ABSTRACT

SULLIVAN, STEPHANIE TOLSTEDT. Functional Biomaterials: Solution Electrospinning and Gelation of Whey Protein and Pullulan. (Under the direction of Saad A. Khan, Ph.D.).

Utilizing biomaterials that are biodegradable, biocompatible and edible serve well for food products as well as biomedical applications. Biomaterials whey protein and pullulan both have these characteristics. Whey proteins (WP) have been used in food products for many years and more recently in pharmaceutical products. They have the ability to form both gels and stable foams. Pullulan (PULL) has also been used in both food and pharmaceutical products, and is a highly water soluble, non-gelling polysaccharide and has been used primarily as a film former. Herein, we investigate the ability of whey protein and pullulan to form nanofibers and gels. Combining their distinct properties allows the ability to uniquely manipulate nanofiber and gel characteristics and behavior for a variety of applications, from food to even tissue scaffolding.

First, we determined the electrospinnability of aqueous whey protein solutions. Both whey protein isolate (WPI) and one of its major components β–lactoglobulin (BLG), either in native or denatured form, yielded interesting micro and nanostructures when electrosprayed; while nanofiber production required blending with a spinnable polymer, poly(ethylene oxide) (PEO). WP:PEO solutions were also successfully electrospun at acidic pH ($2 \leq pH \leq 3$), which could improve shelf life. Fourier Transform Infrared Reflectance (FTIR) analysis of WP:PEO fiber mat indicated some variation in WP secondary structure with varying WPI concentration (as WPI increased, % α-helix increased and β-turn decreased) and pH (as pH decreased from neutral (7.5) to acidic (2), % β-sheet decreased and α-helix increased). X-ray

Photoelectron Spectroscopy (XPS) also confirmed the presence of WP on the surface of the blend fibers, augmenting the FTIR analysis. Interestingly, WP:PEO composite nanofibers maintained its fibrous morphology at temperatures as high as 100 ^{o}C, above the 60 ^{o}C PEO melting point. Further, we show that the blend mats retained a fibrous structure after the heat treatment.

Our second goal was to evaluate the ability of aqueous blends of whey protein and pullulan to form gels. We first looked at WP-PULL blend solutions at room temperature, finding an increasing linear trend in low shear viscosity as the relative concentration of pullulan increased. Blend solution samples were then heated to determine the ability of the blend solutions to form a gelled network. Starting with a homogeneous WP gel, adding PULL, at native mix or alkaline pH, maintained a transparent homogeneous microstructure, but resulted in weaker gels based on its response to stress. At WP isoelectric point (IEP) pH, both protein and blend gels became opaque due to protein aggregation, forming a particulate gel. All gels at the IEP were weaker, yielding at much lower stress and corresponding strain, due to the protein aggregation. The addition of transglutaminase enzyme yielded a stronger network than the native samples, while the addition of sodium trimetaphosphate salt yielded weaker gels and also induced relevant particle and/or course stranded microstructure in both pH 8 and IEP cases.

The third part of this study demonstrated the ability of pullulan to form nanofibers in the solution electrospinning process. Aqueous pullulan solutions were able to form defect-free nanofibers with a minimum concentration of 15 w/w%. Pullulan and PULL:hydroxypropyl-β- cyclodextrin (HPBCD) blend fibers were chemically crosslinked to

form insoluble fibers using ethylene glycol diglycidyl ether (EGDGE), a chemical used in food contact coating applications. Next, solution blends of pullulan with whey protein were prepared and also electrospun at varying pH and relative biomaterial concentrations at 17 total w/w%. PULL-WP blend nanofiber mats were crosslinked via heat treatment and found to be both swellable and insoluble. When dried, the mats did not return to their original fiber state and instead appear to be gelatinous fibers in nature after soaking, and thereby making them potentially useful for tissue scaffolding applications.

A fourth accomplishment was to utilize Near Infrared Reflectance (NIR) Spectroscopy and Chemometrics techniques to analyze commercial whey protein powder characteristics such as protein, fat and moisture content as well as pH. NIR has been utilized in the food and pharmaceutical industries for quality control as a valuable compliment to or replacement for more expensive testing such as High Performance Liquid Chromatography. Analysis resulted in the development of quantitative, linear regression models to correlate whey protein powder characteristics to NIR data.

Whey protein's ability to form gels and pullulan's electrospinnability to form nanofibers is combined herein to form blends of both that can be changed with varying concentration, pH, temperature and supplementation with food-safe additives. The study correlates mechanical properties and microstructure of blend gels and nanofibers and provides a foundation for further study of swellable network for tissue application specifically in the use of pullulan-whey protein heat treated nanofiber mats.

Functional Biomaterials: Solution Electrospinning and Gelation of Whey Protein and Pullulan

by
Stephanie Tolstedt Sullivan

A dissertation submitted to the Graduate Faculty of
North Carolina State University
in partial fulfillment of the
requirements for the degree of
Doctor of Philosophy

Chemical and Biomolecular Engineering

Raleigh, North Carolina

2011

APPROVED BY:

_____	_____
Dr. Saad A. Khan Committee Chair	Dr. Jan Genzer
_____	_____
Dr. Russell E. Gorga	Dr. Richard J. Spontak

DEDICATION

To God, for all the blessings in life you have brought to me. Thank you. You have given me much more than I could possibly deserve.

To both of my parents, for bringing me into this world and giving me their support in every way they could throughout my many years of life. To my mother, for helping me to learn math when I was a kid and making it fun. To my father, for working with me on my tennis so that I could be an athlete for life and for teaching me the art of observation.

To Dr. George Pearsall, Professor Emeritus of Duke University, for career guidance, friendship and support throughout many years. I could not have jumped into or survived these waters without you.

To my brother, Brad, for listening and understanding and even beating me (by a long shot) to the finish of this thing called "P h D." I was not sure that I could finish this endurance event as you did. Whew! Time to vacation in Hawaii! I know where to find you!

To my husband, Michael, for putting up with my long hours away from home and getting the kids where they need to go. You have done your best to understand all this and more. You are a great tennis coach and will be a great elementary school teacher one day. I will support you in every way I can for you to get there, as you have me to finish this effort. Thank you.

To my mother-in-law and father-in-law, Beth and Ray Sullivan, for supporting Michael's dream that ultimately brought me back to the PhD path and for helping us in every way that you could.

To Bill, for supporting my change to become chemical engineer. I will be forever proud of that "A" in Dr. Roberts graduate reaction kinetics course, as I never thought I could do better than you in anything chemical engineering. You are forever a smart man and no doubt could do this "P h D" thing too, if you had wanted to finish.

To my friend, Mandy Peacock (Raleigh, NC), for giving me friendship, refuge and hospitality so I could afford to work away from home.

To my favorite "little old lady in tennis shoes" - the late Isabella Cannon - who was a pioneer as well as wonderful leader, friend and role model to me in her little house on Brooks Ave.

To my cousin, Jonathan Tolstedt (Fargo, ND). for sharing wisdom and humor – you are a joy to all in your life; and my aunt, Velma McCarthy (Burke, SD), who is a pillar of strength, endurance and love for her family. I am so glad we have reconnected and I look forward to visiting you again soon. I have missed you all dearly.

To Steven (Huron, SD), for giving me a dream and an example of leadership, spirituality and stature to follow. I love and miss you always.

Finally, to my wonderful children – Brooke, Breanna and Blakelyn - my world – that you will be happier, healthier and more successful than I could ever dream in all areas of life. I do everything I do for you. I have missed you every moment I am away from you and will continue to each and every day wherever I may be. Please know that your dad and I love you all no matter what, always. Strive to be the best you can be!

BIOGRAPHY

Stephanie Tolstedt Sullivan was born in Columbus, Ohio in 1968. She was blessed to receive the Glenna R. Joyce Scholarship to attend the University of Notre Dame, where she attended from 1986 until 1990, graduating *cum laude* with a Bachelor of Science degree in Mechanical Engineering and had an opportunity to play varsity women's tennis too. While there, she was fortunate to earn the opportunity to participate in the National Science Foundation Research Experience for Undergraduates program, working with Professor Patrick F. Dunn in the summer of 1989. Following completion of her undergraduate degree, she went to work for Amoco Oil Company in Whiting, Indiana and moved with that company to their Texas City, Texas refinery, working as a project engineer. As she trained towards the next step in her career there, to be a maintenance engineer, a personal decision had her move to a new company and work for Stone & Webster Engineering Corporation in Katy, Texas as a fluid systems engineer. After working for these companies and with chemical engineers, she decided to attend graduate school at North Carolina State University (NCSU) in their Department of Chemical Engineering beginning in 1993.

During her studies at NCSU, she worked as a teaching assistant and also received the Patricia Roberts Harris Fellowship. She completed her Master of Science degree in May 1996 under the direction of Dr. Christine Grant and Dr. Ruben Carbonell. Meanwhile, she received a fellowship to attend Duke University graduate school in their Department of Mechanical Engineering and Materials Science. She took courses while there and began research efforts, but a personal decision to be close to her now husband Michael (married 1997) had her take a position in industry in eastern North Carolina. She worked as a

maintenance engineer for PCS Phosphate's (Aurora, NC) phosphoric acid plants, and later as a production engineer for their diammonium phosphate plants (DAP). In this latter position, she had the opportunity to work with experts (she found at the University of Queensland, Australia, in Chemical Engineering) on the granulation process utilized in DAP production. This process is similar to a high shear granulation process used in solid dosage form manufacturing in the pharmaceutical industry, in which she in 1998 earned a position for Merck & Co., Inc. (Wilson, North Carolina) working for Dr. Harry Suryakusuma. After eight years in various positions at that location, where she stayed in order to support her husband's local business, she learned of a new engineering program starting at East Carolina University in Greenville, North Carolina. The ultimate Chair of that new department, Dr. Paul Kauffmann, recruited her so that she could develop courses for both engineering and technology systems programs as well as return to North Carolina State University to complete her PhD starting in 2006. Upon finishing graduate studies at NCSU in 2011, she will continue to support her family as faculty in the Department of Engineering at East Carolina University as she has since Fall of 2006 and, from there, follow whatever path presents itself to continue to do so.

ACKNOWLEDGMENTS

I would like to express my deep gratitude to my advisor, Professor Saad Khan, for his support, help, advice and guidance during the course of this work. You inspired me during my Masters degree about the study of polymers and rheology, and I was so thrilled to be able to return to NCSU to work with you in this area. Thank you for permitting me to work with you and for all of your time and understanding - priceless. I have adored you and your family since we lived in the same apartment building starting in 1993. Thank you so much to my committee – Dr. Jan Genzer, Dr. Richard Spontak and Dr. Russell Gorga. You are all brilliant, amazing engineers, scientists, researchers and men. It has been an honor to present my work to you and learn from you. I wish I had had more time with all of you – to learn and apprentice. Your students are so very blessed.

The wonderful graduate students in the Khan group are all my idols. You, too, are all brilliant engineers and researchers. It has been such an honor to know you and I wish I could have learned more from you. Special thanks to Dr. Ahmed Eissa and fellow students Dr. Christina Tang, Dr. Sachin Talwar, Dr. Sara Arvidson, Dr. Christopher Bonino, Dr. Annie Chu as well as post-doctoral fellow Dr. Carl Saquing for guidance and discussion; along with new fellow students MAJ Christopher Johnson (US Army) and Alina Higham helping me out the door. Christina, you are amazing and no doubt will be running your own research organization one day; I enjoyed our adventure to Switzerland – my only trip to Europe!

To the faculty of the Department of Chemical & Biomolecular Engineering, especially those here when I first started in 1993, thank you. Although some may not even remember me, you are all near and dear to my heart, especially Dr. Ruben Carbonell and Dr.

Christine Grant, my M.S. thesis advisors; Dr. David Ollis, especially for liking my use of color on my TRANSPARENCIES (note not power point slides back then) during my proposal course practice presentations in 1994; and Dr. Peter Kilpatrick who was always a supportive and smiling face as well as taught a great course in colloids & surface science – and now at my alma mater! Thanks to Dr. Hubert Winston - always welcoming and helpful; Dr. Peter Fedkiw, for welcoming me back… I was happy to survive your class years ago; Dr. Carol Hall who was a supportive ear in my younger days, as well as great teacher, making fun links between chemical thermodynamics and certain elements of life – my needing more help on the latter than the former! Notably, Dr. George Roberts who really made the connection for me between the work I had done in industry and the theoretical. I knew I was in the right place after taking your course. I was so pleased to have the opportunity to talk with you several times after returning to NCSU in 2006, and you are sorely missed by all. I only wish I had learned more from you and all at NCSU.

The great staff of the Department of Chemical & Biomolecular Engineering has always been so sweet and helpful – Sandra Bailey, Diane Harper and Sheila Hayes especially have well tolerated me – bless you! Also, thanks to Dr. Michelle Casper, Dr. Kirill Efimenko, Casey Galvin, Erich Bain for technical support of this effort. Thank you to Dr. Allen Foegeding and Yie Hui Yong, Dr. Orlin Velev and Dr. Jan Genzer all for support and utilization of their facilities. Kit has always been amazing.

Thank you again to Dr. George Pearsall, Professor Emeritus of Duke University for providing extra help with my efforts at East Carolina University (ECU), as well as thanks to Dr. David Stepp for his support. If only I could download from both of your brains all of

your materials science knowledge. I also want to thank Paul Kauffmann and for bringing me to ECU and supporting me more than perhaps I even realize. I hope to be able to "toot my own horn" better one day. Thanks to Dr. Evelyn Brown, Dr. Melani Duffrin, Dr. William (Ed) and Darlene Howard, Becky Foster, Dr. John Reis, Dr. David White, Dr. Hayden Griffin, and Bruce Peterson for listening, support and kindness. Certainly, thanks to all Department of Engineering and other College of Technology & Computer Science faculty and staff for understanding and support! Joel Sweatte, Steve Mockbee and Randy Godwin for computer and data storage support. Melani, your support as neighbor, especially in helping my children, has been priceless.

Thanks to ECU Professors Dr. Cathy Hall, Dr. Bill Swart and Dr. Steve Duncan for their collaboration as well as reminders and prodding to finish my doctoral work, in addition to support of my leadership initiatives for ECU students – especially to Steve for making several connections for my leadership speaker series. Special thanks to my friends COL (Retired) Worth Carter (USAF) and CPT Annie Khamphengphet Hester (US Army) for support over the last three years and keeping me somewhat sane. You have gone above and beyond service to your country! Also, thanks to the wonderful athletes with whom I have had the honor to attempt to keep up including Matt Maloney and Tricredibles Mike Columbo and Super Bob Morrison! I have appreciated your smiling and welcoming faces.

Thanks to Dr. Jason Bond, Dr. Tom Fink, Dr. Eva Johannes and Dr. David Cistola, Michelle Robinson, H. Ray Tichenor and Andrew Cathey for their support of this work. Thanks also to Chad Spruill for laboratory support. And to all of my undergraduate research assistants who worked long hours for little to no pay. You are true leaders and will achieve

whatever you put your mind to: Jamelle Simmons, Thomas A. Deaton, Joseph A. Rose, Clay Rice, Victoria Miller, Eric Franson, Adam Hussaini, Lauren Bridgers, Michael Cannon, Christopher Eckert, Dao Dinh, and Mohammed Akbar. Jamelle, you have worked with me for four years and it has been an honor. I would also like to thank my good friends Waz Miller and Bedie & Ron Kohake for helping with countless things for my children; and good friends Gary Crecelius, Beverly Day, and Betsy Whitley who provided encouragement.

One final acknowledgment I feel I must make is to the good Samaritan medical doctor who, after being in a car accident, got out of his hospital bed and worked all night long in pain from several broken ribs and other injuries to save my dad's life in 1962. Without you, my father would not have survived or gone on to do his incredible works of art and inspire his lifetime of students to do the same. Also, my brother and I and my children would not be here without your help, as we were born well after 1962. Since I learned of the details of the event in which my dad's appendix had burst, his abdomen became riddled with infection, and he was administered his last rites – with all attending to him having given up on providing him the care he needed to help him survive and keep him alive (and important to note that you were NOT on staff at the hospital but a PATIENT and nurses were telling you to get back in bed!), I have wanted to find out who you are. I hope to one day soon. You would be in your mid to late seventies by now. I have no riches or rewards to give you, just hugs, thanks and prayers. I hope one day that I and my children can do proud the sacrifice and gift you delivered to us all through saving my father's life. I hope you and your family have had and continue to have a blessed life. You were an angel sent by God that night, and you suffered and sacrificed on behalf of another. No greater gift. Thank you.

TABLE OF CONTENTS

LIST OF TABLES

LIST OF FIGURES

CHAPTER 1 Motivation, Goals and Background

ABSTRACT

In this chapter, we introduce the reader to the dissertation topic: the biomaterials whey protein and pullulan. Utilizing materials that are biocompatible, biodegradable and safe for human consumption and contact for food and medical applications is essential for the well being of the consumer. Both whey protein and pullulan have these characteristics. Better understanding the capability of these materials will allow further product development and use of such safe materials. The focus of the dissertation is to understand their performance as elements of the biomaterial forms nanofibers and gels. In the preparation of these biomaterial forms, both heat and chemical methods are used to modify and potentially enhance these forms.

1.1 Motivation and Goals

The objectives of this study are to develop and examine novel functional gels and solution electrospun nanofibers of biomaterials. In particular, we are interested in two such materials – whey protein (WP), a cheese manufacturing co-product, and pullulan (PULL), a polysaccharide. Currently, both of these biomaterials are utilized in food, pharmaceutical and biomedical applications. Each is biocompatible, edible, and generally regarded as safe (GRAS) by the US FDA[1], and used not just to modify food and other material's properties, but as nutritional supplements as well.[2-5] The three primary objectives of this study are to:

I. Examine strategies to develop WP nanofibers and correlate morphology to solution properties
II. Investigate formation and microstructure of WP-pullulan gels and ways to manipulate gel properties using enzyme and salt
III. Explore creation and crosslinking of pullulan and pullulan blend nanofibers to render this highly water soluble material insoluble

We will demonstrate the electrospinnability of whey protein, pullulan, and blends of these biomaterials as well as analyze the formation and microstructure of their blend gels.

Electrospinning, a process first patented in 1934, can yield fibers smaller than 100nm.[6] Equipment for two electrospinning methods, melt and solution electrospinning, has been thoroughly discussed and summarized in review.[6, 7] Solution electrospinning utilizes polymer dissolved in solvent that is pumped at a controlled flow rate from a syringe to which a high voltage is applied. Electrostatic forces between the positively charged syringe needle

and a grounded collector plate pull solution away from the Taylor cone[8] formation at the tip of the syringe to the collector. As the solution is pulled away from the syringe, solvent evaporates, leaving the polymer drawn into fibers and collected as a fiber mat.[9] The process control parameters can be divided into two categories, one of which is solution/melt properties including viscosity/concentration, surface tension, and conductivity; the other is the operating parameters during electrospinning process including electric field (or voltage applied and distance between spinneret and collector), flow rate, and other environmental parameters, which make it a complicated process for the achievement of defect-free fiber morphology and chemical composition.

Benefits of solution electrospinning include encapsulation of insoluble particles within a nanofiber mat, and the incorporation of soluble drugs in a uniform fashion [6]. Nanofiber systems also can serve as wound dressings[10] or as a scaffold for tissue engineering[1112]. Advanced nanofiber designs include modifying the nanofiber surface with bioactive peptides and proteins[9]; [13] and immobilizing enzymes.[14]

With the surge of electrospinning research, several proteins have been electrospun, although not whey proteins such as β-lactoglobulin (BLG) or α-lactalbumin (ALA). Table 1.1 lists studies found to date involving the electrospinning of proteins, including silk fibroin, zein, keratin, collagen, fibrinogens, egg protein and bovine serum albumin. Based on the desirable functional and health benefits whey proteins provide, possible uses of whey protein-based nanofibers would include food and pharmaceutical design, wound healing, flavor control release, material texture and strength enhancement, immobilizing enzymes for improved stability, and tissue scaffolding.

Our **first goal** is to demonstrate that whey proteins can be electrospun and to evaluate those resultant nanofiber mats, including the impact of pH on electrospinning. Also, we evaluate the impact of heat treatment on WP fiber mats. Thus, the first challenge is to electrospin aqueous whey protein solutions. Sister milk protein casein could not be electrospun without the addition of spinnable polymer. [15] Also, due to the globular nature of whey proteins such as BLG and ALA, the low viscosity of their aqueous solutions, and expectations of entanglement being an issue, this will be a challenge.[16-18] The addition of spinnable polymer may be required, as was executed with other proteins such as silk fibroin and egg proteins.[19-21] Solution pH could also play a role in successful solution electrospinning, as it influences whey protein solution behavior.[22] Certainly, formulation via solution electrospinning at various pH would likely be critical to its ability to tailor it to the sensitivity of the drug or flavenoid requiring delivery. Therefore, to be able to demonstrate that aqueous whey protein solutions can form nanofibers at acidic pH would then facilitate the consequential benefit of formulation flexibility and improved shelf life. Heat treatment of fibers could also play a role in the fiber mat structure, as whey protein can be heat denatured.[23] Whey protein has also been investigated for use in drug delivery systems because it is edible, biocompatible and biodegradable. Thus, forming drug-loaded nanofibers of whey protein is desirable.[24]

For our **second goal**, we examine whey protein-pullulan gel formation. Gels of whey protein have been utilized in food formulations for some time,[23, 25-44,45-58] as have gels of whey protein and some polysaccharides (specifically galactomannans).[23, 25, 59, 60] However, use of whey protein-pullulan blends has been limited to film formation[61-69], solution

demixing.[70-72] and interfacial complex formation.[73] Pullulan's properties, such as highly mobile, water soluble and non-gelling on its own will provide greater flexibility in, not to mention its potential health benefits especially for diabetics.[74] Development of new gel and fiber nanostructures of non-gelling pullulan and whey protein will provide additional opportunities for biotechnology application development as well as fundamental understanding of relationships between aqueous whey protein, pullulan and blend solution properties and their ability to form gelatinous structures not currently available.

Our **third goal** will further explore the use of edible, biocompatible and biodegradable pullulan to form both hydrophilic and hydrophobic nanofibers via solution electrospinning. Pullulan is a natural, water-soluble polysaccharide that is excreted extracellularly by the fungus Aureobasidium pullulans and comprised of maltotriose units (α-1,4 linked glucose molecules) polymerized by α-1,6-glucosidic bonds.[575] The molecule is linear, amorphous,[75] and forms a stair-step like structure (Figure 1.1). It is odorless, flavorless and highly stable. Pullulan has many current and potential uses in the food and pharmaceutical industries,[76] and is being considered for part of therapeutic diets for individuals with type 2 diabetes mellitus because it helps maintain blood glucose levels.[77-89, 895] Reports on native pullulan pharmacokinetics are minimal.[5] Aqueous pullulan solutions are stable and viscous but do not gel, even in the presence of ions like borate that form complexes with hydroxyl groups.[89] Although several group studies of hydrophobically-modified pullulans,[88], the unmodified pullulan has GRAS status.[79-83]

Unmodified pullulan has limited solubility, [1] and has been utilized in primarily water and dimethyl sulfoxide (DMSO) solutions. Use of DMSO has been very controversial and

United States Food & Drug Administration (US FDA) approved for only one human use.[83] Thus, we are specifically interested in better understanding of pullulan aqueous solutions and their ability to form both hydrophilic and hydrophobic nanofibers. Since our study initiated in 2006, only two groups have explored pullulan electrospinning. The first prepared nanofiber mats blended with montmorillonite (MMT) clay to form nanocomposites[90] and the second prepared *in situ* crosslinked pullulan fibers with food safe sodium trimetaphosphate (STMP) and sodium hydroxide (NaOH)[91] following their work developing hydrogels of pullulan crosslinked with the same crosslinker (STMP) and initator (NaOH).[92] We investigate other means of pullulan nanofiber crosslinking, including using chemical means with ethylene glycol diglycidyl ether (EGDGE) and using heat treatment of blends with whey protein that show promise for applications such as tissue scaffolding and food texture modification.

In summary, we will utilize whey protein and pullulan biomaterials for our **study goals** to develop novel electrospun nanofibers and gels while evaluating the influence of rheological and other solution properties on nanofiber and gel structure. Ultimately, this understanding will aid the further development of novel food, pharmaceutical and biomedical materials, such as the evaluation of drug and flavor release from these gels and nanofibers.

1.2 Background

This section discusses the background of whey protein, whey protein gelation, pullulan, and protein-polysaccharide complexation and pullulan nanofibers while outlining

specific questions we address in this study. The chapters that follow address these issues in more detail.

1.2.1 Whey protein

Whey proteins are one of two milk protein groups, with the other being caseins. Formerly considered a by-product of the cheese-making process, researchers have found that whey protein is a valuable dietary supplement in addition to serving as a functional food enhancer. Suppliers such as Davisco Foods, Inc. now consider it a co-product of cheese production due to its increased value. For many years, whey proteins have been used in food design due to its variety of functional uses including water and flavor binding as well as gelation, emulsification and foaming.[93] From a medicinal standpoint, whey proteins are being studied and recognized for their antimicrobial, antiviral, anticarcinogenic and other beneficial metabolic and physiological effects.[94,95] For example, whey in its natural conformation is rich in the amino acid cysteine, which is important in synthesizing the "major intracellular antioxidant" glutathione.[2, 3, 96] Data also suggest that the human body's ability to quickly absorb whey protein may enhance its ability to better utilize protein after eating.[3] Whey proteins consist primarily of BLG, ALA, serum albumin (SA), immunoglobulin (IG) and lactoferrin (LF). Figure 1.2 indicates the composition of bovine whey protein. From a functionality standpoint, the behavior of BLG is known to dominate commercial whey protein ingredients, especially those with higher protein contents such as whey protein isolate (WPI) and some whey protein concentrate (WPC).[3] BLG is a globular protein with an isoelectric point (IEP) of approximately 5.2. The IEP of a protein is the pH at

which the molecule has a neutral charge. At their IEP, whey proteins tend to aggregate extensively. Table 1.2 lists the whey proteins and their properties.

Whey proteins have a variety of beneficial nutritional and product development properties. They have a balance of hydrophilic and hydrophobic residues, contain cysteine and cystine (antioxidant properties), have a globular structure with considerable helical content, are easily heat denatured and are stable in mildly acidic conditions. They are purified from milk using filtration, ion exchange or heat-precipitation techniques.[97] Their ability to gel is utilized for food and other applications.[98] Utilizing whey proteins at acidic pH is desirable to increase product shelf life and stability of biomaterials including those for pharmaceutical and food applications.

Whey proteins are also considered to have positive health effects including reducing the risk of heart disease and cancer as well as lowering blood pressure.[63] Because of this, whey protein is considered to have significant nutritional value and is used in both human and animal food manufacture, including formulation for nutritional supplementation. For example, formulators of nutritious drinks such as yogurt employ low pH acid-heat denatured whey proteins due to their high solubility.[95] Past and current studies of whey proteins involve various forms including gels, emulsions, and foams.[99] Table 1.3 summarizes some functional properties of whey proteins such as gelation and foaming while Table 1.4 provides specific BLG characteristics with pH. Based on the strong impact of pH on structure and performance of whey proteins, including during heat treatment, we consider pH impact in our study.

1.2.2 Whey Protein Gelation

Gelation involves the construction of a continuous network of macroscopic dimensions.[100] In this regard, whey protein gelation requires denaturation of the protein molecules [56] followed by intermolecular interactions. Denaturation is required to expose the reactive functional groups of the protein. Interactions between these functional groups involve chemical bonding and physical interactions. A schematic representation of gelation mechanism is illustrated in Figure 3. Chemical bonding typically involves disulfide bonds formation, which is crucial for protein aggregation.[101] Physical interactions include van der Waals interactions, hydrogen bonding, electrostatic and hydrophobic interactions. [57, 102, 103] A minimum protein concentration is required for gelation. This concentration is a function of temperature, pH and ionic strength.

Gelation is usually done via heat treatment at a temperature higher than denaturation temperature. This is known as thermally induced – or heat induced – gelation. Several publications have extensively studied thermally induced gelation of whey proteins.[104] Whey protein gels are usually characterized by their rheological properties. Rheological characterization includes small strain and large strain properties, and such properties of the whey protein gels have been discussed in various publications.[47, 105-108, 108, 109]

During heat induced gelation, BLG – which is considered the most thermally active of the whey proteins – denatures (unfolds) exposing reactive sites such as thiol groups, hydrophobic or ionized locations. At a high enough concentration, the protein chains also become entangled, facilitating gelation. Linden & Lorient (1999) show three possible heat induced BLG structural modifications, two of which are described as follows:[33, 35-37, 39]

1. Neutral or alkaline medium: gelation improves if electrostatic repulsion stabilizes unfolded BLG molecules (gel firm, elastic)
2. IEP: precipitation occurs (gel opaque, brittle, granular)

The third, acidic gelation, has also been investigated. Gelation of whey proteins at low pH may be thermally induced [110] or cold set.[48, 53, 111] Thermally induced gelation at pH close to isoelectric point creates opaque gels with particulate microstructure, compared to the more transparent gels far from the isoelectric point. Several studies have been performed on gelling properties of whey proteins under acidic conditions.[39, 104] Although gels formed at low pH (< 4) were brittle with low strain and stress at fracture, as opposed to those formed at high pH, which were rubber-like with high strain and stress at fracture,[54,58, 112] the low pH environment is advantageous as it limits the microbial growth and increases product shelf life.[45] Therefore, utilization of heat-induced whey protein gels at acidic conditions would be beneficial in reducing spoilage, but the rheological properties – i.e. weakness and brittleness –has limited the uses of the gels at such pHs. Acid induced cold gelation has showed promise, however, noticeably increasing strength and elasticity of the gels.[34] Enhancing the textural properties of whey protein gels at low pH is viable through acid induced, cold-set gelation, in which disulfide bonds are created in a neutral pH and then the pH is dropped to the required acidic pH.[34] An alternative route is to induce enzymatic crosslinks to strengthen the protein network and enhance the texture.[45]

Evaluation of whey protein at acidic pH is very desirable for food and pharmaceutical formulation to extend product shelf life. Our **first goal** – in electrospinning whey protein

solutions into nanofibers – also looks at the influence of acidic pH on fiber morphology and even the impact of heat treatment and resultant formation of a gelatinous fiber mat. Critical issues we address for this **first goal** include the following:

- Can native aqueous solutions of whey protein (WP) electrospin?
- What is the impact of chemically denaturing WP?
- What is the impact of blending with spinnable synthetic polymer poly(ethylene oxide)?
- How do acidic solutions perform?
- What is the impact of heat treatment?
- What can we understand from microstructure?
- What is the impact of loading a small molecule for release?

Whey protein will also be used in blends with the polysaccharide pullulan for gelation for the dissertation **second goal** and in combining with pullulan in nanofiber blends in the dissertation **third goal** discussed below. Thus, understanding whey protein characteristics and behavior is critical to this effort

.

1.2.3 Pullulan

Pullulan is a glucan that is synthesized extracellularly by the fungus Aureobasidium pullulans. This synthesis occurs when the fungus is grown on media contacting sucrose or glucose. Its existence was first reported in 1938; production conditions and structure were first reported in 1959-1965 timeframe by three different research groups. Hayashibara

Company (Japan) first produced pullulan commercially in 1976.[22, 30, 34, 113, 114] Currently, Hayashibara uses potato, corn or tapioca starch in the fermentation process.[88]

Pullulan applications include food and pharmaceutical products such as confections, pharmaceutical tablets and capsules, films, beverages, binders, sauces,[115] coatings and films, and even molded products by solution casting or thermoplastic extrusion. In fact, melt spinning of pullulan into fibers has been accomplished.[75]

Many of these applications are "biodegradable, transparent, oil resistant and impermeable to oxygen."[86, 116] Pullulan serves as an excellent adhesive, stronger than dextrin and gum arabic by nearly five times.[76] In fact, when compression molded, it is claimed to be as strong and rigid as expanded polystyrene.[75] Also, as a food additive, it helps to maintain food texture, such as refrigerated creamy formulations like mayonnaise.[117] Hayashibara's pullulan received GRAS status in the US in 2002, showing that pullulan is not mutagenic in a bacterial system and that no harmful effects resulted from pullulan consumption.[118] Table 1.5 summarizes how pullulan is resolved in humans.

Several studies have evaluated properties of pullulan. In fact, pullulan has been used for some time as a standard in Size Exclusion Chromatography[1] to determine average molecular weights (M_n, M_w, and M_z) because of its narrow polydispersity[119]. Also, many have investigated pullulan as a viscous fermentation product.[120] The rheology of the fermentation broth is considered an important factor in pullulan production. However, only a few studies have reported rheological property evaluation of pullulan solutions for application development.[17, 76,121-128] These are summarized in Table 1.6.

For example, Matsumura et al. examined rheological behavior of some polysaccharide solutions including pullulan. A next step to his work would be to evaluate solutions at higher pullulan concentrations and/or higher shear rates to determine if the solutions will behave more solid-like. Lazaridou et al. (2003) achieved coil entanglement. They analyzed aqueous solutions of various pullulan molecular mass fractions, determining intrinsic viscosity [η], critical concentration c*, and coil overlap parameters (c*[η]) Lazaridou et al. values for the commercial Hayashibara pullulan are given in Table 1.7, along with other pullulan fractions and polysaccharides. Extending rheological evaluation with dynamic oscillatory measurements to determine if solutions become more elastic at higher concentrations, particularly above c* may be desirable. Ding et al. (2005) used rheometry to analyze pullulan/gelatin phase separated mixtures. [118, 129-131] Spyropoulos et al. (2007, 2008) analyzed pullulan/sodium dodecyl sulfate (SDS) surfactant mixture rheology and microstructure. [118] Such mixtures like these already investigated as well as what we propose would be useful for food and other industry product development.

1.2.4 Protein-polysaccharide gelation complexes

Protein-polysaccharide complexes are being evaluated for food, pharmaceutical and biomedical applications. For development of these applications, considerable work has been done with specific biomaterial-biomaterial-water systems. Both salt concentration and pH have an impact on protein conformation.[129, 130] Acidic solutions of whey protein are desirable for food and pharmaceutical development due to improved shelf life. Controlling the pH of the solution also changes the protein conformation, and thus the ability of whey

protein to interact with other small molecules (such as drug and flavor molecules). Pullulan viscosity is "essentially unaffected by pH over a wide range of pH values (< 2 to > 11)."[73] Therefore, pullulan can be utilized in both acidic and alkaline formulations with whey proteins. Some scientific challenges for the evaluation of these mixtures include both gel formation and nanofiber electrospinning.

For example, the food industry has been interested in biomaterial mixtures, especially those that may form emulsions, as a food texture improvement tool.[88] However, it seems the literature lacks information on nonionic polysaccharides and in particular on the interaction between a widely used biomaterial – whey protein – and pullulan.

Recent studies have evaluated mixture properties of whey protein and other polysaccharides, primarily galactomannans. These are summarized in Table 1.8. Also, an extensive review of whey protein isolate-starch systems was completed by Pogaku et al.[132] Starch is a "naturally occurring polysaccharide composed of semi-crystalline particles consisting entirely of anhydroglucopyranose residues"[133] linked either by 1→4 or 1→6 glycosidic links.

Of note from Table 1.8 and the Tavares et al. (2003) study with WPI and locust bean gum is their conclusion that even if phase separation is occurring in the protein-polysaccharide solution prior to gelation, it may cause a local concentration effect in the gel, but "would not change appreciably the gelation mechanism of the protein."[133] Baeza et al. (2003) reports that incompatible polysaccharides greatly impact protein gelation kinetics and characteristics, in which thermodynamic incompatibility occurs for protein-polysaccharide systems at[61] pH > protein IEP and high ionic strength. Furthermore, his work has evaluated

the non-gelling gums propyleneglycol alginate, xanthan and λ-carrageenan, and he found that the addition of each of these polysaccharides allowed the lowering of the BLG critical gelation concentration as well as the gel formation time (at pH 7).[64] We are interested in extending this challenge by examining of whey protein-pullulan gelation at acidic pH (pH < IEP of whey protein) in comparison to that at neutral pH, for example.

Durand et al. (2001) analyzed BLG and κ-carrageenan systems undergoing aggregation and gelation. Similar to what has been observed so far in our preliminary experiments, Durand et al. (2001) concluded that their mixed protein-polysaccharide system experienced micro-phase separation. This micro-phase separation resulted in gel structures that were similar to pure BLG gels at[64] high ionic strength and the protein IEP. In this case the gel structure could be influenced by this phase separation. Recently, Cakir et al. further investigated whey protein and κ-carrageenan gels, observing phase separation influence on gel microstructure.[40]

Based on these many challenges investigated, we answer some questions specific to the gelation of the pullulan-WP system:

- How does blend ratio concentration impact viscoelastic properties?
- What are limitations for blend gels to form?
- How does pullulan influence gel viscoelasticity?
- Do blend gels have observable microstructure?
- Can blend gels carry a hydrophobic model drug?
- What is the impact of foodsafe additives such as transglutaminase enzyme and sodium trimetaphosphate?

Protein-polysaccharide solutions and gels will be evaluated for the dissertation **second goal** to demonstrate the value of whey protein-pullulan mixtures for food texture and nutrition enhancement, flavor delivery and for controlled pharmaceutical drug delivery systems, for example.

1.2.5 Pullulan nanofibers

Potential exists to use pullulan to produce non-wovens for surface and food texture modification, drug delivery, tissue scaffolding and wound healing. Moreover these polymers can be electrospun in an environmentally benign way without the use of organic solvents. The ease of modulating the interactions of these polymers in solution by varying pH, using additives or even by blending with a second polymer allows the ability of the construct to carry other molecules such as small molecule drugs or flavorings to be promising.

A further objective in this direction is to correlate the properties of the electrospun nanofibers with solution properties. Viscoelastic properties of the polymer solution exert a profound influence on the morphology and diameter of the electrospun fibers. For instance, one of the common problems in electrospun fibers is the presence of beads. It has been reported in the literature that increasing polymer solution viscosity leads to a reduction in fiber bead defects [134]. Efforts to correlate rheology with nanofiber properties studies are until just recently [135] concentrated primarily on the intrinsic and zero shear viscosity of the polymer solutions. However both elastic and viscous properties of the polymer play an important role in the formation of the nanofibers as is evident from the viscoelastic

dumbbells model by Reneker and co-workers for bending instability during electrospinning.[136]

Previous studies concluded that the solutions, although viscoelastic, have low viscosity due to relatively low molecular weight and relatively high pullulan chain flexibility[137, 138] and that solution behavior is primarily viscous.[76] Thus, we are specifically interested in (a) better understanding of pullulan aqueous solution, (b) the ability to use food safe modifiers to crosslink nanofibers and (c) effects of process variables such as temperature and pH for product development.

Pullulan is stable at acidic pH of 2 through alkaline pH levels. Evaluating solutions and resultant nanofibers at acidic pH for prolonged shelf life pharmaceutical and food formulation applications is desirable. One pullulan solution modifier we investigate is hydroxypropyl-β-cyclodextrin (HPBCD). Thus, we would be interested in comparing solution characteristics and electrospun nanofiber mats of HPBCD-pullulan aqueous mixtures. The cyclodextrins are water soluble. The interior of the cyclodextrin "cup" has a hydrophobic micro-environment, while the outside of the cup is hydrophilic. They are used in a variety of applications, including pharmaceutical and biomedical.[139] Pullulan "protected" by cyclodextrin could serve as an effective drug delivery substrate to better help drug molecules reach a colon target in humans, for example. Pullulan and cyclodextrin have joined forces before – with pullulan microspheres formed that contained cyclodextrin and model drug.[140]

Developing, analyzing and crosslinking aqueous solution electrospun pullulan nanofibers is our dissertation **third goal**. Specific questions to be addressed include the following:

- What is the impact of pullulan concentration on electrospinning?
- Can we crosslink pullulan nanofibers to form a hydrophobic mat?
- What microstructure is observed?
- What is the impact of blending pullulan with cyclodextrin on electrospinning & fiber crosslinking?
- Can we crosslink blends of pullulan and whey protein?
- What is the impact of pH on pullulan – WP blend electrospinning?

Investigating the ability of pullulan to electrospin is relevant to both food, pharmaceutical and biomedical formulation. Specific uses that have arisen since the start of this work include using pullulan and pullulan-WP blend nanofibers for fine chocolate texture modification as well as for tissue scaffolding and cardiac cell seeding which are anticipated for future work beyond the scope of this dissertation.

1.3 Organization of Dissertation

Chapter 2 addresses the issue of whether or not we can aqueous solution electrospin whey protein. Gelation of whey protein and pullulan is the focus of Chapter 3. Chapter 4 evaluates the development and crosslinking of pullulan nanofibers. Chapter 5 analyzes whey protein powders by near infrared reflectance spectroscopy and the effort was led by one of

her undergraduate students. Chapter 6 summarizes the key findings of this study of biomaterials and identifies future areas of research.

1.4 References

1. Rulis, A. M. **2002**, 1-4.

2. Madureira, A. R.; Pereira, C. I.; Gomes, A. M. P.; Pintado, M. E.; Xavier Malcata, F. *Food Research International,* **2007**, *10,* 1197-1211.

3. Ha, E.; Zemel, M. B. *The Journal of Nutritional Biochemistry,* **2003**, *5,* 251-258.

4. Fogliano, V.; Vitaglione, P. *Molecular Nutrition & Food Research* **2005**, *3,* 256-262.

5. Wolf, B. W.; Garleb, K. A.; Choe, Y. S.; Humphrey, P. M.; Maki, K. C. *J. Nutr.* **2003**, 1051-1055.

6. Frenot, A.; Chronakis, I. S. *Current Opinion in Colloid and Interface Science* **2003**, 64-75.

7. Li, D.; Xia, Y. *Advanced Materials* **2004**, 1151-1170.

8. Taylor, G. *Proceedings of the Royal Society of London Series a-Mathematical and Physical Sciences* **1969**, *1515,* 453.

9. Sun, X. -.; Shankar, R.; Börner, H. G.; Ghosh, T. K.; Spontak, R. J. *Advanced Materials* **2007**, 87-91.

10. Katti, D. S.; Robinson, K. W.; Ko, F. K.; Laurencin, C. T. *Journal of Biomedical Materials Research Part B: Applied Biomaterials* **2004**, 286-296.

11. Li, W.; Laurencin, C. T.; Caterson, E. J.; Tuan, R. S.; Ko, F. K. *Journal of Biomedical Materials Research* **2002**, 613-621.

12. Boudriot, U.; Dersch, R.; Greiner, A.; Wendorff, J. H. *Artificial Organs* **2006**, *10*, 785-792.

13. Suk Choi, J.; Sang Yoo, H. *Journal of Bioactive and Compatible Polymers* **2007**, 508-524.

14. Jia, H.; Zhu, G.; Vugrinovich, B.; Kataphinan, W.; Reneker, D. H.; Wang, P. *Biotechnol. Prog.* **2002**, *5*, 1027-1032.

15. Xie, J.; Hsieh, Y. *Journal of Materials Science* **2003**, *10*, 2125-2133.

16. Nie, H.; He, A.; Zheng, J.; Xu, S.; Li, J.; Han, C. C. *Biomacromolecules* **2008**, *5*, 1362-1365.

17. Woerdeman, D. L.; Shenoy, S.; Breger, D. *The Journal of Adhesion* **2007**, 785-798.

18. Dror, Y.; Ziv, T.; Makarov, V.; Wolf, H.; Admon, A.; Zussman, E. *Biomacromolecules* **2008**, 2749-2754.

19. Wongsasulak, S.; Kit, K. M.; McClements, D. J.; Yoovidhya, T.; Weiss, J. *Polymer*, **2007**, *2*, 448-457.

20. Yi, F.; Guo, Z.; Fang, Z.; Yu, J.; Li, Q. *Macromolecular Rapid Communications* **2004**, 1038-1043.

21. Jin, H.; Fridrikh, S. V.; Rutledge, G. C.; Kaplan, D. L. *Biomacromolecules* **2002**, 1233-1239.

22. Eissa, A. S. Enzymatic modification of whey protein gels at low pH, North Carolina State University, Raleigh, NC, 2005.

23. Anema, S. G. *Food Chemistry,* **2008**, *1*, 110-118.

24. Satpathy, G.; Rosenberg, M. *J. Microencapsul.* **2003**, *2*, 227.

25. Euston, S. R.; Ur-Rehman, S.; Costello, G. *Food Hydrocolloids* **2007**, *7*, 1081-1091.

26. Ngarize, S.; Adams, A.; Howell, N. *Food Hydrocolloids* **2005**, *6*, 984-996.

27. Resch, J. J.; Daubert, C. R.; Foegeding, E. A. *Food Hydrocolloids* **2005**, *5*, 851-860.

28. Yamul, D. K.; Lupano, C. E. *Food Research International* **2005**, 511-522.

29. Alting, A. C.; Weijers, M.; deHoog, E. H. A.; vandePijpekamp, A. M.; CohenStuart, M. A.; Hamer, R. J.; deKruif, C. G.; Visschers, R. W. *J. Agric. Food Chem.* **2004**, *3*, 623-631.

30. Eissa, A. S.; Bisram, S.; Khan, S. A. *Journal of Agriculture and Food Chemistry* **2004**, 4456-4464.

31. Moon, B.; Mangino, M. E. *Milchwissenschaft-Milk Science International* **2004**, *5-6*, 294-297.

32. Hinrichs, R.; Götz, J.; Weisser, H. *Food Chemistry* **2003**, *1*, 155-160.

33. Ikeda, S. *Food Hydrocolloids* **2003**, *4*, 399-406.

34. Eissa, A. S.; Khan, S. *Journal of Agricultural and Food Chemistry* **2005**, *12*, 5010-5017.

35. Lowe, L. L.; Foegeding, E. A.; Daubert, C. R. *Food Hydrocoll.* **2003**, *4*, 515-522.

36. Chantrapornchai, W.; McClements, D. J. *Food Hydrocolloids* **2002**, *5*, 461-466.

37. Chantrapornchai, W.; McClements, D. J. *Food Hydrocolloids* **2002**, *5*, 467-476.

38. Ramirez-Suarez, J. C.; Xiong, Y. L. *J. Food Sci.* **2002**, *8*, 2885-2891.

39. Britten, M.; Giroux, H. J. *Food Hydrocolloids* **2001**, 609-617.

40. Durand, D.; Le Bon, C.; Croguennoc, P.; Nicolai, T.; Clark, A. H. Aggregation and gelation of globular proteins with and without addition of polysaccharides. In *Gums and Stabilisers for the Food Industry 11;* Williams, P. A., Phillips, G. O., Eds.; Royal Society of Chemistry: Cambridge, 2001; pp 263-270.

41. Vardhanabhuti, B.; Foegeding, E. A.; McGuffey, M. K.; Daubert, C. R.; Swaisgood, H. E. *Food Hydrocoll.* **2001**, *2*, 165-175.

42. Liu, G.; Xiong, Y. L.; Butterfield, D. A. *J. Food Sci.* **2000**, *5*, 811-818.

43. Shinya Ikeda, K. N.,E.Allen Foegeding *Biopolymers* **2000**, *2*, 109-119.

44. Bauer, R.; Rischel, C.; Hansen, S.; Øgendal, L. *Int. J. Food Sci. Tech.* **1999**, *5/6*, 557-563.

45. Errington, A. D.; Foegeding, E. A. *Journal of Agricultural and Food Chemistry* **1998**, 2963-2967.

46. Verheul, M.; Roefs, S. P. F. M. *Food Hydrocolloids* **1998**, *1*, 17-24.

47. Gezimati, J.; Singh, H.; Creamer, L. K. *Journal of Agricultural and Food Chemistry* **1996**, 804-810.

48. Lupano, C. E.; Renzi, L. A.; Romera, V. *J. Agric. Food Chem.* **1996**, *10*, 3010-3014.

49. Panyam, D.; Kilara, A. *Trends in Food Science & Technology* **1996**, *4*, 120-125.

50. Barbut, S. *Food Research International* **1995**, *5*, 437-443.

51. Taylor, S. *Food hydrocolloids* **1994**, *1*, 45.

52. Foegeding, E. A. The effect of cations on rheological properties of whey protein gels. In *Food Proteins, Structure and Functionality;* Schwenke, K. D., Ed.; VCH Verlagsgesellschaft: Weinheim, Germany, 1993; pp 341-343.

53. Lupano, C. E.; Dumay, E.; Cheftel, J. C. *International Journal of Food Science and Technology* **1992**, 615-628.

54. Stading, M.; A.M., H. *Food Hydrocolloids* **1991**, 339-352.

55. Xiong, Y. L.; Kinsella, J. E. *J. Agric. Food Chem.* **1990**, *10*, 1887-1891.

56. Ziegler, G. R.; Foegeding, E. A. *Advanced Food Nutrition Research* **1990**, 203-298.

57. Shimada, K.; Cheftel, J. C. *Journal of Agricultural and Food Chemistry* **1989**, 161-168.

58. Shimada, K.; Cheftel, J. C. *Journal of Agricultural and Food Chemistry* **1988**, 1018-1025.

59. Gunasekaran, S.; Xiao, L.; Eleya, M. M. O. *J Appl Polym Sci* **2006**, *5*, 2470-2476.

60. Reddy, T. T.; Lavenant, L.; Lefebvre, J.; Renard, D. *Biomacromolecules* **2006**, *1*, 323-330.

61. Tavares, C.; Lopes da Silva, J. A. *International Dairy Journal* **2003**, *8*, 699-706.

62. Tavares, C.; Monteiro, S. R.; Moreno, N.; Lopes da Silva, J. A. *Colloids and Surfaces A: Physicochemical and Engineering Aspects* **2005**, 213-219.

63. Monteiro, S. R.; Tavares, C.; Evtuguin, D. V.; Moreno, N.; Lopes da Silva, J. A. *Biomacromolecules* **2005**, 3291-3299.

64. Baeza, R.; Gugliotta, L. M.; Pilosof, A. M. R. *Colloids and Surfaces B: Biointerfaces Food Colloids, Biopolymers and Materials Special Issue* **2003**, *1-4*, 81-93.

65. Sittikijyothin, W.; Sampaio, P.; Gonçalves, M. P. *Food Hydrocolloids* **2007**, *7*, 1046-1055.

66. Ould Eleya, M. M.; Leng, X. J.; Turgeon, S. L. *Food Hydrocolloids* **2006**, 946-951.

67. Leng, X. J.; Turgeon, S. L. *Food Hydrocolloids* **2007**, *7*, 1014-1021.

68. Bertrand, M.; Turgeon, S. L. *Food Hydrocolloids* **2007**, *2*, 159-166.

69. Spahn, G.; Baeza, R.; Santiago, L. G.; Pilosof, A. M. R. *Food Hydrocolloids* **2008**, *8*, 1504-1512.

70. Gounga, M. E.; Zu, S.; Wang, Z.; Yang, W. G. *Journal of Food Science* **2008**, *4*, E155-E161.

71. Gounga, M. E.; Xu, S.; Wang, Z. *Journal of Food Engineering* **2007**, *4*, 521-530.

72. Gounga, M. E.; Xu, S.; Wang, Z. *Journal of Food Biochemistry* **2010**, *3*, 501-519.

73. Wang, S.; van Dijk, P. A. P. P.; Odijk, T.; Smit, J. A. M. *Biomacromolecules* **2001**, 1080-1088.

74. Ganzevles, R. A.; Kosters, H.; vanVliet, T.; CohenStuart, M. A.; deJongh, H. H. J. *J. Phys. Chem. B* **2007**, *45*, 12969-12976.

75. Hayashibara **2007**, 8.

76. Lazaridou, A.; Biliaderis, C. G.; Kontogiorgos, V. *Carbohydrate Polymers* **2003**, 151-166.

77. Fundueanu, G.; Constantin, M.; Ascenzi, P. *Biomaterials* **2008**, *18*, 2767-2775.

78. Autissier, A.; Letourneur, D.; Le Visage, C. *Journal of Biomedical Materials Research Part A* **2006**, 336-342.

79. Dulong, V.; Cerf, D. L.; Picton, L.; Muller, G. *Colloids and Surfaces A: Physicochemical and Engineering Aspects* **2006**, *1-3,* 163-169.

80. Lack, S.; Dulong, V.; Le Cerf, D.; Picton, L.; Argillier, J. F.; Muller, G. *Polymer Bulletin* **2004**, 429-436.

81. Lee, I.; Akiyoshi, K. *Biomaterials* **2004**, *15,* 2911-2918.

82. Sallustio, S.; Galantini, L.; Gente, G.; Masci, G.; LaMesa, C. *J. Phys. Chem. B* **2004**, *49,* 18876-18883.

83. Shingel, K. I. *Carbohydrate Research* **2004**, *3*, 447-460.

84. Fundueanu, G.; Constantin, M.; Mihai, D.; Bortolotti, F.; Cortesi, R.; Ascenzi, P.; Menegatti, E. *Journal of Chromatography B* **2003**, 407-419.

85. Diab, T.; Biliaderis, C. G.; Gerasopoulos, D.; Sfakiotakis, E. *Journal of the Science of Food and Agriculture* **2001**, 988-1000.

86. Yang, K. S.; Lee, E. Y.; Park, M. S.; Lee, K. Y.; Lee, Y. H. *Han'guk Somyu Konghakhoechi* **1998**, *8,* 465.

87. Vandamme, E. J.; Bruggeman, G.; De Baets, S.; Vanhooren, P. T. *Agrofoodindustry hi-tech* **1996**, *5,* 21.

88. Tsujisaka, Y.; Mitsuhashi, M. Pullulan. In *Industrial Gums: Polysaccharides and their derivatives;* Whistler, R. L., BeMiller, J. N., Eds.; Academic Press, Inc.: San Diego, 1993; pp 447-460.

89. Mehvar, R. *Current Pharmaceutical Biotechnology* **2003**, 283-302.

90. Muir, M. DMSO: Many Uses, Much Controversy. *http://www.dmso.org/articles/information/muir.htm*2008).

91. Karim, M. R.; Lee, H. W.; Kim, R.; Ji, B. C.; Cho, J. W.; Son, T. W.; Oh, W.; Yeum, J. H. *Carbohydr. Polym.* **2009**, *2*, 336-342.

92. Shi, L.; Le Visage, C.; Chew, S. Y. *Journal of Biomaterials Science, Polymer Edition* **2011**, *11*, 1459-1472.

93. Autissier, A.; Letourneur, D.; Le Visage, C. *Journal of Biomedical Materials Research Part A* **2007**, *2*, 336-342.

94. Chandan, R. C. Milk Composition, Physical and Processing Characteristics. In *Manufacturing Yogurt and Fermented Milks;* Chandan, R. C., Ed.; Blackwell Publishing: Ames, IA, 2006; pp 17-39.

95. Chandan, R. C.; Shah, N. P. Functional Foods and Disease Prevention. In *Manufacturing Yogurt and Fermented Milks;* Chandan, R. C., Ed.; Blackwell Publishing: Ames, IA, 2006; pp 311-325.

96. Chatterton, D. E. W.; Smithers, G.; Roupas, P.; Brodkorb, A. *International Dairy Journal*, **2006**, *11*, 1229-1240.

97. Kinsella, J. E.; Whitehead, D. M. *Advanced Food Nutrition Research* **1989**, 343-438-343-438.

98. Haylock, S. J.; Sanderson, W. B. Milk Protein Ingredients: Their Role in Food Systems. In *Interactions of Food Proteins;* Parris, N., Barford, R., Eds.; 1991; pp 59-72.

99. Pearce, R. J. Whey Protein Recovery. In *Whey and lactose processing;* Zadow, J. G., Ed.; Elsevier Applied Science: London, 1992; pp 271.

100. Sullivan, S. T.; Khan, S. A.; Eissa, A. S. Whey proteins: functionality and foaming under acidic conditions. In *Whey Processing, Functionality and Health Benefits* Onwulata, C. I., Huth, P. J., Eds.; Wiley-Blackwell: Ames, Iowa, 2008; pp 99-132.

101. Wong, D. W. S. *Mechanism and Theory in Food Chemistry;* Avi, Van Nostrand Reinhold Eds.: New York, 1989; .

102. Sawyer, W. H. *Journal of Dairy Science* **1968**, 323-329.

103. Roefs, P. F. M.; de Kruif, C. G. *Progress in Colloid & Polymer Science* **1994**, 262-266.

104. Alting, A. C.; Hamer, R. J.; de Kruif, C. G.; de Jongh, H. H. J.; Simons, J. -. F. A.; Visschers, R. W. *Special Publication - Royal Society of Chemistry* **2003**, 49-57.

105. Gezimati, J.; Singh, H.; Creamer, L. K. *ACS Symposium Series* **1996**, 113-123.

106. Kavanagh, G. M.; Clark, A. H.; Ross-Murphy, S. B. *Rheologica Acta* **2002**, 276-284.

107. Kavanagh, G. M.; Clark, A. H.; Ross-Murphy, S. B. *Langmuir* **2000**, 9584-9594.

108. Tobitani, A.; Ross-Murphy, S. B. *Macromolecules* **1997**, 4855-4862.

109. Kavanagh, G. M.; Clark, A. H.; Ross-Murphy, S. B. *International Journal of Biological Macromolecules* **2000**, 41-50.

110. Linden, G.; Lorient, D. *New ingredients in food processing;* CRC Press: Boca Raton, 1999; .

111. Lupano, C. E. *Journal of Dairy Science* **1994**, 2191-2198.

112. Stading, M.; Langton, M.; Hermansson, A. -. *Journal of Rheolgy* **1995**, 1445-1450.

113. Eissa, A. S.; Puhl, C.; F.Kadla, J.; Khan, S. A. *Biomacromolecules* **2006**, *6*, 1707-1713.

114. Eissa, A. S.; Khan, S. A. *Food Hydrocolloids* **2006**, *4*, 543-547.

115. Hayashibara **2008**.

116. Yang, K. S.; Lee, E. Y.; Park, M. S.; Lee, K. Y.; Lee, Y. H. *Han'guk Somyu Konghakhoechi* **1998**, *8*, 465-471.

117. McNeil, B.; Harvey, L. M. *Critical Reviews in Biotechnology* **1993**, *4*, 275-304.

118. Ding, P.; Pacek, A. W.; Frith, W. J.; Norton, I. T.; Wolf, B. *Food Hydrocolloids* **2005**, 567-574.

119. Tayal, A.; Kelly, R. M.; Khan, S. A. *Macromolecules* **1999**, 294-300.

120. Kasaai, M. R. *Journal of Applied Polymer Science* **2005**, 4325-4332.

121. Lazaridou, A.; Roukas, T.; Biliaderis, C. G.; Vaikousi, H. *Enzyme and Microbial Technology* **2002**, 122-132.

122. Roukas, T.; Mantzouridou, F. *Journal of Chemical Technology and Biotechnology* **2001**, 371-376.

123. Roukas, T. *Journal of Industrial Microbiology & Biotechnology* **1999**, 617-621.

124. Gaidhani, H. K.; McNeil, B.; Ni, X. *Journal of Chemical Technology and Biotechnology* **2003**, 260-264.

125. Madi, N. S.; McNeil, B.; Harvey, L. M. *Journal of Chemical Technology and Biotechnology* **1996**, 343-350.

126. Goksungur, Y.; Dagbagli, S.; Ucan, A.; Guvenc, U. *Journal of Chemical Technology and Biotechnology* **2005**, 819-827.

127. West, T. P. *Journal of Basic Microbiology* **2000**, *5-6*, 397-401.

128. Li, G.; Qiu, H.; Zheng, Z.; Cai, Z.; Yang, S. *Journal of Chemical Technology and Biotechnology* **1995**, 385-391.

129. Spyropoulos, F.; Frith, W. J.; Norton, I. T.; Wolf, B.; Pacek, A. W. *Journal of Rheology* **2007**, *5*, 867-881.

130. Spyropoulos, F.; Frith, W. J.; Norton, I. T.; Wolf, B.; Pacek, A. W. *Food Hydrocolloids* **2008**, *1*, 121-129.

131. Matsumura, Y.; Satake, C.; Egami, M.; Mori, T. *Bioscience, biotechnology, and biochemistry* **2000**, *9*, 1827-1835.

132. Syrbe, A.; Fernandes, P. B.; Dannenberg, F.; Bauer, W.; Klostermeyer, H. Whey Protein + Polysaccharide Mixtures: Polymer Incompatibility and Its Application. In *Food Macromolecules and Colloids;* Dickinson, E., Lorient, D., Eds.; The Royal Society of Chemistry: Cambridge, 1995; pp 328-339.

133. Pogaku, R.; Seng, C. E.; Boonbeng, L.; Kallu, U. R. *International Journal of Food Engineering* **2007**, *6*, 1-28.

134. Çakıra, E.; Vinyardb, C. J.; Essick, G.; Daubert, C. R.; Drakea, M.; Foegeding, E. A. *Food Hydrocolloids* **2011**.

135. McKee, M. G.; Wilkes, G. L.; Colby, R. H.; Long, T. E. *Macromolecules* **2004**, *5*, 1760-1767.

136. Talwar, S.; Hinestroza, J.; Pourdeyhimi, B.; Khan, S. A. *Macromolecules* **2008**, *12*, 4275-4283.

137. Yarin, A. L.; Koombhongse, S.; Reneker, D. H. *Journal of Applied Physics* **2001**, *9*, 4836-4846.

138. Reneker, D. H.; Yarin, A. L.; Fong, H.; Koombhongse, S. *Journal of Applied Physics* **2000**, *9 Pt. 1*, 4531-4547.

139. Hemar, Y.; Pinder, D. N. *Biomacromolecules* **2006**, *3*, 674-676.

140. Davis, M. E.; Brewster, M. E. *Nature Reviews: Drug Discovery* **2004**, *December*, 1023-1035.

141. Woerdeman, D. L.; Ye, P.; Shenoy, S.; Parnas, R. S.; Wnek, G. E.; Trofimova, O. *Biomacromolecules* **2005**, 707-712.

142. Min, B.; Lee, G.; Kim, S. H.; Nam, Y. S.; Lee, T. S.; Park, W. H. *Biomaterials*, **2004**, *7-8*, 1289-1297.

143. Stephens, J. S.; Fahnestock, S. R.; Farmer, R. S.; Kiick, K. L.; Chase, D. B.; Rabolt, J. F. *Biomacromolecules* **2005**, 1405-1413.

144. Buchko, C. J.; Chen, L. C.; Shen, Y.; Martin, D. C. *Polymer*, **1999**, *26*, 7397-7407.

145. Wnek, G. E.; Carr, M. E.; Simpson, D. G.; Bowlin, G. L. *Nano Letters* **2003**, *2*, 213-216.

146. Yang, L.; Fitie, C. F. C.; van der Werf, Kees O.; Bennink, M. L.; Dijkstra, P. J.; Feijen, J. *Biomaterials* **2008**, 955-962.

147. Li, M.; Mondrinos, M. J.; Gandhi, M. R.; Ko, F. K.; Weiss, A. S.; Lelkes, P. I. *Biomaterials* **2005**, 5999-6008.

148. Zoccola, M.; Montarsolo, A.; Aluigi, A.; Varesano, A.; Vineis, C.; Tonin, C. *e-Polymers* **2007**, *105*, 1-19.

149. Miyoshi, T.; Toyohara, K.; Minematsu, H. *Polymer International* **2005**, 1187-1190.

150. Minato, K.; Ohkawa, K.; Yamamoto, H. *Macromolecular Bioscience* **2006**, 487-495.

151. Huang, L.; McMillan, R. A.; Apkarian, R. P.; Pourdeyhimi, B.; Conticello, V. P.; Chaikof, E. L. *Macromolecules* **2000**, 2989-2997.

152. Nagapudi, K.; Brinkman, W. T.; Thomas, B. S.; Park, J. O.; Srinivasarao, M.; Wright, E.; Conticello, V. P.; Chaikof, E. L. *Biomaterials*, **2005**, *23*, 4695-4706.

153. Zeng, J.; Aigner, A.; Czubayko, F.; Kissel, T.; Wendorff, J. H.; Greiner, A. *Biomacromolecules* **2005**, 1484-1488.

154. Jiang, H.; Hu, Y.; Li, Y.; Zhao, P.; Zhu, K.; Chen, W. *Journal of Controlled Release*, **2005**, *2-3*, 237-243.

155. Barnes, C. P.; Smith, M. J.; Bowlin, G. L.; Sell, S. A.; Tang, T.; Matthews, J. A.; Simpson, D. G.; Nimitz, J. C. *Journal of Engineered Fibers and Fabrics* **2006**, *2*, 16-29.

156. Jensen, R. G. *Handbook of Milk Composition;* Academic: San Diego, 1995; , pp 919.

157. Alizadeh-Pasdar, N.; Nakai, S.; Li-Chan, E. C. Y. *J. Agric. Food Chem.* **2002**, 6042-6042-6052.

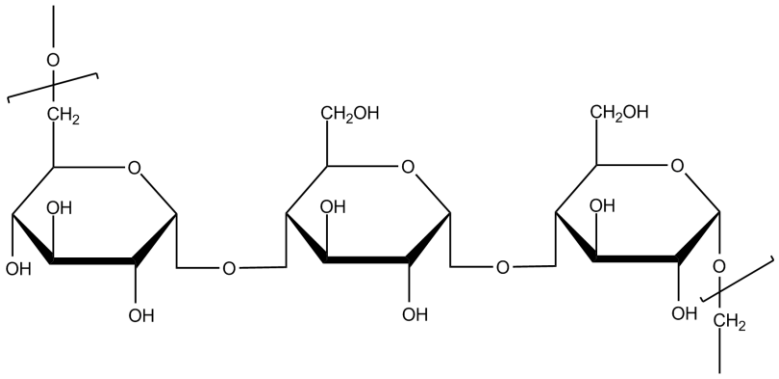

Figure 1.1. Molecular structure of pullulan.

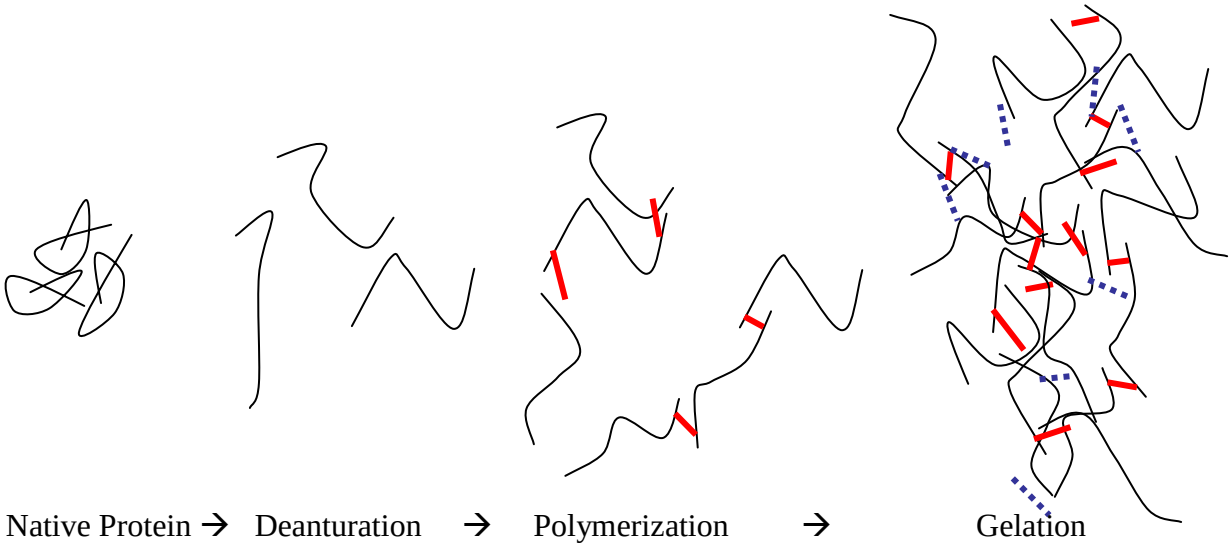

Figure 1.2. Schematic representation of gelation of globular proteins. Solid short connections refer to chemical bonding (disulphide), while dotted connections refer to physical interactions (hydrogen bonding, hydrophobic interactions and electrostatic interactions). (Khan Laboratory)

Table 1.1. Solution electrospun proteins.

Protein	Spinnable polymer in solution	Solvent	Analytical Techniques	Applications	Ref
Casein	PVA or PEO in water	aqueous triethanolamine	DSC, TGA, SEM	immobilize or encapsulate enzyme	[84]
wheat gluten	native, denatured, and with PVOH	1, 1, 1, 3, 3, 3 Hexafluoro-2-propanol	FESEM, OM, SEM (a); EDS, DSC, EDS	tissue scaffolds, hemostatic products	[15]
Silk fibroin		formic acid	SEM, porosimeter, post-fiber formation added cells	normal human keratinocytes and fibroblast cell culture	[17, 141]
Bombyx mori silk fibroin	PEO (900,000 g/mol)	aqueous silk solution in 1, 1, 1, 3, 3, 3 Hexafluoro-2-propanol	SEM, FTIR (ATR), XPS	high performance filters and scaffolds	[142]
spider silk analogue		1, 1, 1, 3, 3, 3 Hexafluoro-2-propanol	FT-Raman, FESEM, CD	tissue engineering, sutures, wound dressing, protective apparel	[21]
silk-like polymer with fibronectin functionality		formic acid	SEM, SPM, TEM, OM, WAXS	prosthetic device for central nervous system implant	[143]
human & bovine fibrinogen		1, 1, 1, 3, 3, 3 Hexafluoro-2-propanol + minimal essential medium	SEM, TEM,	tissue scaffolds	[144]
collagen	with & without x-link with glutaraldhyde vapor	1, 1, 1, 3, 3, 3 Hexafluoro-2-propanol	CD, SEM, AFM	tissue scaffolds	[145]
collagen gelatin (denatured collagen) solubilized α-elastin recombinant human tropoelastin		1, 1, 1, 3, 3, 3 Hexafluoro-2-propanol	SEM, AFM, microtensile test, fluorescent microscopy	tissue engineering matrices	[146]
keratin	polyamide 6	formic acid	SEM, steady shear rheometry, FTIR, DSC, polarizing light microscopy	biomedical applications, active water filtration, biodegradable plastics, textile fibers, etc.	[147]

Table 1.1. Solution electrospun proteins (continued).

Protein	Spinnable polymer in solution	Solvent	Analytical Techniques	Applications	Ref
soluble eggshell membrane protein	PEO (900,000 g/mol)	0.2% aqueous NaOH	SEM, diffractometer, DSC, XRD	heavy metal adsorption, burn dressings, cell culture substrates, enzyme immobilization platforms	[148]
egg albumen	PEO (MW 300kDa)	aqueous formic acid	steady shear rheometry, tensiometry, conductivity, TGA, DSC, FTIR, SEM	biodegradable packaging materials	[20]
zein		80 wt% ethanol	SEM	renewable, biodegradable packaging	[19]
poly (γ -benzyl-L-glutamate)		Triethylamine & dichloromethane	CD, SEM, WAXD, FTIR (ATR)	non-woven fibers	[149]
elastin mimetic peptide polymers		deionized water	TEM, FESEM, tensile testing	artificial blood vessel	[150]
elastin-mimetic protein triblock copolymers		deionized water, TFE	SEM, rheometry, uniaxial tensile strength	control midblock structure for tuning material properties	[151]
bovine serum albumin	Poly(vinyl) alcohol	water	SEM, UVVis, IR	protein delivery system	[152]
luciferase	Poly(vinyl) alcohol	PBS water	SEM, UVVis	control enzyme release	
bovine serum albumin	PEG in water, electrospun coaxially with PCL in DMF/chloroform	double distilled water	NMR, SEM, TEM, CD, SDS-PAGE, BCA assay, enzymatic analysis	scaffolds for tissue engineering, drug delivery, gene therapy	[153]
lysozyme					
hemoglobin		2, 2, 2, -trifluoroethanol	SEM, uniaxial tensile testing	optimal wound healing device	[154]
myoglobin					
oligopeptide (Ser-Glu-Glu)$_3$ - PEO	PEO	deionized water	SEM, XPS, AFM	multifunctional textiles & bioactive tissue scaffolds	[155]

Table 1.2. Whey protein properties.

Whey protein	Concentration in milk (g/l) *	No. of Amino Acid Residues **	Approx. MW (kDa)**	Isoelectric Point** (pH)
β-lactoglobulin (BLG)	**3.2**	**162**	**18**	**5.2**
α-lactalbumin (ALA)	**1.2**	**123**	**14**	**5.1**
Serum albumin	0.4	582	69	4.8
Immunoglobulin	0.8	-	150-1,000	4.6-6.0
Protease-peptones	1.0	-	4-40	3.7

* [9]

** [156]

Table 1.3. Functional Properties of Whey Proteins.[94]

Functionality	Properties of Whey Proteins
Water binding	Water binding capacity increase with denaturation of protein
Solubility	Soluble at all pH levels. If denatured, insoluble at pH 5.
Viscosity	Low for native protein; higher if denatured
Gelation	Heat gelation at 70 C or higher and influenced by pH and salts
Emulsification	Good except at pH 4-5, if heat denatured
Foaming	Good foam/overrun. β-lactoglobulin better than α-lactalbumin
Flavor Binding	Retention varies with degree of denaturation

Table 1.4 β–lactoglobulin (BLG) characteristics with pH [94]

BLG characteristics with pH	pH
Solubility limits	2-10
Monomer structure with 2 disulfide bonds	< 3.5 >8.0
Conformational changes and molecule expansion	7.5
Increase in reactivity of thiol group	> 7.0
Dissociation of the dimer	> 7.0

Table 1.5 Destiny of pullulan in human consumption[157]

Human GI system	Impact on pullulan	by
Upper gastrointestinal tract	Partially hydrolyzed	Salivary & other enzymes
Distal intestinal tract	1. Further hydrolyzes 2. Ferments hydrolysis products to short chain fatty acids	Bacteria
Colon	1. Completely hydrolyzes 2. Ferments hydrolysis products	Bacteria

Table 1.6 Studies that included rheological evaluation of pullulan solutions.

Study	Solutions	Results	Method
Matsumura et al., 2000 [1]	18 w/w% pullulan in phosphate buffer	Viscoelastic behavior G″>G′ → molecules not entangled at this concentration	Dynamic oscillatory rheometry
Lazaridou et al., 2003 [131]	0.4-12 w/v% aqueous pullulan of different mass fractions	Determined: • intrinsic viscosity [η] → low for all solutions • critical concentration c* = c where random coils begin to entangle (by transition of the zero shear specific viscosity vs. concentration plots from a lower to higher slope value) • coil overlap parameters (c*[η]) = total volume occupied by coils in polymer solution regardless of MW	Capillary viscometry & steady shear rheometry
Ding et al., 2005 [76]	Gelatin/pullulan mixtures (phase separated mixtures used for zero/low fat food product manufacture)	Pullulan-rich phases were non-Newtonian only at high shear rates G′ = G″ criteria determined gelling & melting temperatures	Rheometry, parallel plates 1.5 mm gap
Spyropoulos et al. [118]	Aqueous Pullulan/SDS and salt (texture enhancement in food and home/personal care industries)	Viscosity • increased with SDS addition • decreased with salt addition Explanation 1. Pullulan is being “salted out” 2. Changes in biopolymer molecular structure in presence of salt	microscope-video computer system and Couette device, which showed that mixture morphology/ microstructure and rheology

Table 1.7. Molecular characteristics of commercial Hayashibara pullulan[129, 130]

	Hayashibara pullulan	Other Pullulan fractions	
Mw (kDa) #	361	12-564	
Mn (kDa) #	150	9-297	
Rg (nm) #	32	16-32	
Mw/Mn polydispersity index #	2.4	1.3-2.3	
			Other polysaccharides
[η] (dl/g)	0.56	0.38-0.70	0.37-35
c* (g/dl)	1.8	1.4-3.1	Wheat arabinoxylan 0.26-3.8
c*[η]	1.0	1.0-1.2	Guar 1.0 Locust bean gum 1.3 Dextran 0.8-2.2 λ-carrageenan 4.0

determined by HPSEC with multiangle laser light scattering and differential refractive index detectors

Table 1.8. Whey protein-polysaccharide gelled systems analyzed using rheometry.

Polysaccharides	Solvent/conditions	Rheology	Geometry
Locust bean gum (LBG) [76] (neutral) (purified by ethanol precipitation)	Ultrapure water (with WPI BiPRO) pH 5.0 & 7.0	Dynamic measurements at low strain Controlled stress rheometer	Cone-plate (isothermal) Parallel plate (non-isothermal – gel formation)
Propyleneglycol alginate (PGA) [61, 63]	Double filtered distilled water pH 7	Dynamic measurements at low strain Controlled stress rheometer	Parallel plate
Locust bean gum[64] (neutral) (purified by ethanol precipitation)	Ultrapure water (with WPI BiPRO) Modified LBG with enzyme	Dynamic measurements - small deformation Controlled stress rheometer	Cone-plate (isothermal) "Roughish" Parallel plate (non-isothermal – gel formation)
Guar LBG Tara gum[63]	Ultrapure water (with WPI BiPRO) Guar - some samples enzymatically treated Confocal with Rh-B	Dynamic measurements at low strain Temp sweeps Controlled stress rheometer	Wrinkled Parallel plate
Tara gum[62]	Aqueous BLG Varied pH – 7 and 4.6 Confocal with RITC	Controlled stress rheometer	Rough acrylic plate
κ-carrageenan[65]	Aqueous BLG pH 5 Confocal with Fast Green fluorochrome	Small deformation oscillatory Controlled strain rheometer	Couette

Table 1.8. Whey protein-polysaccharide gelled systems analyzed using rheometry (continued).

Polysaccharides	Solvent/conditions	Rheology	Geometry
κ-carrageenan pectin[66]	Aqueous WPI Varied concentration of each (separately) in aqueous WPI	Controlled strain rheometer Varied pre-shear and shear Analyzed with modified Carreau and Carreau models	Parallel plate
Xanthan gum[67]	Aqueous WPI pH 6.5, 6.0, 5.5 added salt Confocal with Fast Green fluorochrome	Controlled strain rheometer Small deformation oscillatory measurements	Plate-plate
λ-carrageenan[68]	Aqueous whey protein concentrate (WPC) Compared mixtures and spray-dried mixtures	Controlled stress rheometer Dynamic measurements at low strain	Parallel-plate

CHAPTER 2 Solution Electrospinning Whey Protein

Chapter 2 is essentially a manuscript by Stephanie T. Sullivan, Christina Tang, Anthony Kennedy, Sachin Talwar, and Saad A. Khan to be submitted to *Biomacromolecules.*

Solution Electrospinning Whey Protein

Stephanie T. Sullivan, Christina Tang, Anthony Kennedy ǂ, Sachin Talwar, and Saad A. Khan*

Department of Chemical and Biomolecular Engineering, North Carolina State University, Raleigh, NC 27695-7905,
ǂDepartment of Chemistry, East Carolina University, Greenville, NC 27858

ABSTRACT

We report the fabrication of a variety of whey protein (WP) nanostructures ranging from nanoparticles to nanofibers via solution electrospinning, which may be particularly well suited for flavor delivery. Aqueous whey protein solutions, both whey protein isolate (WPI) and one of its major components β–lactoglobulin (BLG), either in native or denatured form yielded interesting micro and nanostructures; while nanofiber production required blending with a spinnable polymer, poly(ethylene oxide) (PEO). WP:PEO solution composition was as high as 3:1 and average fiber diameters ranged from 312 to 690 nm depending on polymer composition and concentration. WP:PEO solutions are also successfully electrospun at acidic pH ($2 \leq pH \leq 3$), which could improve shelf life. FTIR analysis of WP:PEO fiber mat indicates some variation in WP secondary structure with varying WPI concentration (as WPI increased, % α-helix increased and β-turn decreased) and pH (as pH decreased from neutral (7.5) to acidic (2), % β-sheet decreased and α-helix increased). XPS also confirms the presence of WP on the surface of the blend fibers, augmenting the FTIR analysis. Interestingly, WP:PEO composite nanofibers maintain its fibrous morphology at temperatures as high as 100 ^{o}C, above the 60 ^{o}C PEO melting point. Further, we show that

the blend mats retained a fibrous structure after the heat treatment. In addition, the mats swell in water and retain a fibrous quality which makes them ideal for tissue scaffolding. Finally, we incorporated a small hydrophobic molecule (RhB) as a model flavenoid into WP:PEO nanofiber mats. The BLG:PEO nanofibers qualitatively exhibit improved fiber quality and RhB distribution compared to PEO nanofibers; however, no effect on the release profile was observed.

2.1 Introduction

Whey proteins, one of two milk protein groups along with the caseins, have been found to be a valuable dietary supplement and a functional food enhancer. Whey proteins are used in food design due to the variety of functionalities including: binding of water and flavor, gelation, emulsification and foaming.[(1),(2)] Furthermore, whey proteins are being evaluated and recognized for their antimicrobial, antiviral, and anticarcinogenic effects.[(3)-(5)] The predominant whey proteins, β-lactoglobulin (BLG) and α-lactalbumin (ALA), are globular proteins with an isoelectric point of approximately 5.2 and 4.3, respectively.[(6)] The most abundant bovine milk protein, native BLG has 162 amino acid residues, eight anti-parallel □-sheets, one □-helix chain and a molecular weight of 18 kDa [(7)]; while ALA has 123 amino acid residues, a secondary structure consisting of α-helix (~31%), 3_{10}-helix (~21%) and a small contribution of β-strands (~6%) [(8)], and a molecular weight of 14 kDa.[(6)]

A significant fraction of whey protein research has focused on gelation and gel characteristics [(6)-(30)] because these gels can provide food products with unique functional performance and favorable textural properties. Recently, structures made from milk proteins

such as whey, have been recognized as an important tool in vehicles for the delivery of bioactives and pharmaceuticals.[31]-[33] Nanofibers, in particular, are considered promising for drug delivery due to high specific surface area leading to efficient drug release[34],[35],[36] and industry has patented.[37] Nanofiber structures of whey protein may be especially well suited for such applications.

Electrospinning is a simple process used to produce nanofibers, in some cases smaller than 100nm in diameter.[38] Equipment for two electrospinning methods, melt and solution electrospinning, have been thoroughly discussed in the literature.[38] Solution electrospinning utilizes polymer dissolved in solvent that is pumped at a controlled flow rate from a syringe to which a high voltage is applied. Electrostatic forces between the positively charged syringe needle and a grounded collector plate pull solution away from the syringe tip into a Taylor cone formation and to the collector. As the solution is pulled away from the syringe, the solvent evaporates, leaving the polymer drawn into fibers and collected as a fiber mat.[39]-[47] Solution properties including viscosity, conductivity, and surface tension as well as process parameters such as solution flow rate, tip to collector distance and applied voltage all affect the electrospinning process. Solution electrospinning allows for encapsulation of insoluble particles within a nanofiber mat, and the incorporation of soluble drugs in a uniform fashion.[38] Nanofiber systems also can serve as wound healing dressings [48] or as a scaffold for tissue engineering.[49],[50] Other nanofiber designs include modifying the nanofiber surface with nanoparticles,[44] bioactive peptides and proteins[51],[52] and immobilizing enzymes.[45] Most recently, electrospun biomaterial nanofibers have been

highlighted as a novel tool for food industry applications such as nutraceutical and flavor release.[53]

Some milk proteins have been utilized in solution electrospinning. Bovine serum albumin, for example, has been successfully electrospun both with[54]-[56] and without[57] the use of a carrier polymer; while caseins yielded successful nanofibers only when blended with spinnable polymer.[58] Nanofibers have also been obtained from other proteins including silk fibroin,[46],[59],[60] zein,[61] keratin,[62] collagen,[63],[64] fibrinogens,[65] egg protein,[66],[67] and wheat protein.[68],[69] However, neither of the two primary whey proteins BLG and ALA nor a commonly utilized combination of the two - whey protein isolate (WPI) have been electrospun into nanofibers.

In this study, we address critical issues such as whether whey proteins can be electrospun into nanofibers in their native, chemically or heat denatured forms; or must they, similar to the caseins, be solution electrospun with the help of a spinnable polymer in solution.[58] Thus, the first goal is to electrospin aqueous whey protein solutions. The globular nature of whey proteins such as BLG and ALA, the low viscosity of their aqueous solutions, and potential lack of molecular entanglement makes producing nanofibers challenging.[69],[70] The addition of spinnable polymer may be required, as was executed with other proteins such as egg proteins.[66],[67] We also explore the effect of solution pH on electrospinning, as it influences whey protein solution behavior.[6] Further, changing the pH of the solution expands the ability to incorporate drugs or flavenoids. Electrospinning aqueous whey protein solutions at acidic pH would facilitate formulation flexibility and improved shelf life.[71] In order to improve the stability of the fibers, we examine covalent

crosslinking by heat treatment as whey protein can be heat denatured[72] at approximately 70°C when it forms disulfide bonds between neighboring chains. Finally, we incorporate and monitor the release of a fluorescent dye as a model hydrophobic molecule.

2.2 Materials & Methods

2.2.1 Solution Preparation

BiPRO Whey Protein Isolate (WPI) and BIOPURE β-lactoglobulin (BLG) were both obtained from Davisco Foods Inc. (Eden Prairie, MN) and used as received (98% protein). Some BIOPURE BLG was purified[73] and verified with NuPAGE. Poly(ethylene oxide) (PEO) Polyox WSR205 (MW 600kDa, Polydispersity Index 12,[74] was obtained from The Dow Chemical Company (Midland, MI) and was used as received. Hydrochloric acid, ethanol, urea and Rhodamine B were used as received from Sigma. WPI, BLG, and PEO were dissolved in deionized water (DW) and stirred for a minimum of 3 hours to ensure complete dissolution. Solution pH and conductivity were measured with a Fisher Scientific Accumet AB15 pH meter and Accumet AB30 conductivity meter, respectively. The viscosities of pertinent samples were measured at 25°C in a TA Instruments AR-2000 stress controlled rheometer using a cone and plate geometry.

2.2.2 Solution Electrospinning

The electrospinning apparatus, described previously [44] included a precision syringe pump (Harvard Apparatus, Holliston, MA) operated at flow rate of 0.1-2.0 mL/hour, and a high-voltage power supply (Gamma High Voltage Research, model D-ES30 PN/M692 with a

positive polarity between 0 and 30 kV) Electrospinning solutions were loaded in a 10 ml syringe to which a stainless steel capillary metal-hub needle (22 gauge) was attached. The positive electrode of the high voltage was connected to the needle tip. The grounded electrode was connected to an aluminum foil-covered metallic collector.[75] The tip-to-collector distance varied from 12 – 17 cm.

2.2.3 Morphology & Surface Analysis

Specimens from solution electrospinning efforts were mounted on stubs; sputter coated with ~ 15-40 nm layer of gold and examined using scanning electron microscopy (SEM, FEI Quanta 200 Environmental Scanning Electron Microscope). Fiber size distributions were obtained by measuring a minimum of 100 fibers using Image J software (NIH). A Riber X-ray Photoelectron Spectrometer (XPS) operated at 12kV with a 1mm spot size was used for nanofiber mat surface analysis. Differential scanning calorimetry (DSC) was utilized to analyze fiber mat thermal properties (model DSCQ200, TA Instruments, New Castle, DE) at a heating rate of 10 °C/minute under inert Argon gas.

The infrared spectra of nanofiber mats were recorded at room temperature using a Nicolet Magna-IR 750 spectrometer (Madison, WI). Dry air was continuously run through the spectrometer. The infrared spectra were recorded at 2 cm^{-1} resolution. A total of 128 transmission scans were recorded, averaged, and apodized with the Happ-Genzel function. Additional Infrared spectra were obtained on a Nicolet 6700 FTIR (Thermo Scientific, Madison WI) equipped with a DTGS detector and continually purged with dry air. Samples were analyzed directly on a single bounce diamond ATR (45°) by acquiring 128 scans at

$4cm^{-1}$ resolution at ambient temperature. Spectra were corrected for water vapor and then ATR corrected using the advanced ATR correction routine (Omnic 8.0) prior to secondary structure analysis. Secondary structure analysis was performed by using a curve resolution technique and determining the areas of the individual components. Band positions were confirmed with Fourier self deconvolution and also by obtaining second derivative spectra.

Confocal laser scanning microscopy (CLSM) fluorescent images were taken with a FV 300 scanner of the Olympus BX-61 system, equipped with high-resolution DP70 digital charge coupled device (CCD) camera (Olympus America Inc.) with objective magnifications ranging from 4× to 50×. Two and three dimensional LSM nanofiber images were taken with the Olympus LEXT OLS4000 confocal laser scanning microscope metrology system. Reflected light microscope images were taken with an Olympus BX-51 microscope system with objective magnifications ranging from 10× to 100×. Release studies were conducted directly in deionized water-filled cuvets. Readings were taken every two minutes using a Perkin Elmer Lambda 45 Spectrometer at 543 nm (Waltham, MA).

2.3 Results and Discussion

2.3.1 Electrospinning aqueous whey protein solutions

We began by electrospinning aqueous whey protein solutions at various concentrations. Electrospinning of native WPI and BLG at concentrations up to 35 w/w% resulted in microparticles. WP concentrations above 35 w/w% yielded viscous nonhomogeneous solutions that could not be elecrospun. Figure 2.1(a) shows a representative micrograph of WPI sample.

We were not able to produce whey protein fiber by electrospinning, possibly due to a lack of molecular engtanglement; however, denatured proteins may be more likely to entangle than when in their native, globular state as has been previously reported with BSA denatured with β-mercaptoethanol (BME). We also attempted to electrospin chemically denatured whey protein, but avoiding the use of BME due to its high toxicity. Whey protein in 8M urea (Figure 2.1(b)), in 5M ethanol and 20 mM hydrochloric acid (HCl) (Figure 2.1(c)), or in deionized water (pH 8) and ethanol (5:1 by volume) (Figure 2.1(d)), identified means of unfolding whey proteins, were electrospun and yielded interesting micro and nanoparticles. For example, in the case of urea, which at the concentration used indirectly affects the protein structure by interacting and perturbing water [(76),(77)] particles with crystal-like structure were produced. When dissolved in the mixture of water (pH 8) and ethanol (5:1 v:v ratio) and electrospun, it formed a nanoparticle film, evenly coating the collector with a white nanoparticle layer. As an alternative to chemically denaturing proteins, we also explored heat treatment. Whey protein solutions at concentrations low enough to avoid gelation (less than 11 w/w%) were heat treated and electrospun. Depending on concentration, these results either yielded microstructures or simply liquid buildup on the collector (results not shown). These results suggest that denaturing WPI or BLG via chemical means or heat treatment does not provide sufficient molecular entanglement required for fiber formation during electrospinning, possibly due to their relatively low molecular weights compared to BSA. Figure 2.1(e) shows viscosity of aqueous whey protein solutions of both BiPRO and BetaLAC material. Electrospinning these solutions did not yield fibers.

2.3.2 Electrospinning WP:PEO blends

We hypothesize that whey proteins in their native or denatured state do not have sufficient entanglement to electrospin, so in the next set of experiments we blend them with a water soluble, electrospinnable polymer, polyethylene oxide (PEO), to determine if that can facilitate fiber formation as has been previously reported.[56],[58] As shown in Figure 2.2, these WPI:PEO blends successfully yielded nanofiber mats, and a maximum of 75 w/w% whey protein was achieved. Interestingly, at 4 w/w% PEO produces beaded fibers (Figure 2.2(a)), but the addition of the WPI (maintaining 4 w/w% PEO) leads to uniform bead-free fibers. As expected, the fiber diameter increases as the total polymer (protein and PEO) concentration increases, but the process parameters also play a role in uniformity. For example, WPI:PEO 50:50 and 60:40 mats are very close in mean diameter. Both were electrospun with a 15 cm tip-to-collector distance, 1 ml/hr flow rate and 22 gauge 2 inch needle, but the 60:40 utilized a higher voltage (10 kV vs. 9 kV). The stronger electrostatic force of the higher 10 kV could explain the slightly smaller fibers achieved at a higher concentration. However, the 50:50 WPI:PEO fiber mats had a mean fiber diameter of 321 ± 56 nm with the lowest standard deviation, thus the most uniform fibers produced. This result agrees with qualitative assessment that the fibers were less uniform both above and below the 8 total w/w%. Fibers with the highest WPI concentration are somewhat less uniform in diameter and even "wavy" in appearance, with a higher mean diameter and standard deviation (668 ± 135 nm) with some minor fiber breakage present (Figure 2.2(e)).

We also electrospun blends of BLG and PEO holding the total weight of polymer in solution constant (10 w/w%) (Figure 2.3). At various blend ratios, the nanofibers appeared

to be consistent with respect to total polymer weight, with mean diameters ranging from 381 – 466 nm. Comparing the 75:25 BLG/PEO blend with the WPI:PEO blend, total polymer concentration of 10 and 5.5 w/w%, respectively, the BLG/PEO blend fibers did not appear to have issues of "waviness" or breakage. This could be due to the increased total polymer concentration or solution homogeneity with BLG in lieu of the mixture of proteins in the WPI formulation.

2.3.3 Effect of pH on whey protein/PEO electrospinning

The use of whey proteins at acidic pH is often desirable for reduced bacterial growth and increased product shelf life;[69] therefore, we electrospun acidic whey protein/PEO solutions. However, previous results indicate that pH of the solution affects the electrospinning process due to changes in solution conductivity.[78, 79] For example, Son et al. [79] investigated the effect of pH variation (from 2 to 12) on polyvinyl alcohol electrospinning. Beaded nanofibers were obtained under acidic conditions whereas finer, defect-free fibers resulted from basic solutions. Further, pH also affects the structure and net charge of proteins. For example, whey proteins are known to extensively aggregate at pH near their isoelectric points. Changes in pH of the electrospinning solution are expected to affect fiber morphology as previously reported with zein, and the effect of pH on protein electrospinning is likely protein dependant.[80,81] In our case, we examine electrospinning whey protein and PEO at acidic pH no lower than 2.0 to avoid polymer degradation.[78]

The desirable attributes of electrospinning whey protein PEO blends at pH 2 led us to examine the effect of blend composition on nanofiber characteristics at low pHs using WPI and a total polymer concentration of 5.5 w/w%. Figure 2.4 shows SEMs of each electrospun

fiber mat (Figure 2.4 (a) – (d)) and provides information on the precursor solution concentrations, pH, zero shear viscosity and mean nanofiber diameter (Figure 2.4(e)). Several features are apparent from the data. First, we find all four solutions of PEO:WPI ratios ranging between 50:50 to 80:20 produced bead-free nanofibers. Secondly, these nanofibers exhibit similar diameters between 262 to 312 nm even though the viscosity changes greatly (by a factor of seven). In the case of the low pH studies shown in Figure 2.4, addition of WPI to PEO increased conductivity of the sample from ~0.1 mS/cm for a PEO solution to 1.5 mS/cm for the 80:20 sample, but decreases with increasing PEO concentration, changing from 1.5 mS/cm for the 80:20 sample to 3.4 mS/cm for the 50:50 sample. These results suggest that fiber diameter is not being solely dictated by polymer concentration or viscosity. The slight differences in mean nanofiber diameter may be due to the variation in electrospinning applied voltage (the applied voltage for the 66:34 solution was 9.5 kV whereas that for the 80:20 solution was 11.0 kV) or due to the globular nature of the protein. Previous work by Son et al.[82] revealed that addition of a polyelectrolyte to PEO decreased fiber diameter to a constant value, with a concomitant increase in conductivity. However, further addition of polyelectrolyte did not change the fiber diameter but increased conductivity monotonically. We believe our results are consistent with this scenario.

We also studied the effect of pH on BLG/PEO blends. Solutions of 50:50 BLG and PEO were prepared at total 7 w/w% for pH of 7.5 (native solution pH), 5.2 (isoelectric point of BLG), 4.0 (near isoelectric point of ALA and other whey proteins in WPI), and acidic 2.0. Solutions at pH 7.5 and 2.0 were transparent and yellow in color; whereas solutions at pH 5.2 and 4.0 were milky white, indicating protein aggregation as expected. Conductivity of the

solutions increased with decreasing pH (Figure 2.5(g)), as expected, since BLG becomes more positively charged as the solution pH changes from 7.5 to 2.0. Solution viscosity was also affected by pH Figure 2.5(e); it was lowest for pH 2.0 solution, likely due to the BLG being in a monomer state compared to the other three solutions. Also, pH 5.2 solution viscosities are slightly higher than other solutions, likely due to the impact of the BLG aggregation at its isoelectric point.

At pH 7.5 and 2.0, uniform fibers are produced (Figure 2.5(a) and (Figure 2.5(d), respectively). When the average fiber diameter at pH 7.5 and 2.0 are compared (453 nm to 391 nm, respectively), the trend of decreasing fiber diameter with increasing solution conductivity agrees with that found in the literature.[10] However, the pH 5.2 (Figure 2.5(b)) and 4.0 (Figure 2.5(c)) fibers both contain bead defects (~1 μm in diameter), possibly due to whey protein agglomeration in the solution. Viscosity does not appear to play a strong role in fiber quality in this case compared to the influence of protein aggregation and/or structural state.

2.3.4 WPI:PEO blend fiber analysis

FTIR analysis of the PEO and WPI:PEO blend fiber mats were conducted to confirm that both the PEO and WPI are present in the blend fiber mats as well as obtain information regarding the structure of the protein in the fiber. Spectra for all of the sample compositions shown in Figure 2.2(a)-(e) were collected and were similar. One blend fiber mat spectra is shown in Figure 2.6(a) for comparison to raw materials. Spectra for the WPI:PEO blend fiber mats show broad new bands at approximately 3280 cm^{-1}, 1650 cm^{-1}, and 1530 cm^{-1} compared to the PEO fiber and PEO powder spectrum. The 3280 cm^{-1} peak may represent

NH stretching intensity that increases with molecular weight, while the 1650 cm^{-1} band, which is found in proteins, is assigned to the Amide I band. This combination band arises due to C=O stretching vibrations coupled to N-H and C-N vibrations. The band that appears at approximately 1530 cm^{-1} is assigned as the Amide II band which arises primarily due to N-H in-plane bending vibrations.[83] All of these are indicative of the presence of protein or more specifically in this case the whey protein isolate, which as noted before is primarily BLG and ALA. Previous FTIR analyses of BLG[22] reveal different structural characteristics (e.g., □ sheets, □ helices) of BLG in the 1600 – 1700 cm^{-1} range. The WPI:PEO fiber peak at 1650 cm^{-1} obtained from our samples is broad across this range, indicating that BLG may be present in some or all of these conformations. Eissa et al. also discussed that a change occurred in the magnitude of the spectra with increasing BLG concentration, although the shape of the spectra were similar.[22] Slight shifts in band position between very low (i.e., 0.25%) and the higher concentrations (3-7%) indicated that some molecular interaction may be influencing results with increasing concentration.[22] Our data also indicates a slight shift with overall whey protein concentration.

ALA, the other primary protein in WPI, also absorbs in the 1610-1700 cm^{-1} region, as would be expected.[84] Wongsasulak et al. (2007) found pure PEO electrospun nanofiber characteristic peaks at ~2900 (methylene group CH_2 molecular stretching), and at 1100 cm^{-1} and 958 cm^{-1} (C-O-C group stretching),[66] which agrees with the PEO fiber peaks seen in our data (Figure 2.6). A change in bandwidth for the absorption centered around 2880 cm^{-1} also occurs and increases with WPI concentration, thus decreasing with relative PEO concentration, which agrees with Eissa's observation of peak shifts with whey protein

concentration.[22] We would expect this also due to more contributions and resultant heterogeneity of the WPI in the solution and resultant mat. Zeng et al. used FTIR to evaluate PVA/BSA fibers, concluding that BSA, which is classified as a whey protein, generated FTIR peaks at 1710 cm^{-1} and 1665 cm^{-1} representing amide bonds from BSA.[54] The WPI:PEO fibers are not expected to show a dominant BSA representation, as WPI was processed to approximately a 98% protein concentration using ionic exchange chromatography which retained the BLG and ALA; thus, BSA should not be present in significant quantities in the WPI:PEO fiber mats. Rather, our WPI:PEO fiber mat FTIR data is dominated in this range by the ALA.

Where possible, secondary structural analysis was performed on spectra utilizing curve fitting routines and conforming band positions using second derivatives and Fourier self-deconvolution techniques. The original spectrum and the inverted second derivative of the WPI:PEO 50:50 fiber sample are shown in Figure 2.6(b) for illustrative purposes. This sample showed a strong absorption band in the Amide I region centered at 1644cm^{-1} and an Amide II absorption band at 1542cm^{-1}, which would indicate a high content of β-type structures and analysis of the band supports this observation. Curve resolution of the Amide I band (Figure 2.6(c)) revealed that the protein secondary structure is approximately 12% α-helix, 38% β-sheet, 30% β-turn and 20% random coil. On the other hand, the 100% PEO fiber and powder samples, consistent with Figure 2.6(a), showed no absorption in the amide I region between 1600 and 1700cm^{-1}.

Fiber samples were compared by FTIR analyses of BLG:PEO at both neutral and acidic pH. Some differences are observed between the analyses of the WPI:PEO and

BLG:PEO fiber samples prepared from neutral pH solutions, with shifts in both Amide I and II band peak maxima. This difference can be explained by the composition of WPI, which contains both ALA and BLG proteins. For comparison of fiber samples prepared from different pH, we used BLG as the protein component. The neutral pH BLG:PEO sample shows a peak maximum at 1632cm^{-1} for the Amide I band and a strong Amide II band at 1535cm^{-1} (Figure 2.5(f)); while the acidic pH sample has similar Amide I and Amide II band peaks at 1633cm^{-1} and 1535^{-1}, respectively. The pH change induces only a slight change in overall conformation of the BLG: PEO samples based on this peak shift, which could be simply limited to measurement resolution and not a true shift. Secondary structural analysis of samples reveals small but significant changes in the overall conformation between neutral and acidic pH (Table 1). The overall trend indicates a higher helical and lower β-sheet content. At pH below the protein's isoelectric point, one would expect the protein to be highly protonated and therefore to exhibit more hydrogen bonding which could increase the percentage of helical character.

While FTIR analyses of the WPI:PEO blends shows the presence of both PEO and WPI in the mats as expected, perhaps of greater interest is the composition of the blend present on the surface of the fibers. In order to examine this issue x-ray photoelectron spectroscopy (XPS) was used to determine surface (< 5 nm) constituents in atomic concentration. XPS survey scans utilizing PEO fiber mats with and without WPI are shown in Figure 2.7. On the surface of the PEO fibers, both carbon and oxygen atoms are found as expected. In the WPI:PEO blend fiber, an additional nitrogen peak is observed, indicating the presence of whey protein on the fiber surface. The atomic nitrogen content on the surface

of the fiber was approximately 10.6% slightly higher than the theoretical 7.5% atomic nitrogen concentrated calculated based on the uniform bulk solution concentration. This suggests that the whey protein is more concentrated on the surface of the fiber which is consistent with previous studies by Sun et al.[51]

XPS was also employed to examine the fiber mats made from BLG/PEO blends at various pH. Figure 2.5(g) provides the atomic % of each element present on the nanofiber surface for each mat produced from acidic solution (pH 2.0), solution at the BLG isoelectric point (5.2) and approximately neutral solution (7.5). Oxygen concentration peaks at the isoelectric point, while nitrogen is at a minimum. The opposite effect is seen at pH 7.5, where nitrogen is nearly 2% higher than on the surface of the pH 5.2 fibers. Based on this, one could conclude that at the isoelectric point the BLG agglomerates with the more hydrophilic oxygen portions of the protein being on the surface of the fiber, while at pH 7.5, nitrogen is in higher quantity at the surface. At acidic pH, the oxygen on the surface also is lower compared to that at the isoelectric point. Conformational changes of the BLG including a change from dimer to monomer expose a slight increased amount of nitrogen. Also, XPS results indicate a new element present in significant quantities – that of chlorine – likely due to the lowering of solution pH using HCl solution. As shown in Table Figure 2.5(g), sodium is present at the same order of magnitude in all three samples, indicating the possible presence of salt as a contaminant in the solution. The BLG used for these fiber preparations was purified, the PEO was not. Although, some NaOH solution may have been used during the pH adjusting process of the pH 5.2 and 2.0 solutions; the pH 7.5 solution was not modified with NaOH.

2.3.5 Nanofiber heat treatment

We explored heat treatment to increase the thermal stability of the WP:PEO blend nanofibers, since covalently crosslinking of the whey protein is expected to occur upon heating above the gelation temperature. An enclosed vial containing BLG/PEO fiber sample was placed in a water bath at 80°C for one hour. We used optical microscopy techniques (RLM and CLSM) to qualitatively examine the effect of heat treatment on the structure of the mats (Figure 2.8 and TOC graphic). The PEO mat melts (Figure 2.8(a)), while the blend fiber mats each retain a fibrous structure. The heat treated mats appear to transition from a molten state to a gel state with increasing WPI concentration. The 40:60 WPI:PEO mat shown in Figure 2.8(b) and (e) looks very similar to the 50:50 WPI:PEO mat (image not shown).

Using electron microscopy, we looked more closely at the structure of the PEO fiber mats with (Figure 2.9(a, b)) and without (Figure 2.9(c,d)) BLG, both before and after this heat treatment. We observe that the fiber mat containing whey protein maintain both its fibrous structure and fiber diameter following heating (Figure 2.9(a)). However, when the PEO–only fibers are heated to 80°C, they melt to form a PEO film as shown in Figure 2.9(d). Impressively, the addition of BLG to the blend and resultant fibers improves the stability and higher available surface area of the heated mat compared to a heated mat of 100% PEO. We also used XPS to evaluate changes in composition at the surface of the fiber after heat treatment. The atomic nitrogen concentration of the heat treated sample, measured using XPS, was 9.5%, which is slightly (~1.1%) lower than the fiber sample prior to heating. The decrease in the atomic nitrogen concentration was countered by an atomic oxygen

concentration increase of 1.5%, while that of carbon stayed relatively constant, indicating that some conformational changes may have occurred to expose more oxygen laden portions of the amino acid chains. Additionally, mobility of PEO during heat treatment may explain the slight changes in atomic surface composition. This could lead to the development of a heat treatment process in order to control surface amino acid content taking advantage of this PEO mobility as well as the crosslinking occurring between denatured proteins. Nonetheless, even after heating, the protein is still on the fiber surface. This, along with the ability of the whey protein to permit the PEO fiber system to retain its fibrous-like network after heating above PEO's melting point could extend the potential of nanofibers to higher temperature applications as needed for food or other production processes that would require heating. Also, heating BLG increases the reactivity of its thiol group, especially above pH 7; thus, heat treating the WP:PEO blend mats could regulate their reactivity.[85]

Thermal properties of the native and heat treated WP:PEO blend fiber mats were determined using DSC evaluation. Figure 2.9(e) shows DSC thermograms of PEO, 50:50 purified BLG:PEO blend mats before and after heat treatment at 80 °C (of Figure 2.9(b) and 9(a), respectively) and then the curve for purified BLG powder. According to Faridi-Majidi et al. (2007), the intense melting peaks of each nanofiber mat indicates the presence of semicrystalline products.[85] We were able to examine the crystallinity of the WP:PEO blends. The crystallinity relative to crystalline PEO is calculated from Xc (%) = $(\Delta H_f/\Delta H_f^o)$ x 100, where ΔH_f is the heat of fusion of the mat and ΔH_f^o is the heat of fusion of crystalline PEO (213.7 J/g).[85] Similar to Faridi-Majidi et al. (2007), our PEO mat has a higher heat of fusion at 141.5 J/g than the blend mats, as well as a higher calculated nanofiber mat

crystallinity of 66%. These values are lower than their powder PEO data (166.0 J/g; 77.68%) as expected. From this, we can similarly conclude that the PEO nanofiber production process reduces its crystallinity. [85] The addition of the WP to the formulation significantly reduces this relative crystallinity to 22 – 27%. We also note that the addition of BLG to the PEO nanofibers lowers the melting point of the mat compared to PEO from 67 °C to 55 °C, which indicates that the ability of the BLG to form some bonds as it is heated to above its denaturation temperature (approximately 71 °C).[85] The addition of BLG to the PEO nanofibers lowers the melting point of the mat compared to an all PEO (from 67 °C to 55 °C), but a heat treatment of the mat will increase that melting point to 62 °C. Similarly, as shown in Figure 2.9(f), blending WPI in the PEO mat formulation will decrease the melting point, but heat treatment of this mat even further lowers its melting point. This is likely due to the presence of ALA and other proteins in the WPI blend which do not crosslink upon heating like the purified BLG (Figure 2.9(g)).

2.3.6 Incorporation and release of a small molecule

As an initial step towards using these WP:PEO blend fibers as potential delivery vehicles, we incorporated and examined the release of a water soluble dye molecule Rhodamine B (RhB). We conducted a qualitative visual study to determine the distribution of RhB in PEO nanofibers with or without the addition of BLG to the solution prior to electrospinning. To do this, we examined the fibers containing RhB with SEM and CLSM (Figure 2.10). At 4 w/w% in water with 0.02 w/w% RhB, PEO forms beaded nanofibers as shown in Figure 2.10(a) with fibers "bunched" in the mat, possibly due to dye clusters. The

corresponding confocal microscopic image in Figure 2.10(b) shows brighter areas of dye near voids where these bunches or clusters have formed. The fiber mat electrospun from solution containing an additional 4 w/w % purified BLG in Figure 2.10(c) does not contain the presence of these clusters on the confocal image (Figure 2.10(d)) indicating, qualitatively, a more uniform distribution of dye. Thus, the BLG addition to solution appeared to improve the uniformity of the fiber mat as well as the distribution of the model flavenoid molecule RhB. FTIR comparison between the RhB-BLG-PEO, BLG-PEO and WPI-PEO blend fibers showed no strong difference or additional peaks (data not shown). However, secondary structure of the BLG was slightly affected by the presence of RhB (Table 1). This indicates that incorporating a molecule into a protein-based nanofiber system may influence protein secondary structure, but may not influence system performance. This would require evaluating each protein and delivery-molecule system.

Release of RhB from both PEO and BLG/PEO blend into DI water at room temperature was monitored over several minutes. In both cases, approximately 90% of the RhB was released within 10 minutes. Interestingly, despite the difference in distribution of the dye within the PEO and BLG/PEO fiber mats, there was no significant difference in the release profiles (Figure 2.11(d)) and samples were dissolving.

In order to establish an insoluble nanofiber mat of these materials, we heat treated mats of PEO and BLG/PEO for 24 - 44 hours at 100 °C (Figure 2.11(a)), which is well above the gelation temperature of the WP and above the melting point of PEO. After heat treatment, we found that the mats did not dissolve even after days of soaking in water and ultimately air drying (Figure 2.11(b)), since we believe the protein crosslinks during the heat

treatment. However, the mats did not return to their original state after soaking and drying, possibly since much of the PEO may be free to dissolve.

We examined the FTIR spectra after electrospinning, heat treatment, and soaking in water (data shown for the PEO/BLG blend (Figure 2.11(c)). While no difference in the spectra is seen between the native and heat treated mat, we believe that after exposure to water the majority of the PEO dissolves and the mat appears to be predominantly whey protein as indicated by the changes in the peak at approximately 1250 cm^{-1}. Results for the WPI:PEO blend mats were similar to that for the BLG/PEO. Figure 2.12(a) provides SEM image of the original heat treated mat, (b) this sample suspended and soaking in water, (c) sample after removal from water and (d) the dry, post-soaking mat under SEM. The sample in Figure 2.12(b) swelled with a minimum swelling ratio of 5.7 (= $(m-m_o)/m_o$ where m_o is initial sample mass and m is mass after soaking) after removal from water and blot dry with filter paper). The success of heat treatment we found dependent on heat treatment time and sample thickness (data not shown). For example, the same sample heat treated 18 hours dissolved in water immediately; while after 44 hours it swelled and maintained stability in water as shown in Figure 2.12(b). During heat treatment of the PEO:WP fiber mats, the BLG unfolds and forms disulfide bonds resulting in crosslinks in and between fibers. Further work is moving these heat treated WP:PEO fiber mats to the tissue engineering laboratory as a variant to other biomaterial scaffolding options. [87]

2.4 Conclusions

In this study, we demonstrated fabrication of electrospun nanofibers from whey proteins (WP) and its component beta lactoglobulin (BLG). Aqueous whey protein solutions either in native or denatured form yielded interesting micro and structures; while the addition of poly(ethylene oxide) to the system led to bead-free nanofiber formation. Nanofibers with WP:PEO composition as high as 3:1 could be obtained with diameters ranging between 312 to 690 nm depending on composition and total polymer concentration. Further, WP:PEO blends at a pH of 2.0 could be electrospun, which is desirable for reduced bacterial growth and increased product shelf life. However, beaded nanofibers resulted near the isoelectric point (pH~5) possibly from protein aggregation. XPS analysis of the blend fibers confirmed the presence of the protein and showed whey proteins were more concentrated on the fiber surface than the bulk. FTIR analysis also confirmed the presence, and revealed the secondary structure changed as a function of pH. Heat treatment of the blend fibers using temperatures above the gelation temperature of the protein increased the thermal stability of the fibers and with prolonged heat treatment, enabled the mat to become less soluble in water primarily due to the WP crosslinks. This heat treatment and resultant soaking mat stability shows promise for tissue scaffolding applications and is subject of ongoing work.

2.5 Acknowledgements

Thank you to Davisco Foods International, Inc. for providing the BiPRO and BetaLAC whey protein products. We thank Dr. Jason Bond, Dr. Thomas Fink and the East Carolina

University Biology Department Imaging Core for Scanning Electron Microscope utilization and Mr. Chris Dunkley of Olympus for reflected light microscopy support. We thank the Dr. Orlin Velev group at North Carolina State University for assistance with confocal microscopy. Also, we are grateful to East Carolina University students H. Ray Tichenor, Jamelle Simmons, Adam Hussaini, Joseph A. Rose, Clayton D. Rice and Thomas A. Deaton for support of this work.

2.6 References

(1) Chandan, R. C. Milk Composition, Physical and Processing Characteristics. In Manufacturing Yogurt and Fermented Milks; Chandan, R. C., Ed.; Blackwell Publishing: Ames, IA, 2006; pp 17-39.

(2) Chandan, R. C.; Shah, N. P. Functional Foods and Disease Prevention. In Manufacturing Yogurt and Fermented Milks; Chandan, R. C., Ed.; Blackwell Publishing: Ames, IA, 2006; pp 311-325.

(3) Chatterton, D. E. W.; Smithers, G.; Roupas, P.; Brodkorb, A. International Dairy Journal, 2006, 11, 1229-1240.

(4) Madureira, A. R.; Pereira, C. I.; Gomes, A. M. P.; Pintado, M. E.; Xavier Malcata, F. Food Research International, 2007, 10, 1197-1211.

(5) Ha, E.; Zemel, M. B. The Journal of Nutritional Biochemistry, 2003, 5, 251-258.

(6) Eissa, A. S. Enzymatic modification of whey protein gels at low pH, North Carolina State University, Raleigh, NC, 2005.

(7) Jung, J-M; Savin, G.; Pouzot, M.; Schmitt, C.; Mezzenga, R. Biomacromolecules, 2008, 9, 2477-2486.

(8) Alting, A. C.; Weijers, M.; deHoog, E. H. A.; vandePijpekamp, A. M.; CohenStuart, M. A.; Hamer, R. J.; deKruif, C. G.; Visschers, R. W. J. Agric. Food Chem. 2004, 3, 623-631.

(9) Eissa, A. S.; Khan, S. A. Food Hydrocolloids 2006, 4, 543-547.

(10) Bertrand, M.; Turgeon, S. L. Food Hydrocolloids 2007, 2, 159-166.

(11) Liu, G.; Xiong, Y. L.; Butterfield, D. A. J. Food Sci. 2000, 5, 811-818.

(12) Renard, D.; Robert, P.; Garnier, C.; Dufour, E.; Lefebvre, J. Journal of Biotechnology 2000, 3, 231-244.

(13) Britten, M.; Giroux, H. J. Food Hydrocolloids 2001, 609-617.

(14) Roefs, S. P. F. M.; Peppelman, H. A. Aggregation and gelation of whey proteins: specific effect of divalent cations.? In Food Colloids: Fundamentals of Formulation; Dickinson, E., Miller, R., Eds.; The Royal Society of Chemistry: London, 2001; pp 358-358-368.

(15) Vardhanabhuti, B.; Foegeding, E. A.; McGuffey, M. K.; Daubert, C. R.; Swaisgood, H. E. Food Hydrocoll. 2001, 2, 165-175.

(16) Burke, M. D.; Ha, S. Y.; Pysz, M. A.; Khan, S. A. International Journal of Biological Macromolecules 2002, 1-3, 37-44.

(17) Foegeding, E. A.; Davis, J. P.; Doucet, D.; McGuffey, M. K. Trends in Food Science & Technology 2002, 5, 151-159.

(18) Kavanagh, G. M.; Clark, A. H.; Ross-Murphy, S. B. Rheologica Acta 2002, 276-284.

(19) Lowe, L. L.; Foegeding, E. A.; Daubert, C. R. Food Hydrocoll. 2003, 4, 515-522.

(20) Eissa, A. S.; Bisram, S.; Khan, S. A. Journal of Agriculture and Food Chemistry 2004, 4456-4464.

(21) Daubert, C. R.; Hudson, H. M.; Foegeding, E. A.; Prabhasankar, P. LWT - Food Science and Technology 2006, 3, 206-215.

(22) Eissa, A. S.; Puhl, C.; Kadla, J. F.; Khan, S. A. Biomacromolecules 2006, 6, 1707-1713.

(23) Kinsella, J. E.; Whitehead, D. M. Advanced Food Nutrition Research 1989, 343-438-343-438.

(24) Shimada, K.; Cheftel, J. C. Journal of Agricultural and Food Chemistry 1989, 161-168.

(25) Taylor, S. Food hydrocolloids 1994, 1, 45.

(26) Barbut, S. Food Research International 1995, 5, 437-443.

(27) Stading, M.; Langton, M.; Hermansson, A. -. Journal of Rheolgy 1995, 1445-1450.

(28) Lupano, C. E.; Renzi, L. A.; Romera, V. J. Agric. Food Chem. 1996, 10, 3010-3014.

(29) Errington, A. D.; Foegeding, E. A. Journal of Agricultural and Food Chemistry 1998, 2963-2967.

(30) Ikeda, S.; Nishinari, K.; Foegeding, E. A. Biopolymers 2000, 2, 109-118.

(31) MaHam, A.; Tang, Z.; Wu, H.; Wang, J.; Lin, Y. Small 2009, 5, 1706-1721.

(32) Livney, Y.D. Current Opinion in Colloid and Interface Science, 15, 73-83.

(33) Satpathy, G.; Rosenberg, M. J. Microencapsul. 2003, 2, 227.

(34) Srikar, R.; Yarin, A. L.; Megarides, C. M.; Bazilevsky, A. V.; Kelley, E. Langmuir 2008, 965-974.

(35) Cui, W.; Zhou, Y.; Chang, J. Science and Technology of Advanced Materials 2010, 11, 014108 (11pp).

(36) Ignatious, F.; Sun, L.; Lee, C.; Baldoni, J. Pharmaceutical Research 2010, 27, 4, 576-588.

(37) Ignatious, F.; Sun, L. Electrospun amorphous pharmaceutical compositions. U.S. Patent 2006/0013869 A1, January 19, 2006.

(38) Frenot, A.; Chronakis, I. S. Current Opinion in Colloid and Interface Science 2003, 64-75.

(39) Li, D.; Xia, Y. Advanced Materials 2004, 1151-1170.

(40) Huang, Z.; Zhang, Y.; Kotaki, M.; Ramakrishna, S. Composites Science and Technology 2003, 2223-2253.

(41) Andrady, A. L. Science and Technology of Polymer Nanofibers; Wiley: 2008; , pp 404.

(42) Reneker, D. H.; Yarin, A. L.; Fong, H.; Koombhongse, S. Journal of Applied Physics 2000, 9 Pt. 1, 4531-4547.

(43) Yarin, A. L.; Koombhongse, S.; Reneker, D. H. Journal of Applied Physics 2001, 9, 4836-4846.

(44) Saquing, C.D., Manasco, J.L., Khan, S.A., Small, 2009, 5, 944-951.

(45) Jia, H.; Zhu, G.; Vugrinovich, B.; Kataphinan, W.; Reneker, D. H.; Wang, P. Biotechnol. Prog. 2002, 5, 1027-1032.

(46) Jin, H.; Fridrikh, S. V.; Rutledge, G. C.; Kaplan, D. L. Biomacromolecules 2002, 1233-1239.

(47) MacDiarmid, A. G.; Jones, W. E.; Norris, I. D.; Gao, J.; Johnson, A. T.; Pinto, N. J.; Hone, J.; Han, B.; Ko, F. K.; Okuzaki, H.; Llaguno, M. Synthetic Metals 2001, 1-3, 27-30.

(48) Katti, D. S.; Robinson, K. W.; Ko, F. K.; Laurencin, C. T. Journal of Biomedical Materials Research Part B: Applied Biomaterials 2004, 286-296.

(49) Li, W.; Laurencin, C. T.; Caterson, E. J.; Tuan, R. S.; Ko, F. K. Journal of Biomedical Materials Research 2002, 613-621.

(50) Boudriot, U.; Dersch, R.; Greiner, A.; Wendorff, J. H. Artificial Organs 2006, 10, 785-792.

(51) Sun, X.; Shankar, R.; Börner, H. G.; Ghosh, T. K.; Spontak, R. J. Advanced Materials 2007, 87-91.

(52) Suk Choi, J.; Sang Yoo, H. Journal of Bioactive and Compatible Polymers 2007, 508-524.

(53) Kriegel, C.; Arrechi, A.; Kit, K.; McClements, D. J.; Weiss, J. Critical Reviews in Food Science and Nutrition 2008, 775-797.

(54) Zeng, J.; Aigner, A.; Czubayko, F.; Kissel, T.; Wendorff, J. H.; Greiner, A. Biomacromolecules 2005, 1484-1488.

(55) Jiang, H.; Hu, Y.; Li, Y.; Zhao, P.; Zhu, K.; Chen, W. Journal of Controlled Release, 2005, 2-3, 237-243.

(56) Kowalczyk, T.; Nowicka, A.; Elbaum, D.; Kowalewski, T.A. Biomacromolecules, 9, 2087-2090.

(57) Dror, Y.; Ziv, T.; Makarov, V.; Wolf, H.; Admon, A.; Zussman, E. Biomacromolecules 2008, 2749-2754.

(58) Xie, J.; Hsieh, Y. Journal of Materials Science 2003, 10, 2125-2133.

(59) Kim, So Hyun; Nam, Young Sik; Lee, Taek Seung; Park, Won Ho. Polymer Journal 2003, 35(2), 185-190

(60) Min, B.; Lee, G.; Kim, S. H.; Nam, Y. S.; Lee, T. S.; Park, W. H. Biomaterials, 2004, 7-8, 1289-1297.

(61) Miyoshi, T.; Toyohara, K.; Minematsu, H. Polymer International 2005, 1187-1190.

(62) Zoccola, M.; Montarsolo, A.; Aluigi, A.; Varesano, A.; Vineis, C.; Tonin, C. e-Polymers 2007, 105, 1-19.

(63) Yang, L.; Fitie, C. F. C.; van der Werf, Kees O.; Bennink, M. L.; Dijkstra, P. J.; Feijen, J. Biomaterials 2008, 955-962.

(64) Li, M.; Mondrinos, M. J.; Gandhi, M. R.; Ko, F. K.; Weiss, A. S.; Lelkes, P. I. Biomaterials 2005, 5999-6008.

(65) Wnek, G. E.; Carr, M. E.; Simpson, D. G.; Bowlin, G. L. Nano Letters 2003, 2, 213-216.

(66) Wongsasulak, S.; Kit, K. M.; McClements, D. J.; Yoovidhya, T.; Weiss, J. Polymer, 2007, 2, 448-457.

(67) Yi, F.; Guo, Z.; Fang, Z.; Yu, J.; Li, Q. Macromolecular Rapid Communications 2004, 1038-1043.

(68) Woerdeman, D. L.; Ye, P.; Shenoy, S.; Parnas, R. S.; Wnek, G. E.; Trofimova, O. Biomacromolecules 2005, 707-712.

(69) Woerdeman, D. L.; Shenoy, S.; Breger, D. The Journal of Adhesion 2007, 785-798.

(70) Nie, H.; He, A.; Zheng, J.; Xu, S.; Li, J.; Han, C. C. Biomacromolecules 2008, 5, 1362-1365.

(71) "Microorganisms in Foods 6. Microbial Ecology of Food Commodities.," ICMSF, 1998. ICMSF, International Commission for the Microbiological Specifications for Foods. Blackie Academic and Professional, 1998.

(72) Anema, S. G. Food Chemistry, 2008, 1, 110-118.

(73) Malliart, P.; Ribadeau-Dumas, B. Journal of Food Science 1988, 53, 3, 743-752

(74) Little, Ralph C.; Ting, Robert Y.; Journal of Chemical and Engineering Data 1976, 21, 422-423.

(75) Talwar, S.; Hinestroza, J.; Pourdeyhimi, B.; Khan, S. A. Macromolecules 2008, 12, 4275-4283.

(76) Tobi, D.; Elber, R.; Thirumalai, D. Biopolymers 2003, 359-369.

(77) Czarnik-Matusewicz, B.; Kim, S. B.; Jung, Y. M. The Journal of Physical Chemistry B 2009, 2, 559-566.

(78) Song, J.; Kim, H.; Kim, H. J Mater Sci: Mater Med 2008, 95-102.

(79) Son, W. K.; Youk, J. H.; Taek, S. L.; Park, W. H. Materials Letters 2005, 1571-1575.

(80) Zhu, J.; Shao, H.; Hu, X. International Journal of Biological Macromolecules, 2007, 4, 469-474.

(81) Torres-Giner, S.; Gimenez, E.; Lagaron, J. M. Food Hydrocolloids, 2008, 4, 601-614.

(82) Son, W. K.; Youk, J. H.; Lee, T. S.; Park, W. H. Polymer, 2004, 9, 2959-2966.

(83) Socrates, G. Infrared Charateristic Group Frequencies: Tables and Charts; John Wiley & Sons: Chichester, 1994; , pp 249-752.

(84) Zhong, H.; Gilmanshin, R.; Callender, R. J. Phys. Chem. B 1999, 19, 3947-3953.

(85) Phillips, L. G.; Whitehead, D. M.; Kinsella, Structure-Function Properties of Food Proteins 1994 (Academic Press, Inc.).

(86) Faridi-Majidi, R.; Sharifi-Sanjani, N. J Appl Polymer Sci, 2007 105, 1351-1355.

(87) Van Vlierberghe, S.; Dubruel, P.; Schacht, E. Biomacromolecules 2011, 12, 1387-1408.

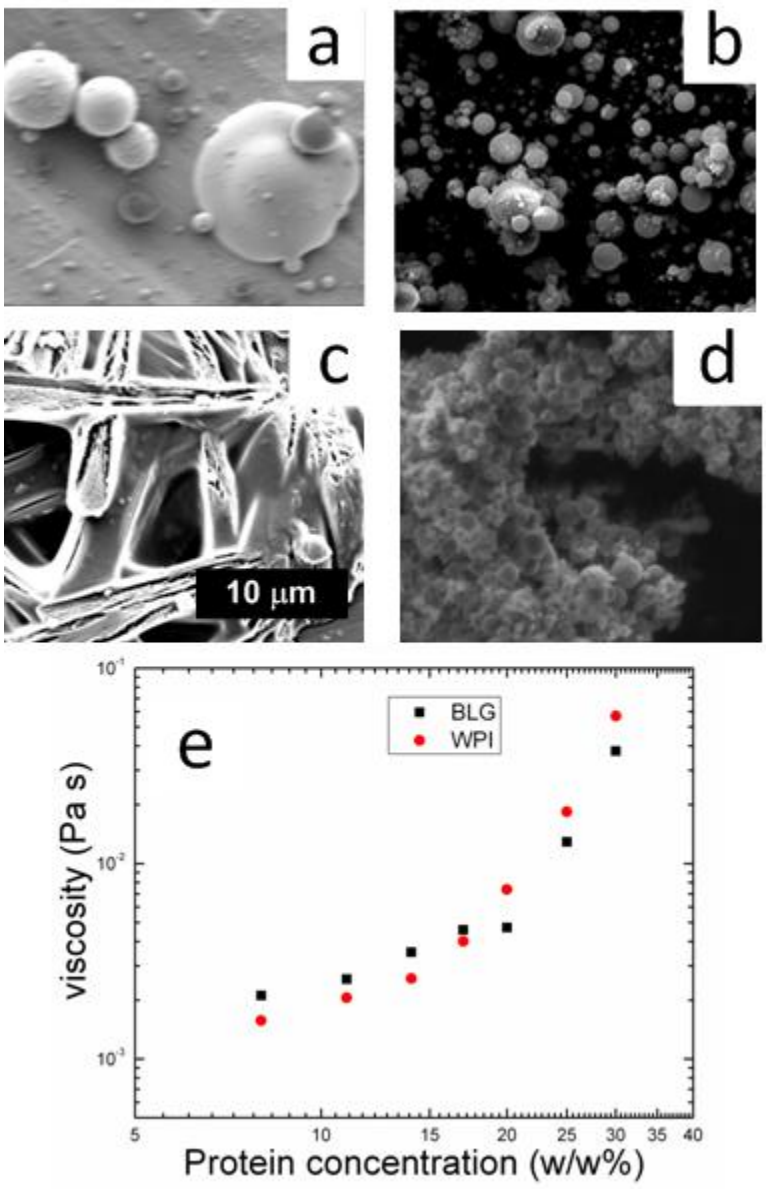

Figure 2.1. Electrospun whey protein microstructures (a) whey protein isolate (WPI) 25 w/w% in deinonized water (DW) [flowrate 1 ml/hr, 12 cm TCD, 30kV]; (b) 17 w/w% □-lactoglobulin (BLG), 5M ethanol, 20mM HCl in DW [flowrate 2 ml/hr, 17 TCD, 15 kV]; (c) 10 w/w% BLG 8M urea in DW [flowrate 1 ml/hr, 12 cm TCD, 30kV]; (d) 17 w/w% WPI in DW mixed with ethanol 5:1 by volume [flowrate 1 ml/hr, 15 cm TCD, 26 kV]. 10 □m scale bar shown applies to all SEM images. (e) Viscosity of aqueous whey protein solutions.

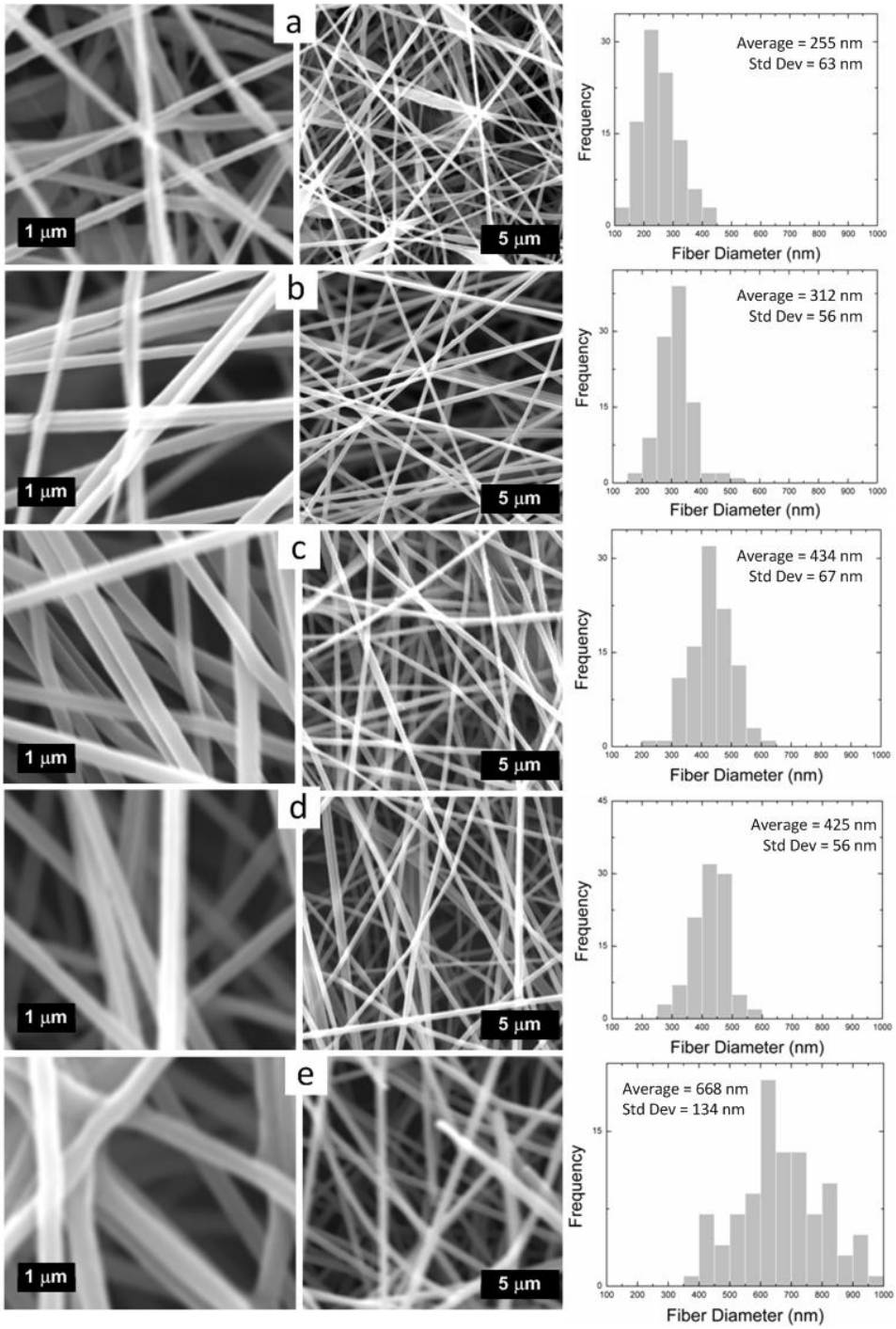

Figure 2.2. Scanning electron micrographs and fiber diameter analysis of whey protein isolate (WPI) and poly(ethylene oxide) (PEO) blend solution electrospun nanofibers. PEO 4 w/w% with increasing WPI (and thus total weight) concentration, with WPI:PEO ratio (a) 0:100; (b) 40:60; (c) 50:50; (d) 60:40; (e) 75:25.

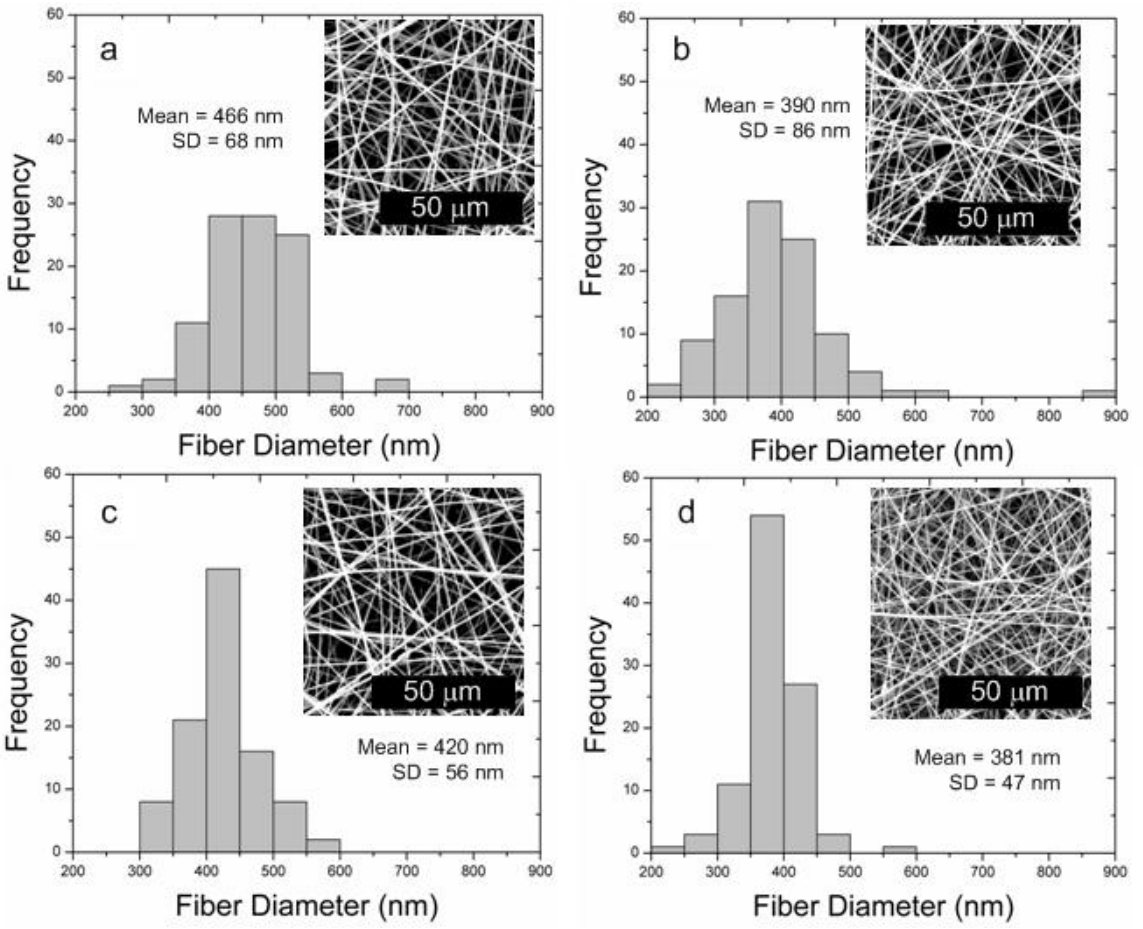

Figure 2.3. Scanning electron micrographs and fiber diameter analysis of □-lactoglobulin (BLG) and poly(ethylene oxide) (PEO) blend solution electrospun nanofibers. Fibers spun at 15 cm tip-to-collector distance and 22 gauge needle. Total 10 w/w% with BLG:PEO ratio (solution viscosity Pa s; flow rate ml/hr; voltage) (a) 75:25 (0.5; 1.0; 9.5 kV); (b) 60:40 (3.2; 0.5 ml/hr; 10.5 kV); (c) 50:50 (10; 0.2 ml/hr; 10 kV); (d) 40:60 (23; 0.1 ml/hr; 15 kV).

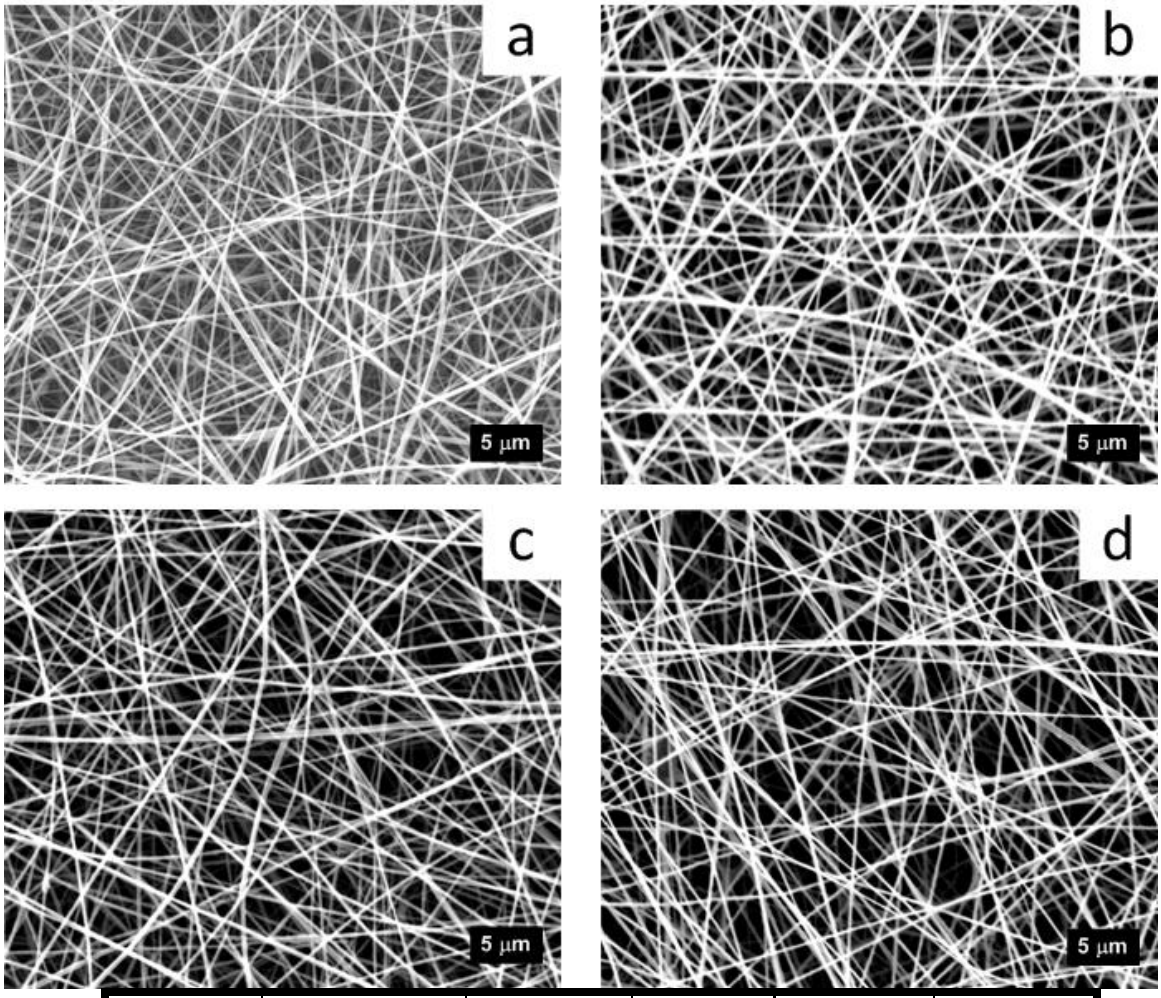

e

PEO:WPI ratio	PEO concentration (w/w%)	Solution pH	Solution viscosity (Pa s)	Nanofiber mean diameter* (nm)	standard deviation* (nm)
50:50	2.7%	2.36	0.34	312	69
57:43	3.2%	2.43	0.65	301	52
66:34	3.6%	2.55	1.04	304	51
80:20	4.4%	2.92	2.33	262	44

Figure 2.4. Scanning electron micrographs of total weight 5.5 w/w% PEO:WPI acidic blend mats (a) 50:50, (b) 57:43, (c) 66:34 and (d) 80:20 by weight blend solution electrospun nanofiber mats produced. (e) provides solution and nanofiber data, with *nanofiber data determined from NIH Image J analysis with minimum 100 measurements.

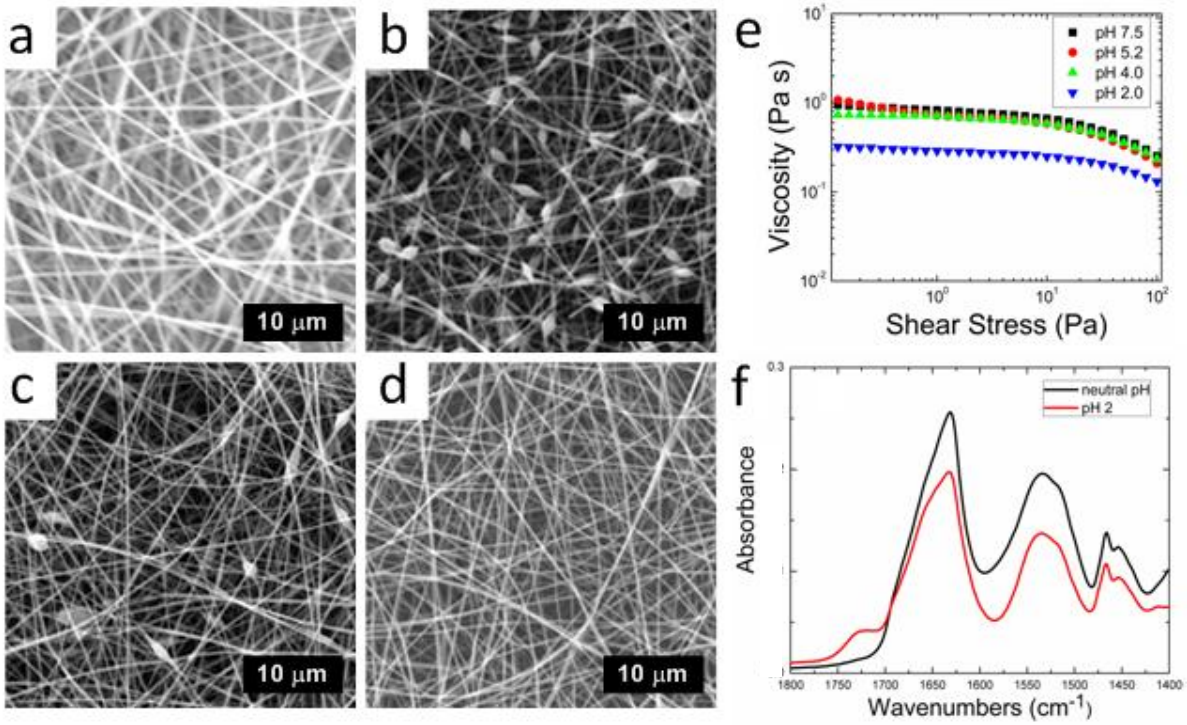

g

Solution pH	Solution Conductivity (mS/cm)	Nanofiber mean diameter (nm)	standard deviation (nm)	XPS Elemental Fiber Mat Content (%)				
				O	C	N	Cl	Na
7.5	2.5	453	82	24.62	63.84	11.27	0	0.28
5.2	3.8	Bead defects		28.42	62.01	9.35	0	0.23
4	5.6	Bead defects		*				
2	12.6	391	94	26.69	62.07	9.65	1.32	0.27

Figure 2.5. Scanning electron micrographs of solution electrospun nanofibers from total 7 w/w % solution of 50:50 purified BLG:PEO at pH (a) 7.5; (b) 5.2; (c) 4.0, (d) 2.0. (e) shows solution steady shear viscosity vs. shear stress; (f) provides FTIR comparison of 50:50 WP:PEO fiber mat prepared from neutral pH and acidic pH 2; and (g) provides mean nanofiber diameter, X-ray photoelectron spectroscopy (XPS) and solution data for these mats of varying pH. Fiber mats at pH 5.2 and 4.0 each contained bead defects. For example, fibers formed with pH 5.2 solution had bead defects with measured average diameter of 1 μm. *Note that XPS was only completed on fiber mats of pH 2, 5.2 and 7.5.

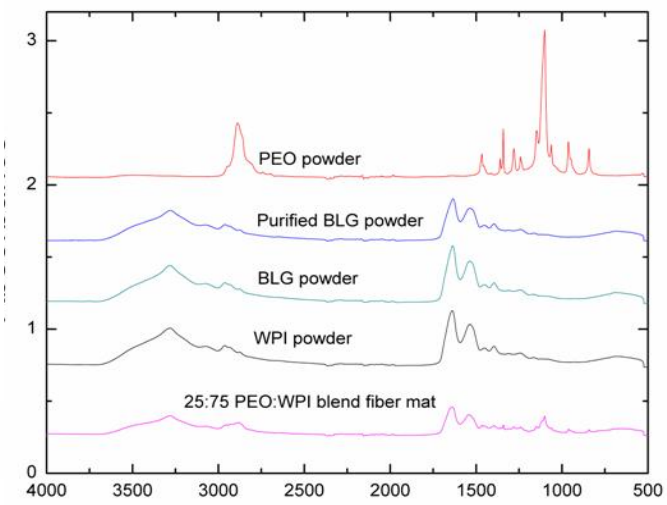

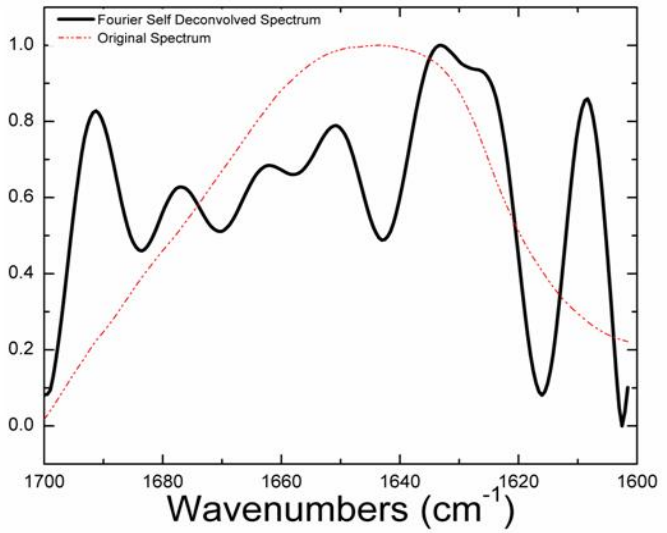

C

Sample	Peak position (cm^{-1})	Assignment	Peak position (cm^{-1})	Assignment
50:50 WPI:PEO	1616	β-sheet	1656	α-helix
	1624	β-sheet	1664	turns
	1634	β-sheet	1678	turns
	1647	unordered	1691	β-sheet

Figure 2.6. (a) FTIR absorbance spectra for raw materials and representative PEO/WPI blend nanofiber mat; (b) Amide I Region of the 50:50 PEO:WPI sample showing the original spectrum and the Fourier self-deconvolved spectrum (Bandwidth 42 cm-1, enhancement: 3.5); (c) Peak positions of the resolved Amide I region of whey protein isolate on PEO fibers. Protein secondary structure information for source material and nanofiber mats is given in Table 1.

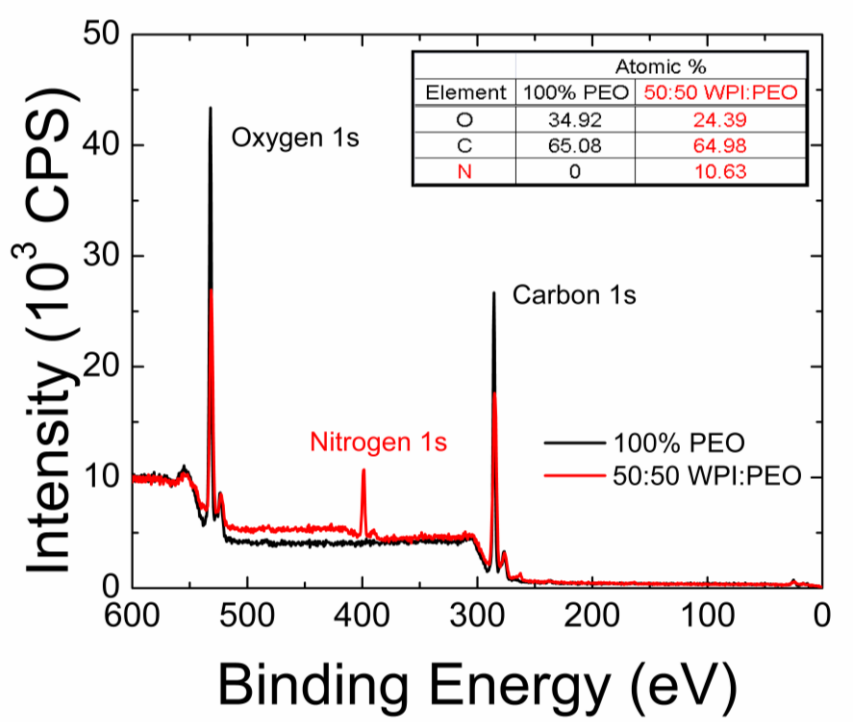

Figure 2.7. An XPS survey scan is displayed for electrospun nanofibers generated from 4 w/w% PEO solutions with and without WPI. The inset table provides the atomic percent of each element present on the nanofiber mat surface.

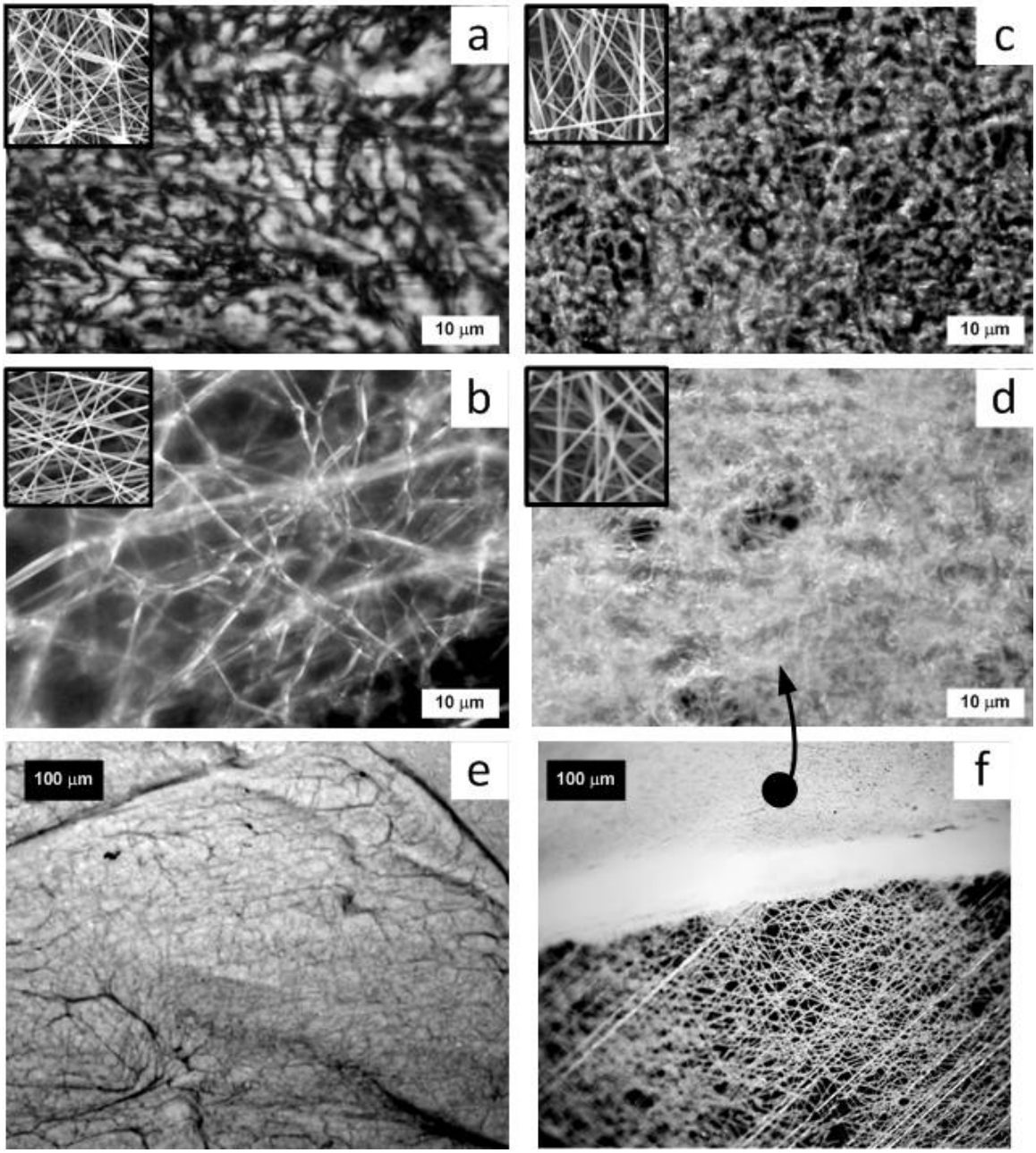

Figure 2.8. Reflected light dark field microscope images of heat treated whey protein isolate (WPI) and poly(ethylene oxide) (PEO) blend solution electrospun nanofiber mats. PEO 4 w/w% with increasing WPI concentration, with WPI:PEO ratio (a) 0:100; (b) 40:60; (c) 60:40; (d) 75:25. Insets in (a) – (d) are SEM images of original mats (before heat treatment) at same scale as reflected light microscope images. (e) is reflected light image of (b) 40:60 WPI:PEO at lower magnification, showing melt appearance; while (f) is reflected light image of (d) 75:25 WPI:PEO at lower magnification, showing networked fiber gel appearance with thinner fibrous sample edge that was formed from pulling mat apart.

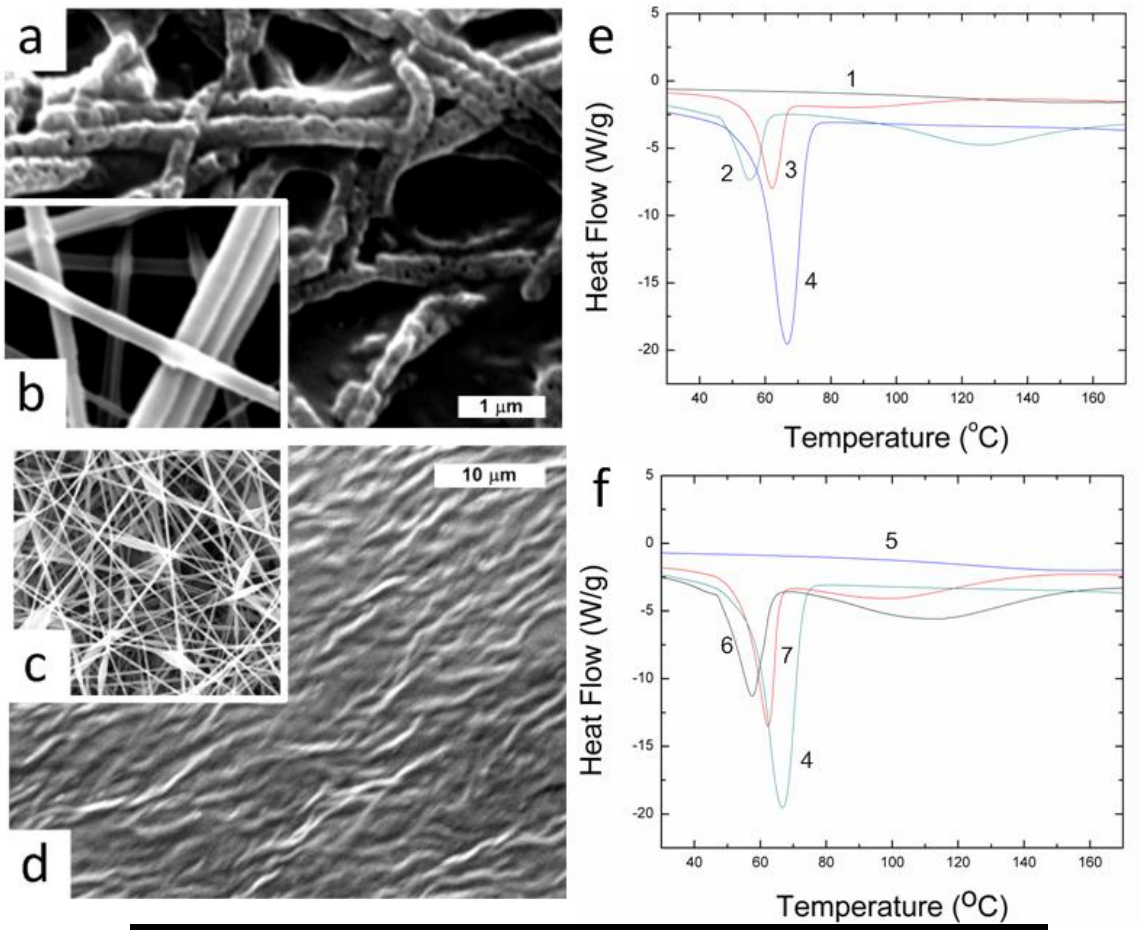

g

Sample composition	prior heat treatment at 80 °C?	melting point (° C)	ΔHf (J/g)	Xc (%)
100% PEO (4)	no	66.82	141.50	66%
50:50 PEO:pBLG (2)	no	55.12	48.63	23%
50:50 PEO:pBLG (3)	yes	62.07	49.11	23%
50:50 PEO:WPI (7)	no	62.38	56.76	27%
50:50 PEO:WPI (6)	yes	57.51	46.43	22%

Figure 2.9. Scanning electron microscope images of 8 w/w% purified BLG (pBLG)/PEO blend nanofibers (a) after and (b) before (inset) heat treatment at 80°C; PEO nanofibers (c) before (inset) and (d) after heat treatment at 80 °C. Images (a) and (b) are at same scale; as are (c) and (d). (e) and (f) provide DSC thermographs of nanofiber mats and powders: scan (1) purified BLG (pBLG) powder; (2) pBLG:PEO 50:50 native nanofiber mat (b); (3) pBLG:PEO 50:50 heat treated nanofiber mat (a); (4) PEO nanofiber mat (c); (5) BiPRO WPI powder; (6) WPI:PEO 50:50 heat treated nanofiber mat; (7) WPI:PEO 50:50 native nanofiber mat; (g) summarizes DSC data.

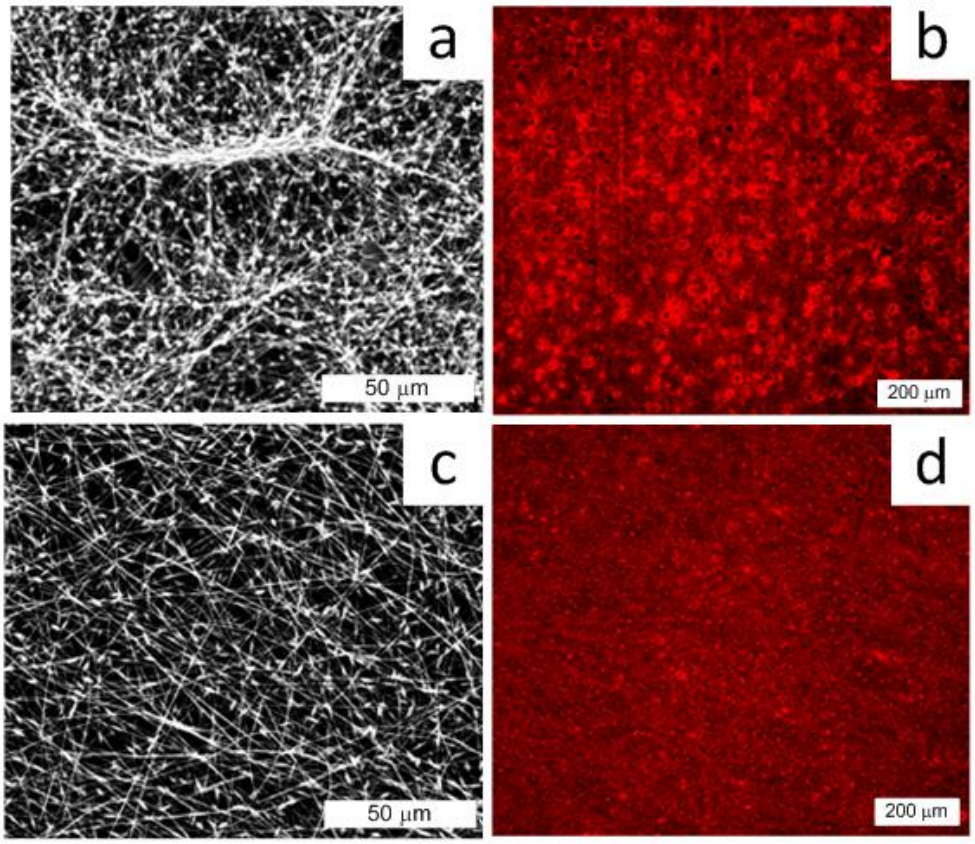

Figure 2.10. PEO fiber mat with 4 w/w% PEO and 0.02% RhB in deionized water *without* BLG (a) scanning electron micrograph, (b) confocal microscope image of RhB distribution; and *with* BLG (50:50 BLG:PEO for total 8 w/w%) (c) scanning electron micrograph, (d) confocal microscope image of RhB distribution.

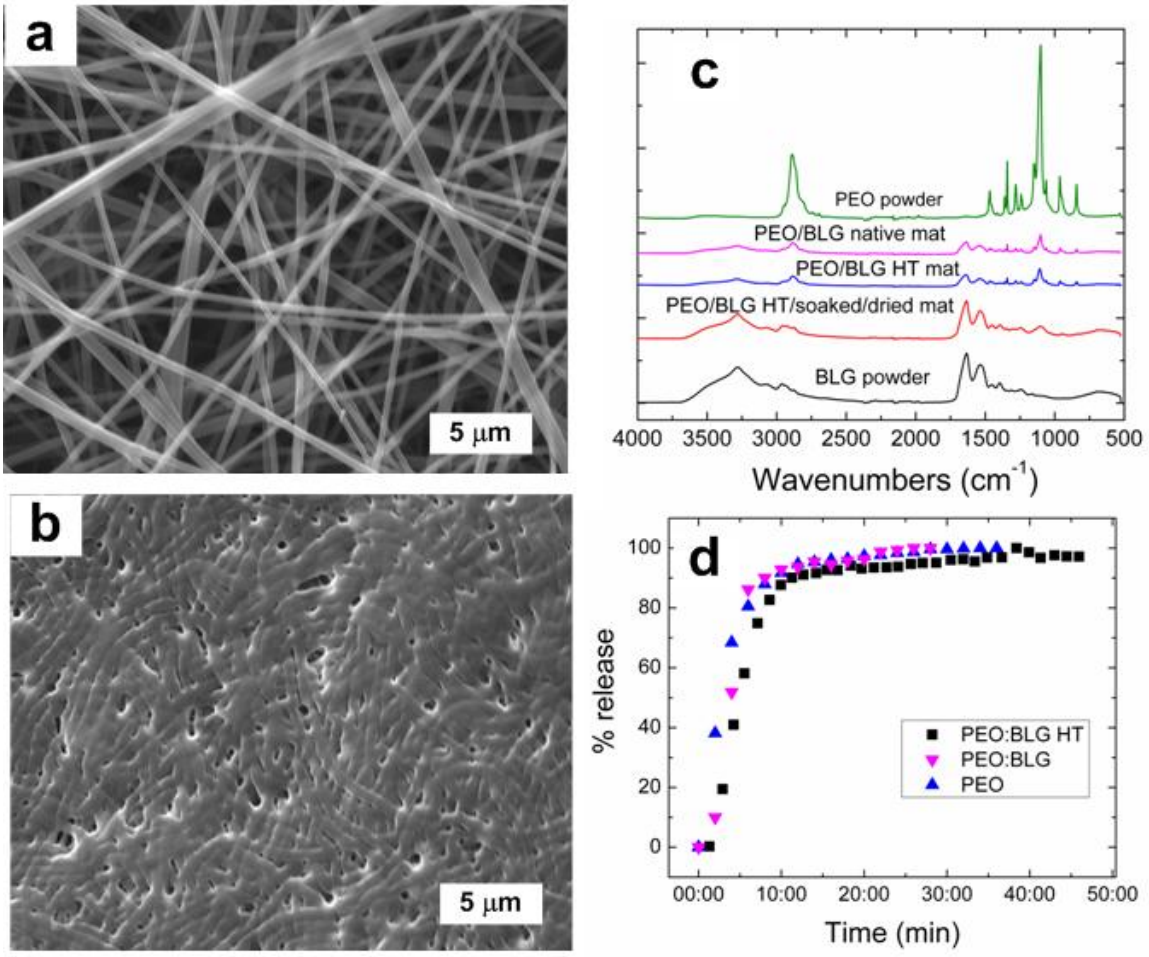

Figure 2.11. PEO:BLG (50:50 BLG:PEO for total 8 w/w%) blend fiber mat (a) post heat treatment at 100 °C for 18 hrs, (b) post heat treatment then after soaking in water and air drying, (c) FTIR comparison between native, heat treated, heat treated/immersed/dried mats and raw material powder, (d) release of RhB over time from fiber mat samples of PEO, BLG:PEO and heat treated BLG:PEO.

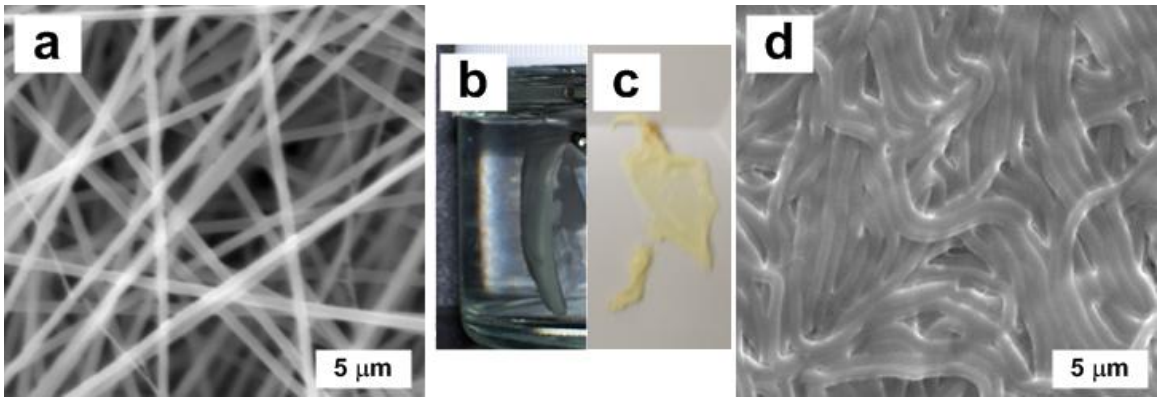

Figure 2.12. PEO:WPI (25:75 for total 16 w/w%) nanofiber mat with post heat treatment at 100 °C for 44 hrs (a) post heat treatment, (b) suspended soaking in deionized water, (c) sample removed from water soak, (d) SEM of sample (c) air dried and sputter coated with gold.

Table 2.1. Conformational analysis of WP:PEO nanofiber sample protein secondary structure showing the effect of concentration, pH and dye addition. *BioPURE BLG used as received. pBLG is BioPURE BLG that has been purified.

Sample	β-sheet	α-helix	β-turn	random coil
50:50 WPI:PEO (neutral pH) mat	38%	12%	30%	20%
75:25 WPI:PEO (neutral pH) mat	38%	16%	26%	20%
WPI powder	41%	12%	28%	19%
BLG* powder	43%	12%	26%	19%
Purified BLG powder	44%	11%	26%	19%
50:50 BLG*:PEO (neutral pH) mat	44%	12%	25%	19%
50:50 BLG*:PEO (pH 2) mat	36%	19%	24%	21%
50:50 pBLG:PEO with RhB mat	37%	15%	28%	20%

CHAPTER 3 Functional gels of whey protein and pullulan blends

Chapter 3 is essentially a manuscript by Stephanie T. Sullivan, Jamelle M. Simmons, Thomas J. Fink, Michelle D. Robinson, David Cistola, and Saad A. Khan to be submitted to *Food Hydrocolloids*.

Functional gels of whey protein and pullulan blends

Stephanie T. Sullivan, Jamelle M. Simmons[ǂa], Thomas J. Fink[ǂb], Michelle D. Robinson[ǂc], David Cistola[ǂc], and Saad A. Khan*

Department of Chemical and Biomolecular Engineering, North Carolina State University, Raleigh, NC 27695-7905,
[ǂa] Department of Engineering, East Carolina University, Greenville, NC 27858
[ǂb] Department of Biology, East Carolina University, Greenville, NC 27858
[ǂc] Brody School of Medicine, East Carolina University, Greenville, NC 27858

ABSTRACT

Continuous improvement and development of safe and effective food, flavor and active ingredient delivery systems are biotechnology industry missions. Gels are utilized as foundations of food and biotechnology products. Controlling gel properties varies not only product texture, but also potential flavor and pharmaceutical compound delivery. Heat set gels of aqueous whey protein have been utilized in many food applications. We prepared aqueous blends of whey protein (WP) and a non-gelling polysaccharide pullulan (PULL) to correlate heat set gels composition, structure and yield response. Biomaterial blend heat-set gelation as a function of WP-PULL blend composition was evaluated using microscopy and rheological techniques. Using a dynamic rheological technique, we evaluated the large strain behavior of samples. From this evaluation, yield or fracture stresses of the pure protein gels were higher by an order of magnitude over 50:50 protein-polysaccharide blend gels. Both

blend gel microstructure and yield stress varied with pH relative to the β-lactoglobulin (BLG) isoelectric point, with particulate blend gel at pH 5.2 having lower yield stress than the blend at the native mix 6.8 pH. Hydrophobic model drug Rhodamine B loading was observed via confocal microscopy, with large gaps in blend particle gel microstructure found, which could be responsible for the lower blend yield stress. Via ESEM, a polysaccharide smoothing effect on the protein gel microstructure was observed. Additionally, at both the isoelectric point (IEP) and pH 8, we evaluated the impact of the addition of transglutaminase enzyme and sodium trimetaphosphate on the formation of whey protein-pullulan blend heat set gels at 17 w/w% using this large strain behavior dynamic rheological analysis. One critical observation noted is that gels at pH 8 had yield stress an order of magnitude larger than those at the BLG IEP.

3.1 Introduction

Gels of whey protein have been utilized in food formulations for some time.[1-24] For many years, whey proteins have been used in food design due to its variety of functional uses including water and flavor binding as well as gelation, emulsification and foaming.[25-27] From a medicinal standpoint, whey proteins are being studied and recognized for their antimicrobial, antiviral, anticarcinogenic and other beneficial metabolic and physiological effects.[28-30] For example, whey in its natural conformation is rich in the amino acid cysteine, which is important in synthesizing the "major intracellular antioxidant" glutathione.[30] Data also suggest that the human body's ability to quickly absorb whey protein may enhance its ability to better utilize protein after eating. [30]

Whey proteins are considered globular proteins with (1) compact and ordered molecular structure, (2) tight conformation organization (α-helices and β-sheets), (3) stabilization by physical (hydrogen & hydrophobic) and covalent (primarily disulfide bridges) bonds, and (3) upon adsorption, secondary structure is retained while tertiary structure changes.[31] Whey proteins consist primarily of BLG, α-lactalbumin (ALA), serum albumin (SA), immunoglobulin (IG) and lactoferrin (LF). For functionality such as gelation, , the behavior of BLG is known to dominate commercial whey protein ingredients, especially those with higher protein contents such as whey protein isolate (WPI) and some whey protein concentrates (WPC).[32] BLG is a globular protein with an isoelectric point (IEP) of approximately 5.2, monomer molecular weight of 18.3 kDa, and 3 nm diameter in its native state. The IEP of a protein is the pH at which the molecule has a neutral charge. At their IEP, whey proteins tend to aggregate extensively.

Heating aqueous whey protein solution of at least 11 w/w% above the BLG denaturation temperature (70 °C) will form gels.[1,27] Varying conditions such as protein content, pH, salt concentration and salt composition can result in formation of a variety of gels "from fine-stranded particles to large particulate gel structures"[33], thus making whey protein a highly suitable food ingredient due to the ability to control its structure and textures with these different conditions.

Complexes of protein with polysaccharides have been evaluated for food, pharmaceutical and biomedical applications, specifically biomaterial-biomaterial-water systems. For example, the food industry has been interested in biomaterial mixtures, especially those that may form emulsions, as a food texture improvement tool.[34] Mixed gels of whey protein and galactomannans have been the subject of many recent studies.[35-43] However, one polysaccharide that has not been explored in whey protein gelation systems is pullulan.

Pullulan is considered a non-gelling polysaccharide and is edible, biodegradable and generally regarded as safe (GRAS) by the United States Food and Drug Administration.[44] Pullulan is a natural, water-soluble polysaccharide that is excreted extracellularly by the fungus *Aureobasidium pullulans* and comprised of maltotriose units (α-1,4 linked glucose molecules) polymerized by α-1,6-glucosidic bonds.[45] The molecule is linear, amorphous and forms a stair-step like structure. It is odorless, flavorless and highly stable. Pullulan has many current and potential uses in the food and pharmaceutical industries, [46-58] and is being considered for part of therapeutic diets for individuals with *type 2 diabetes mellitus* because it

helps maintain blood glucose levels.[59] Aqueous pullulan solutions are stable and viscous but do not gel.[57]

Whey protein and pullulan blends could be used not just to modify food and other material properties, but as nutritional supplements as well.[29, 30, 59, 60] Analysis of whey protein-pullulan blends has been limited to coating applications.[61-63] Gels of edible whey protein and pullulan will provide additional opportunities for biotechnology application development as well as fundamental understanding of relationships between aqueous whey protein, pullulan and blend solution properties and their ability to form gels.

Within this work, we report correlations between whey protein-pullulan gel rheological properties to microstructure. We start with a homogenous protein gel and transform the microstructure with addition of pullulan, change in pH, heating time, as well as the addition of either chemical phosphorylation agent sodium trimetaphosphate (STMP) or transglutaminase (TG) enzyme, both of which serve to crosslink biomaterials.

3.2 Materials and Methods

3.2.1 Materials

BiPRO Whey Protein Isolate (WPI) and BIOPURE β-lactoglobulin (BLG) were both obtained from Davisco Foods Inc. (Eden Prairie, MN) and used as received. Some BIOPURE BLG was utilized following a purification procedure [64] that was verified with NuPAGE (see Appendix B). Pullulan PI-20 (200 kDa, Polydispersity Index 2.4 [65]) was obtained from Hayashibara Company, Limited (Okayama, Japan) and was used as received. Hydrochloric acid (HCl), sodium azide, sodium hydroxide (NaOH), and Rhodamine B were used as

received from Sigma. A commercial version (Activia TI TG) of Transglutaminase (TG) enzyme (1 % enzyme and 99 % maltodextrin, by weight) was provided by Ajinomoto Co., Japan and used as received. Sodium trimetaphosphate (STMP) (Alfa Aesar) was used as received.

3.2.2 Gel Preparation and Rheological Evaluation

Whey protein: pullulan blend solution preparation

Total weight of solutions prepared for rheological studies was 17 w/w%, with relative amount of WP and pullulan varying. To prepare the biomaterial blend solutions, WP and pullulan powders were dissolved in deionized water (DW) and solutions were stirred for a minimum of 3 hours to ensure complete dissolution and stored under refrigeration. If any time had passed between initial solution preparation and use, they were stirred again for a minimum of 15 minutes to insure that phase separation was not a factor. Solution pH was measured with a Thermo Orion 5 Star pH meter. The viscosity of solution samples were measured at 25°C in a TA Instruments AR-2000EX stress controlled rheometer using a cone (40 mm, 2°) and plate geometry. WP and pullulan solutions were prepared measured at their resultant mixing pH. Additional solutions at varied pH were used to prepare gels for microscopic evaluation. Solution pH was modified using requisite amounts of either HCl or NaOH.

Whey protein: pullulan blend gel rheology

Dynamic shear rheological experiments were conducted on a TA Instruments AR-

2000EX stress controlled rheometer. Heat set gels were prepared *in situ* on the TA Instruments AR-2000EX stress controlled rheometer using both smooth and serrated parallel plate geometries with the Peltier plate controlled at 80 °C during gel formation. In dynamic experiments, samples were subjected to a sinusoidal deformation as a function of increasing oscillation frequency, and corresponding elastic (G′) and viscous (G″) moduli were measured. The frequency spectrum of the elastic and viscous moduli provided indication of level of gelation accomplished by the solution sample. Strain sweep experiments were conducted at a constant frequency of 1 rad/s, providing a method to examine sample yield stress. Exposed sample edges were covered with mineral oil to prevent evaporation.

Whey protein: pullulan blend gel rheology with enzyme and STMP addition

17w/w% solutions of Pullulan and Whey Protein Isolate (WPI) were made in stock solutions then divided into smaller stocks (native, enzyme, and STMP). These solutions were made in advance then split into ratios of 100% WPI, 100% Pullulan, 70WPI:30PULL, 50WPI:50PULL, 30WPI:70PULL either in the native state, with TG enzyme, or with STMP. Solutions were adjusted to pH 5.2 or 8. Rheological studies were conducted on a TA Instruments AR-2000ex stress-controlled rheometer using serrated upper and lower parallel plate geometries. Samples were heated on the rheometer *in situ* for 90 minutes at 80°C during the time sweep to observe gelation kinetics of the solutions. Frequency sweeps were then completed at 25 °C from 0.1 to 100 rad/s with the sample given time to equilibrate for 10 minutes. The last test was a strain sweep that imposed a 0.01 – 20000 %strain. The elastic stress was derived from the elastic properties of the gel multiplied by the resulting strain of

the gel, which was plotted against the %strain. Samples were taken before and after the rheological tests to visually see if the samples gelled before and after the heating as well as changed in turbidity.

3.2.3 Microscopic Observation

For Environmental Scanning Electron Microscopy (ESEM) evaluation, gels were prepared for a minimum of 30 minutes in a Despatch LDB laboratory heater for at 80 °C. A Quanta 200 Scanning Electron Microscope was operated in Environmental mode with a chamber pressure of 4.2-5.2 Torr, using water vapor as the chamber gas. A Peltier cooling stage was used to maintain a working temperature of 2 °C.

For initial confocal microscopy evaluation, gels containing 0.02 w/w% Rhodamine B were prepared on microscope slides in a nylon composite formed well, covered with a glass cover slide and heated for 30 minutes. Confocal microscopy was conducted using an Olympus IX81 Inverted Microscope with tandem Spinning Disk Confocal unit at 100X magnification. Additional confocal laser scanning microscopy images were recorded on a Zeiss LSM 710. Specimens were cut to fit a 1 cm diameter glass microscope slide and stained with aqueous Rhodamine B solution (0.2 % w/w) minutes prior to imaging. The set-up was configured with an inverted microscope (model Zeiss Axio Observer Z1) and a 40 × objective lens (LD C-Apochromat 40x/1.1 W Korr M27). The light source was a multiline argon laser with an excitation wavelength at 514 nm. The emission of Rhodamine B was recorded between 531 and 703 nm.

3.2.4 WP and WP:PULL blend FTIR and NMR

The infrared spectra of solution and gel samples between silver chloride crystals were recorded at room temperature using a Nicolet Magna-IR 750 spectrometer (Madison, WI). Dry air was continuously run through the spectrometer. The infrared spectra were recorded at 2 cm-1 resolution. A total of 128 transmission scans were recorded, averaged, and apodized with the Happ-Genzel function. Additional Infrared spectra were obtained on Nicolet 6700 FTIR spectrometer (Thermo Scientific, Madison WI) continually purged with nitrogen. Samples were analyzed directly on a germanium ATR by acquiring 128 - 512 scans at 4cm-1 resolution at ambient temperature.

The relative mobilities of the content species were evaluated through transverse relaxation time analysis (T_2) as measured by benchtop time-domain ^{1}H NMR. The data were accumulated on a Bruker HyperQuant mq-40 benchtop instrument resonating at 40 MHz. A Carr-Purcell-Meiboom-Gill (CPMG) pulse sequence was employed to measure T_2 values. The data was acquired with a 180° pulse separation of 0.04 ms, 8192 data points, and 15 dummy echoes (one echo data point saved for every 16 echoes generated). All data were collected at a sample temperature of 37 ± 0.2°C. A purified BLG solution was prepared at 17 w/w% in a 5:1 ratio of D_2O to H2O. The D_2O served to partially suppress the dominant signal from solvent H2O. One aliquot of the sample was heated to 80°C for 1 hour, which exceeds the gelation temperature of BLG and a gel was formed; the other aliquot was untreated and remained as liquid.

3.3 RESULTS & DISCUSSION

3.3.1 Effect of protein-polysaccharide solution properties on gel formation

We begin by investigating the impact of native biomaterial solution dynamics on gelation properties. We prepared blend aqueous solutions of different WP and PULL compositions while keeping constant the total biomaterial concentration at 17 w/w%. This concentration was chosen to exceed the WP gelation concentration of approximately 11 w/w% as well as the observed pullulan entanglement concentration in our laboratory as well as others,[65] yet still yield blends that will have an overall protein concentration less than this gelation concentration. It is important to note that the overall protein concentration of the blend is less than the established gelation concentration of 11 w/w%. This would then demonstrate that the addition of PULL would allow the lowering of the BLG critical gelation concentration. As seen in Figure 3.1(a), solution viscosity measured at room temperature all exhibit a Newtonian region, with only higher pullulan concentration solutions (greater than 50% of the blend weight as pullulan) exhibiting shear thinning as applied shear stress approached 100 Pa. Figure 3.1(b) shows a linear trend of viscosity increasing with increasing proportion of pullulan in the blend.

Blend solution samples were then heated in situ on the rheometer and viscoelastic properties were evaluated to verify the presence of a gel-like network. Figure 3.2 shows elastic and viscous moduli with evolution of frequency after solutions underwent a heating period. The 100% WPI samples were prepared on the rheometer with a heat set period of 30 minutes, while 50:50 WPI:pullulan blend gels were prepared for 90 minutes to insure a gel

network could form. Blend solutions that contained at least 50% WP exhibited gel characteristics in tilting and rheological tests, namely at relative concentrations of 85:15, 70:30 and 60:40 WP:Pullulan (data not shown). For all WPI and WPI-pullulan blend gels, elastic and viscous moduli had very weak frequency dependence, with G′ larger than G″ over the entire frequency spectrum, which is characteristic of a gel. A 100% pullulan solution was also subjected to *in situ* heating on the rheometer for 60 minutes prior to the dynamic experiment. As shown in Figure 3.2, the sample's viscous modulus dominated in the frequency spectrum, and both G′ and G″ demonstrated a much stronger dependence on frequency. This indicated that the 17 w/w% aqueous pullulan solution did not form a gel upon heating, which confirms prior observation.[57]

Many complex materials exhibit yield stress, which has been described as the largest applied shear stress before material flow occurs.[66] Figure 3.3a shows the dynamic moduli of the WP and blend samples as a function of increasing strain amplitude. Similar to WPI gel observations by Eissa et al. (2004), the dynamic moduli are flat at low strains exhibiting a LVE-like regime.[1] As strain increases, both G′ and G″ decrease slowly which indicates nonlinear behavior. As strain amplitude continues to increase, G′ and G″ begin to decrease as gel microstructure is disrupted, cross over and then decrease rapidly upon gel fracture. We determined fracture strain by plotting elastic stress, the product of the elastic modulus and strain (G′γ), as a function of increasing strain.[1, 66] Figure 3.3b shows the elastic stress as a function of strain for 100% WPI and 50:50 WPI:pullulan blend gels at both mix pH 6.8 and the WP isoelectric point pH 5.2. Data indicated that the 100% WPI gels have a higher fracture stress than their blend counterparts. However, the fracture strain of the 50:50 blend at

native (mix) pH 6.8 was higher than both WPI and BLG gels, perhaps due to the longer heat set duration of 90 minutes.

Table 3.2 summarizes fracture stress and strain for protein and blend gels evaluated in the first phase of our study. First, we can compare 100% WPI gels that were heated for 30 minutes, but of different pH: 5.2 (the BLG IEP) and pH 6.8. The protein gel formed from pH 6.8 solution was able to withstand higher strain (57%) while the gel formed at the BLG IEP only achieved 37% before fracture. However, the IEP gel did reach a larger maximum elastic stress of 5275 Pa while the native mix gel reached 4639 Pa. Yet, the pH 6.8 protein gel's broad maximum suggests yielding occurs more gradually[66], unlike the distinct sharp failure of the pH 5.2 gel as shown in Figure 3.3. This agrees with observation that gels at the IEP are more brittle, as particulate gels. During heat induced gelation of WPI aqueous solution, BLG – which is considered the most thermally active whey protein – denatures (unfolds) exposing reactive sites such as thiol groups, hydrophobic or ionized locations. At a high enough concentration, the protein chains also become entangled, facilitating gelation. Figure 3.4(a) and (b) shows two possible heat induced BLG structural modifications,[67] which are described by Linden & Lorient (1999) as follows:[67]

3. Neutral or alkaline medium: gelation improves if electrostatic repulsion stabilizes unfolded BLG molecules (gel firm, elastic)
4. IEP: precipitation occurs (gel opaque, brittle, granular)

Our visual observation of opaque, granular gels at the IEP as well as brittle behavior exhibited upon fracture confirms this.

We next compare 50:50 WPI:PULL blend gels formed with one at pH 6.8 and one at

the IEP. These were heated for the same period of time at 90 minutes. The pH 6.8 gel had both higher maximum elastic stress and maximum fracture stress. The pH 5.2 gel this time had a more broad peak, and thus a more gradual yield. As we will see when we evaluate microstructure, this is likely due to having larger liquid regions and less homogeneity than the neutral formed gel. Lastly, we evaluate (Table 3.2) the effect of heating time on the pH 5.2 50:50 WPI:PULL blend. The blend that only heated 30 minutes was able to withstand more strain before yielding due to its more liquid-like state; while the blend heated for 90 minutes did exhibit some signs of fracture but appeared to yield at 22% while fracturing at a higher strain similar to that of the pH 6.8 gel at approximately 150%. Data for the 50:50 pH 5.2 90 minute sample could indicate some signs of slip,[66] which we address later in this work by adding a bottom cross-hatched plate to *in situ* gel formation and analysis.

The protein gel higher values of fracture stress and elastic modulus both were attributed to the disulfide bonding crosslinks formed during heat set gelation. The presence of pullulan in the blend reduced the fracture stress likely due to a reduction in the number of crosslinks. As noted previously, pullulan does not form gels with increasing concentration or upon heat treatment. It must be noted that heat set gels formed from solutions near the isoelectric point are considered particulate gels in which whey protein is forming particle aggregates. The presence of these aggregates limits the ability of the blend gel protein component to crosslink, which explains the marked difference between the fracture stress and strain of the native and isoelectric point pH gels of more than an order of magnitude.

3.3.2 Blend Gel Microstructure

To further understand how WP:PULL blends behave, we observe gel microstructure using both ESEM and confocal microscopy. While standard SEM has been used to observe WPI gel microstructure in many studies,[1] this has required at least five preparation steps including glutaraldehyde fixing, osmium tetraoxide soaking, ethanol dehydration, carbon dioxide critical point drying and then, following gentle gel fracture, Au/Pd sputter coating. As Rizzieri et al. (2003) note, the ESEM allows the study of moist material in its most natural state.[68] We observed our samples at approximately 95% relative humidity in the ESEM chamber. While the beam of 20-25 kV accelerating voltage did cause some sample drying over time, we believe the ESEM allowed us to more accurately view the gel microstructure over standard SEM. Figure 3.4 shows ESEM images of a 60:40 WPI:pullulan 20 total w/w% pH 6.8 blend sample. This is a representative sample of many gels we observed at the native mix pH that had a very smooth surface as well as section, as seen in the top/side view in Figure 3.4(c).

Both ESEM and confocal microscopy comparison of 100% WPI and 50:50 WPI:pullulan blend 17 total w/w% pH 5.2 gels are shown in Figure 3.5. These are particulate gels, as noted by the appearance of aggregates. The smooth areas of the protein polysaccharide blend gel are likely pullulan regions as polysaccharide have previously observed to have a smoothing effect on heat set protein particle gels. [69] The confocal images are highlighted by the presence of the fluorescent dye and hydrophobic molecule Rhodamine B (RhB). The ESEM samples did not contain RhB. The blend gel had larger voids than its

protein counterpart, and a less homogenous particulate structure. The voids are likely responsible for the lower fracture stress values of the blend gels. However, controlling gel properties utilizing the presence of the non-gelling pullulan amongst the crosslinked protein structure could allow both flavor and active ingredient exposed surface area and diffusion control in food and pharmaceutical applications. The three dimensional image at the bottom of Figure 3.5 shows protein microparticles or aggregates that formed in a 50:50 WPI:PULL blend at the IEP after heat treatment. The blend had a particulate appearance as expected and shows similar features to the ESEM blend image, especially the lower left hand corner of the middle left image which looks identical to the surface of the aggregates in the three dimensional image.

Further investigation into the WP and WP:PULL blends utilized FTIR before and after heating and full spectra results are given in Figure 3.6. After heating, in both the WP and WP:PULL blend gels, a new peak is identified at approximately 1456 cm^{-1} that corresponds to the formation of disulfide bonds. In the WP:PULL blend gel sample, an additional peak is also identified at 2962 cm^{-1} which is identified as C-H asymmetric stretching. This would indicate that the addition of pullulan in the gel state would make the gel much more flexible when less water is present compared to the all protein gel and low viscosity solution.

From the NMR evaluation, the T_2 relaxation times were obtained for purified BLG, purified BLG:PULL and PULL solution samples before and after heating and are provided in Figure 3.7. The liquid sample yields a solvent (water) peak at approximately 1370 ms. Both samples then appear to have corresponding peaks. The different peaks indicate species with different mobility in the system. In each, there may be dimers or monomer of protein as well

as BLG variants, as these samples are at pH less than 7 where dimers are expected to be BLG's native state. Further study is warranted to determine the impact of solution preparation as well as impact of pH and blend with the mobile polysaccharide pullulan. The gel sample has shorter relaxation times, indicating less mobile species, as well as fewer peaks. This method can not only evaluate the impact of heating on water mobility,[70] but also of the BLG species themselves; preliminary pullulan/BLG blend system data are generating additional peaks as expected from a commercial material.

From examining microstructure with these tools for both WP and WP:PULL blends, we can identify that the addition of pullulan to a protein solution at various concentrations will permit flexibility for biomaterial design with these nutritional substances.

3.3.3 Modifying WP:PULL blends with enzyme and STMP addition

To permit additional design flexibility and even nutritional gains to our protein gels and protein-polysaccharide blends, we can employ the use of additives to our aqueous solution prior to heat treatment with both TG enzyme and STMP. TG enzyme has been well studied as a whey protein crosslinker.[1, 17, 71-77] Activia TI TG that we use here is a commercially available form of the transglutaminase enzyme with the ability to crosslink protein. Various forms of TG can be found in animal, plant, and microbial sources. This TG crosslinks proteins through covalent bonding of the two amino acids glutamine and lysine; proteins high in these amino acids may be effectively crosslinked. TG is active over a wide range of pH and temperatures but is inactivated at higher temperatures which vary with the conditions and composition of the food system.[78]

STMP has been used as a phosphorylation agent for both protein and sugars as a means of enhancement for improving their functional properties.[79, 80] STMP is often used in the food industry as a cross-linker as it is non-toxic to humans. It works by linking the polymer chains with phosphates.[49,81] We employ both of these food additives to investigate their influence on heat treating of WP and WP:PULL blend solutions.

Heating protein solutions above their denaturing temperature (80-90 °C) will unfold the protein and decrease gelation time[76,78] As we have discussed, BLG needs to be partially denatured or fully denatured by raising the pH to around 8 to begin to cross-link and form gels. Transglutaminase can be introduced into the protein solution when the protein is partially or completely denatured and this will decrease gelation time. Optimal pH and temperature for TG impact has been shown to be 8 and 50 °C, respectively.[78] STMP has been used as a chemical in the phosphorylation of protein[79,82] to supplement food with phosphorus; as well as reactant with sodium hydroxide initiator to form pullulan hydrogels.[49, 81, 83] We investigate the interaction of enzyme and STMP in WP:PULL blend solutions at both pH 5.2 (BLG IEP) and pH 8 (where TG is active and STMP has some initiator (NaOH) present to begin reaction with PULL) to see if the combination of these additives will further enhance or inhibit gel formation and viscoelastic properties.

Initial studies were completed by heat treating blend solutions in vials and viewing qualitatively with tilting tests (see Appendix A). All whey protein only and blend solutions formed gels at pH 8, whether native or containing TG enzyme. However, pullulan only solutions did not form complete gels in any case. When comparing the pullulan solutions to those solutions utilized to form hydrogels with STMP in previous work[81], the concentration

of both pullulan and NaOH in our blends was not as high as the pullulan concentration in their work (we used a maximum of 17 w/w% at pH 8 while they used 20 w/v% and resulting in pH 12+, respectively).[81] Therefore, we did not have adequate pullulan or NaOH concentration to achieve gelation of the pullulan-only solution.

Based on our qualitative analysis of the samples at pH 8 (Appendix A), we found that STMP initiated aggregation in the 100% WP samples. The 70:30 WP:PULL blend with enzyme exhibited phase separation and at this blend ratio all samples with additive showed some protein aggregation yielding a milky sample compared to the transparent native sample, with the strongest one being that with STMP only. None of the 50:50 WP:PULL blend samples indicated any phase separation, but again both samples containing STMP were milky and opaque, indicating the occurrence of protein aggregation. In the predominately pullulan blend sample set (30:70 WP:PULL), native and enzyme samples were clear, but samples containing STMP were milky and the one with STMP-only had some minor phase separation. All 100% pullulan samples were clear and did not form complete gels after heating. All pH 8 samples that contained WP formed a gel with no residual liquid upon tilt. For samples at pH 5.2, all WP:PULL blends exhibited some degree of phase separation which agrees with the Wang study discussed above, but also did form gels.

Impact of pH and composition on gelation kinetics

To understand gelation kinetics of our WP and WP-PULL blend systems, we completed rheological evaluation using dynamic time sweeps during heat set and then frequency and strain sweeps following a heat treatment of 90 minutes at 80 °C. Figure 3.8

shows the evolution of the sinusoidal stress phase shift δ over time during heating for 100% WPI, 50:50 WPI:PULL blends and 100% PULL solutions at both pH 8 and the IEP pH 5.2. δ = 45° has often been used as a rough gel point estimation although final frequency plots dictate if the sample is a true gel. [84] Figure 3.8 shows that for the pH 8 100% WPI samples, the native solution drops quickly to a small value (~ 4), indicating rapid gelation. The pH 8 100% WPI solution with TG enzyme δ also drops quickly, while the solution with STMP gels more gradually. For the pH 8 WPI:PULL blends, even though the systems each take longer to reach a δ < 45° , they begin exhibiting gel-like properties each with similar shape of the δ curve to that of the 100% WPI samples. The pH 8 enzyme gelation kinetics are slower, making a more gradual decrease with the blend. The native blend solution gelation occurs much more rapidly, once it starts, signified by a steeper slope in the δ curve which indicates rapid gelation by protein denaturation and disulfide bonding at pH 8. The presence of either TG or STMP does seem to prevent protein-protein network formation; their presence drives bond formation leading to an alternative network structure. For pH 8 100% PULL solutions, all three systems, native, enzyme and STMP, take considerably longer to see a significant change in δ. During the end of the 90 minute heating, the native and enzyme pH 8 pullulan solutions do reach the δ < 45°, while the STMP-containing sample only reaches a δ of about 60°.

The pH 5.2 samples follow much different kinetics thus a different shape of the δ-curve and time to reach δ plateau. The first sample of the 100% WPI solutions to drop in δ, and most sharply, is the one containing enzyme, which is counterintuitive to what we would expect, as the enzyme is not considered as active at this pH.[1] However, the enzyme

containing sample also plateaus more quickly to approximately 20. The sample containing STMP eventually δ-plateaus later, but at a lower value as well at around 10. The blends take considerably longer to δ-drop, and with the blend samples we do not observe a plateau in the time frame used. However, no 100% pullulan samples gelled based on observed tilting studies and rheological data.

Impact of TG enzyme and STMP on gel "strength"

Figure 3.9 provides frequency sweep data for samples. This data was collected just following heat treatment. For pH 8 blend systems (Figure 9a), TG provided more elasticity to WPI only gels with a higher elastic modulus plateau compared to that of pH 5.2 systems, which do not appear to be completely gelled due to some frequency dependence. In 100% WPI only gels, protein aggregation at the BLG IEP (Figure 9b) decreased gel elasticity by anywhere from one to three orders of magnitude. 50WPI:50PULL blends showed a marked decrease in elasticity as well as gel formation with a two to three order of magnitude drop in G'. The change to IEP pH had less impact on the protein-only gels, dropping just one order of magnitude. As realized in studies without additive above, PULL impeded the ability of the WP to form networks. At the IEP, the addition of enzyme did appear to increase gel elasticity compared to the blend without enzyme. As seen in microstructure evaluation (in previous section above) at the IEP, non-aggregated regions of the gel are likely fluidic containing the non-gelling pullulan. The addition of TG is likely adding bond formation here, although not expected to be active at this pH, it is playing a role, perhaps regionally within the blend. Overall, for 100% pullulan solutions, the addition of additives for the

conditions applied (polymer concentration, pH and heating) had minimal effect (data not shown).

As shown in Figure 3.9c, the addition of STMP has minimal impact on the 100% WPI sample, but lowers the magnitude of the WP:PULL blend below that of native solutions. The STMP is likely facilitating formation of an alternative, but weaker, network to that of the native blend sample. Figure 3.9d shows the impact of STMP on gels prepared at BLG's IEP. Again, as with enzyme, the protein aggregation has a strong impact on the elasticity of the blend gels by several orders of magnitude. The elastic modulus also is reduced much more by the presence of STMP in the WP only gel, perhaps getting in the way of WP networks forming or unable to react with protein or polymer with not enough initiator present. However, in comparing the blend gels, the one containing STMP is actually stronger, perhaps due to the ability of STMP to form bonds between proteins as well as the polysaccharide. STMP forms bonds by linking the alcohol groups of two different polymer chains, but needs an alkaline environment to do this.[85]

To further interpret relative gel strength, we determine tanδ as it evolves with frequency, as shown in Figure 3.10, from frequency sweep data. Shim & Mulvaney (2001) evaluated gels of WPI and corn starch observing that paste-like weak gels had a tanδ of > 0.1 while firm true gels tanδ was < 0.1.[86] The delta is related to the ratio of the viscous to elastic modulus as follows[87]:

$$\tan \delta = G''/G'$$

where G″ is the viscous modulus and G′ is the elastic modulus. For both pH 5.2 and pH 8, all 100% PULL solutions showed the most frequency dependence. At pH 8, values for both

100% WPI and WPI:PULL blends all exhibited the character of a crosslinked network near to that of a "true gel;" while at pH 5.2, WPI:PULL blend systems regardless of additive all demonstrated some frequency dependence. Samples containing STMP appeared to have the most frequency dependence as well; while the blend with added enzyme had less frequency dependence by its value of tanδ was approximately 0.5 – and these results indicate that the WPI:PULL blend with enzyme can form a weak network under these conditions. In taking a closer look at the value of tanδ none of the 9 samples at any of these conditions actually achieve < 0.1, or even 0.2 consistently. To completely eliminate a measured frequency dependence, perhaps a longer heating time is required, or even time for additional reactions to occur.

Figure 3.11 provides elastic stress versus strain data for both WP and WP:PULL blend gels prepared at pH 8 and pH 5.2, in the native state as well as with the addition of enzyme and STMP. First, in comparing the native WP to the WP:PULL blend, both gels exhibit approximately the same maximum elastic stress and corresponding fracture strain. The blend sample with enzyme, however, has a fracture strain at maximum elastic stress an order of magnitude lower than the protein only sample, yet achieves a higher maximum elastic stress than the WP only sample. Both samples with STMP appear to only yield after achieving a similar maximum elastic stress in the WP sample, but an order of magnitude lower maximum in the blend. Pullulan, although it does not achieve a true gel on its own, is easily "plasticized", forming films and adhesives, and is highly water soluble, mixed with WP provides additional flexibility in gel formation. Gounga et al. (2010) reported that the addition of pullulan to the film forming solution decreased tensile strength and the elastic

modulus of films, but increased the elongation at break – its ability to "stretch."[63] The mobility and flexibility of the pullulan in solution may account for this.

Samples without additive (native) show little variation with pH and concentration except for the 100% WPI gel samples where alkaline pH 8 (where WP is denatured) has a much higher fracture strain at maximum elastic stress than its acidic or IEP counterparts. It is interesting to again note here that the replacement of WP by PULL in the blends does not have significant impact on the yield strain, so that WP:PULL can be effectively used. In looking at native samples of yield or fracture stress, all gels at the protein IEP have a very low yield stress, while the alkaline pH have higher, indicating that the unfolded protein is reacting to form covalent bonds and this stronger network.

The addition of enzyme is most effective at pH 8 for the highest concentrations of WP in increasing the ability of the gel to withstand more strain. For the fracture stress, alkalinity is important to achieve the highest maximums – again indicating that bonding is important even in the blends, of both the disulfide as well as enzyme induced protein bonds. 50:50 blend and higher do exhibit higher fracture stress than native samples on the whole, even of the pH 5.2 sample. The pH 8 blend sample also demonstrates this, while the yield stresses of the pH 8 sample blends indicate a nice increasing trend with increasing protein content, which also implies that phosphorylation between protein and STMP is having an influence on the maximum yield stress, as opposed to reaction with pullulan.

Impact of TG enzyme and STMP on network formation at pH 8

FTIR spectra for all nine samples at pH 8 are given in Figure 12. All samples show hydroxyl band peaks in the 3368-3384 cm-1 range as well as 1044 cm-1 C-O stretching, Amide I (1640 cm-1). As Gounga et al. notes, subtle changes in shape, shift and/or intensity of FTIR peaks indicates intramolecular alteration. [63] All protein samples contain the Amide II (1548-1550 cm-1) peak due to stretching of N-H and vibration of C-N[63], while pullulan may be exhibiting C-O stretching at 1153-1155 cm-1. All samples containing pullulan are exhibiting a peak at 2047 cm-1 which is indicative of N=N stretching. This peak is present because this stock pullulan solution was prepared with a small amount of sodium azide preservative.

STMP's presence in each of the samples is indicated by sample-containing peaks at 1267 cm-1 and P=O stretching. C-O stretching at 1080-1087 cm-1 is also present in all but the native protein sample, but strongest in peak magnitude in each of the STMP containing samples. This is likely indicating that indeed C-O bonds have formed with the presence of the STMP through a crosslinking reaction. Each STMP-containing sample has a peak 1004-1017 range, which also is likely indicative of P-O-C stretching, also due to the formation of STMP-biomaterial crosslinks. Gounga et al. concluded that WPI:PULL film had "greater water-binding capacity and contained more water associated with protein" than WPI alone.[63] The PULL made the film more water soluble – with hydrogen bonding being more predominant in PULL-containing films. This would also be expected for the WP:PULL blend gels.

Impact of additives on gel microstructure at pH 8

In the confocal microscope microstructure images in Figure 3.12, the protein network is indicated by the bright areas which are stained by RhB; dark areas correspond to areas without protein, similar to Figure 3.5. Samples of 100% pullulan did not form gels and were not evaluated. Samples of 100% WPI and WPI:PULL blends either native or with TG were homogeneous and continuous and did not have observable microstructure, as shown in Figure 3.12(a), (b), (e) and (f). This is also the case for all pullulan solutions, as all solutions remained clear and transparent with both additives and heat treatment. However, both WP and blend samples containing STMP showed microstructure. Sample in Figure 3.12(c) appears to be more like a particulate gel, while the blend sample with STMP in Figure 3.12(f) appears to be more have some particulate and course stranded regions, along with more voids due to the protein aggregation rich areas leaving pullulan in its network voids. In each of these samples, protein-protein interactions were stronger due to the formation of aggregates.

In comparing data in Figure 3.11 to microstructure, it is apparent that although WPI-STMP and WPI:PULL-STMP have a similar fracture strain at maximum stress, the more particulate WPI-STMP gel sample was able to withstand a higher maximum stress than the sample without PULL. Also, both samples containing enzyme exhibited a higher yield strain than native (homogenous continuous) samples. The WPI:PULL-STMP sample, which has the most dark regions in its course particulate microstructure, had an order of magnitude lower elastic modulus than the other microstructure samples and is thus behaves and appears more liquid like.

3.4. Conclusion

Whey protein and pullulan blend gels have been evaluated using microscopy and rheological methods. Protein gels had higher fracture stress than its blend counterparts. Also, blend gels formed at the protein isoelectric point of pH 5.2 exhibited fracture stresses more than an order of magnitude lower than its native mix counterpart; while 100% WPI gels of different pH had fracture stresses and strains of the same order of magnitude. The presence of the pullulan in the protein aggregated solution inhibited protein heat induced crosslinking. ESEM and confocal imaging showed smooth gel microstructure at pH 6.8, but particulate gel microstructure at isoelectric point pH 5.2. Particulate blend gels contained larger voids, which indicated less crosslinking and thus may explain the lower fracture stresses. Changing the continuous network from protein to protein-pullulan blend appeared to cause an increase in water holding properties as well.

As shown by the varying gel fracture stress and strain as well as microstructure, the addition of pullulan to the whey protein gel permits new concentration controlled protein-polysaccharide blend gel design for biomedical, food and pharmaceutical application. WP:PULL blend solution and gel properties can be manipulated by heat treatment and addition of TG and STMP. Gel yield strength was increased by TG at higher WPI concentrations, while STMP reduced the magnitude of the system viscoelastic response. Depending on the pullulan/WPI blend concentration desired, TG or STMP can be used to manipulate system properties. Enzyme enhanced gel yield strain over native gels; while pullulan and STMP reduced the elasticity of the gels. ESEM revealed gels with microstructure at the protein isoelectric point, but smooth transparent gels at near neutral and

pH 8. Benchtop NMR is a promising tool for evaluating species mobility in protein solutions.

ACKNOWLEDGMENTS

Special thanks to: Davisco Foods for providing BiPRO whey protein isolate and BioPURE beta-lactoglobulin. Hayashibara International for providing PI-20 pharmaceutical/food grade pullulan. East Carolina University Department of Biology Dr. Jason Bond for ESEM use and Drs. Timothy Christensen and Matthew Schrenk for Olympus confocal microscope use, and to Dr. Eva Johannes for Zeiss confocal microscope support. Thank you for support of Thomas A. Deaton, Eric W. Franson, Mohammed S. Akbar, Christopher A. Eckert and Michael S. Cannon for assistance.

.

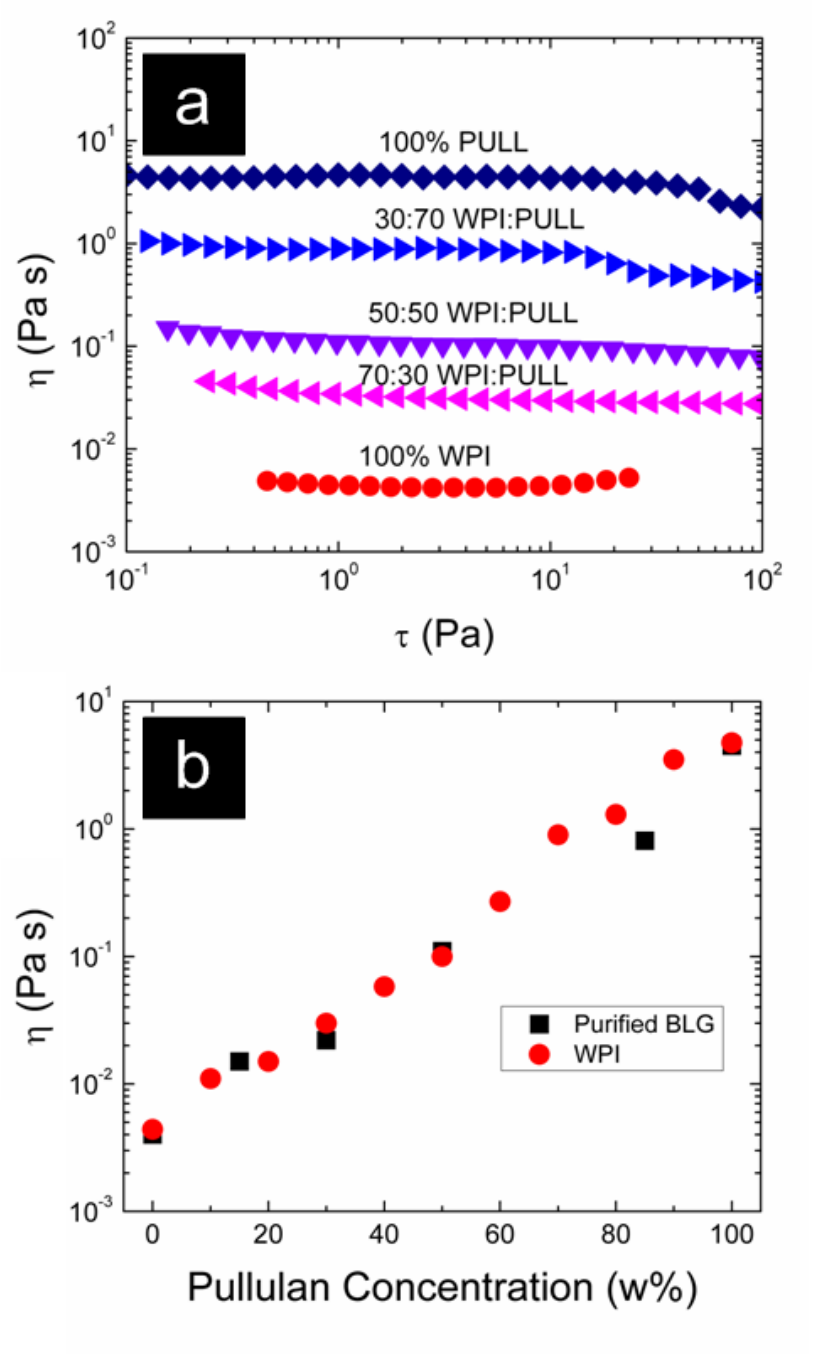

Figure 3.1: (a) Solution viscosity vs. Shear Stress for 100% WPI, 50:50 WPI:PULL blend and 100% PULL 17 total w/w% aqueous solutions. (b) Solution low shear viscosity of 17 total w/w% whey protein and pullulan blend solutions. X-axis denotes pullulan percent of total weight.

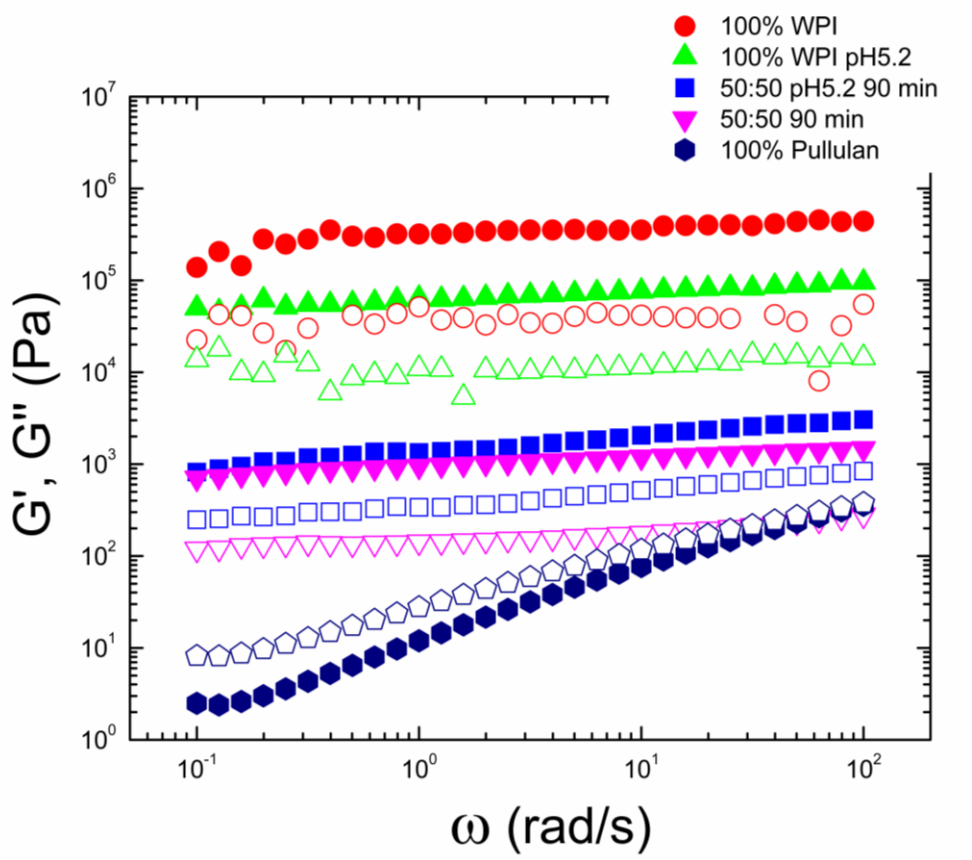

Figure 3.2: Dynamic frequency spectrum of the Elastic (G′) (closed symbols) and viscous (G″) (open symbols) moduli of protein and protein-polysaccharide blend heat set gels and pullulan heat treated 17 total w/w% solutions.

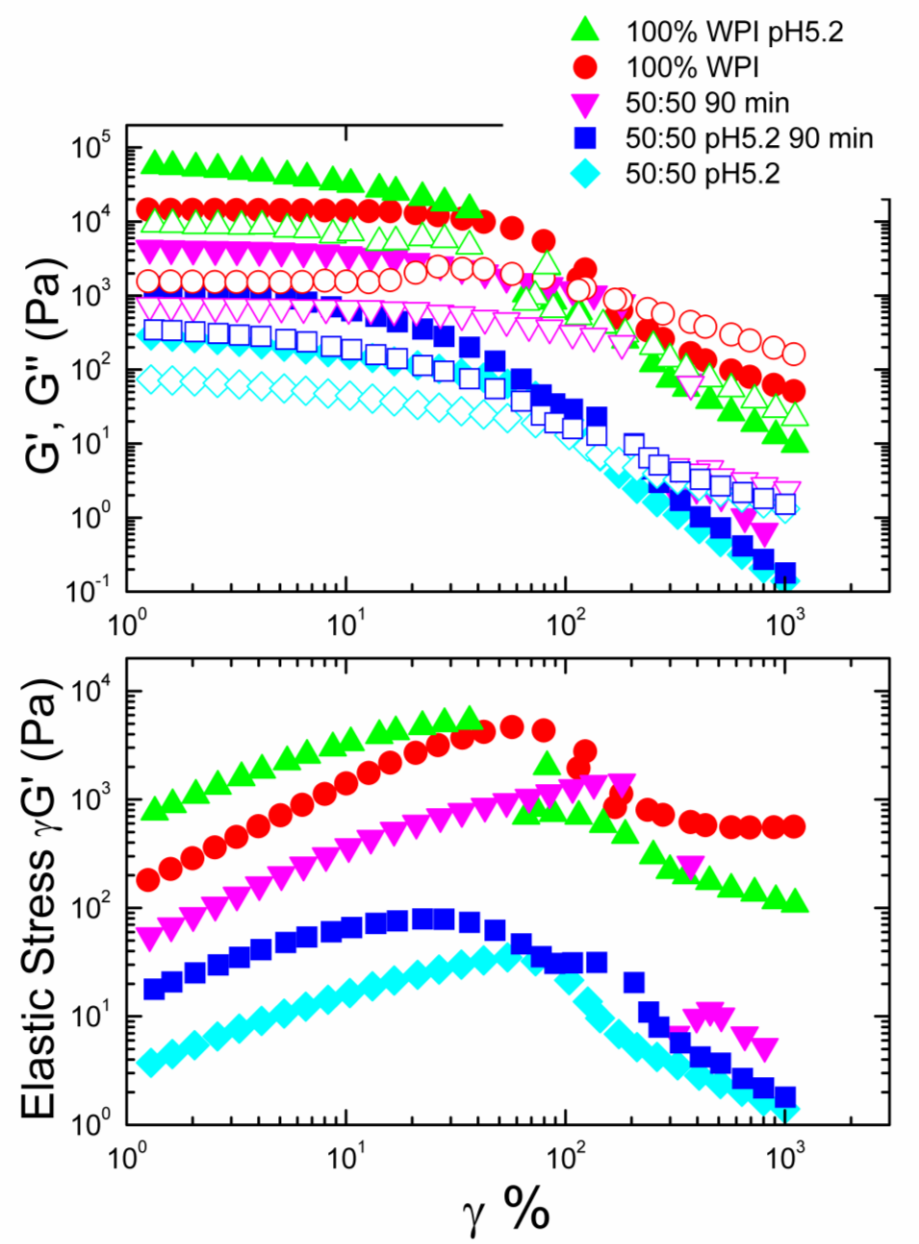

Figure 3.3: Effect of increasing strain amplitude on top: Elastic (closed symbols) and Viscous (open symbols) moduli and bottom: Elastic stress G′γ.

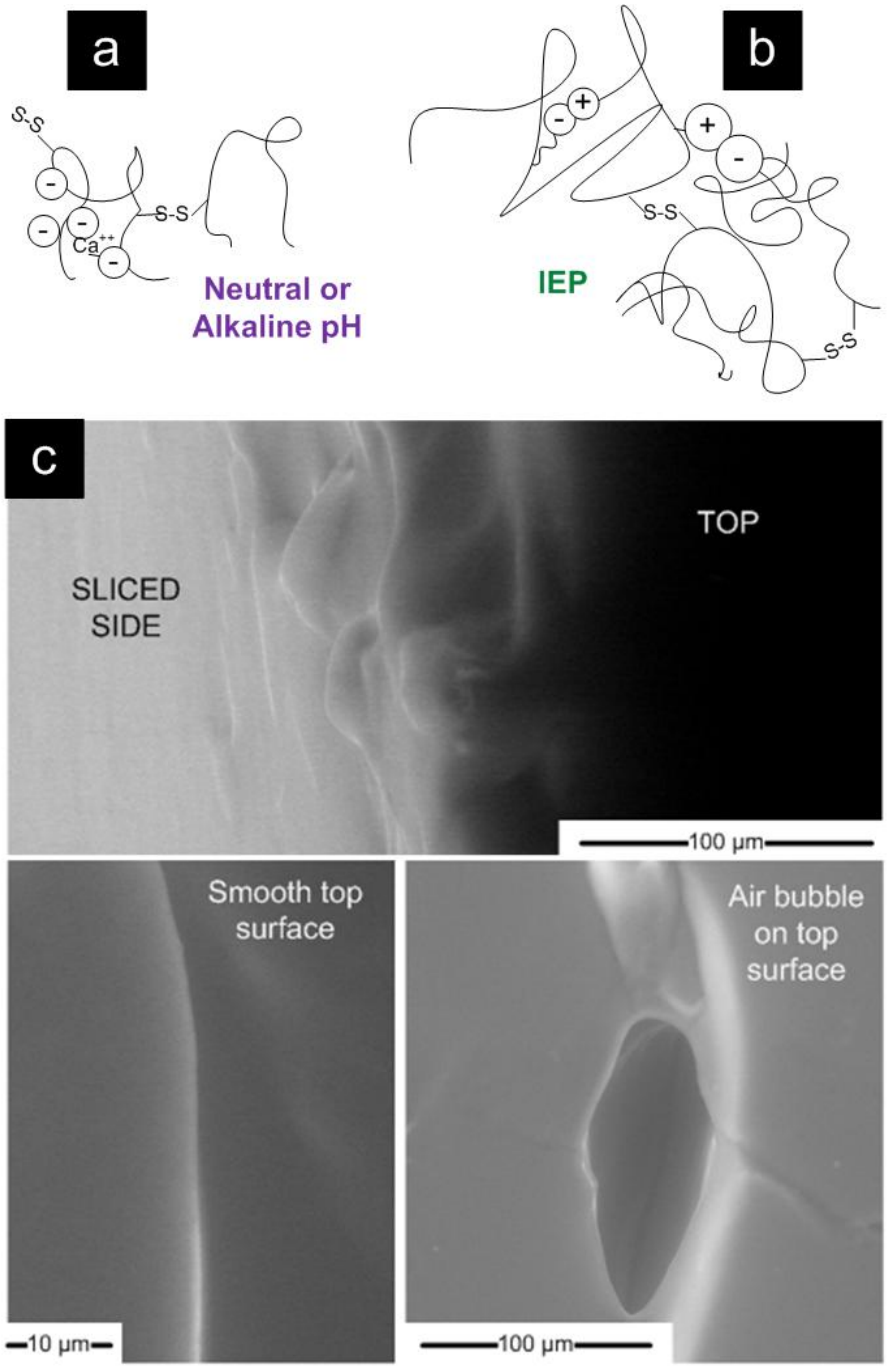

Figure 3.4: Schematics for heat induced structural modifications of BLG for (a) neutral or alkaline medium such as pH 6.8 or (b) at the BLG isoelectric point (IEP) [recreated from Linden et al., 1999][67] with (c) ESEM of WPI:PULL blend gel slice. Representative sample of homogeneous continuous gel samples; this formed from pH 6.8 20 total w/w% solution 60:40 WPI:pullulan by weight. Surface of gel has smooth topography and no visible particles and thus is not a particulate gel.

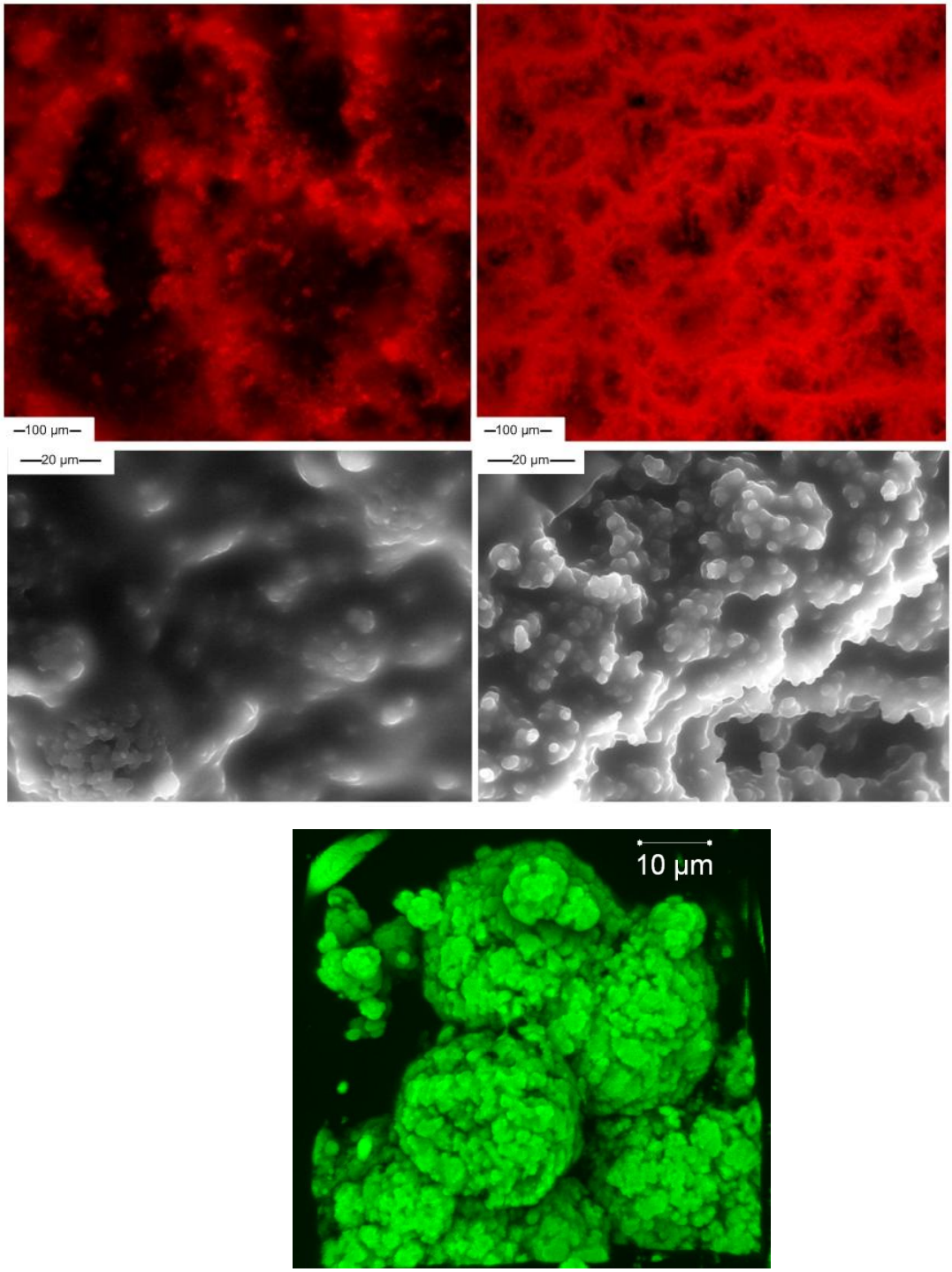

Figure 3.5: Confocal (top) and ESEM (middle) images of WPI:Pullulan 50:50 blend (left) and 100% WPI (right) particulate gels slice. Gel formed from pH 5.2 17 total w/w% solution. Bottom is 3D confocal image of protein aggregation observed in 50:50 WPI:Pullulan blend.

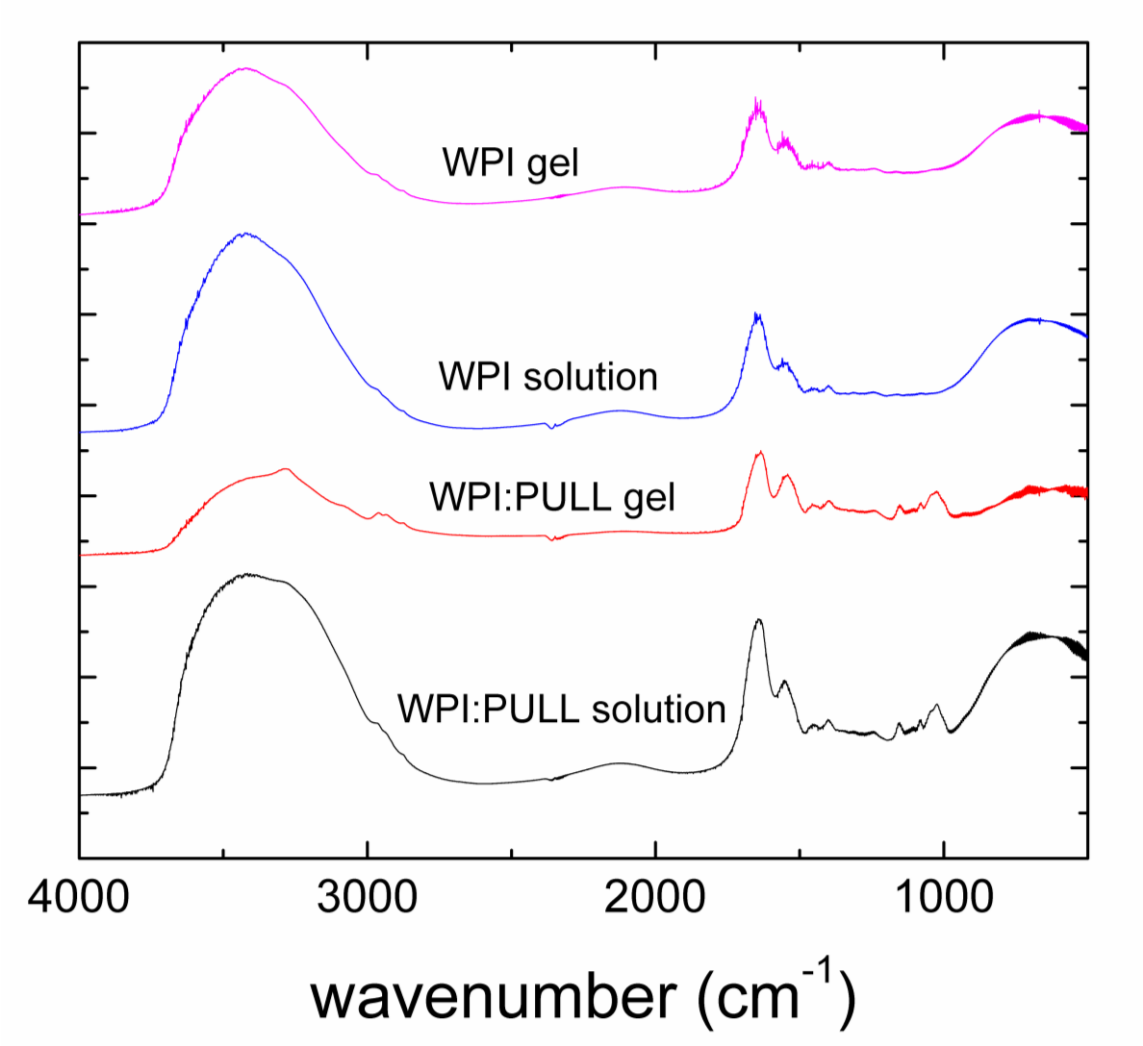

Figure 3.6: FTIR spectra of WP only and WP-PULL blends before and after heating at native mix pH. In the blend solution, there is a noticeable shift in the hydroxyl band including a more predominant peak at 2962 cm^{-1} indicating C-H asymmetric stretching.

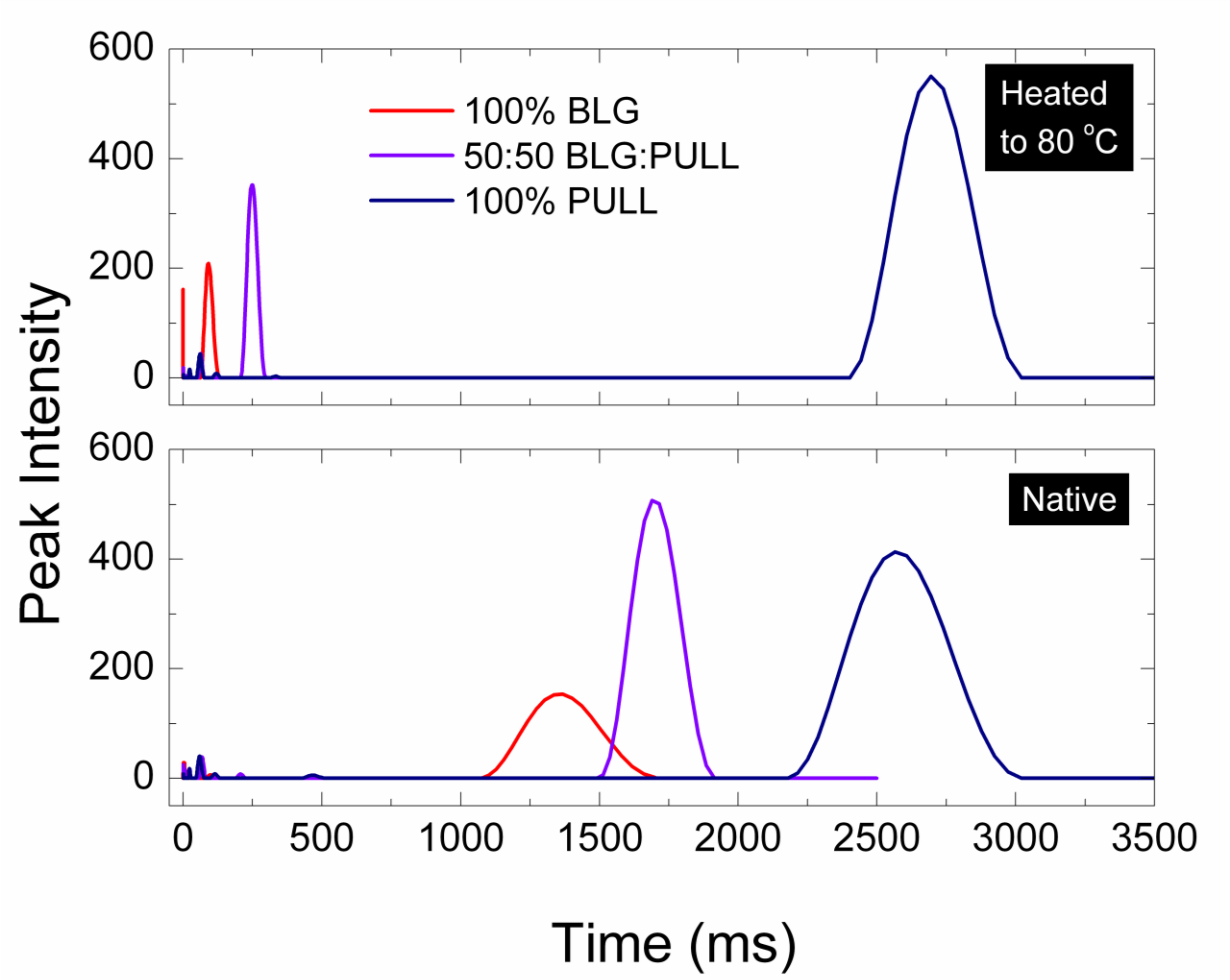

Figure 3.7: Benchtop time-domain NMR transverse relaxation times (T_2) for purified BLG, purified BLG:PULL and PULL native and heat treated aqueous solutions

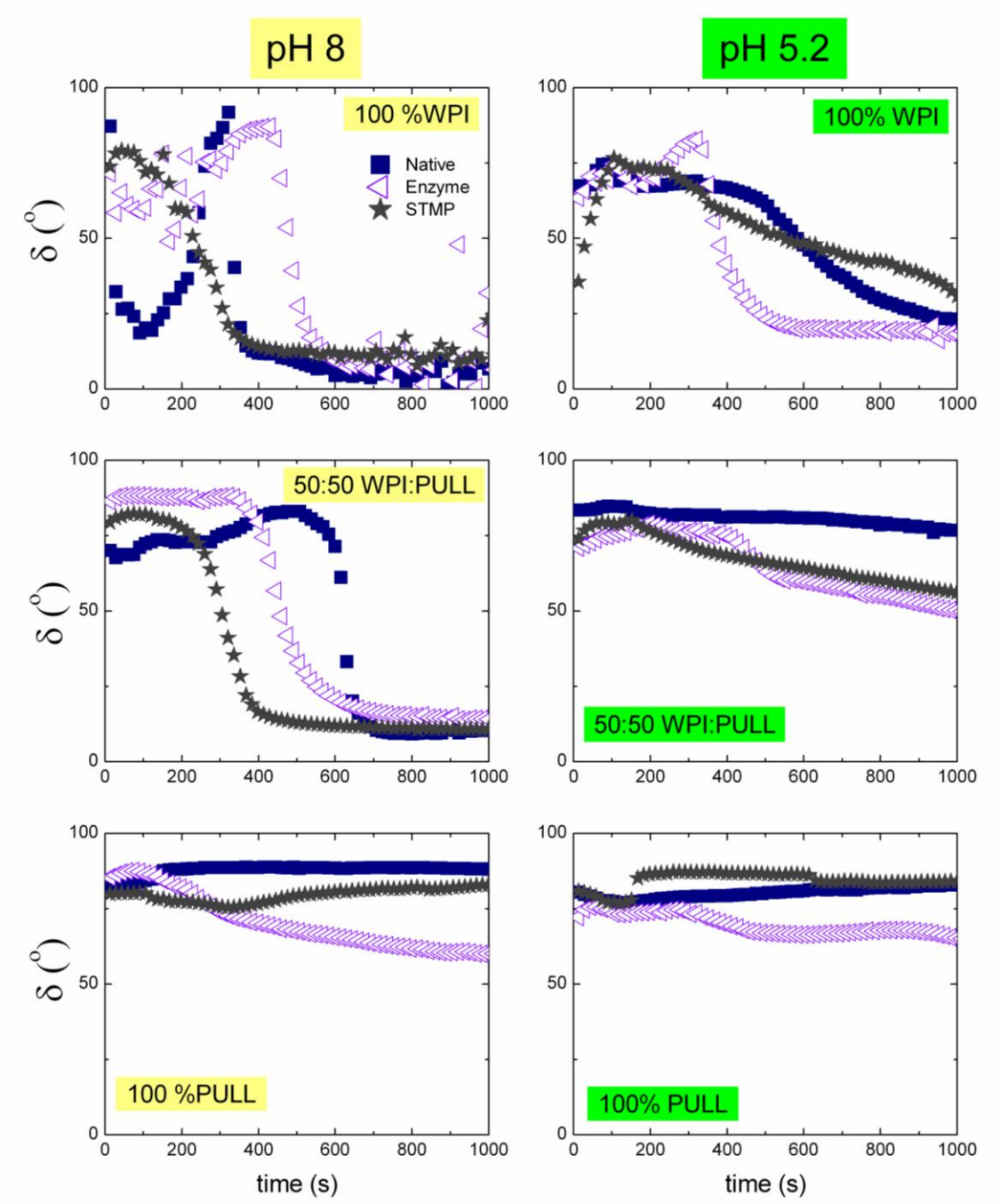

Figure 3.8. δ evolution during heating at 80 °C (ω = 1 rad/s) as a function of time for 100% WPI, 50:50 WPI:PULL blend and 100% PULL solutions at pH 8 (left) and pH 5.2 (right). Blend solutions were prepared at 17 total w/w% with as received native whey protein isolate and pullulan.

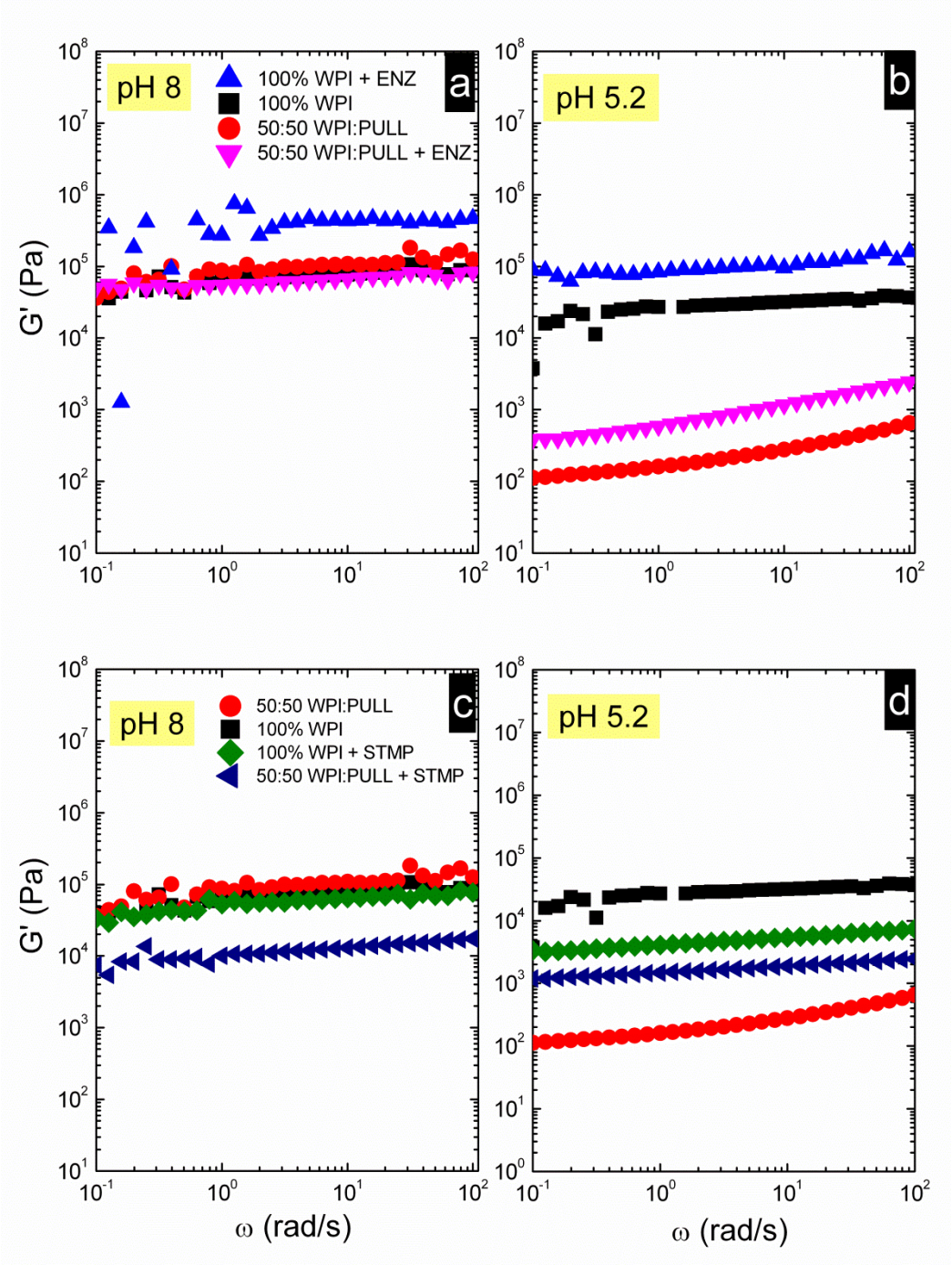

Figure 3.9. G′ elastic modulus evolution during dynamic oscillatory frequency sweep comparing WP and WP:PULL blend solutions comparing (a) at pH 8 and (b) at pH 5.2 the addition of TG enzyme; while comparing (c) at pH 8 and (d) at pH 5.2 the addition of STMP.

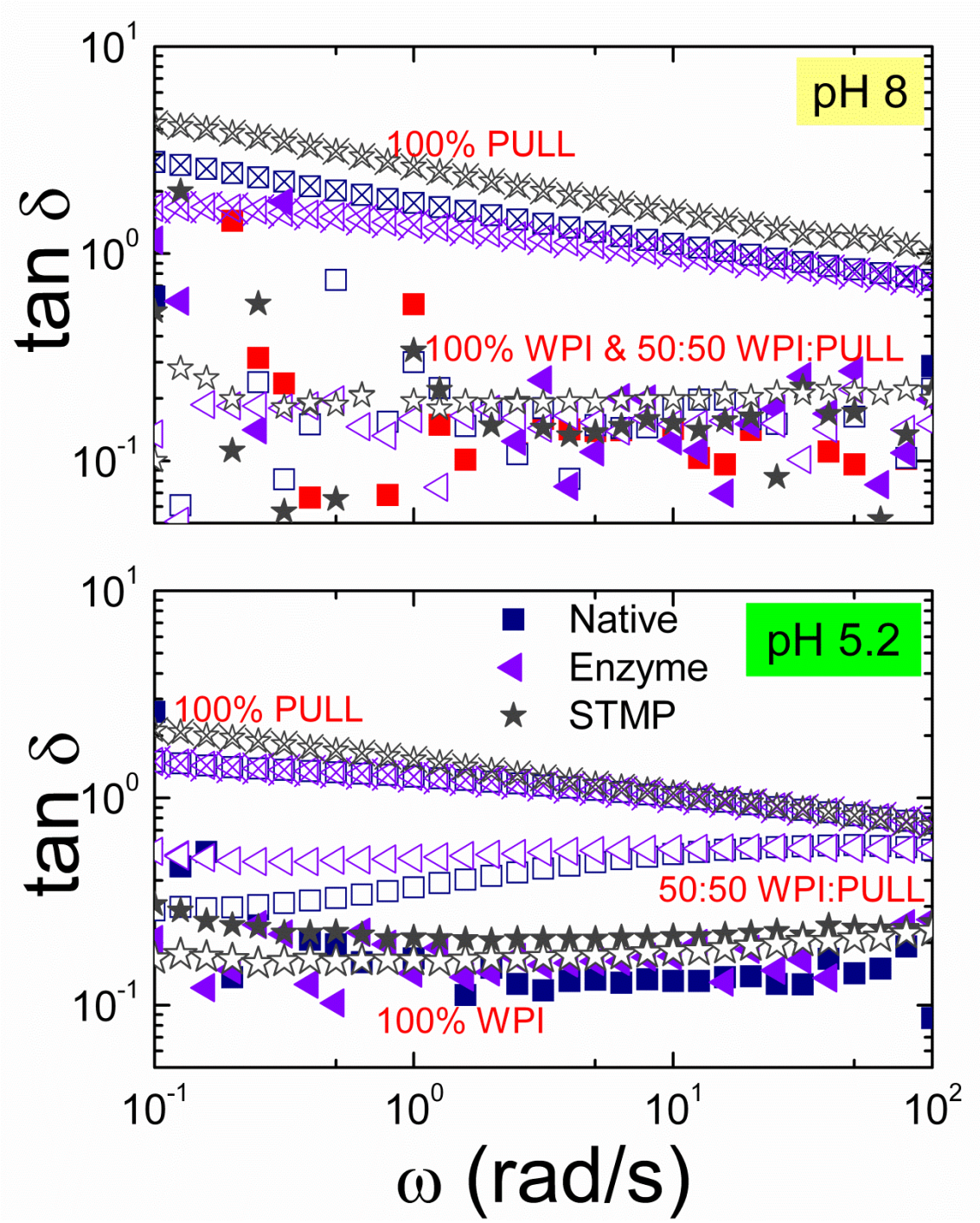

Figure 3.10. Effect of frequency (ω) on tan δ for pH 8 (top) and pH 5.2 (bottom) formed gels with additive transglutaminase enzyme (Enzyme) or sodium trimetaphosphate (STMP) and without (Native), where solid symbols are 100% WPI, open symbols are 50:50 WPI:PULL blends, and x-centered symbols are 100% PULL.

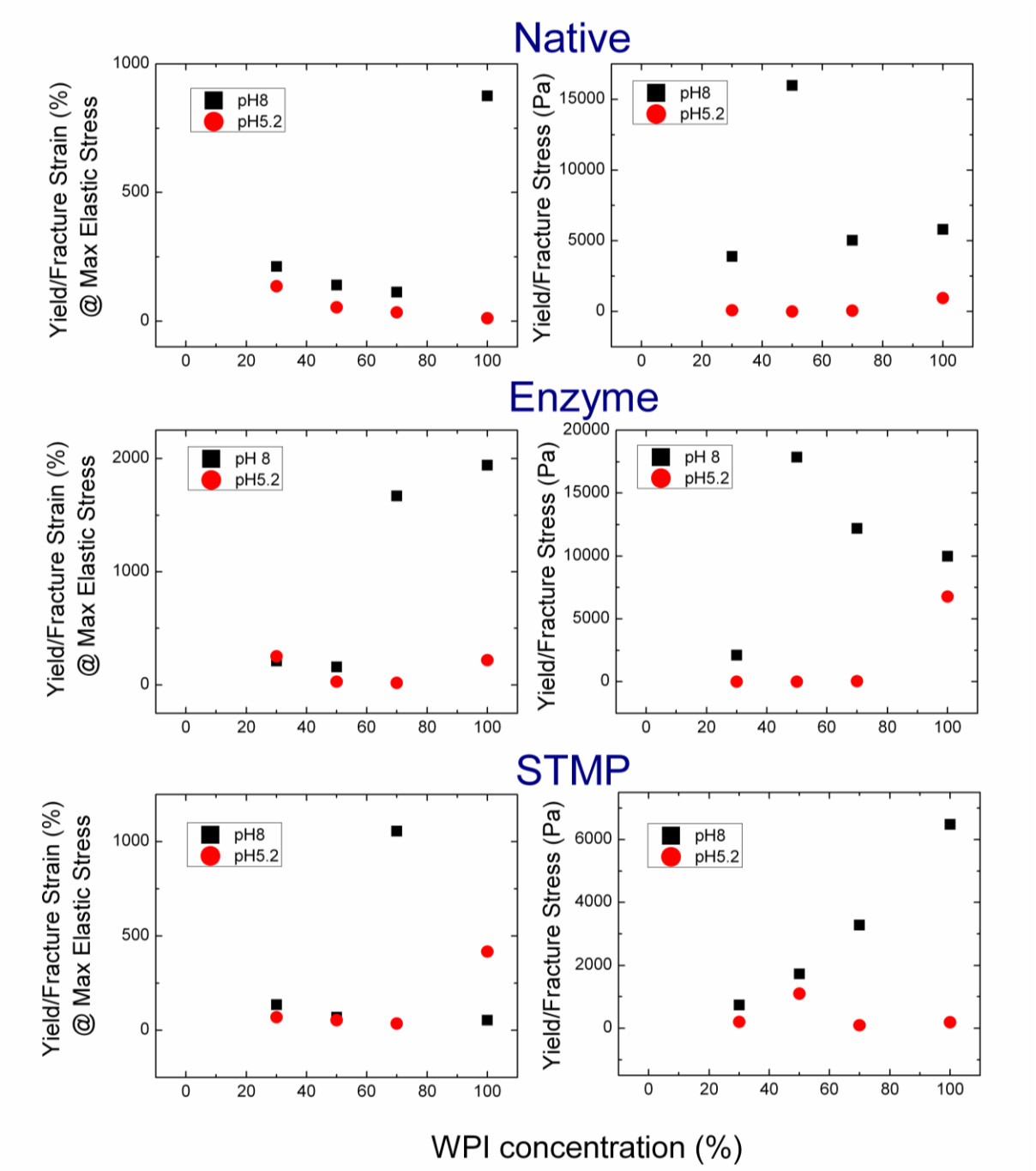

Figure 3.11. Yield/Fracture Stress and Yield/Fracture strain % at maximum elastic stress versus WPI concentration as % of total of 17 w/w% original solution concentration for native (top), TG enzyme (middle) and STMP (bottom) gels.

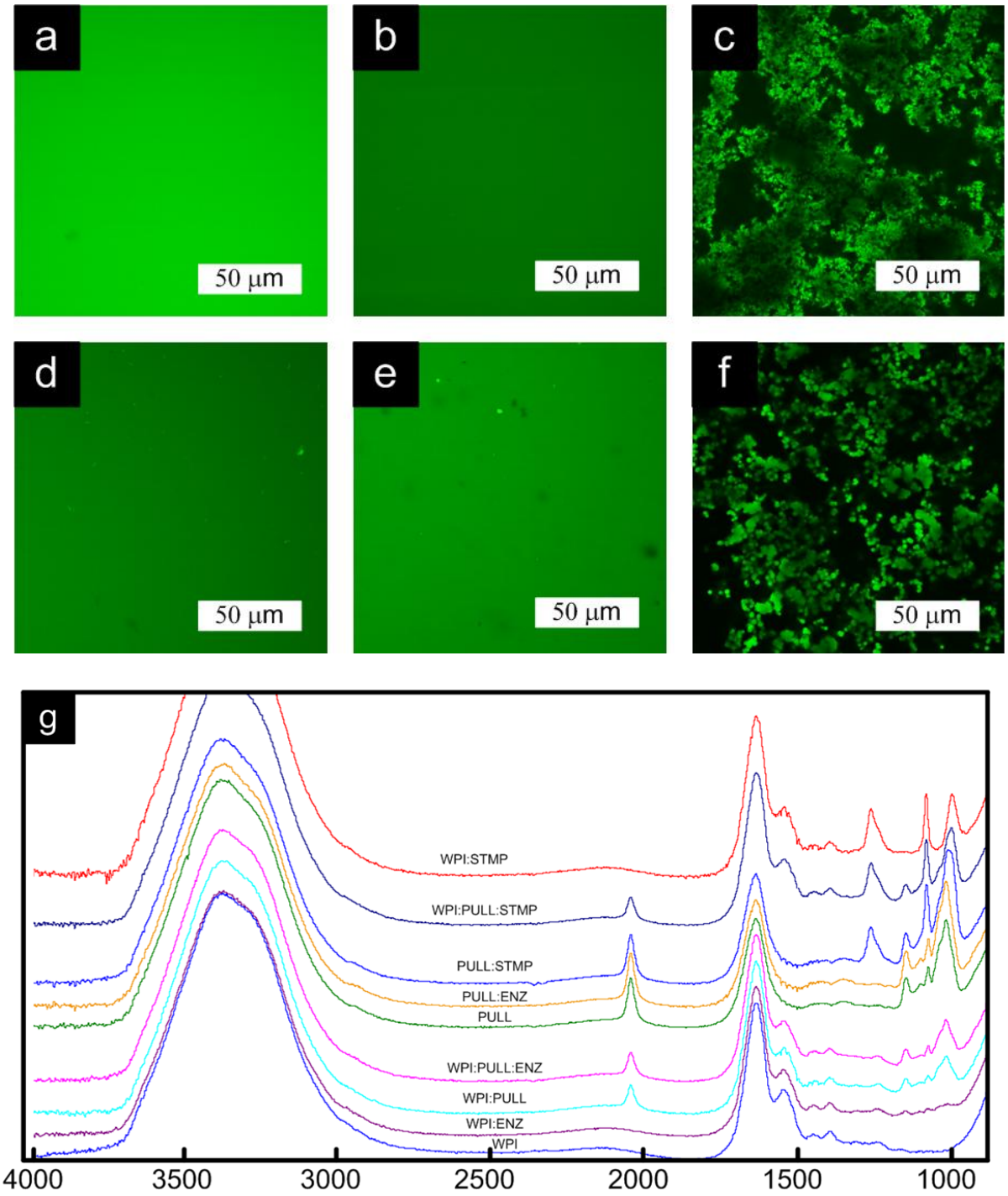

Figure 3.12. Top images show confocal microscope images of samples that showed microstructure. FTIR spectra of WP and WP:PULL blend gels at pH 8 showing changes with addition of enzyme and STMP.

.

Table 3.1. Protein and blend gel fracture stress and strain.

Gel preparation	Fracture Strain (%) at max elastic stress	Fracture Stress (Pa) max elastic stress
100% WPI pH 5.2 (30 min)	37	5274
100% WPI pH 6.8 (30 min)	57	4639
50:50 WPI:pullulan pH 6.8 (90 min)	181	1448
50:50 WPI:pullulan pH 5.2 (90 min)	22	79
50:50 WPI:pullulan pH 5.2 (30 min)	54	35

APPENDIX A. Pre-rheological study of blend gel formation at pH 8.

	WPI:Pullulan 100:0	Color Change (Heating)		Gelation (Heating)	
	Sample	Before	After	Before	After
1	NATIVE	beige	beige	no	yes
2	ENZYME	beige	beige	yes	yes
3	STMP	milky-white	milky-white	no	yes
4	STMP/ENZ	translucent milky-white	milky-white	no	yes

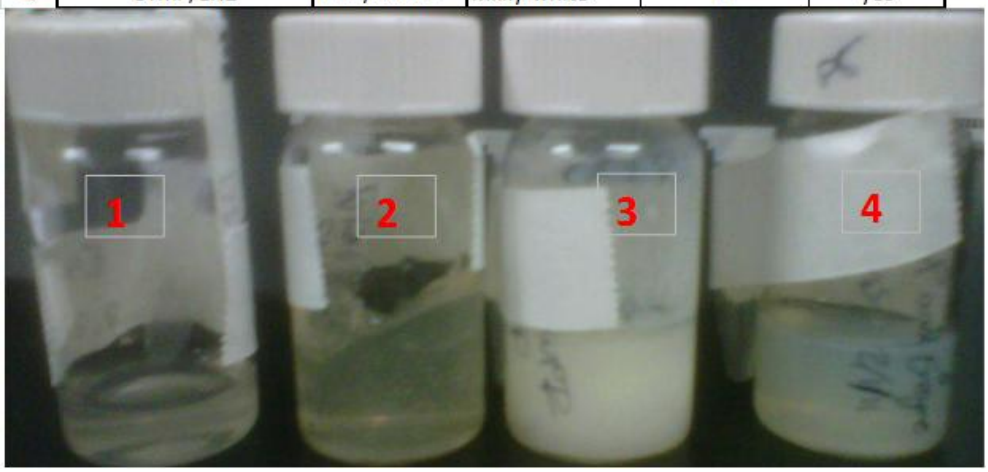

	WPI:Pullulan 70:30	Color Change (Heating)		Gelation (Heating)		Phase
	Sample	Before	After	Before	After	Separation?
1	NATIVE	beige	beige	no	yes	no
2	ENZYME	milky-beige	milky-beige	no	yes	yes
3	STMP	milky-white	milky-white	no	yes	no
4	STMP/ENZ	milky-beige	milky-white	initiating	yes	no

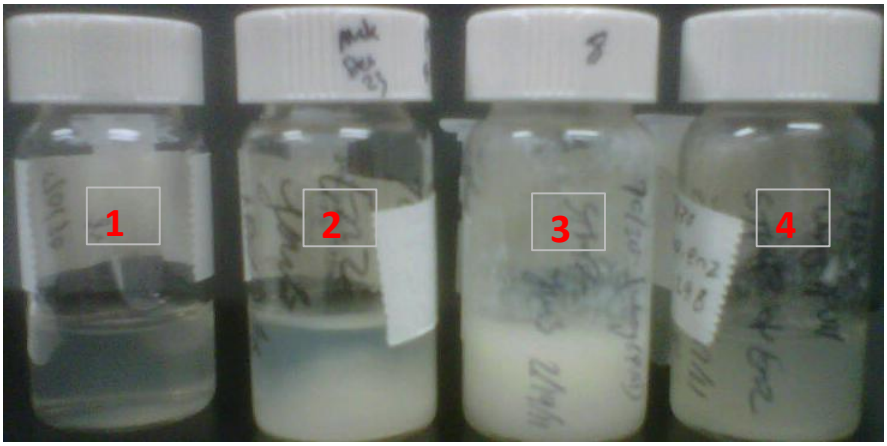

	WPI:Pullulan 50:50	Color Change (Heating)		Gelation (Heating)		Phase
	Sample	Before	After	Before	After	Separation?
1	NATIVE	clear-beige	clear-beige tint	no	yes	no
2	ENZYME	clear-beige	clear-beige tint	no	yes	no
3	STMP	milky-beige	milky-white	no	yes	no
4	STMP/ENZ	milky-white	milky-white	no	yes	no

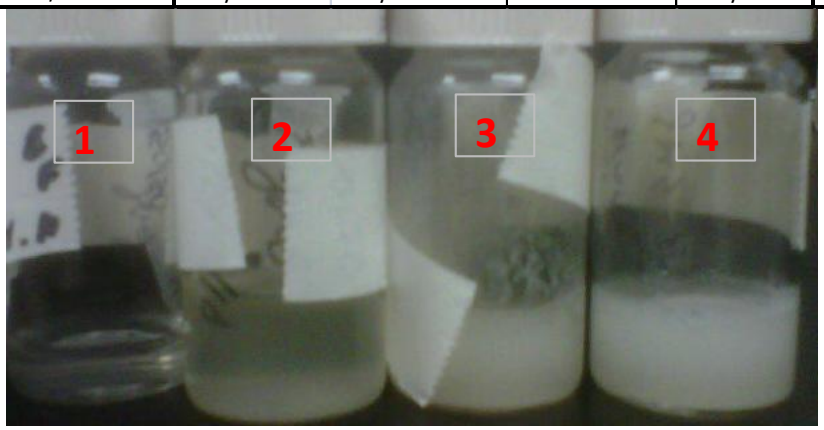

	WPI:Pullulan 30:70	Color Change (Heating)		Gelation (Heating)		Phase
	Sample	Before	After	Before	After	Separation?
1	NATIVE	clear-beige	clear-beige	no	yes	no
2	ENZYME	clear-beige	clear-beige	no	yes	no
3	STMP	milky-white	milky-white	no	yes	yes
4	STMP/ENZ	milky-white	milky-white	no	yes	no

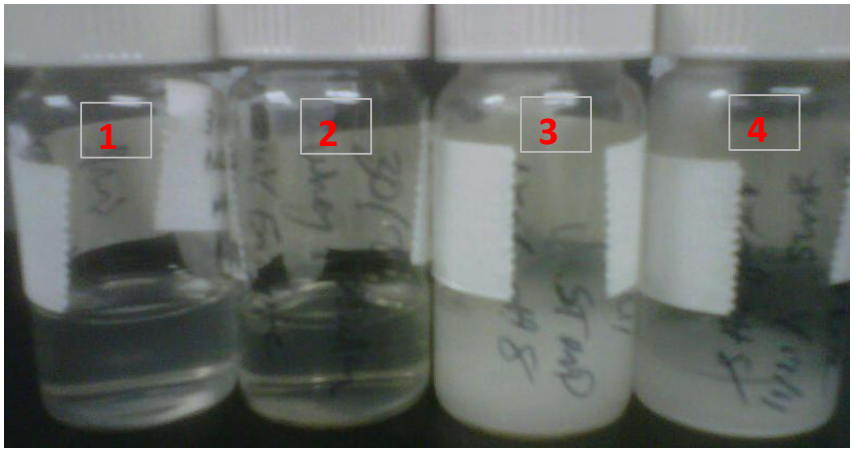

WPI:Pullulan 0:100	Color Change (Heating)		Gelation (Heating)	
Sample	Before	After	Before	After
NATIVE	clear	clear	no	no
ENZYME	clear	clear	no	no
STMP	clear	clear	no	no
STMP/ENZ	clear	clear	no	no

APPENDIX B. NuPAGE results from purification of BLG.

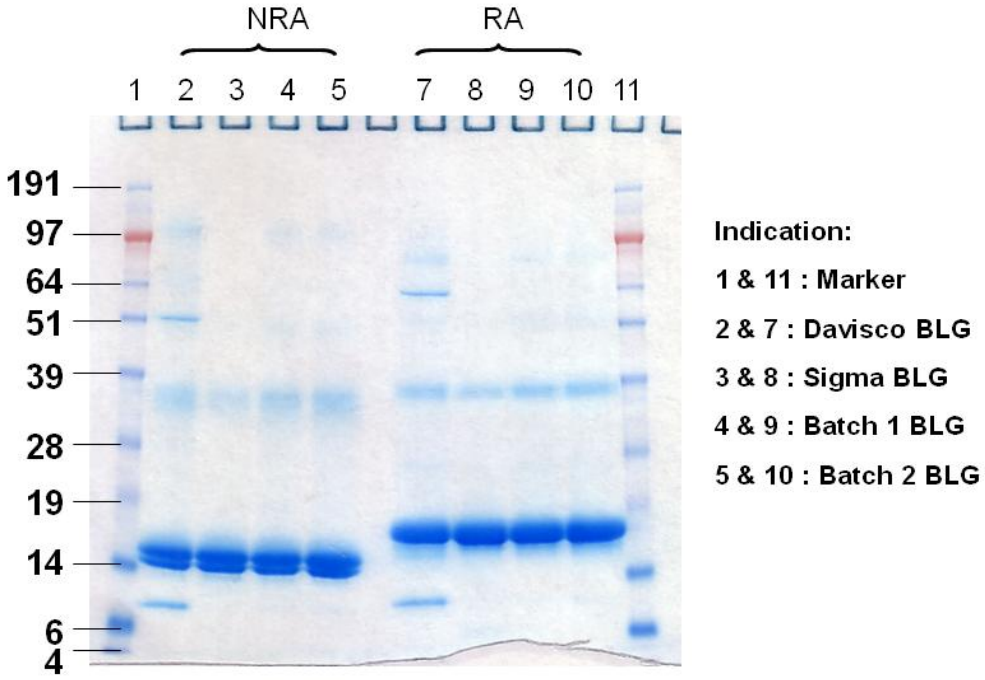

3.5 REFERENCES

1. Eissa, A. S.; Bisram, S.; Khan, S. A. *Journal of Agriculture and Food Chemistry* **2004**, 4456-4464.

2. Vardhanabhuti, B.; Foegeding, E. A.; McGuffey, M. K.; Daubert, C. R.; Swaisgood, H. E. *Food Hydrocoll.* **2001**, *2*, 165-175.

3. Bot, A.; van Amerongen, I. A.; Groot, R. D.; Hoekstra, N. L.; Agterof, W. G. M. *Polymer Gels and Networks* **1996**, *3*, 189-227.

4. Anema, S. G. *Food Chemistry*, **2008**, *1*, 110-118.

5. Euston, S. R.; Ur-Rehman, S.; Costello, G. *Food Hydrocolloids* **2007**, *7*, 1081-1091.

6. Ngarize, S.; Adams, A.; Howell, N. *Food Hydrocolloids* **2005**, *6*, 984-996.

7. Resch, J. J.; Daubert, C. R.; Foegeding, E. A. *Food Hydrocolloids* **2005**, *5*, 851-860.

8. Yamul, D. K.; Lupano, C. E. *Food Research International* **2005**, 511-522.

9. Alting, A. C.; Weijers, M.; deHoog, E. H. A.; vandePijpekamp, A. M.; CohenStuart, M. A.; Hamer, R. J.; deKruif, C. G.; Visschers, R. W. *J. Agric. Food Chem.* **2004**, *3*, 623-631.

10. Moon, B.; Mangino, M. E. *Milchwissenschaft-Milk Science International* **2004**, *5-6*, 294-297.

11. Hinrichs, R.; Götz, J.; Weisser, H. *Food Chemistry* **2003**, *1*, 155-160.

12. Ikeda, S. *Food Hydrocolloids* **2003**, *4*, 399-406.

13. Eissa, A. S.; Khan, S. *Journal of Agricultural and Food Chemistry* **2005**, *12*, 5010-5017.

14. Lowe, L. L.; Foegeding, E. A.; Daubert, C. R. *Food Hydrocoll.* **2003**, *4*, 515-522.

15. Chantrapornchai, W.; McClements, D. J. *Food Hydrocolloids* **2002**, *5*, 461-466.

16. Chantrapornchai, W.; McClements, D. J. *Food Hydrocolloids* **2002**, *5*, 467-476.

17. Ramirez-Suarez, J. C.; Xiong, Y. L. *J. Food Sci.* **2002**, *8*, 2885-2891.

18. Britten, M.; Giroux, H. J. *Food Hydrocolloids* **2001**, 609-617.

19. Durand, D.; Le Bon, C.; Croguennoc, P.; Nicolai, T.; Clark, A. H. Aggregation and gelation of globular proteins with and without addition of polysaccharides. In *Gums and Stabilisers for the Food Industry 11;* Williams, P. A., Phillips, G. O., Eds.; Royal Society of Chemistry: Cambridge, 2001; pp 263-270.

20. Liu, G.; Xiong, Y. L.; Butterfield, D. A. *J. Food Sci.* **2000**, *5*, 811-818.

21. Shinya Ikeda, K. N.,E.Allen Foegeding *Biopolymers* **2000**, *2*, 109-119.

22. Bauer, R.; Rischel, C.; Hansen, S.; Øgendal, L. *Int. J. Food Sci. Tech.* **1999**, *5/6*, 557-563.

23. Gunasekaran, S.; Xiao, L.; Eleya, M. M. O. *J Appl Polym Sci* **2006**, *5*, 2470-2476.

24. Reddy, T. T.; Lavenant, L.; Lefebvre, J.; Renard, D. *Biomacromolecules* **2006**, *1*, 323-330.

25. Chandan, R. C. Milk Composition, Physical and Processing Characteristics. In *Manufacturing Yogurt and Fermented Milks;* Chandan, R. C., Ed.; Blackwell Publishing: Ames, IA, 2006; pp 17-39.

26. Chandan, R. C.; Shah, N. P. Functional Foods and Disease Prevention. In *Manufacturing Yogurt and Fermented Milks;* Chandan, R. C., Ed.; Blackwell Publishing: Ames, IA, 2006; pp 311-325.

27. Sullivan, S. T.; Khan, S. A.; Eissa, A. S. Whey proteins: functionality and foaming under acidic conditions. In *Whey Processing, Functionality and Health Benefits* Onwulata, C. I., Huth, P. J., Eds.; Wiley-Blackwell: Ames, Iowa, 2008; pp 99-132.

28. Chatterton, D. E. W.; Smithers, G.; Roupas, P.; Brodkorb, A. *International Dairy Journal*, **2006**, *11*, 1229-1240.

29. Madureira, A. R.; Pereira, C. I.; Gomes, A. M. P.; Pintado, M. E.; Xavier Malcata, F. *Food Research International*, **2007**, *10*, 1197-1211.

30. Ha, E.; Zemel, M. B. *The Journal of Nutritional Biochemistry*, **2003**, *5*, 251-258.

31. van Aken, G. A. Coalescence Mechanisms in Protein-Stabilized Emulsions. In *Food Emulsions;* Friberg, S. E., Larsson, K. and Sjoblom, J., Eds.; Marcel Dekker: New York, 2004; pp 299-299-325.

32. Kinsella, J. E.; Whitehead, D. M. *Advanced Food Nutrition Research* **1989**, 343-438-343-438.

33. Roefs, S. P. F. M.; Peppelman, H. A. Aggregation and gelation of whey proteins: specific effect of divalent cations? In *Food Colloids: Fundamentals of Formulation;* Dickinson, E., Miller, R., Eds.; The Royal Society of Chemistry: London, 2001; pp 358-358-368.

34. Syrbe, A.; Fernandes, P. B.; Dannenberg, F.; Bauer, W.; Klostermeyer, H. Whey Protein + Polysaccharide Mixtures: Polymer Incompatibility and Its Application. In *Food Macromolecules and Colloids;* Dickinson, E., Lorient, D., Eds.; The Royal Society of Chemistry: Cambridge, 1995; pp 328-339.

35. Tavares, C.; Lopes da Silva, J. A. *International Dairy Journal* **2003**, *8*, 699-706.

36. Tavares, C.; Monteiro, S. R.; Moreno, N.; Lopes da Silva, J. A. *Colloids and Surfaces A: Physicochemical and Engineering Aspects* **2005**, 213-219.

37. Monteiro, S. R.; Tavares, C.; Evtuguin, D. V.; Moreno, N.; Lopes da Silva, J. A. *Biomacromolecules* **2005**, 3291-3299.

38. Baeza, R.; Gugliotta, L. M.; Pilosof, A. M. R. *Colloids and Surfaces B: Biointerfaces Food Colloids, Biopolymers and Materials Special Issue* **2003**, *1-4*, 81-93.

39. Sittikijyothin, W.; Sampaio, P.; Gonçalves, M. P. *Food Hydrocolloids* **2007**, *7*, 1046-1055.

40. Ould Eleya, M. M.; Leng, X. J.; Turgeon, S. L. *Food Hydrocolloids* **2006**, 946-951.

41. Leng, X. J.; Turgeon, S. L. *Food Hydrocolloids* **2007**, *7*, 1014-1021.

42. Bertrand, M.; Turgeon, S. L. *Food Hydrocolloids* **2007**, *2*, 159-166.

43. Spahn, G.; Baeza, R.; Santiago, L. G.; Pilosof, A. M. R. *Food Hydrocolloids* **2008**, *8*, 1504-1512.

44. Rulis, A. M. **2002**, 1-4.

45. Hayashibara **2007**, 8.

46. Fundueanu, G.; Constantin, M.; Ascenzi, P. *Biomaterials* **2008**, *18*, 2767-2775.

47. Autissier, A.; Letourneur, D.; Le Visage, C. *Journal of Biomedical Materials Research Part A* **2006**, 336-342.

48. Dulong, V.; Cerf, D. L.; Picton, L.; Muller, G. *Colloids and Surfaces A: Physicochemical and Engineering Aspects* **2006**, *1-3*, 163-169.

49. Lack, S.; Dulong, V.; Le Cerf, D.; Picton, L.; Argillier, J. F.; Muller, G. *Polymer Bulletin* **2004**, 429-436.

50. Lee, I.; Akiyoshi, K. *Biomaterials* **2004**, *15*, 2911-2918.

51. Sallustio, S.; Galantini, L.; Gente, G.; Masci, G.; LaMesa, C. *J. Phys. Chem. B* **2004**, *49*, 18876-18883.

52. Shingel, K. I. *Carbohydrate Research* **2004**, *3*, 447-460.

53. Fundueanu, G.; Constantin, M.; Mihai, D.; Bortolotti, F.; Cortesi, R.; Ascenzi, P.; Menegatti, E. *Journal of Chromatography B* **2003**, 407-419.

54. Diab, T.; Biliaderis, C. G.; Gerasopoulos, D.; Sfakiotakis, E. *Journal of the Science of Food and Agriculture* **2001**, 988-1000.

55. Yang, K. S.; Lee, E. Y.; Park, M. S.; Lee, K. Y.; Lee, Y. H. *Han'guk Somyu Konghakhoechi* **1998**, *8*, 465.

56. Vandamme, E. J.; Bruggeman, G.; De Baets, S.; Vanhooren, P. T. *Agrofoodindustry hi-tech* **1996**, *5*, 21.

57. Tsujisaka, Y.; Mitsuhashi, M. Pullulan. In *Industrial Gums: Polysaccharides and their derivatives;* Whistler, R. L., BeMiller, J. N., Eds.; Academic Press, Inc.: San Diego, 1993; pp 447-460.

58. Mehvar, R. *Current Pharmaceutical Biotechnology* **2003**, 283-302.

59. Wolf, B. W.; Garleb, K. A.; Choe, Y. S.; Humphrey, P. M.; Maki, K. C. *J. Nutr.* **2003**, 1051-1055.

60. Fogliano, V.; Vitaglione, P. *Molecular Nutrition & Food Research* **2005**, *3*, 256-262.

61. Gounga, M. E.; Zu, S.; Wang, Z.; Yang, W. G. *Journal of Food Science* **2008**, *4*, E155-E161.

62. Gounga, M. E.; Xu, S.; Wang, Z. *Journal of Food Engineering* **2007**, *4*, 521-530.

63. Gounga, M. E.; Xu, S.; Wang, Z. *Journal of Food Biochemistry* **2010**, *3*, 501-519.

64. Mailliart, P.; Ribadeau-Dumas, B. *Journal of Food Science* **1988**, *3*, 743-752.

65. Lazaridou, A.; Biliaderis, C. G.; Kontogiorgos, V. *Carbohydrate Polymers* **2003**, 151-166.

66. Walls, H. J.; Caines, S. B.; Sanchez, A. M.; Khan, S. A. *Journal of Rheology* **2003**, *4*, 847-868.

67. Linden, G.; Lorient, D. *New ingredients in food processing;* CRC Press: Boca Raton, 1999; .

68. Rizzieri, R.; Baker, F. S.; Donald, A. M. *Polymer* **2003**, *19*, 5927-5935.

69. Nayebzadeh, K.; Chen, J.; Dickinson, E.; Moschakis, T. *Langmuir* **2006**, *21*, 8873-8880.

70. Indrawati, L.; Stroshine, R. L.; Narsimhan, G. *J. Sci. Food Agric.* **2007**, *12*, 2207-2216.

71. Gauche, C.; Barreto, P. L. M.; Bordignon-Luiz, M. T. *LWT - Food Science and Technology* **2010**, *2*, 214-219.

72. Gauche, C.; Vieira, J. T. C.; Ogliari, P. J.; Bordignon-Luiz, M. T. *Process Biochemistry* **2008**, *7*, 788-794.

73. Eissa, A. S.; Puhl, C.; Kadla, J. F.; Khan, S. A. *Biomacromolecules* **2006**, *6*, 1707-1713.

74. Eissa, A. S.; Khan, S. A. *Food Hydrocolloids* **2006**, *4*, 543-547.

75. Wilcox, C. P.; Swaisgood, H. E. *J. Agric. Food Chem.* **2002**, *20*, 5546-5551.

76. Song, F.; Zhang, L. *The Journal of Physical Chemistry B* **2008;** *44*, 13749-13755.

77. YILDIRIM, M.; HETTIARACHCHY, N. S. *J. Food Sci.* **1997**, *2*, 270-275.

78. Eissa, A. S. Enzymatic modification of whey protein gels at low pH, North Carolina State University, Raleigh, NC, 2005.

79. Li, C.; Enomoto, H.; Hayashi, Y.; Zhao, H.; Aoki, T. *LWT--Food Science and Technology* **2010**, *9*, 1295-1300.

80. Li, C. P.; Enomoto, H.; Ohki, S.; Ohtomo, H.; Aoki, T. *J Dairy Sci* **2005**, 4137-4145.

81. Autissier, A.; Letourneur, D.; Le Visage, C. *Journal of Biomedical Materials Research Part A* **2007**, *2*, 336-342.

82. Li, C.; Salvador, A. S.; Ibrahim, H. R.; Sugimoto, Y.; Aoki, T. *J. Agric. Food Chem.* **2003;** *23*, 6808-6815.

83. Dulong, V.; Forbice, R.; Condamine, E.; Le Cerf, D.; Picton, L. *Polymer Bulletin* **2011**, *3,* 455-466.

84. Tang, C.; Saquing, C. D.; Harding, J. R.; Khan, S. A. *Macromolecules* **2009;** *2,* 630-637.

85. Li, Y.; de Vries, R.; Slaghek, T.; Timmermans, J.; Cohen Stuart, M. A.; Norde, W. *Biomacromolecules* **2009;** *7,* 1931-1938.

86. Shim, J.; Mulvaney, S. J. *J. Sci. Food Agric.* **2001**, *8,* 706-717.

87. Macosko, C. W. *Rheology: Principles, Measurements and Applications;* Wiley-VCH: New York, 1994 .

CHAPTER 4 Pullulan Nanofiber Crosslinking by heat and chemical methods

Chapter 4 is essentially a manuscript by Stephanie T. Sullivan, Christina Tang, H. Ray Tichenor, Jamelle M. Simmons, Thomas A. Deaton, Anthony Kennedy, and Saad A. Khan to be submitted to *Carbohydrate Polymers.*

Pullulan Nanofiber Crosslinking by heat and chemical methods

*Stephanie T. Sullivan, Christina Tang, H. Ray Tichenor[‡a], Jamelle M. Simmons[‡b], Thomas A. Deaton[‡b], Anthony Kennedy[‡c], and Saad A. Khan**

Department of Chemical and Biomolecular Engineering, North Carolina State University, Raleigh, NC 27695-7905
[‡a] Department of Geology, East Carolina University, Greenville, NC 27858
[‡b] Department of Engineering, East Carolina University, Greenville, NC 27858
[‡c] Department of Chemistry, East Carolina University, Greenville, NC 27858

Abstract

We examine aqueous pullulan solution electrospinning, correlating solution properties with electrospun mat morphology and crosslinking the highly water soluble pullulan mats to render them insoluble. Aqueous pullulan solutions were electrospun into sub-micron fibers at a minimum concentration of 15 w/w%. We associate changes in solution dynamics to changes in fiber morphology for three regions: (1) above the critical concentration to electrospin pullulan fiber mats (c_c ~ 13.7 w/w%), (2) below the critical concentration in a semidilute entangled region (11-12 w/w%) to produce beaded fibers with increased uniformity over those (3) above the critical overlap concentration (1.76 w/w%) in a semidilute unentangled region where nonuniform beaded fibrous materials are produced (6-9 w/w%). Ex-situ crosslinking techniques are examined for this highly water soluble polymer along with PULL blends with whey protein (WP) and hydroxypropyl-β-cyclodextrin (HPβCD). PULL-WP blends formed fibers with only 8.5 w/w% spinnable polymer pullulan

present in the total 17 w/w% solution; while PULL-HPBCD formed fibers with just 5 w/w% pullulan present in a total 20 w/w% solution. We also associate changes in solution dynamics of PULL:WP blend solutions with fiber morphology for two regions: (1) semidilute unentangled, which closely trends with theoretical $\eta_{sp} \sim c^{1.25}$ with our $\eta_{sp} \sim c^{1.22}$ and (2) semidilute entangled with theoretical $\eta_{sp} \sim c^{4.8}$ compared to our $\eta_{sp} \sim c^{5.5}$ for these regions. When investigating the impact of pH on PULL:WPI blend fibers, as solution pH impacts the secondary structure of the WP, we found mean fiber diameter of the blend mats increased linearly with increasing relative concentration of pullulan. Also, acidic pH of 3 permitted blends with less spinnable polymer to form nanofibers with few defects, when the higher pH blend mats were dominated by the presence of beads. This indicated that acidic pH and resulting WP secondary structure shifted the critical concentration to electrospin pullulan lower. XPS revealed the presence of WP on the surface of the hydrophilic PULL nanofibers, thereby allowing the possibility of nanofiber surface functionalization for different applications including selective binding for pharmaceutical or flavor release. We capitalize on this functionalization by crosslinking PULL:WP blend nanofibers via heat treatment. XRD indicated that fiber mats of pullulan and heat treated PULL:WP blends are amorphous. We also show that a PULL mat can be rendered insoluble in water following submersion in ethylene glycol diglycidyl ether (EGDGE) at 80 °C.

4.1 Introduction

Pullulan is a natural, water-soluble polysaccharide that is excreted extracellularly by the fungus Aureobasidium pullulans and comprised of maltotriose units (α-1,4 linked glucose molecules) polymerized by α-1,6-glucosidic bonds.[11] It is edible, biodegradable and generally regarded as safe (GRAS) by the U.S Food and Drug Administration.[2] The molecule is linear, amorphous [3] and forms a stair-step like structure. It is odorless, flavorless and highly stable. Pullulan has many current and potential uses in the food and pharmaceutical industries,[4-16] and is being considered for part of therapeutic diets for individuals with type 2 diabetes mellitus because it helps maintain blood glucose levels.[17] Reports on native pullulan pharmacokinetics are minimal.[16] Pullulan is stable at acidic pH of 2 through alkaline pH levels while its aqueous solutions are stable and viscous but do not gel, even in the presence of ions like borate that form complexes with hydroxyl groups.[15]

Pullulan applications include food and pharmaceutical products such as confections, pharmaceutical tablets and capsules, films, beverages, binders, sauces[1], coatings and films, and even molded products by solution casting or thermoplastic extrusion. Many of these applications are "biodegradable, transparent, oil resistant and impermeable to oxygen."[3] Pullulan serves as an excellent adhesive, stronger than dextrin and gum arabic by nearly five times.[1] In fact, when compression molded, it is claimed to be as strong and rigid as expanded polystyrene.[18] Also, as a food additive, it helps to maintain food texture, such as refrigerated creamy formulations like mayonnaise.[19] However, because pullulan is extremely water soluble, its applications are limited.

In this study, we will correlate solution properties to solution electrospinnability of pullulan into nanofibers followed by utilizing two crosslinking methods, one with heat and one with chemical submersion, or *ex situ* crosslinking, and show that the mats are insoluble in water. Electrospinning, a process first patented in 1934, can yield fibers smaller than 100nm. [20] Equipment for two electrospinning methods, melt and solution electrospinning, has been thoroughly discussed and summarized in review articles.[20, 21] Solution electrospinning utilizes polymer dissolved in solvent that is pumped at a controlled flow rate from a syringe to which a high voltage is applied. Electrostatic forces between the positively charged syringe needle and a grounded collector plate pull solution away from the Taylor cone formation at the tip of the syringe to the collector. As the solution is pulled away from the syringe, solvent evaporates, leaving the polymer drawn into fibers and collected as a fiber mat.[22]

Forming fibers of pullulan with high surface area and reduced water solubility could provide textural and flavor enhancements to foods, allow improved drug delivery as well as other benefits of nanoparticles and fibers. Melt spinning of pullulan into fibers has been accomplished [13, 23] as has solution electrospinning to form pullulan-clay nanofiber mats.[24] However, these are still water-soluble systems. *In situ* poly(vinyl alcohol) nanofiber crosslinking has been completed using glutaraldehyde and hydrochloric acid;[25] while crosslinking of polysaccharide nanofiber mats includes work by Bonino et al. and others using alginates, demonstrating use in biomedical applications.[26-28] Most recently, pullulan and pullulan/gelatin blends have been solution electrospun in a mixture of water and

dimethylformamide (DMF) and then *in-situ* crosslinked with sodium trimetaphosphate (STMP).[29]

We extend the aqueous solution electrospinning of pullulan with protein and cyclodextrin blends as well as crosslinking the highly water soluble nanofibers to form a swellable fiber mat with both chemical and heat treatment methods. Native pullulan is soluble primarily in water (and dimethyl sulfoxide (DMSO). [10] Use of DMSO has been very controversial and the United States Food & Drug Administration (US FDA) approved for only one human use.[30] Also, using DMF as solvent as Shi et al. (2011)[29] demonstrate is undesirable due to toxicity to humans.[31] Thus, we are specifically interested in producing aqueous solution electrospun nanofibers, forming electrospun nanofiber blends of PULL:WP and PULL:HPBCD, and crosslinking these nanofiber mats to render them hydrophobic to expand their use.

For heat treatment crosslinking, we prepare pullulan fibers containing whey protein. Whey protein and poly(ethylene oxide) blend nanofibers demonstrated the ability to be crosslinked and rendered insoluble in water by a similar method.[32] Other than this use, whey protein-pullulan blends has been limited to film formation,[33-35] solution demixing,[36] interfacial complex formation,[37] and gels.[38] Evaluating solutions and resultant nanofibers at extreme pH for prolonged shelf life pharmaceutical and food formulation applications is also desirable.

In addition, we examine chemical crosslinking of pullulan nanofibers. Several groups have hydrophobically-modified pullulan.[6-10] However, we would like to prepare the materials in aqueous solution using native pullulan. Some groups have cross-linked pullulan

to form hydrogels using sodium trimetaphosphate (STMP),[7, 39, 40] and Le Visage's group extends this to electrospinning pullulan.[29] Finally, we also look at the ability of pullulan nanofibers to carry hydroxypropyl-β-cyclodextrin (HPBCD) and subsequent crosslinking of these mats using a chemical method. PULL:HPBCD crosslinked mats could allow many applications from flavor and drug delivery to hydrophobic molecule capture for environmental cleaning, and even tissue culture.[26]

Biodegradable, biocompatible, hydrophobic pullulan and pullulan blend nanofiber mats may provide a system that proves useful for many biomedical applications. Critical objectives of this study are to correlate aqueous pullulan solution properties with fiber morphology as well as to crosslink pullulan nanofiber mats, establishing that they are insoluble in water from the crosslinking process. Potential exists to use these nanofibers to produce non-wovens for surface modification, drug delivery and wound healing as well as the development of novel foods.

4.2 Materials & Methods

4.2.1 Solution Preparation

Pullulan (PULL) was provided by Hayashibara International (Japan) with an average molecular weight of 274 kDa and a polydispersity of 1.634.[41] BiPRO Whey Protein Isolate (WPI) (98% protein) and BIOPURE β-lactoglobulin (BLG) (95% protein) were both obtained from Davisco Foods Inc. (Eden Prairie, MN) and used as received. Some BIOPURE BLG was purified [42] and verified with NuPAGE (see Appendix A). Hydrochloric acid, acetone, ethanol, and Rhodamine B were used as received from Sigma.

Sodium dodecyl sulfate (99% purity) was used as received from Fisher. 2-mercaptoethanol (99% purity) was used as received from Acros Organics. Urea (99% purity) was used as received from Fisher. Ethylene glycol diglycidyl ether (Polysciences, Inc.) was used as received. Hydroxypropyl-β-cyclodextrin (HPBCD) was purchased from CTD, Inc (High Springs, Fl, technical grade, product code THPB-T) and was used without further purification. The purity of THPB-T grade HPBCD was 91.2%, and included the presence of impurities such as water (3.4%), propylene glycol (<5.0%) and unsubstituted β-CD (<1.0%). The average degree of substitution for this derivative was 5.6 (computed mol. wt.-1460). All solutions were made with deionized water.

To prepare the biomaterial mixtures, PULL and specified components were dissolved in deionized water (DW) and solutions were stirred for a minimum of 3 hours to ensure complete dissolution. Solution pH and conductivity were measured with a Fisher Scientific Accumet AB15 pH meter and Accumet AB30 conductivity meter, respectively. The viscosities of pertinent samples were measured at 25°C in a TA Instruments AR-2000 stress controlled rheometer using a 40 mm, 2° cone and plate geometry.

4.2.2 Solution Electrospinning

The electrospinning apparatus included a precision syringe pump (Harvard Apparatus, Holliston, MA), which is operated at flow rate of 0.1-2.0 mL/hour, and a high-voltage power supply (Gamma High Voltage Research, model D-ES30 PN/M692 with a positive polarity) that provided voltages in the range of 0-30 kV. Electrospinning solutions were loaded in a 10 ml syringe to which a stainless steel capillary metal-hub needle was

attached. The positive electrode of the high voltage was connected to the needle tip. The grounded electrode was connected to an aluminum foil-covered metallic collector. The tip-to-collector distance was 15 cm. The needle was by Jensen Global, JG 2.0-22, 2 inches long and 22 gauge.

4.2.3 Morphology & Surface Analysis

Specimens from solution electrospinning efforts were mounted on stubs, sputter coated with gold and examined using scanning electron microscopy (SEM, FEI Quanta 200 Environmental Scanning Electron Microscope). Thirty sample fiber diameter measurements were taken with National Institutes of Health Image J software using SEM images. A sample of n = 30 measurements is statistically considered a "large sample." With depth of field and duplication of measurements a concern from randomly selecting 100 fibers from SEM images, we completed a statistical evaluation of our SEM image evaluation protocol. A t-test evaluated the null hypothesis that H_0: $\mu_1 = \mu_2$ for n=100 and n=30 independent random width measurements from individual fibers from the sample. A p-value > 0.05 allows us to accept the null hypothesis that the mean fiber width is not significantly different between 100 and 30 independent random measurements of individual fiber widths from the same sample. To evaluate this protocol, measurements were randomized by using Image J to place a 200-point grid over the electron micrographs at each of 100 points of fiber intersection (where depth of field was judged to be minimal) a measurement was made. This grid was offset for independent random measurement of 30 fiber widths to compare. Statistical analysis was performed using SPSS version 17.0. Therefore, for all fiber diameter measurements, a large

sample of n = 30 measurements using our grid protocol selecting measurement positions with minimal depth of field was utilized.

Some specimens were evaluated using Environmental Scanning Electron Microscopy (ESEM) in which the Quanta 200 Scanning Electron Microscope was operated in Environmental mode with a chamber pressure of 4.2-5.2 Torr, using water vapor as the chamber gas. A Peltier cooling stage was used to maintain a working temperature of 2 °C.

Confocal laser scanning microscopy images were recorded on a Zeiss LSM 710. Specimens were cut to fit a 1 cm diameter glass microscope slide and stained with 100 µL of aqueous Rhodamine B solution (0.2 % w/w) just prior to imaging. The set-up was configured with an inverted microscope (model Zeiss Axio Observer Z1) and a 40 × objective lens (LD C-Apochromat 40x/1.1 W Korr M27). The light source was a multiline argon laser with an excitation wavelength at 514 nm. The emission of Rhodamine B was recorded between 531 and 703 nm. Reflected light microscope images were taken with an Olympus BX-51 microscope system with objective magnifications ranging from 10× to 100×.

A Riber X-ray Photoelectron Spectrometer (XPS) operated at 12kV with a 1mm spot size was used for nanofiber mat surface analysis. Differential scanning calorimetry (DSC) was utilized to analyze fiber mat thermal properties (model DSCQ200, TA Instruments, New Castle, DE) at a heating rate of 10 °C/minute under inert Argon gas.

The infrared spectra of nanofiber mats were recorded at room temperature using a Nicolet Magna-IR 750 spectrometer (Madison, WI). Dry air was continuously run through the spectrometer. The infrared spectra were recorded at 2 cm^{-1} resolution. A total of 128 transmission scans were recorded, averaged, and apodized with the Happ-Genzel function.

Spectra were subtracted from that of air. Additional Infrared spectra were obtained on Nicolet 6700 FTIR spectrometers (Thermo Scientific, Madison WI) continually purged with dry air or nitrogen. Samples were analyzed directly on a single bounce diamond or germanium ATR (45°) by acquiring 128 - 512 scans at 4cm^{-1} resolution at ambient temperature. Spectra collected by diamond ATR were corrected for water vapor and then ATR corrected using the advanced ATR correction routine (Omnic).

X-ray diffraction studies were conducted with a Cu Kα radiation source (λ = 1.542 Å) at 40 kV x30 mA for 1800 s on a Bruker D-5000 diffractometer equipped with a Highstar area detector. Diffraction patterns were analyzed with Bruker General Area Detector Diffraction System (GADDS) software. In transmission mode, the intensity was recorded for 2θ in the range of 7°- 41°. Scans taken with an empty sample holder served as a background for subtraction.

4.3 Results and Discussion

4.3.1 Effect of polymer concentration

We begin by investigating aqueous solution properties of pullulan and correlating results with the resulting morphology of solution electrospun mats. The molecular structure of pullulan is provided in Figure 4.1(a). This molecule is very flexible and highly water soluble. Steady shear viscosity results of pullulan aqueous solution are shown in Figure 4.1(b) and indicate that aqueous pullulan solutions are Newtonian in stress ranges from 0.01 – 100 Pa, while Figure 4.1(c) shows an increase in solution conductivity with increasing pullulan concentration. Figure 4.2 shows the specific viscosity of pullulan solutions as a

function of polymer concentration, which we will discuss in detail. Also, solution electrospinning has indicated that pullulan solution concentrations > 12w/w% produced uniform nanofibers, while solutions ≤ 12 w/w% formed beaded fibers or beaded structures. The average fiber diameters for 15, 18, 20 w/w% nanofiber mats followed an increasing trend of 421 nm, 439 nm and 584 nm, respectively. Figure 4.3(a) – (h) shows nanofiber specimens electrospun from aqueous solutions of 6 – 25 w/w%. Figure 4.3(i) is a representative histogram from SEM analysis of fiber diameter for a 15 w/w% sample. Figures 4.3(j) and (k) are SEM and confocal images of a nanofiber mat that was electrospun with an 18 w/w% solution that was loaded with 0.02 w/w%, demonstrating that a pullulan mat can be solution electrospun with a model drug or flavenoid loaded in solution and still form uniform, defect free nanofibers.

Viscosity is a measure of polymer entanglement in solution and can be used to predict electrospun material morphology.[43,44] To look more closely at correlating solution properties to solution electrospinnability of pullulan into nanofibers, we look at the specific viscosity data shown in Figure 4.2. Lazaridou et al.[3] did extensive pullulan solution analysis in their work preparing pullulan films. They used the same pullulan (Hayashibara International, they designate received form as P_{360}) as our studies and they thoroughly determined the concentration dependence of zero shear specific viscosity, determining c* to be 1.8 g/dl from intrinsic viscosity determination (0.56 dl/g), with double logarithmic plotted slopes of the dilute and concentrated regimes to be 1.00 and 2.37, respectively.[3] c* is the overlap or crossover concentration where polymer chains begin to overlap.[45]

We fit the data in Figure 2 with three linear fits following McKee's approach[43] The first phase is dilute region and the first change in slope indicates the critical overlap concentration, although experimental data yields a scaling in the dilute region $\eta_{sp} \sim c^{0.7}$, slightly less than the theoretically expected ($\eta_{sp} \sim c^{1.0}$). The second phase of data shows that $\eta_{sp} \sim c^{2.5}$. Based on these slopes, we determined the critical overlap concentration occurs at 1.8 wt. % and indicates the onset of the semidilute regime These results are similar to previous results by Lazaridou.[46] In the third phase, we observe that $\eta_{sp} \sim c^{6.3}$. [43] Based on these fits, we find that the critical concentration c_c for pullulan occurs at ~14 wt.%. The value of the c_c we empirically determine here agrees with our electrospinning results in which we achieved bead free fibers at 15 w/w%, but bead defects at 12 w/w%. The concentration where we confirm the ability to form bead free fibers is 15 w/w% or 8.5c* which is likely due to pullulan's broad polydispersity of 2.4. [45]

We can look at our electrospinning results, as we have observed results from samples within the semidilute regime ($c^* < c < c_c$), to more closely identify a transition between the semidilute unentangled and entangled regimes. Figure 4.3(a) and (b) appear to be dominated by beads in their electrospun mats of 6 and 9 w/w%, respectively. We interpret these samples as falling in the semidilute unentangled regime. Figure 4.3 (c) and (d) both contain bead defects, but are dominated by the presence of fibers for these 11 and 12 w/w% samples. We consider this to fall in a semidilute entangled regime, where fibers can form, but not without producing beads intermittently. Samples were electrospun at 15 w/w% and higher and all achieved uniform fibers – at 15, 18, 20 and 25 w/w% , and are shown in Figures 4.3 (e) – (h), respectively.

Figure 4.3(i) shows the result SEM fiber diameter analysis results using the Image J software for a total of 100 fibers of the 15 w/w% sample. For all samples, as expected, the mean fiber diameter increases with increasing pullulan concentration, and thus increasing viscosity, of the source aqueous solution. Figure 4.3 (j) and (k) show and SEM and confocal image, respectively, of the same nanofiber mat that was prepared with RhB in solution prior to electrospinning. The dye appears to be present on the surface of the fibers.

4.3.2 Blending with WP

Figure 4.4(a) shows the electrospun nanofiber mat from an aqueous pullulan-BLG blend solution. This blend solution, containing just 8.5 w/w% pullulan, successfully electrospun bead-free nanofibers (total 17 w/w% for a 50:50 PULL:BLG ratio, [18cm tip to collector distance (TCD), 0.3 ml/hr flow rate, 9.5 kV]). Therefore, the addition of the BLG to solution permitted the use of less pullulan to achieve quality fibers. Based on this result, the total solution concentration for varying blend composition was chosen to be 17 total biomaterial concentration because it was demonstrated to be successful for both 100% PULL and 50:50 PULL:BLG ratio solutions to electrospin nanofibers, as well as can form gelatinous structures upon heating, which we show to be beneficial later. PULL:WPI blend solution viscosities are shown in Figure 4.4(b) and also have a Newtonian region with viscosity increasing with increasing relative pullulan content in the blend. The four solutions were electrospun to produce fiber mats. The 70:30 and 60:40 PULL:WPI blend solutions both produced bead-free fiber mats, as shown in Figures 4.4 (c) and (d). Both 50:50 and

30:70 PULL:WPI blend mats did contain bead defects, with the number of beads increasing with decreasing pullulan concentration, as expected.

To further correlate PULL:WPI blend solution dynamics, we develop a log-log plot of specific viscosity vs. concentration for the solutions as shown in Figure 4.5(a). This data shows a different contour than the PULL only data in Figure 4.2. Based on Figure 4.5(a), we associate changes in solution dynamics of PULL:WPI blend solutions with fiber morphology for two regions: (1) semidilute unentangled, which closely trends with theoretical $\eta_{sp} \sim c^{1.25}$ with our $\eta_{sp} \sim c^{1.22}$ and (2) semidilute entangled with theoretical $\eta_{sp} \sim c^{4.8}$ compared to our $\eta_{sp} \sim c^{5.5}$ for these regions. An increase in slope indicates increased interactions between polymer. [3] The inset image in Figure 4.5(a) is the result of electrospinning a solution that is 15:85 PULL:WPI blend composition and is a mat of beaded fibers and clearly falls in the semidilute region. Based on the data shown in Figure 4.6(a), the addition of whey protein to the pullulan aqueous solution has shifted the observed critical concentration for electrospinning bead free fibers, which is some value > 8.5 w/w% (PULL:WPI 50:50) where we observed a few minor defects. This is supported by an increase in apparent entanglement with the addition of WP, since fibers formed at lower PULL concentrations.

4.3.3 Impact of pH on morphology and electrospinnability of PULL:WPI blends

We next demonstrate the electrospinnability of pullulan-whey protein blend aqueous solutions at varying pH to prepare mats for crosslinking by heat treatment and determine if pH will shift the critical concentration and fiber quality. For this phase of our study, we continue using the total biomaterial concentration of 17 w/w% and vary solution pH. We had established that this biomaterial concentration in solution could form a gel upon heating

above the gelation temperature of BLG (70 °C). Figure 4.5(b) shows viscosity data and again a Newtonian region for each sample. Figure 4.6 (a) – (o) shows SEM images of fibers prepared from 17w/w% aqueous biomaterial solutions of various PULL:WPI ratios at pH 3, 5.2, 8 and 11 (electrospinning conditions provided in Appendix C). Figure 4.6 (p) summarizes that mean fiber diameter data. Appendix A provides solution properties and electrospinning parameters for the samples. The 30:70 PULL:WPI blend at pH 11 would not electrospin, as the solution gelled. A good correlation of fiber diameter to solution properties is solution conductivity, which, for each pH, fiber diameter decreased with increasing conductivity (data in Appendix A). In turn, as pullulan concentration increases for each pH, fiber diameter also increased. This only appears to not be applicable for the solution at pH 8, where the fiber diameter standard deviation for the 70:30 PULL:WPI blend was higher than that for the 100% pullulan, while its histogram peak was actually lower. This could be a result of the limited number of fibers in the 70:30 image with adequate depth of field for measurement compared to the 100% PULL sample. pH variation from blend mix pH reveals that each solution yielded bead free fibers with 50:50 PULL:WPI blends. Therefore, changes in pH to more acidic or more alkaline from the native blend mix pH also shifted the quality of the fibers and the resultant critical concentration. Even a stronger influence, acidic pH 3 permitted blends with less spinnable polymer to form nanofibers with few defects (30:70 PULL:WPI), when the higher pH were dominated by the presence of beads. This indicated that acidic pH and resulting WP secondary structure shifted the semidilute entangled region to a lower concentration of spinnable polymer pullulan.

FTIR analysis was completed on pullulan mats, PULL:BLG blend mats and BLG powder and is shown in Figure 4.7(a). The pullulan molecule exhibits peaks in the 1500-650 cm^{-1} region. Table 4.1 summarizes the individual bands and what they represent.[24] Similar to Karim et al. observations[24], small shifts in absorption maximum and band shape alteration are indicative of some interactions between the PULL and BLG presence when compared to individual component spectra. We do observe a shift in maxima in the hydroxyl band and slight shifts in their common regions in the 1500-1200 cm^{-1} range.

While FTIR analyses of the PULL:BLG blends shows the presence of both PULL and BLG in the mats as expected, perhaps of greater interest is the composition on the surface of the fibers. In order to examine this issue, x-ray photoelectron spectroscopy (XPS) was used to determine surface (< 5 nm) constituents in atomic concentration. XPS survey scans utilizing PULL fiber mats with and without BLG are shown in Figure 7(b). On the surface of the PULL fibers, both carbon and oxygen atoms are found as expected of significant magnitude. In the PULL:BLG blend fiber, an additional strong nitrogen peak is observed, indicating the presence of whey protein on the fiber surface. The atomic nitrogen content on the surface of the fiber was approximately 11.45%, higher than the theoretical 2% atomic nitrogen concentrated calculated based on the uniform bulk solution concentration. This suggests that the whey protein is more concentrated on the surface of the fiber which is consistent with previous studies by Sun et al.[22]

4.3.4 Crosslinking by heat treatment

Based on studies of fiber blends of WP and poly(ethylene oxide), the fiber surface functionality of the whey protein along with pullulan's amorphous properties could enable

fiber crosslinking via heat treatment.[32] Based on Karim et al.'s evaluation of pullulan fiber mats, they found the degradation temperature of a pullulan mat to be approximately 250 °C using thermogravimetric analysis (TGA).[47] Gounga et al. recently used heating pullulan and WPI blend solutions at 90 °C to form films.[35] They found that the film glass transition temperature (T_g) decreased with increasing pullulan concentration. They thought this could be due to hydrogen bonding between water molecules and pullulan's hydroxyl groups in support of Kilburn et al.'s findings.[48] They also considered the view of Bizot et al. who considered this due to α(1→6) bond plasticization increasing pullulan chain flexibility.[49] Borde et al. (2005) determined that pullulan with 11.6% water content had a T_g of approximately 66 °C, which they considered low relative to the other amorphous polysaccharides they studied, possibly due to its flexible glycosidic linkages.[41] They also explain that a barrier for pullulan crystalline arrangement may be its maltotriose monomer sequence irregularity.[41]

Lazaridou et al. (2003), in evaluating pullulan films, stated that "pullulan is an ideal model system for studying the effects of molecular size on thermal and mechanical properties, i.e. being an amorphous and linear polymer of maltotriosyl units, crystallinity and chain branching are not factors which can complicate the thermomechanical properties of this polysaccharide."[3] Lazaridou et al. (2003) go on to explain that, as an amorphous polymer, pullulan's glass transition, or α-relaxation, is the motion of its long-chain segments.[3] Pullulan is highly water soluble. As a result, water causes pullulan plasticization leading to "increased intermolecular distances (free-volume), decreased local viscosity and increased back-bone chain segmental mobility."[3]

Based on these prior analyses of pullulan films, we wanted to look more closely at both pullulan mobility and thermal properties. First, to investigate the mobility of pullulan in aqueous solution, the relative mobilities of the content species were evaluated through transverse relaxation time analysis (T_2) as measured by benchtop time-domain ^{1}H NMR. Low-resolution NMR evaluation of pullulan solutions before and after heat treatment at 80 °C indicate a slight increase shift in pullulan and water mobility after heat treatment. Due to these characteristics of pullulan and some DSC experiments (data not shown), we decided to next perform XRD experiments with both native and 150 °C annealed fiber mat samples. X-ray diffraction spectra results are given in Figure 4.7(c). The native pullulan powder as well as the 100% pullulan fiber mat both exhibit broad peaks at approximately $2\Theta = 19.4°$ and $2\Theta = 35°$. The heat treated 50:50 PULL:WPI blend samples also have similar peaks at $2\Theta = 19.4°$ and $2\Theta = 35°$. The native blend sample appears to have weak intensity broad amorphous halos at both $2\Theta = 13°$ and $2\Theta = 19.4°$ with no sharp crystalline peaks visible. Biliaderis et al. attributed the broad peak in their pullulan films at $2\Theta = 19°$ to indicate that the material is fully amorphous. [50]

To evaluate the potential of heat-induced crosslinking of PULL:WP blend fiber mats, samples were heat treated at 100 °C. Successful crosslinking was dependent on sample thickness and heat treatment time. The sample shown in Figure 4.8(a) had an initial weight of 0.074 g and after soaking in deionized water for 24 hours increased its weight to 1.613 g, resulting in a swelling ratio exceeding 20 times its original weight. Figure 4.8(b) shows the sample after removal from water soaking. Figure 4.8(c) shows an SEM of the original mat while 4.8(d) shows the mat surface via ESEM after soaking. The surface appears to be more

film like, but indication of a fibrous structure appears to be underlying, confirmed by ESEM views in Figures 4.8 (e) – (h) of a network. Figure 4.8(i) is a confocal microscope image of the same mat that had been soaking in water for four days. Dye was applied just prior to imaging and shows a fiber network still intact.

Figure 4.9 (a) – (c) shows FTIR spectra of BLG material and PULL mats, and then PULL:BLG and PULL:WPI blend heat treated mats before and after soaking in various solutions for approximately 24 hours. Both mats retain some presence of the pullulan, with peaks at 1154 and 1023 cm^{-1}, indicating C-O stretching. The samples were observed to swell considerably and maintain form when removed from the solution. Table 4.2 correlates bands with BLG.[51] The strong peak associated with BLG around 1540 cm^{-1} is no longer present in any of the mats, indicating that some protein structural changes have occurred, at minimum. In all samples, the protein peak in the 1630-1645 cm^{-1} range is maintained, indicating the primary component remaining from all soaking conditions is the BLG and also a water signal as well with the hydroxyl band present. From observation of the mat after having been removed from water soak and exposed to air for several days, it retained a gel-like structure and did not return to its original dry state. This is likely due to the PULL-WP mat retaining bound water. The mat in its original state was dry, but following heat treatment formed covalent bridges. Still, when immersed in water, it becomes a hydrogel. Based on our evaluation of the heat treatment of pullulan-BLG fiber blends, the mats retain a gelatinous network structure which could enable both texture/flavor release modification of food and pharmaceuticals as well as provide a potential cell seeded structure for tissue culture. Crosslinking of pullulan-WP blend fibers was successful.

4.3.5 Blending with HPBCD

Fibers of pullulan and HPBCD have many potential applications for hydrophobic molecule and capture. Previously, PVA-HPBCD blend fibers and HPBCD only fibers were prepared via solution electrospinning.[52] Here we demonstrate the use of spinnable polymer pullulan to form pullulan and HPBCD blend fiber mats. Figure 4.10 (a) – (e) shows SEM micrographs of samples of increasing pullulan concentration in the PULL:HPBCD blends. Also, a linear increase in the bead free nanofiber diameter was found with increasing pullulan concentration as shown in Figure 4.10(f), data for which was determined from image analysis that is presented in Figure 4.10(g)-(j). Additional PULL:HPBCD blend solution properties and electrospinning parameters are given in Appendix B along with SEM images. As shown in Figure 4.10(k), HPBCD blend solutions also achieve a Newtonian region throughout the 0.01 – 100 Pa shear stress in experiments, with viscosity increasing with increasing PULL content. Blends of total 20 w/w% aqueous solution required a minimum of 50% pullulan to yield bead free fibers. Although we do not have enough data to determine regime transitions for PULL:HPBCD blend solutions, we can see good agreement in Figure 4.10(l) where these solution specific viscosities fall, as the 25:75 and 50:50 PULL:HPBCD blend samples both exhibit bead defects, although the 50:50 sample much fewer, yet their corresponding specific viscosities fall in pullulan's semidilute regime, while those solutions that do form defect free mats each fall in the region above the critical concentration. Therefore, our log-log plot of specific viscosity vs. pullulan concentration could be used as a rough guide to determine electrospinnability of solutions that are at least of 5 w/w% pullulan; and fibers with just

minimal bead defects were electrospun with only 10 w/w% pullulan, when PULL-only mats required 15 w/w%.

We were also interested in being able to crosslink PULL:HPBCD blend fibers. Before doing so, we wanted to determine if the HPBCD may add crystalline features to PULL mats. Crystallinity may hamper the ability of the mat to crosslink, similar to findings in examination of cellulose fiber structure. In this work, they found that amorphous cellulose was readily penetrated by and reactive with water and acid; while microfibril bundle crystalline regions could not be penetrated by acid or water molecules, but they were surface reactive.[53] We used XRD to examine PULL:HPBCD blend mats as shown in Figure 4.11(a), which indicated the same peak present as the PULL-only mat at approximately 2Θ = 19°, along with another broad peak at approximately 2Θ = 13°. This blend mat XRD spectra appears to be identical in shape to that of HPBCD–only mat XRD results with 2Θ = 18°, along with another broad peak at approximately 2Θ = 8°, with simply a shift to the left. In evaluating mats using FTIR, Figure 4.11(b) shows FTIR spectra of the native PULL:HPBCD mat which is difficult to distinguish from a PULL only mat. HPBCD visible adsorption bands are present at ~1030, ~1080, and ~1155 cm^{-1} (due to coupled C-C/C-O stretching and antisymmetric stretching vibrations of the C-O-C glycosidic bridge. The XRD peaks are in agreement with findings of Celebioglu & Uyar (2011) that pure HPBCD fibers have amorphous structures.[52]

4.3.6 Impact of crosslinking by chemical treatment

Since heat treatment of pullulan only mats would not yield a water-insoluble substance, we investigate alternative means to crosslink pullulan nanofibers to render them insoluble. Native pullulan mats were crosslinked by placing approximately 1 x 1 cm samples in a 20 ml vial containing 5 ml of EGDGE. Once samples were in the EGDGE, the vial was placed in an oven at 80 °C for approximately 24 hours. After crosslinking in EGDGE, the samples were suspended by a binder clip (as in Figure 4.8(a)) in deionized water for approximately 24 hours. This soaking in water appeared to remove the bulk of the EGDGE component film and leave pullulan crosslinked fibers behind, as shown in Figure 4.12. The inset reflected light microscope image in Figure 4.12(c) shows the EGDGE-crosslinked pullulan film and its underlying fiber structure before being soaked in water, which we will discuss in more detail.

Figure 4.11 shows FTIR spectra for a native pullulan mat, the mat after crosslinking in EGDGE, and then following the water soak. The FTIR peaks in the native pullulan mat are typical of the pullulan as described above. The peaks after EGDGE crosslinking are characteristic of the presence of both pullulan and EGDGE. A new peak emerged in the EGDGE crosslinked sample and is the only one other than the hydroxyl band present in the water soaked mat post crosslink. This peak is broad and centered at 1642 cm^{-1} likely attributed to C=C stretching. Figure 4.12(a)-(c) shows an 18 w/w% pullulan nanofiber mat that was evaluated under a confocal microscope, where (a) is the material cross-section view that is furthest from the microscope slide and closest to the surface on which the RhB dye was placed to stain the sample. (b) is further away from the treated surface and (c) is at the

bottom of the sample. The aqueous dye solution was placed on the sample just minutes prior to imaging. The sequence of images indicates that the application of the water based solution was causing the dissolution of the resin portion of the mat, leaving behind only crosslinked pullulan fibers. Figure 4.12 (d) and (e) are images of the same sample that had been soaking in DW for over 24 hours. This image indicates that the water had, by this time, dissolved the bulk of the EGDGE resin-like residue and left a fiber-only mat. Figure 4.12 (f) shows an ESEM image of the sample. This sample was thicker than the one imaged in (a) – (e). Therefore, the upper right image at this point had still retained some of the resin like properties, yet the bulk of the crosslinked soaking material was a fibrous-like network as indicated by the samples in (d) and (e). EGDGE crosslinking of native pullulan mats successfully achieved an insoluble fibrous network.

We were also interested in crosslinking PULL:HPBCD blend fibers. Based on the XRD and FTIR results, we believed that the PULL:HPBCD blend mats would perform similarly to that of PULL in crosslinking with EGDGE. The crosslinked blend mat post EGDGE (see Figure 4.11) has additional peaks that are difficult to distinguish from those of a PULL only mat. What is most interesting is that after soaking the PULL:HPBCD blend mat in water, it does appear have some peak shifts likely from some PULL:HPBCD complexation, while the PULL only soaked mat has similar peaks to its original. Also of note is the attempt to "crosslink" the HPBCD only mat in EGDGE. This mat dissolved in the EGDGE at 80 °C. However, when PULL:HPBCD fibers are formed, the mat does crosslink and has different properties compared to the PULL-only mat based on FTIR spectra.

Therefore, potential exists for a PULL:HPBCD blend fiber mat to serve in desirable biotechnology applications.

4.4 Conclusion

Within this work, we correlate PULL, PULL:WP and PULL:HPBCD fiber mat morphologies to solution dynamics. We identify three regimes in the pullulan solution specific viscosity data that indicate the pullulan critical concentration to electrospin of a minimum of 13.7 w/w%, confirmed by defect free mat produced with a 15 w/w% solution. Pullulan tends to behave as do other polymers with broad polydispersity having a high c/c* ratio to achieve fibers. All solutions evaluated had dominant Newtonian regions; and solution viscosity increased in each case with increasing pullulan concentration. Blend fibers were able to form defect free mats. The addition of WP to PULL solutions shifted the critical concentration lower, enabling defect free mats to form at lower pullulan concentrations than PULL only mats. pH also impacted the success of electrospinning PULL:WP blends, as 50:50 blends at pH 3, 5.2, 8 and 11 all achieved defect free fibers. The lowest pH of 3 enabled nearly defect free fibers of 30:70 PULL:WPI. Protein on the surface of the PULL:WP fibers, as confirmed by XPS, enabled mats to be heat treated, presumably forming protein-protein linkages during heat treatment that rendered them insoluble in water. In fact, they formed very nice swellable, biodegradable, edible mats that would be ideal for cell seeding and tissue culture. XRD results agreed with literature data interpreted as pullulan being fully amorphous. Chemical crosslinking with EGDGE also yielded a crosslinked

network. In both heat treatment of PULL:WP blends and chemical submersion of PULL or PULL:HPBCD, an insoluble gelatinous/fibrous network was formed.

ACKNOWLEDGMENTS

Special thanks to: Davisco Foods for providing BiPRO whey protein isolate and BioPURE beta-lactoglobulin. Hayashibara International for providing PI-20 pharmaceutical/food grade pullulan. We thank Dr. Jason Bond, Dr. Thomas Fink and the East Carolina University Biology Department Imaging Core for Scanning Electron Microscope and Olympus Confocal Microscope use and Mr. Chris Dunkley of Olympus for reflected light microscopy support, and to Dr. Eva Johannes for Zeiss confocal microscope support. We thank Dr. Michelle Casper and Dr. Sara Arvidson for XRD support. Thank you for support of Andrew Cathey, Joseph A. Rose, Clayton Rice, Victoria L. Miller, Christopher A. Eckert, Adam Hussaini, Dao Dinh, Mohammed S. Akbar, and Michael S. Cannon.

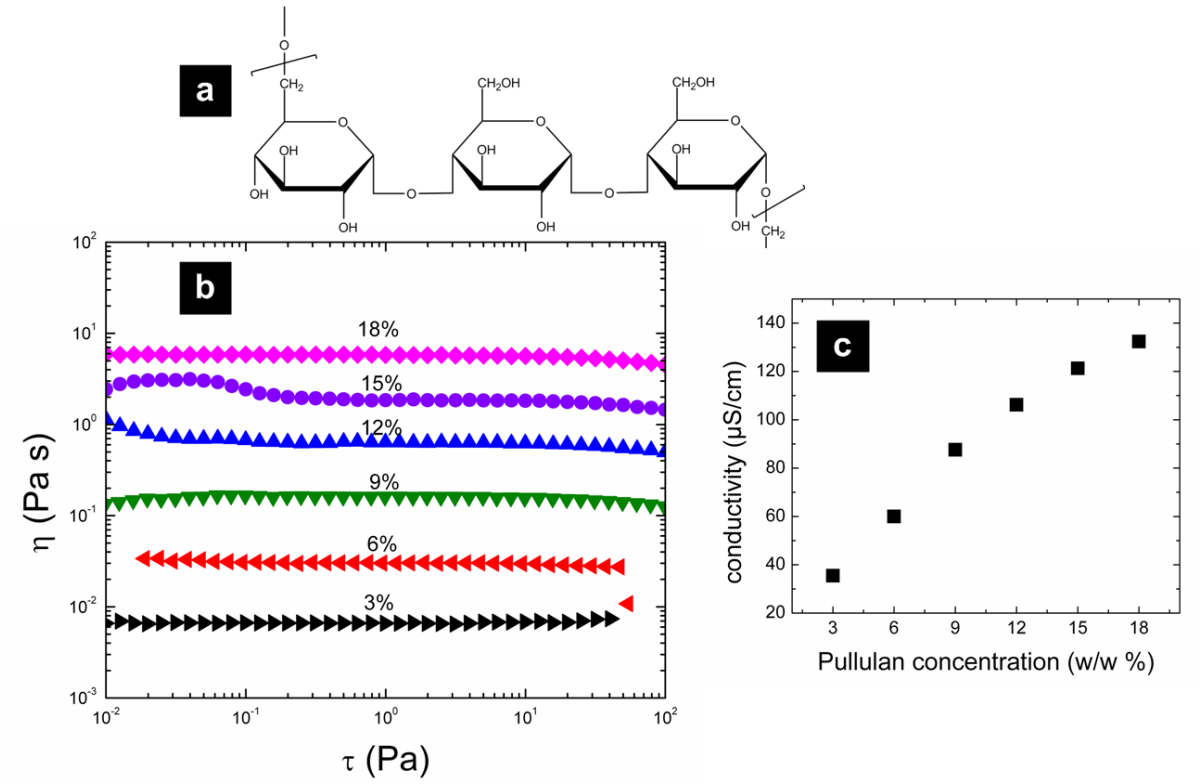

Figure 4.1. (a) molecular structure of pullulan, (b) Solution viscosity vs. shear stress for aqueous pullulan solutions at varying concentrations, and (c) solution conductivity vs. pullulan concentration.

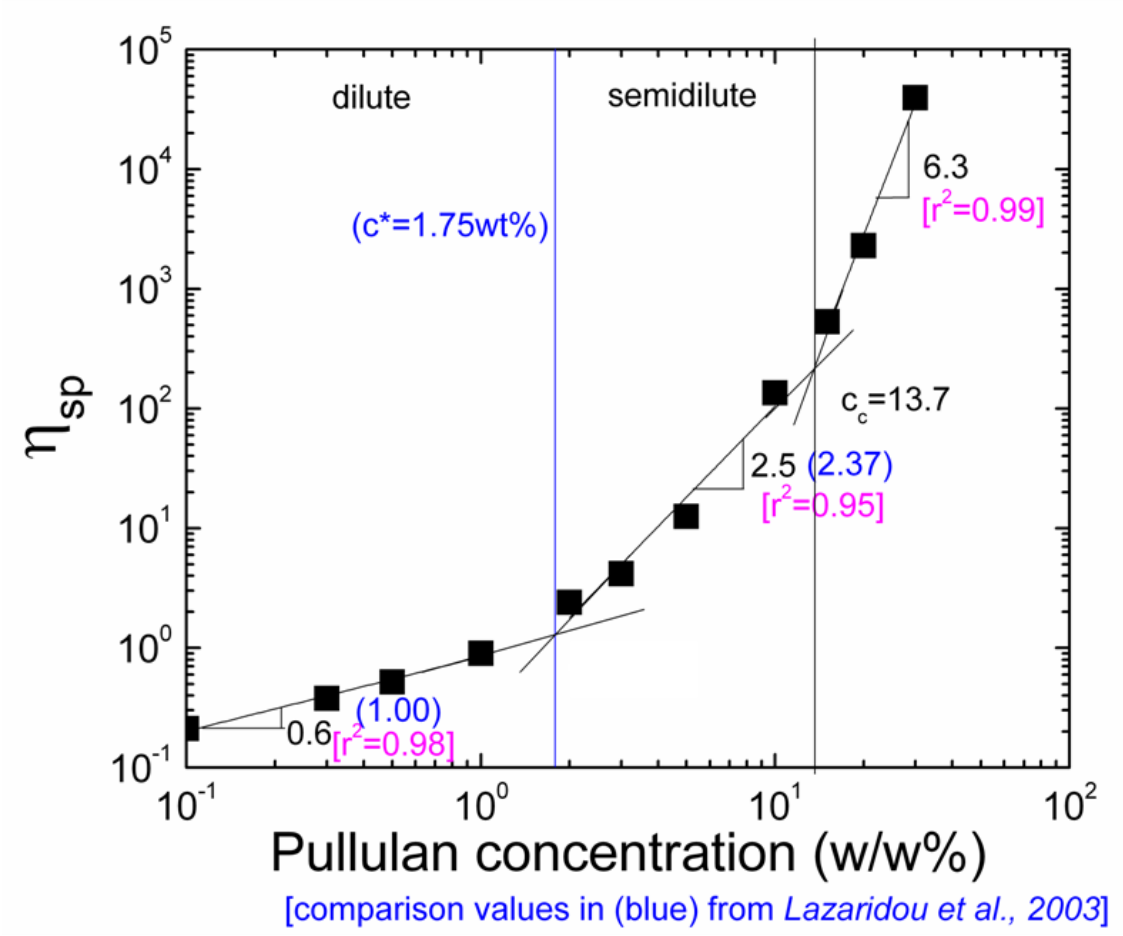

Figure 4.2. Rheological solution properties of pullulan: a log-log plot of specific viscosity vs. concentration for pullulan solutions with a three linear fit model.

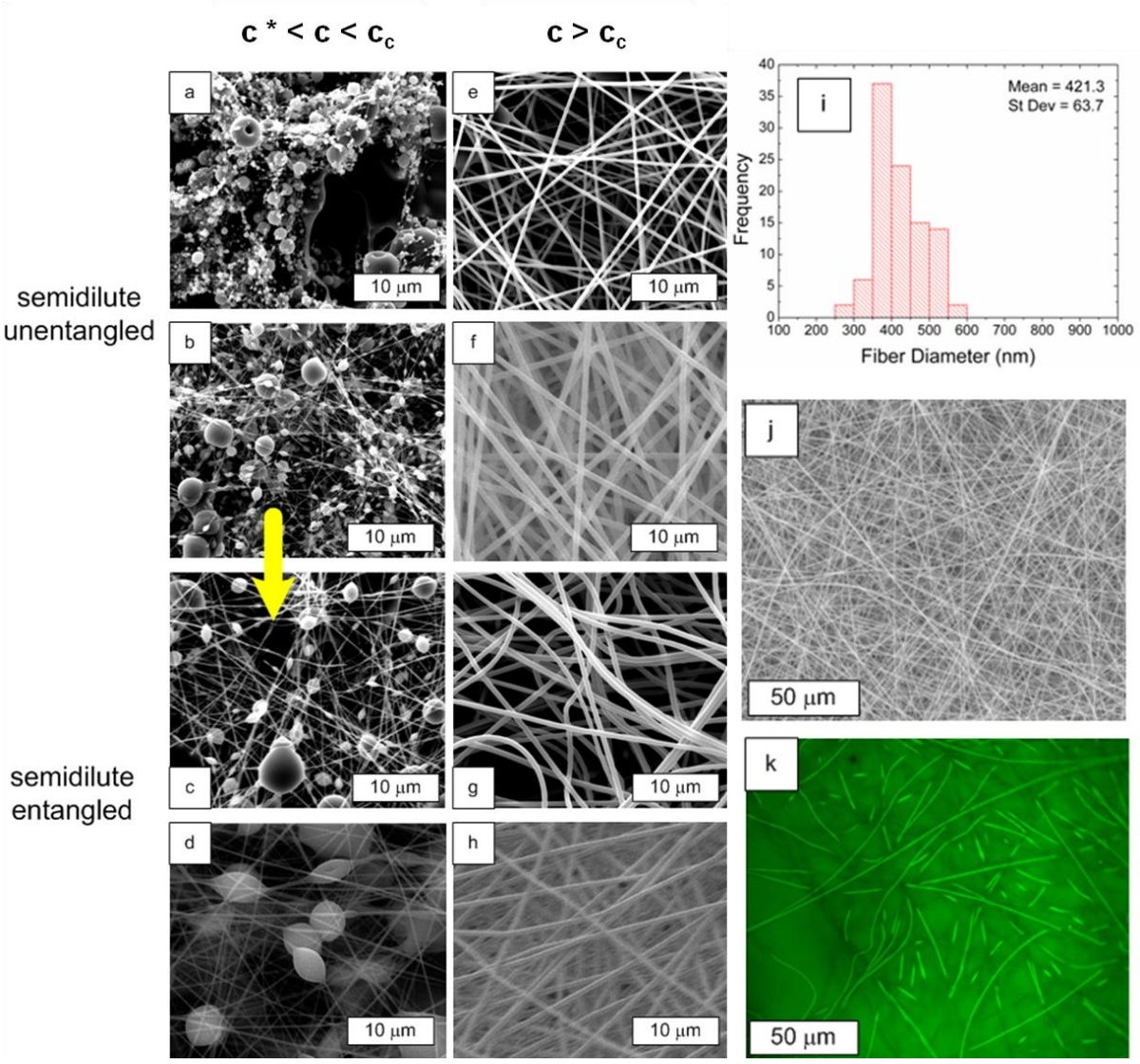

Figure 4.3. SEM micrographs of pullulan at varying concentrations (a) 25 w/w% [15 cm TCD, 0.25 ml/hr, 15.4 kV], (b) 20 w/w% [18 cm TCD, 1.0 ml/hr, 23 kV], (c) 18 w/w% [15 cm TCD, 1.50 ml/hr, 11.7 kV], (d) 15 w/w% [14cm TCD, 1.0 ml/hr, 9kV], (e) 12 w/w% [15 cm TCD, 1.75 ml/hr, 10.9 kV], (f) 11 w/w% [12 cm TCD, 1.0 ml/hr, 7.5 kV], (g) 9 w/w% [14 cm TCD, 1.1 ml/hr, 8.5 kV] (h) 6 w/w% [14cm TCD, 1.4 ml/hr, 9kV], (i) representative histogram results from SEM image analysis while (j) and (k) are SEM and confocal, respectively of 18 w/w% solution electrospun mat containing 0.2 w/w% RhB.

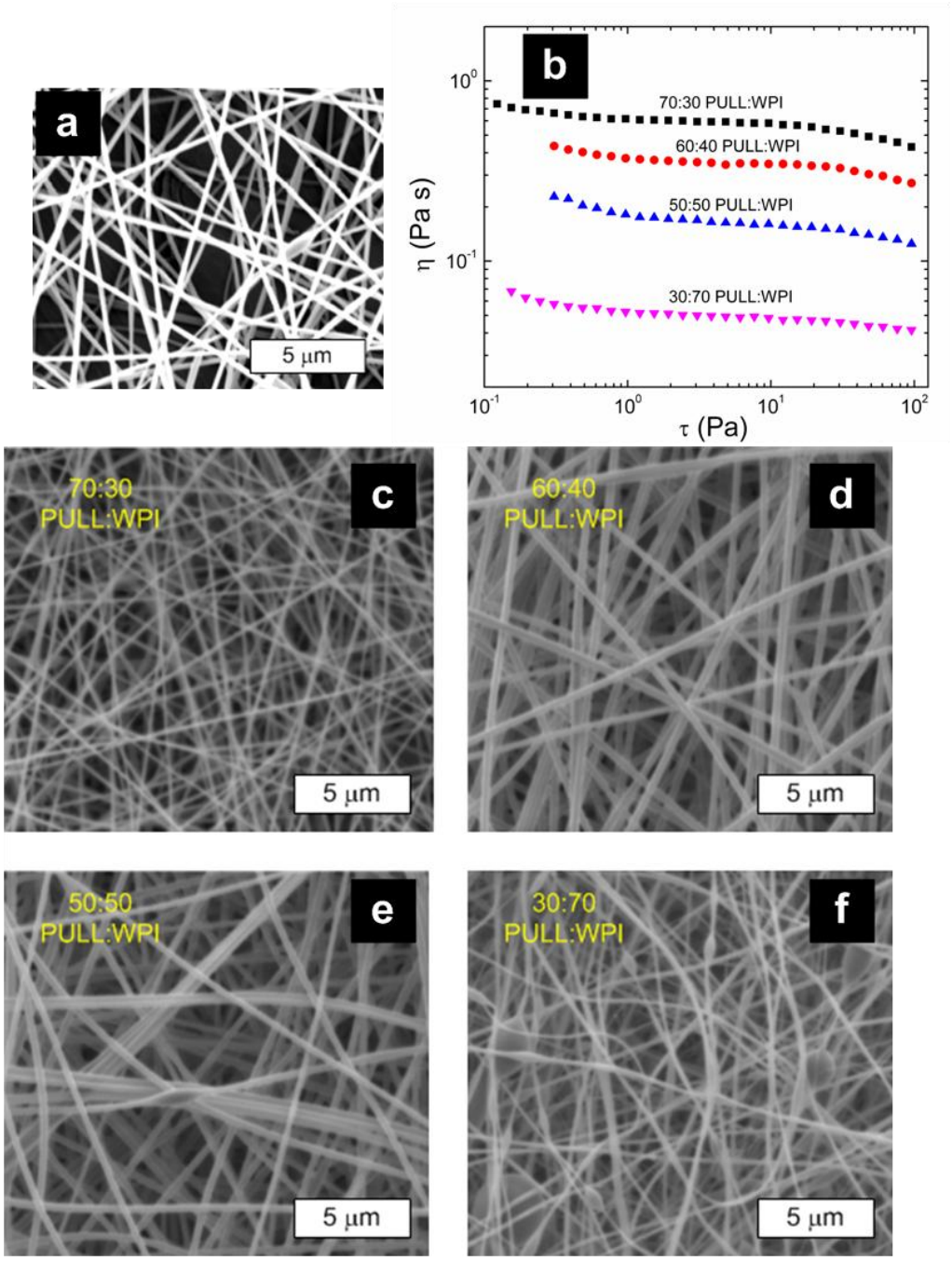

Figure 4.4. (a) Nanofiber mat of PULL:BLG, (b) Solution viscosity vs. shear stress for aqueous pullulan:WPI native mix pH blend solutions of varying composition at 17 total biomaterial w/w% and (c) – (e) are nanofiber mats at various PULL:WPI ratios blend nanofibers at mix pH. (c) 70:30 PULL:WPI (18cm TCD, 1 ml/hr, 26 kV), (d) 60:40 PULL:WPI (16.5 cm TCD, 0.65 ml/hr, 26 kV), (e) 50:50 PULL:WPI (18cm TCD, 1 ml/hr, 25 kV), (f) 30:70 PULL:WPI (14 cm TCD, 0.9 ml/hr, 18kV).

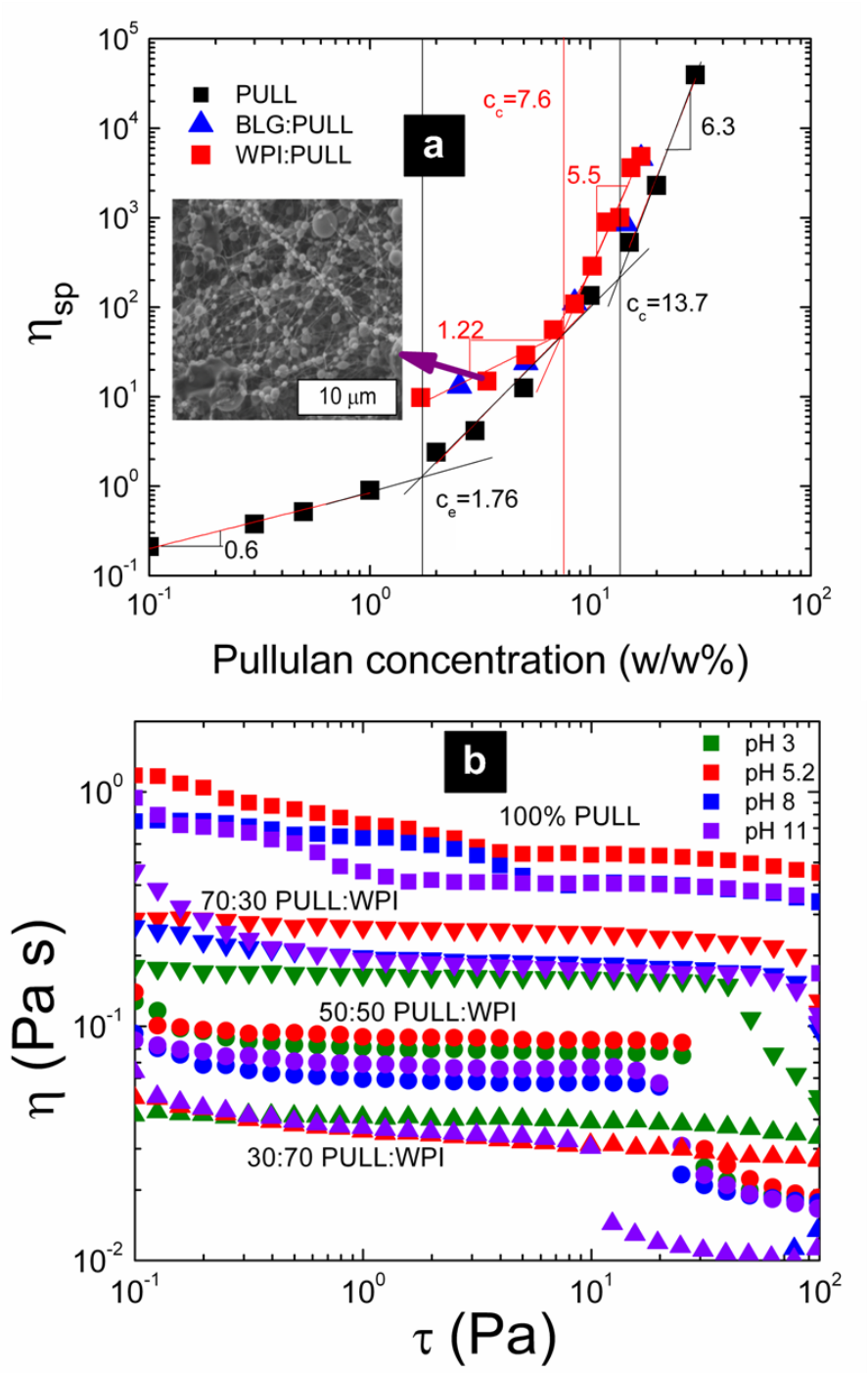

Figure 4.5. (a) Rheological solution properties of pullulan, PULL:WPI and PULL:BLG blends: a log-log plot of specific viscosity vs. concentration for pullulan solutions and (b) viscosity vs. shear stress for solutions of varying blend composition and pH.

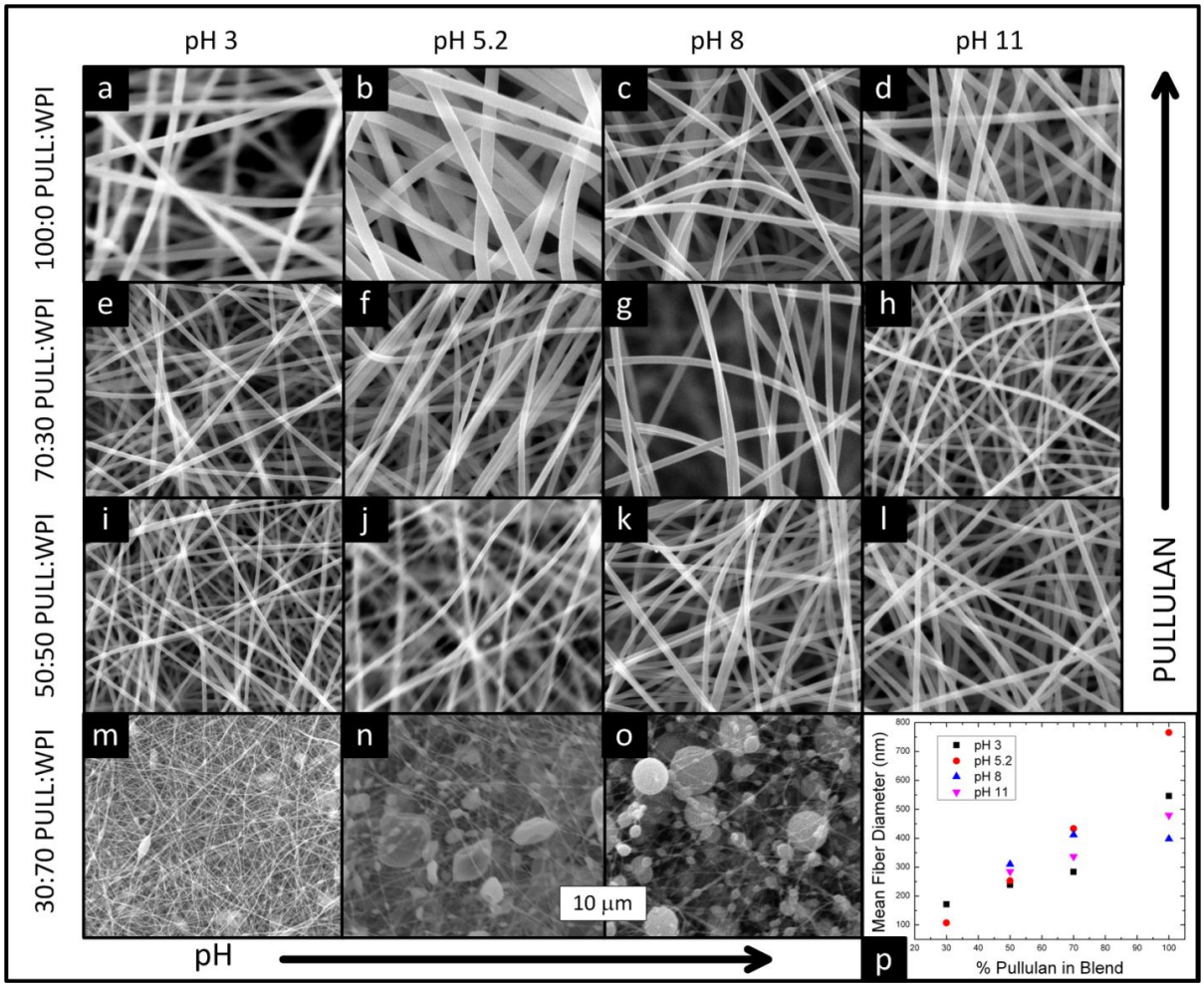

Figure 4.6. (a) – (o) Pullulan-whey protein isolate nanofibers varying concentration and pH. (p) is mean fiber diameter vs. % pullulan in fiber blend for each pH. Only fiber mats that did not have significant bead defects are included in data.

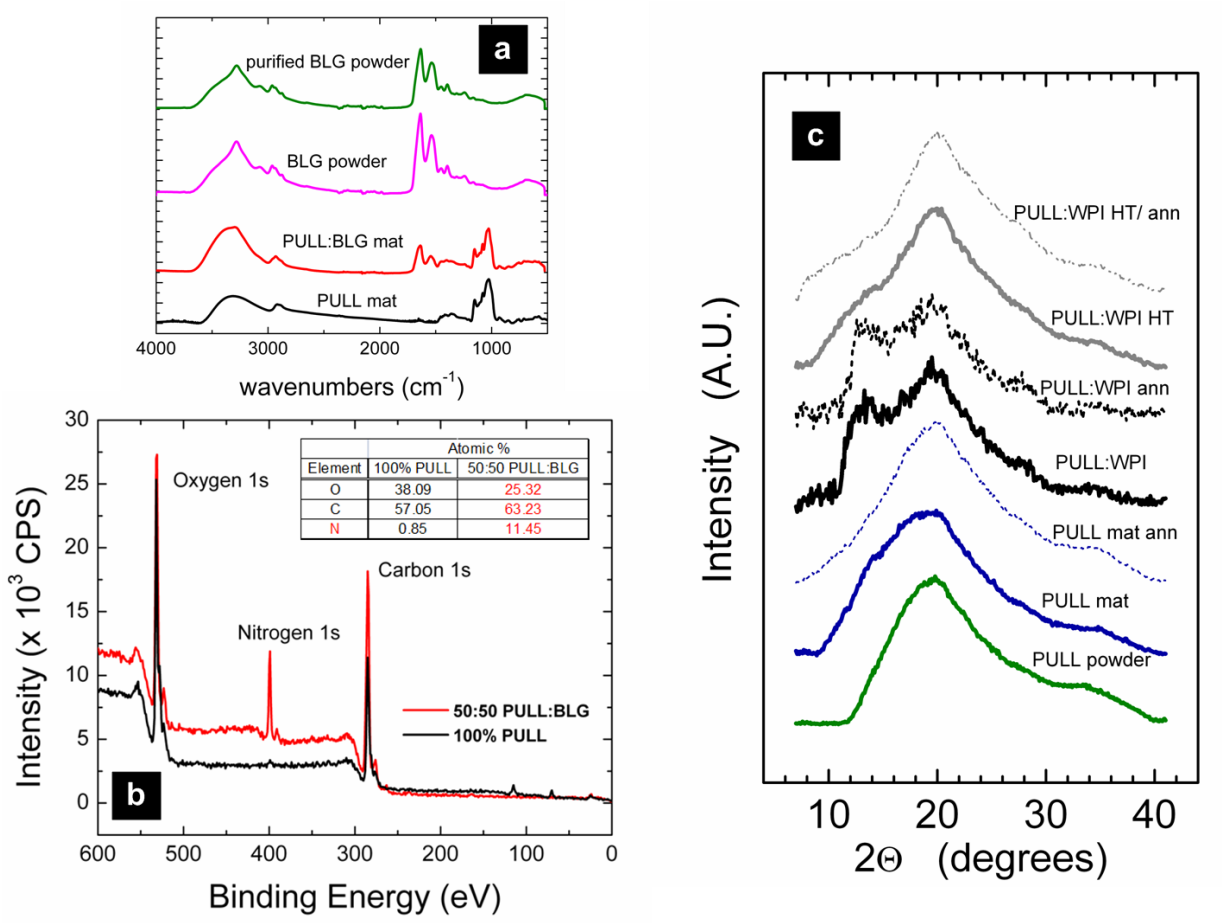

Figure 4.7. (a) FTIR absorbance spectra for raw materials and representative PULL:BLG blend nanofiber mats. (b) An XPS survey scan is displayed for electrospun nanofibers generated from 17 w/w% Pullulan solutions with and without WPI. The inset table provides the atomic percent of each element present on the nanofiber mat surface. Note that an aluminum 2p peak (4.01%) was also present in the 100% pullulan sample along with a trace amount of Nitrogen. This was due to this sample being analyzed while still on aluminum foil and the sample did not entirely cover the surface of the foil, hence yielding the small aluminum peak and trace amounts of nitrogen from foil handling. (c) X-ray diffraction patterns for 100% pullulan and 50:50 WPI:pullulan blend fiber mats. The heat treated blend mat for the pattern shown was heat treated for 18 hours at 100 °C. The solid lines are native samples, while the dashed lines are samples that were annealed at 150 °C before XRD.

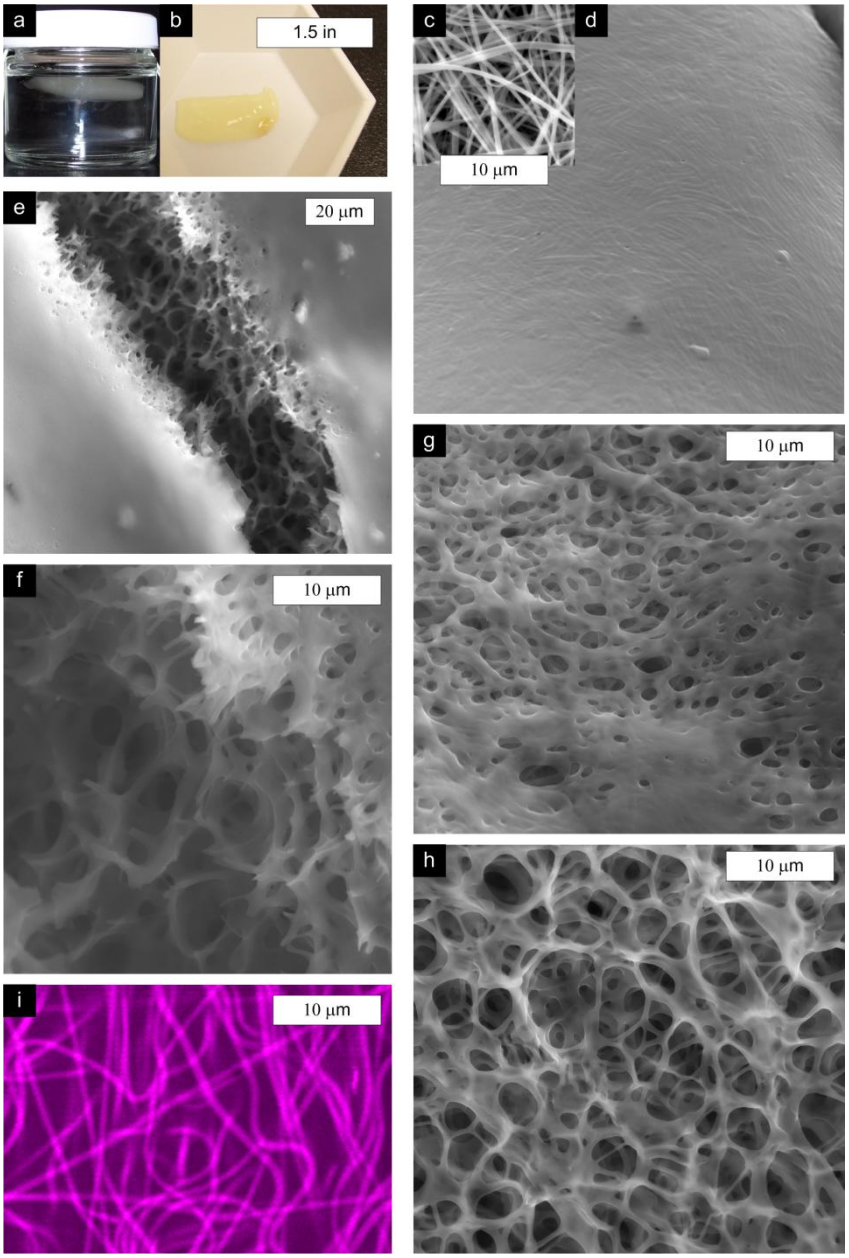

Figure 4.8. During (a) and Post (b) 24-hour room temperature deionized water soaking of 24 w/w% 50:50 PULL:WPI blend fiber mat (15cm TCD, 16.8 kV, 1 mL/hr, 22 gauge 2" Needle) that had been heat treated 46 hours (oven, 100 °C); (c) SEM of same mat during heat treatment (at 18 hour time point). (d) ESEM of surface of (b); (e) and (f) are ESEM of (b) at tear location. (g) and (h) are ESEM of (b) at alternate locations showing structure beneath smooth scaffold-water interface. (i) is confocal image of same 46-hour heat treated mat following 4-day soaking in deionized water.

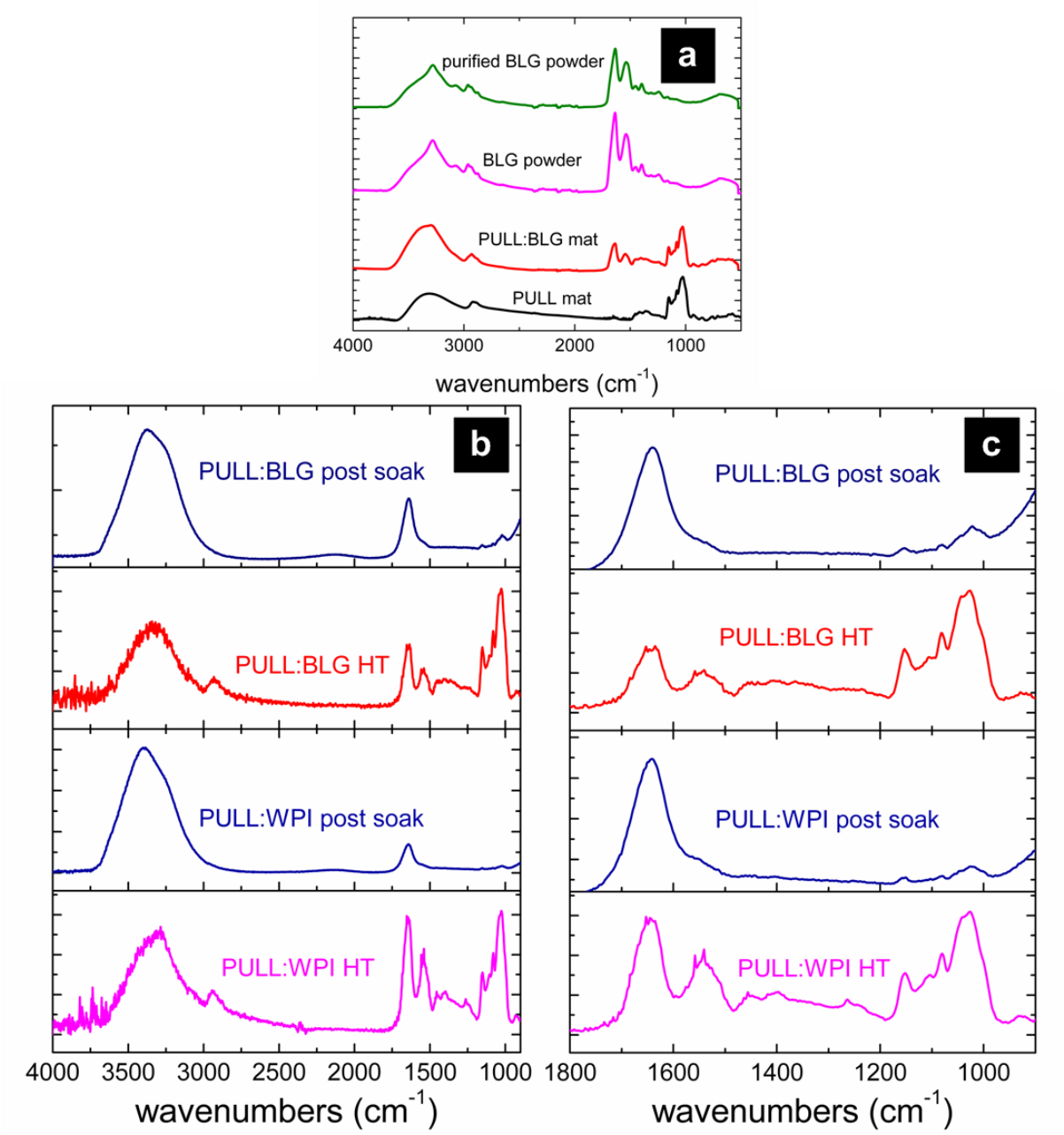

Figure 4.9. FTIR spectra for (a) BLG, pullulan mat and PULL:BLG blend mat, (b) pre and post soak of PULL:WPI and PULL:BLG blend fiber mats – full spectra and (c) partial spectra.

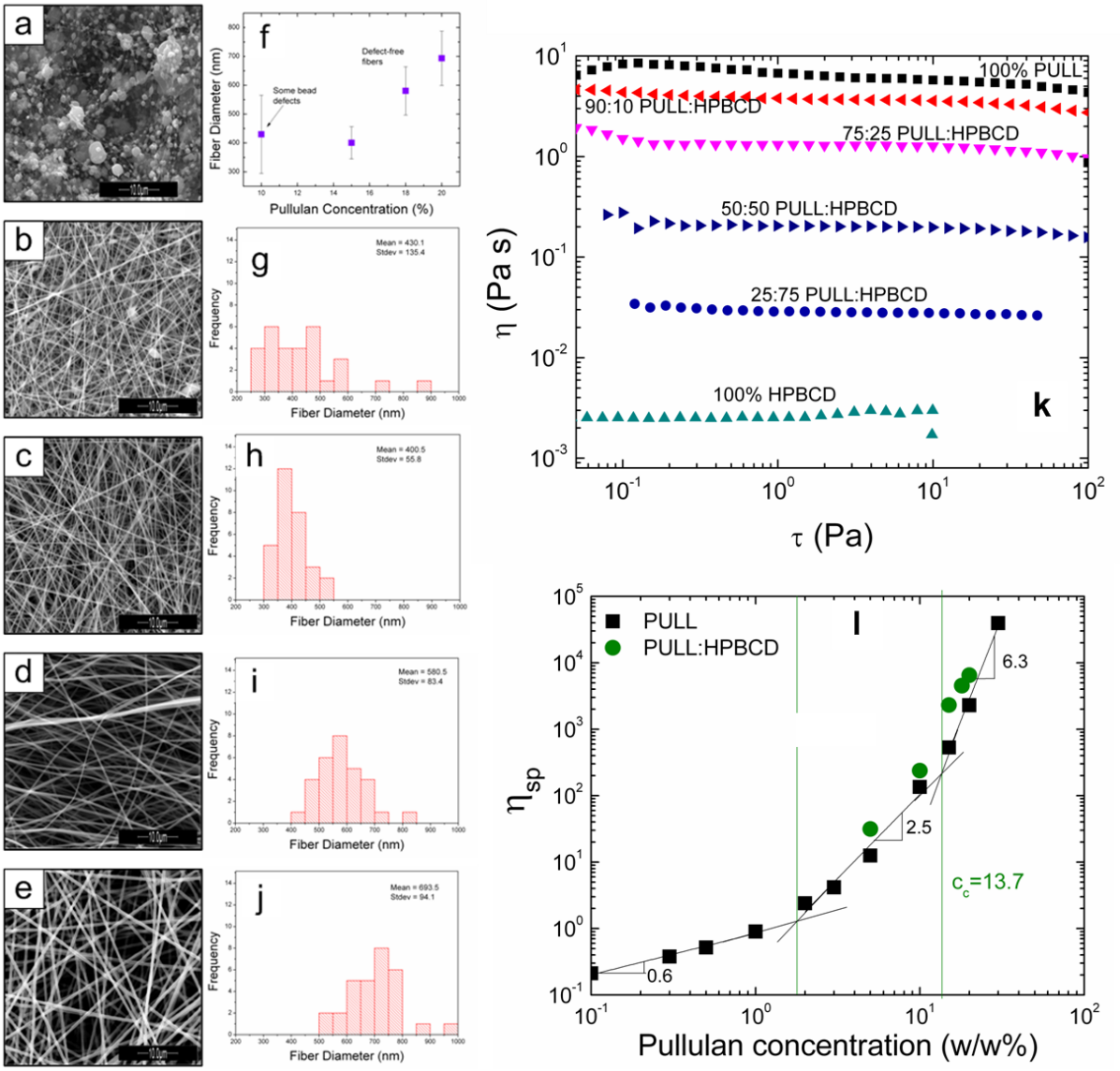

Figure 4.10. PULL-HPBCD fiber mats prepared from total 20 w/w% aqueous solution with PULL:HPBCD (a) 25:75; (b) 50:50 with (g) fiber diameter frequency; (c) 75:25 with (h) fiber diameter frequency; (d) 90:10 with (i) fiber diameter frequency; and (e) 100:0 with (j) fiber diameter frequency. (f) shows linear increase in fiber diameter with increasing pullulan concentration of defect free fibers. (k) viscosity vs. shear stress of PULL:HPBCD blend aqueous solutions and (l) specific viscosity vs. concentration log-log plot to compare data to theory.

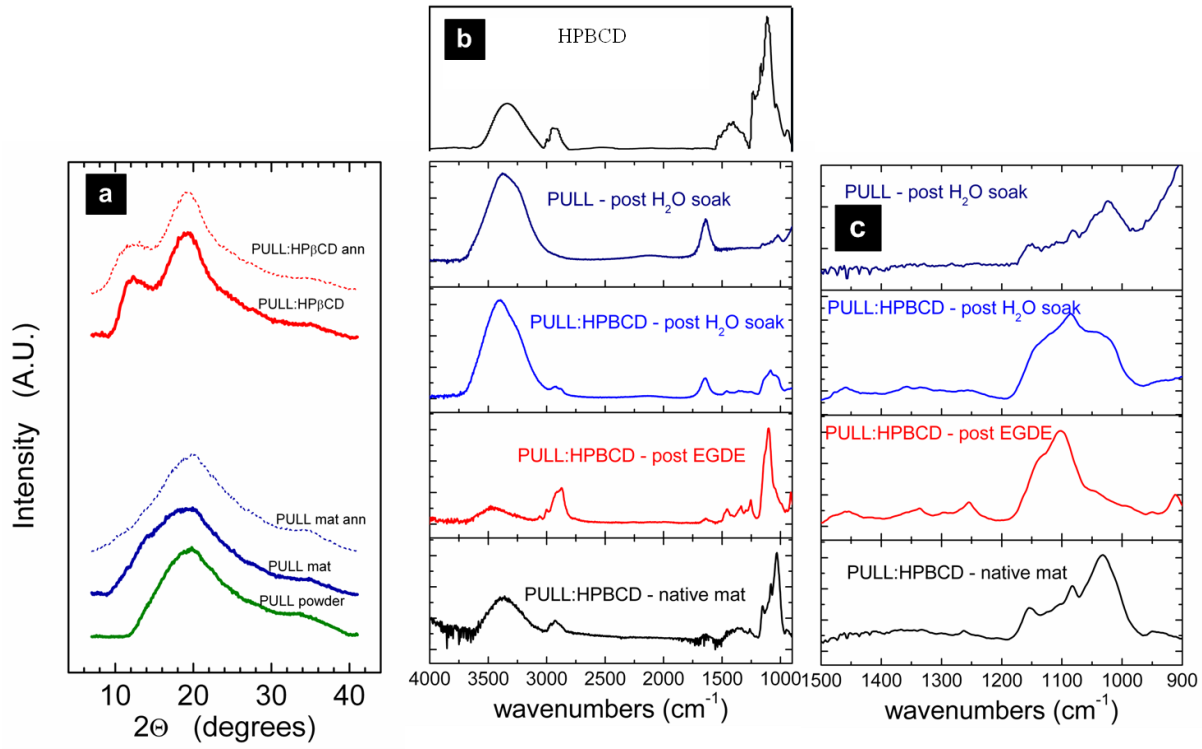

Figure 4.11 (a) XRD of 100% pullulan and PULL:HPBCD blend fiber mats and (b) FTIR of PULL:HPBCD native, EGDGE crosslinked, and crosslinked-water soaked mat in comparison to PULL only EGDGE crosslinked mat, which indicates that the PULL:HPBCD mat does retain some HPBCD in both EGDGE crosslinking and DW immersion. (c) Shows FTIR results in focused 1500 – 900 cm^{-1} wavenumber range.

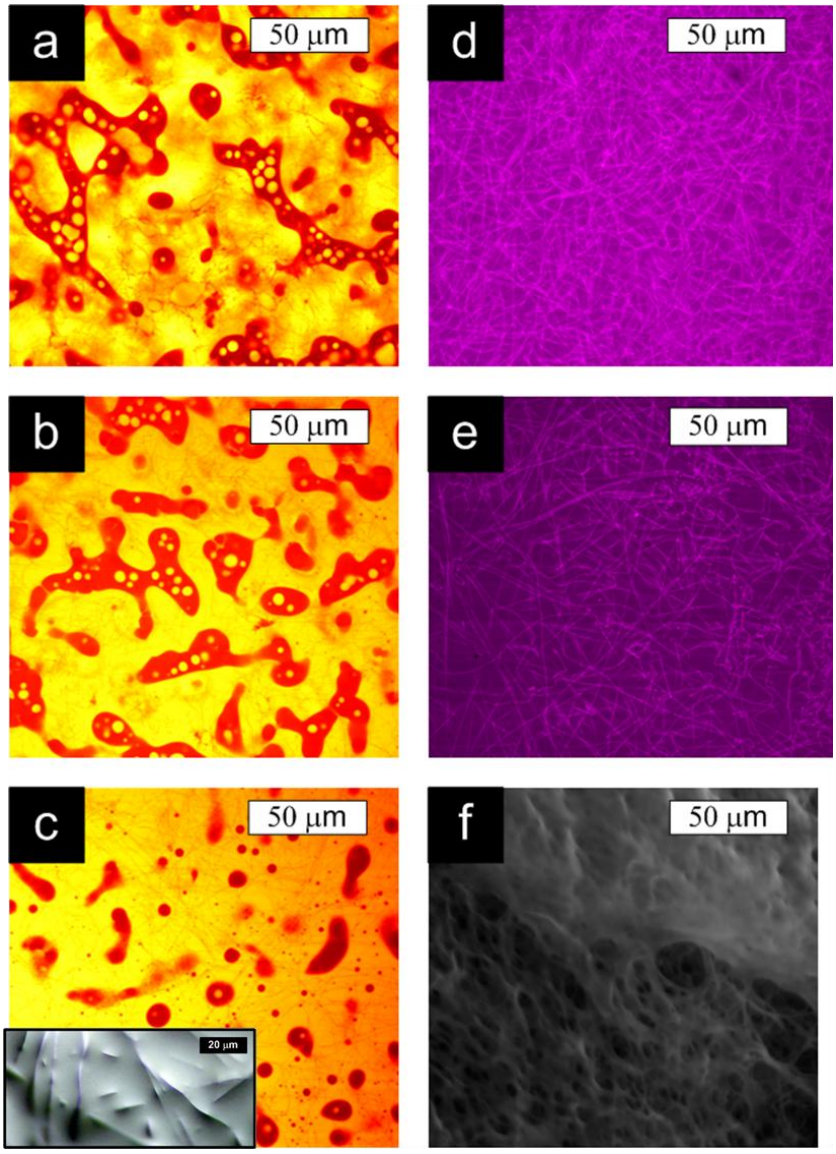

Figure 4.12. Confocal microscope images of pullulan fiber mat after immersion crosslinking in EGDGE at 80 °C for 24 hours. (a) – (c) were treated minutes before imaging with RhB-deionized water solution, with (a) deepest into sample from lens, but closer to surface where solution was applied, with (b) and (c) progressing closer to the objective and surface of microscope slide. (d) and (e) are the same fiber mat that has soaked suspended in deionized water for 48 hours, removed from soaking just before application of RhB dye solution, then imaged with (d) further from objective and (e) closer to objective and surface of microscope slide. The ESEM image in (f) shows the structure of the pullulan mat crosslinked in EGDGE after soaking in DW for 24 hours. The inset in (c) is a reflected light microscope image of an EGDGE-crosslinked mat.

Table 4.1. FTIR peaks representative of pullulan.[24]

Wavenumbers (cm^{-1})	characteristic
850	α-glucopiranosid units
755	α-(1,4) glucosidic bonds
932	α-(1,6) glucosidic bonds
2850-3000	CH and CH_2 stretching vibrations
1300-1500	CH/CH_2 deformation vibrations
3000-3600	Hydroxyl band
1000-1260	C-O stretching
1724	Carbonyl band
2930	CH stretching vibrations

Table 4.2. FTIR spectra analysis of 3-7% BLG in deuterium oxide solution.[51]

Wavenumber (cm-1)	BLG Characteristic region
1600-1700	Amide I region C=O and C-N stretching
1621, 1634, 1692	β-sheets
1649	α-helix
1677	Turns or β-sheets
1663	turns
1605	Side chain residues

APPENDIX A. PULL:WPI blend solution properties and electrospinning parameters.

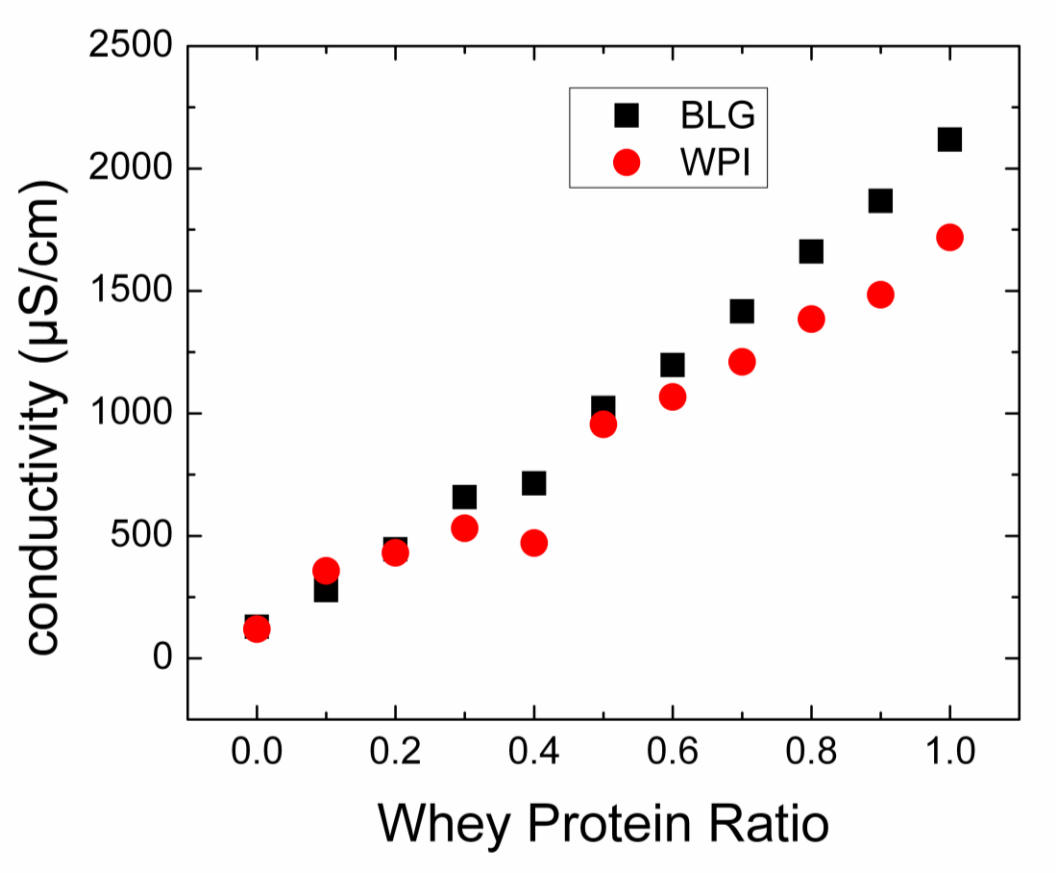

Figure APP.1. Conductivity of whey protein-pullulan 17 w/w% mixtures (at native mix pH).

Table APP1. PULL:WPI blend solution properties and electrospinning parameters.

Solution Properties					E-spin parameters				
Pullulan	**WPI**	**Total Weight Percent**	**Ph**	**Conductivity**	**spacing**	**flow rate (ml/hr)**	**voltage (kV)**	**needle**	**Morphology**
100%	0%	17%	11	623 µs/cm	15cm	0.7	15	22	Fibers
70%	30%	17%	11	1844 µs/cm	15cm	0.7	20.6	22	Fibers
50%	50%	17%	11	3.33ms/cm	15cm	0.7	20.7	22	Fibers
30%	70%	17%	11	3.77ms/cm					Would not spin
0%	100%	17%	11	6.15 ms/cm					Would not spin
Pullulan	**WPI**	**Total Weight Percent**	**Ph**	**Conductivity**	**spacing**	**flow rate (ml/hr)**	**voltage (kV)**	**needle**	**Morphology**
100%	0%	17%	8	777 µs/cm	15cm	0.9	13.3	22	Fibers
70%	30%	17%	8	876 µs/cm	15cm	0.5	15.9	22	Fibers
50%	50%	17%	8	1273 µs/cm	15cm	1.5	18.6	22	Fibers
30%	70%	17%	8	2065 µs/cm	15cm	0.1	19.8	22	Beaded fibers
0%	100%	17%	8	3.16 ms/cm					Would not spin
Pullulan	**WPI**	**Total Weight Percent**	**Ph**	**Conductivity**	**spacing**	**flow rate (ml/hr)**	**voltage (kV)**	**needle**	**Morphology**
100%	0%	17%	5.2	162.6 µs/cm	15cm	0.8	14.7	22	Fibers
70%	30%	17%	5.2	1479 µs/cm	15cm	1	16.5	22	Fibers
50%	50%	17%	5.2	2339 µs/cm	15cm	0.4	15.1	22	Fibers
30%	70%	17%	5.2	3.51 ms/cm	15cm	0.1	15.2	22	Beaded fibers
0%	100%	17%	5.2	4.66 ms/cm					Would not spin
Pullulan	**WPI**	**Total Weight Percent**	**Ph**	**Conductivity**	**spacing**	**flow rate (ml/hr)**	**voltage (kV)**	**needle**	**Morphology**
100%	0%	17%	3	524 µs/cm	15cm	0.5	17.2	22	Fibers
70%	30%	17%	3	5.05 ms/cm	15cm	0.1	17.5	22	Fibers
50%	50%	17%	3	5.53 ms/cm	15cm	0.1	17.5	22	Fibers
30%	70%	17%	3	7.13 ms/cm	15cm	0.5	27.9	22	Fibers with some beads
0%	100%	17%	3	28.32 ms/cm					Would not spin

APPENDIX B. PULL:HPBCD solution and electrospinning parameters.

% Pullulan (w/w)	% HPβCD (w/w)	Total Weight Percent	pH	Conductivity (µs/cm)	Fiber Morphology	Spacing (cm)	Flow Rate (ml/hr)	Voltage (kV)	Needle (mm)
20%	0%	20%	5.15	57.10	Nanofibers	15.00	0.20	11.20	22.00
18%	2%	20%	5.70	53.80	Nanofibers	15.00	0.20	6.80	22.00
15%	5%	20%	5.80	47.80	Nanofibers	15.00	0.20	7.50	22.00
10%	10%	20%	5.37	37.20	Minimal bead defects	15.00	0.20	8.90	22.00
5%	15%	20%	5.03	38.10	Beaded Nanofibers	15.00	0.30	7.50	22.00
0%	20%	20%	6.43	25.06	Did not e-spin	-	-	-	-

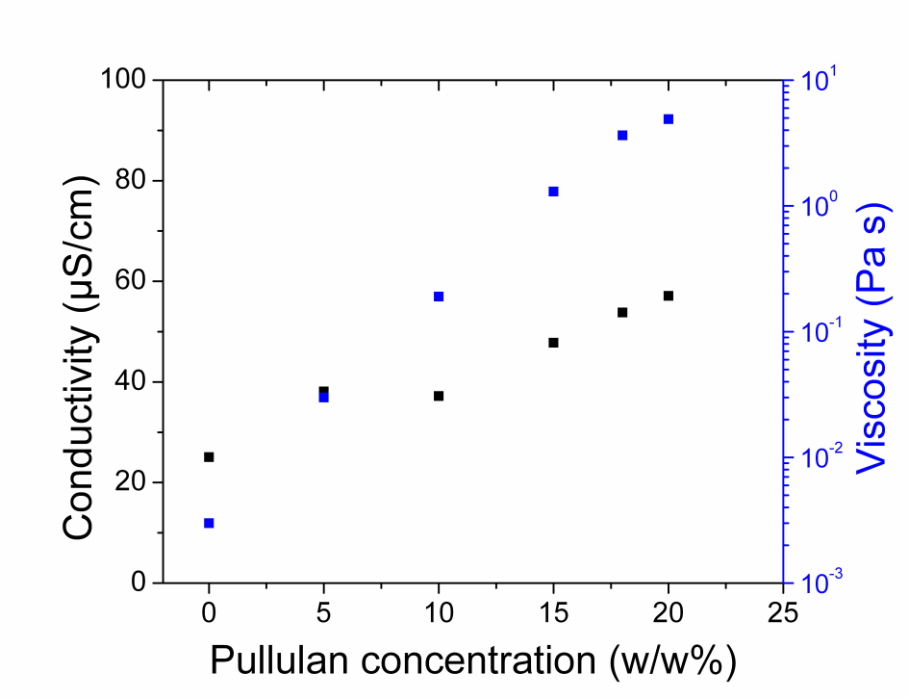

% Pullulan (w/w)	% HPβCD (w/w)	Total Weight Percent	pH	Conductivity (µs/cm)	Fiber Morphology	Spacing (cm)	Flow Rate (ml/hr)	Voltage (kV)	Needle (mm)
20%	10%	30%	5.41	45.50	Nanofibers	15.00	0.30	8.50	22.00
20%	20%	40%	4.86	38.80	Nanofibers	15.00	0.30	7.00	22.00
10%	35%	45%	5.48	25.02	Nanofibers	15.00	0.30	5.30	22.00
10%	45%	55%	5.39	18.32	Beaded Nanofibers	20.00	0.30	5.50	22.00
0%	60%	60%	6.17	7.78	Did not e-spin	-	-	-	-
0%	70%	70%	6.90	2.51	Nanofibers	15.00	0.30	12.10	22.00

% Pullulan (w/w)	% HPβCD (w/w)	Total w/w%	pH	Conductivity (µs/cm)	Fiber Morphology
20%	10%	30%	5.41	45.50	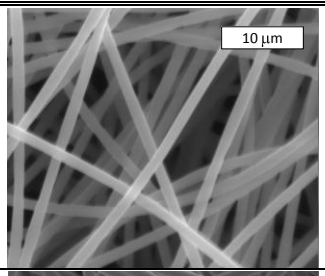
20%	20%	40%	4.86	38.80	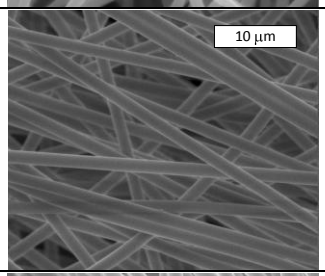
10%	35%	45%	5.48	25.02	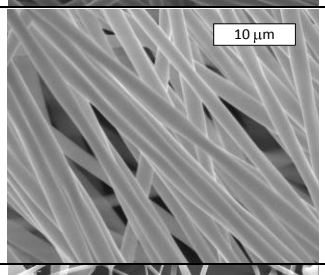
10%	45%	55%	5.39	18.32	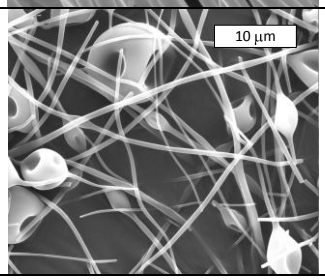
0%	60%	60%	6.17	7.78	Did not e-spin
0%	70%	70%	6.90	2.51	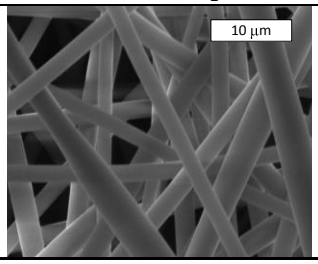

4.5 References

1. Hayashibara **2007**, 8.

2. Rulis, A. M. **2002**, 1-4.

3. Lazaridou, A.; Biliaderis, C. G.; Kontogiorgos, V. *Carbohydrate Polymers* **2003**, 151-166.

4. Fundueanu, G.; Constantin, M.; Ascenzi, P. *Biomaterials* **2008**, *18*, 2767-2775.

5. Autissier, A.; Letourneur, D.; Le Visage, C. *Journal of Biomedical Materials Research Part A* **2006**, 336-342.

6. Dulong, V.; Cerf, D. L.; Picton, L.; Muller, G. *Colloids and Surfaces A: Physicochemical and Engineering Aspects* **2006**, *1-3*, 163-169.

7. Lack, S.; Dulong, V.; Le Cerf, D.; Picton, L.; Argillier, J. F.; Muller, G. *Polymer Bulletin* **2004**, 429-436.

8. Lee, I.; Akiyoshi, K. *Biomaterials* **2004**, *15*, 2911-2918.

9. Sallustio, S.; Galantini, L.; Gente, G.; Masci, G.; LaMesa, C. *J. Phys. Chem. B* **2004**, *49*, 18876-18883.

10. Shingel, K. I. *Carbohydrate Research* **2004**, *3*, 447-460.

11. Fundueanu, G.; Constantin, M.; Mihai, D.; Bortolotti, F.; Cortesi, R.; Ascenzi, P.; Menegatti, E. *Journal of Chromatography B* **2003**, 407-419.

12. Diab, T.; Biliaderis, C. G.; Gerasopoulos, D.; Sfakiotakis, E. *Journal of the Science of Food and Agriculture* **2001**, 988-1000.

13. Yang, K. S.; Lee, E. Y.; Park, M. S.; Lee, K. Y.; Lee, Y. H. *Han'guk Somyu Konghakhoechi* **1998**, *8*, 465.

14. Vandamme, E. J.; Bruggeman, G.; De Baets, S.; Vanhooren, P. T. *Agrofoodindustry hi-tech* **1996**, *5*, 21.

15. Tsujisaka, Y.; Mitsuhashi, M. Pullulan. In *Industrial Gums: Polysaccharides and their derivatives;* Whistler, R. L., BeMiller, J. N., Eds.; Academic Press, Inc.: San Diego, 1993; pp 447-460.

16. Mehvar, R. *Current Pharmaceutical Biotechnology* **2003**, 283-302.

17. Wolf, B. W.; Garleb, K. A.; Choe, Y. S.; Humphrey, P. M.; Maki, K. C. *J. Nutr.* **2003**, 1051-1055.

18. McNeil, B.; Harvey, L. M. *Critical Reviews in Biotechnology* **1993**, *4*, 275-304.

19. Ding, P.; Pacek, A. W.; Frith, W. J.; Norton, I. T.; Wolf, B. *Food Hydrocolloids* **2005**, 567-574.

20. Frenot, A.; Chronakis, I. S. *Current Opinion in Colloid and Interface Science* **2003**, 64-75.

21. Li, D.; Xia, Y. *Advanced Materials* **2004**, 1151-1170.

22. Sun, X. -.; Shankar, R.; Börner, H. G.; Ghosh, T. K.; Spontak, R. J. *Advanced Materials* **2007**, 87-91.

23. Yang, K. S.; Lee, E. Y.; Park, M. S.; Lee, K. Y.; Lee, Y. H. *Han'guk Somyu Konghakhoechi* **1998**, *8*, 465-471.

24. Karim, M. R.; Lee, H. W.; Kim, R.; Ji, B. C.; Cho, J. W.; Son, T. W.; Oh, W.; Yeum, J. H. *Carbohydr. Polym.* **2009**, *2*, 336-342.

25. Tang, C.; Saquing, C. D.; Harding, J. R.; Khan, S. A. *Macromolecules* **2009;**, *2*, 630-637.

26. Ulery, B. D.; Nair, L. S.; Laurencin, C. T. *Journal of Polymer Science Part B: Polymer Physics* **2011**, *12*, 832-864.

27. Bonino, C. A.; Krebs, M. D.; Saquing, C. D.; Jeong, S. I.; Shearer, K. L.; Alsberg, E.; Khan, S. A. *Carbohydr. Polym.* **2011**, *1*, 111-119.

28. Jeong, S. I.; Krebs, M. D.; Bonino, C. A.; Samorezov, J. E.; Khan, S. A.; Alsberg, E. *Tissue Engineering Part A* **2011**, *1-2*, 59-70.

29. Shi, L.; Le Visage, C.; Chew, S. Y. *Journal of Biomaterials Science, Polymer Edition* **2011**, *11*, 1459-1472.

30. Muir, M. DMSO: Many Uses, Much Controversy. *http://www.dmso.org/articles/information/muir.htm*2008).

31. Lynch, D. W.; Placke, M. E.; Persing, R. L.; Ryan, M. J. *Toxicological Sciences* **2003**, *2*, 347-358.

32. Sullivan, S. T.; Tang, C.; Talwar, S.; Kennedy, A.; Khan, S. A. *Draft for Submission from Chapter 1*. **2011**.

33. Gounga, M. E.; Zu, S.; Wang, Z.; Yang, W. G. *Journal of Food Science* **2008**, *4*, E155-E161.

34. Gounga, M. E.; Xu, S.; Wang, Z. *Journal of Food Engineering* **2007**, *4*, 521-530.

35. Gounga, M. E.; Xu, S.; Wang, Z. *Journal of Food Biochemistry* **2010**, *3*, 501-519.

36. Wang, S.; van Dijk, P. A. P. P.; Odijk, T.; Smit, J. A. M. *Biomacromolecules* **2001**, 1080-1088.

37. Ganzevles, R. A.; Kosters, H.; vanVliet, T.; CohenStuart, M. A.; deJongh, H. H. J. *J. Phys. Chem. B* **2007**, *45*, 12969-12976.

38. Sullivan, S. T.; Simmons, J. M.; Fink, T. J.; Robinson, M. D.; Cistola, D.; Khan, S. A. *Draft for submission from Chapter 3*. **2011**.

39. Autissier, A.; Letourneur, D.; Le Visage, C. *Journal of Biomedical Materials Research Part A* **2007**, *2*, 336-342.

40. Dulong, V.; Forbice, R.; Condamine, E.; Le Cerf, D.; Picton, L. *Polymer Bulletin* **2011**, *3,* 455-466.

41. Borde, B.; Bizot, H.; Vigier, G.; Buleon, A. *Carbohydr. Polym.* **2002**, *1,* 83-96.

42. Socrates, G. *Infrared Charateristic Group Frequencies: Tables and Charts;* John Wiley & Sons: Chichester, 1994; , pp 249-752.

43. McKee, M. G.; Wilkes, G. L.; Colby, R. H.; Long, T. E. *Macromolecules* **2004**, *5,* 1760-1767.

44. Klossner, R. R.; Queen, H. A.; Coughlin, A. J.; Krause, W. E. *Biomacromolecules* **2008; 2008**, *10,* 2947-2953.

45. Andrady, A. L. *Science and Technology of Polymer Nanofibers;* Wiley: 2008; , pp 404.

46. Lazaridou, A.; Biliaderis, C. G.; Kontogiorgos, V. *Carbohydrate Polymers* **2003**, 151-166.

47. Karim, M. R.; Lee, H. W.; Kim, R.; Ji, B. C.; Cho, J. W.; Son, T. W.; Oh, W.; Yeum, J. H. *Carbohydr. Polym.* **2009**, *2,* 336-342.

48. Kilburn, D.; Claude, J.; Schweizer, T.; Alam, A.; Ubbink, J. *Biomacromolecules* **2005; 2005**, *2,* 864-879.

49. Bizot, H.; Le Bail, P.; Leroux, B.; Davy, J.; Roger, P.; Buleon, A. *Carbohydr. Polym.* **1997**, *1,* 33-50.

50. Kristo, E.; Biliaderis, C. G. *Carbohydr. Polym.* **2007**, *1*, 146-158.

51. Eissa, A. S.; Puhl, C.; Kadla, J. F.; Khan, S. A. *Biomacromolecules* **2006**, *6*, 1707-1713.

52. Celebioglu, A.; Uyar, T. *Langmuir* **2011; 2011**, *10*, 6218-6226.

53. Zhao, H.; Kwak, J. H.; Conrad Zhang, Z.; Brown, H. M.; Arey, B. W.; Holladay, J. E. *Carbohydr. Polym.* **2007**, *2*, 235-241.

CHAPTER 5 Near Infrared Reflectance (NIR) Spectroscopy of Commercial Whey Protein Powders

Chapter 5 is essentially a manuscript by Jamelle M. Simmons, Paul Gemperline and Stephanie T. Sullivan to be submitted to the *Journal of Chemometrics* or *Applied Spectroscopy.*

Near Infrared (NIR) Spectroscopy of Commercial Whey Protein Powders

Jamelle Simmons[‡a]*, Paul Gemperline*[‡b]*, Stephanie T. Sullivan*

Department of Chemical and Biomolecular Engineering, North Carolina State University, Raleigh, NC 27695-7905
[‡a] Department of Engineering, East Carolina University, Greenville, NC 27858
[‡b] Department of Chemistry, East Carolina University, Greenville, NC 27858

ABSTRACT

Near Infrared Reflectance (NIR) Spectroscopy usage in the rapid quantification of products is gaining more attention in areas of biofuel, dairy, food & beverage, feed & forage, grain, and pharmaceutical industries. Coupled with advances in statistical techniques (such as chemometrics), powerful models can be built to determine product composition of future unknown samples based on known reference standards. NIR Spectroscopy is a quick, non-invasive, non-destructive alternative to traditional chemical methods which take longer to complete. Multivariate methods are used to take a complex matrix of data and extract the most amount of variation which is representative of the original matrix. The new, simplified matrix is then used to build a calibration model with predicative capabilities. The following study investigated the potential of chemometric techniques in the prediction of whey protein samples through the use of Partial Least Squares (PLS) modeling. From all whey protein samples, protein % concentration, fat % concentration, moisture % concentration, and pH concentration were selected for PLS analysis. A calibration model was made for each concentration that was validated by a separate set of samples not used in the calibration

models. We found that of the samples used in this study, four models could be created that determined the concentrations of samples unknown to it. This resulted in four validated models with low Root Mean Square Error of Prediction (RMSEP). NIR shows promise for improvement of quality control and rapid results. However, standardization and robust calibration issues still exist that need to be addressed before NIR Spectroscopy can be implemented in a production process.

5.1 Introduction

5.1.1 Whey Protein Concentrate

Whey proteins are high quality and nutritious proteins that are beneficial to the body's performance. Whey protein isolate is the purest form of protein containing between 90-99% protein with whey protein concentrate containing between 29-89% protein based on the manufacturers specifications. Whey proteins are made up of a number of individual proteins including: β-lactoglobulin, α-lactalbumin, immunoglobulins, Bovine Serum Albumin (BSA), Glycomacropeptide (GMP) and other proteins. Whey proteins can be found in baby formula, protein shakes, muscle formulas, nutritional bars, performance formulas, and meal replacements [1]. In a previous study by Baer, 47 whey powder samples were obtained from different manufacturers around the U.S. with different ranges for protein, moisture, lactose, and fat. Spectral analysis was carried out in triplicate on all samples; regression models were then calculated for each component of the powder mixtures [2].

5.1.2 Chemometrics

Chemometrics is an interdisciplinary field that involves the use of statistics, mathematical modeling, computer science, and analytical chemistry [3]. During chemometric modeling, the maximum amount of relevant information is extracted from data that is analyzed [*4*]. Through multivariate techniques, multiple variables in an NIR spectrum can be related to known analyte properties; through qualitative and quantitative methods properties of future unknown samples can be determined [4]. Variable reduction techniques are used to reduce a large original data set to a few uncorrelated variables containing only information

relevant to samples that were analyzed [4]. Partial Least Squares (PLS) takes advantage of data reduction and finds the direction of greatest variability in the acquired spectral information and the known concentrations, which is plotted on a new axis to determine the "PLS components" or "PLS factors" [4].

5.1.3 NIR Spectroscopy

NIR spectroscopy utilizes the spectral range from 780-2500nm (12,500 – 4,000cm $^{-1}$) and provides complex structural information on the analyzed samples related to the vibration behavior of combinations of bonds [5]. NIR spectroscopy and chemometrics work together in building statistical models with the capability of predicting the components of future unknown samples, with as little error as possible. The whole process can be generalized to a few steps: (1) spectral data acquisition; (2) data pre-processing to eliminate noises and baseline shift from the instrument and background; (3) building a calibration model using a set of samples with known concentrations; (4) validation of the model using samples separate from the calibration set [5].

5.1.4 Multivariate Calibration

Multivariate calibrations models have an advantage over univariate models in that they do not need to be recalibrated frequently, giving them usage over an extended period of time. These models are based on many samples that are collected over a large span of time (possibly years). Linear regression models of the type $\mathbf{y = Xb + e}$ are used where $\mathbf{y}$ is the parameter to be predicted, $\mathbf{X}$, is the matrix with the spectral data, b, are the regression

coefficients and **e**, contains the residuals. Model parameters are estimated by training (calibration) set which use the number of samples and spectral wavelengths. Methods such as Multiple Linear Regression (MLR) use select variables; but in the case of PLS, full spectrum calibration methods are used [6].

*5.2**Materials & Methods***

5.2.1 Overview of Sample Sets

Samples were donated from Brewster Dairy, Inc (Brewster, OH), Foremost Farms, USA (Baraboo, WI), and Agri-Mark, Inc (Lawrence, Ma). Certificates of Analysis (CoA's) were sent from each company and potential areas for analysis were determined by comparing similar mixture components (protein percentage, fat, moisture, pH). Protein concentration ranged from 34.11 to 82.59 percent, fat ranged from 2.45 to 5.21 percent, moisture ranged from 3.7 to 5.19 percent, and pH ranged from 6.14 to 6.45.

5.2.2 NIR Spectroscopy

A Foss NIRSystems Model 6500 was used with a sample transport module attachment for analyzing powder samples. The monochromator chasis contains the grating drive which provides the precision for reliable analysis and a concave holographic grating which separates the wavelengths. A tungsten halogen lamp is used as the energy source. The order sorter filter separates the orders of radiation; first order radiation is preferred in spectrophotometry because it is the most intense. The system has internal standards that are used to compare its peak positions, stored in its software table, with reference positions for

wavelength calibration. The differences are calculated and the instrument software makes necessary corrections. The reflectance detector was used for collecting diffusely scattered radiation from the surface of the samples. Reflectance detectors are designed to gather energy from the sample surface with minimal specular reflection effects. The instrument uses a gain optimization, auto gain, which uses the first scan of each data collection to adjust the gain level for the best resolution of signal. Gain depends on the sample absorbance and requires no user adjustment [7].

The tungsten lamp was allowed ample time to warm up before running reference cell standard in the sample transport module. Multiple reference samples were taken to determine if the lamp had enough time to warm up and detect the presence of instrument drift; tests were alsoexecuted to ensure the instrument performed to company standards. The spectral range used for this study was 1100-2500 nm.

5.2.3 Sample Preparation & Loading

Whey protein samples were used as shipped from the companies and packed into the NIR ring cups with a quartz lens and screw on backing. All protein samples were refrigerated when not in use; whey powders were brought to lab temperature and mixed to loosen any powder clusters. Each powder was analyzed in triplicate; one powder sample was split among three NIR ring cups. Enough whey powder was used so that the backing of the ring cup was not visible through the powder. The fully assembled ring cup was loaded into the sample transport attachment of the NIRSystems 6500 for reflectance analysis.

5.3 ***Chemometric Analysis***

5.3.1 Software and Algorithms

MatLab and statistical algorithms were developed for the evaluation of NIR Spectroscopy data. A GUI program was created to import spectral data into MatLab for processing. The PLS algorithm was developed based on the work by Lorber, Wangen and Kowalski [91]. Two matrices contained the calibration and test spectra and PLS was performed for up to 18 factors. Two matrices contained the concentration data which were determined from the Certificates of Analysis (CoA's) from the companies. Based on these matrices, the models predictions of the concentrations are returned. The code also allows for pre-processing steps (mean correction and variance scaling) to be used. The user is able to specify the number of factors to be used in the model with a matrix of regression coefficients returned in the final model.

5.3.2 Initial Preprocessing

The samples from the NIR spectrometer were saved and exported to MatLab into a GUI program which extracted the spectral data. The matrix of spectra was trimmed off reference cell data used to check the precision of the NIR sample transport, as well as spectra that did not have accompanying known concentrations (determined by CoA's). The trimmed spectra (now totaling 153) were then baseline corrected (Figure 5.1A), followed by the averaging of triplicate samples leaving 51 total spectra, corresponding to 51 usable samples for calibration modeling and validation. The remaining spectra were trimmed to exclude all

signals acquired beyond 2200nm, due to noise, followed by the indexing of all of the spectra from the remaining wavelength range (Figure 5.1B).

5.3.3 Importing CoA Concentrations

A separate Excel spreadsheet (Table 5.1) housed all of the CoA data from all whey protein samples. This file was arranged to include four columns (protein percentage, fat percentage, moisture percentage, and pH). This same file was used to determine which samples were missing CoA's, which resulted in the deletion of the corresponding spectra along with the reference spectra. This spreadsheet was imported into MatLab and assigned a variable for later use in building four individual models for each mixture component (protein, fat, moisture, pH). This spreadsheet holds the information regarding concentrations of each component while the NIR file holds the corresponding spectral data.

5.3.4 Selection of Training and Validation Sets

Before the selection of training (calibration) and test (validation) sets, MatLab's random generator was reset , which is later used to pseudo-randomize the spectra in each data set. All 51 spectra are arranged randomly in a vector and sorted, followed by the splitting of the first 27 spectra into the training set and the remaining 24 spectra were used as the test set. This same split was used for all mixture components of the samples. The first column in the matrices represented the protein percentages; fat, moisture, and pH were represented by the second, third, and fourth columns respectively.

5.3.5 Partial Least Squares (PLS) Models

PLS was applied to the data to create four separate calibration models for each mixture component (protein, fat, moisture, pH). The following code set-up was used to construct each model:

[p_conc.1, p_conc.2, SEC, SEP, b] = pls (spec_trn, mc_trn, spec_tst, mc_tst, nuse, mn_corr, var_scale, nfac).

The matrix of 27 training spectra was represented by **spec_trn**, with the test (validation) spectra represented by **spec_tst**. The concentrations of mixture components (determined by CoA's) were entered for training (**mc_trn**) and test (**mc_tst**). The user specified the number of factors to use (**nuse**); preprocessing steps such as mean correction (**mn_corr**) and variance scaling (**var_scale**) could be specified. The variable **nfac** limited the maximum number of factors to calculate to 18. Once PLS was executed, the predicted (estimated) concentrations of the calibration set (**p_conc.1**) and the predicted (estimated) concentrations of the validation set (**p_conc.2**) were determined. The Square Error of Calibration (**SEC**) and Square Error of Prediction (**SEP**) were returned as row vectors for each model evaluated; the regression coefficients are returned in the **b** row vector. Residuals can be calculated by subtracting the CoA concentrations from the values estimated through the NIR spectra.

The SEP values generated from the 18 factors would determine the minimum number of factors needed to accurately explain the largest amount of variability in each model. Exceeding the minimum number of factors would result in data over-fitting which would decrease the model's predictive capabilities of future unknown samples.

*5.4**Results***

5.4.1 PLS for Protein Model

Only two factors were needed to explain the largest amount of variability in the protein concentration data as determined by the SEC and SEP values (Table 5.2 & Figure 5.2A). Using two factors gave a Root Mean Square Error of Prediction (RMSEP) of 6.258. Although the addition of more factors would reduce the RMSEP, the model would be over-fitted to the samples used in this study, decreasing its predictive capability for future unknowns. The calibration model and validation model (Table 5.2 & Figure 5.2B) were plots generated from the data; calibration and validation residual plots were also generated for the models (Table 5.2 & Figure 5.2C). As many samples contained 30-40% protein (24 calibration sets), the introduction of 3 samples with a protein concentration of over 80%, to the previous 24 samples, had influence on the model.

5.4.2 PLS for Fat Model

Only two factors were needed to explain the largest amount of variability in the fat concentration data as determined by the SEC and SEP values (Table 5.3 & Figure 5.3A). Using two factors gives a Root Mean Square Error of Prediction (RMSEP) of 0.270. The calibration model and validation model (Table 5.3 & Figure 5.3B) were plots generated from the data; calibration and validation residual plots were also generated for the models (Table 5.3 & Figure 5.3C).

5.4.3 PLS for Moisture Model

Only three factors were needed to explain the largest amount of variability in the moisture concentration data as determined by the SEC and SEP values (Table 5.4 & Figure 5.4A). Using two factors gives a Root Mean Square Error of Prediction (RMSEP) of 0.190. The calibration model and validation model (Table 5.4 & Figure 5.4B) were plots generated from the data; calibration and validation residual plots were also generated for the models (Table 5.4 & Figure 5.4C).

5.4.4 PLS for pH Model

Only four factors were needed to explain the largest amount of variability in the pH data as determined by the SEC and SEP values (Table 5.5 & Figure 5.5A). Using two factors gives a Root Mean Square Error of Prediction (RMSEP) of 0.149. The calibration model and validation model (Table 5.5 & Figure 5.5B) were plots generated from the data; calibration and validation residual plots were also generated for the models (Table 5.5 & Figure 5.5C).

5.5 ***Discussion***

5.5.1 PLS Models

For the four models that were created, only a few factors were needed to represent the entire data sets that were analyzed. Two factors cannot be ignored in the data analysis: (1) for the protein model, a few samples greatly deviated from the average range of the remaining samples which added error in predictability in the model; (2) the models are specific to the samples run on the NIRSystem Spectrometer and cannot be used to analyze samples of

similar ranges on a different NIRSystem even if it is the same model type from the manufacturer.

5.5.2 Sample Size & Range

A large enough sample size is needed for both the calibration and test sets that will be representative of the sample range that would be expected in the whey protein production environment. For NIR Spectroscopy and Chemometrics to be applied in a production setting, companies that specialize in a certain range of whey protein samples need to acquire a large library of samples over the entire range of acceptability for their production. As with any analytical method used for quality control, demonstration of method repeatability would need to be validated and documented.

5.5.3 Advantages and Disadvantages of NIR Spectroscopy

Some advantages of NIR analysis: (1) non-invasive and non-destructive to samples; (2) requires minimal sample preparation; (3) quick measurements and results; (4) no need for reagents. A few disadvantages: (1) chemometric techniques have to be used in the extraction of relevant information for data analysis; (2) accurate and robust models are hard to obtain; (3) large libraries of data are required of known samples across the range of interest to have a high predictive accuracy for future samples; (4) trusted reference methods need to be used which spectral data can be compared against [4].

5.5.4 NIR Calibration Standardization

Multivariate calibrations have a few set-backs that need to be addressed before implementing the system in a production setting. The calibrations can become invalid when

they are carried out on one instrument which is later replaced. Even instruments of the same model can have differences that will influence the calibration model. Drift or a shift in an instrument response, measurements taken at different temperatures, or changes in the physical constitutions of samples can all invalidate a calibration model [6]. To make a model more robust, sources of error that can have an effect on the model's predictive capabilities need to be incorporated during the calibration stage. Sources of variation can be eliminated through preprocessing. Also, parts of the wavelength spectrum which are robust against variations between instruments and experimental conditions should be selected. The selection of wavelengths does not apply to full spectrum calibrations such as PCR and PLS models [6].

5.6 ***Conclusion***

NIR Spectroscopy and Chemometric techniques have been used to build quantitative, linear regression models for whey protein concentrate property analyses (protein, fat, moisture, pH). PLS was used to explain a large dimension of data with only a few factors which led to the models with a highly accurate predictive capability of the validation samples. For this process to be implemented in a production setting, the disadvantages of NIR Spectroscopy and multivariate calibration need to be addressed. However, the implementation of NIR Spectroscopy in a production environment would lead to improved quality control, time saved on chemical testing, and a reduction in the use of chemical reagents for an alternative non-destructive method.

5.7 Acknowledgments

Special thanks to Brewster Dairy, Foremost Farms, and Agri-mark for donating samples for this project. East Carolina University graduate students Teresa Byers, John Blanton, and Patrick Cutler for their assistance with chemometrics analyses and NIR.

REFERENCES

[1] (2008). Whey protein facts. Retrieved March 22, 2009, from Whey Protein Institute Web site: http://www.wheyoflife.org/facts.cfm#3

[2] Baer, R .J.(1983). *Compositional analysis of nonfat dry milk and whey powder using near infrared diffuse reflectance spectroscopy*. Unpublished doctoral dissertation, University of Georgia, Athens.

[3] Gemperline, Paul J. *Practical guide to chemometrics: 2nd edition*. Boca Raton London, New York: Taylor & Francis Group.

[4] Blanco, M., & Villarroya, I. (2002). NIR spectroscopy: A rapid-response analytical tool. *TrAC Trends in Analytical Chemistry, 21*(4), 240-250. doi:DOI: 10.1016/S0165-9936(02)00404-1

[5] Cen, H., & He, Y. (2007). Theory and application of near infrared reflectance spectroscopy in determination of food quality. *Trends in Food Science & Technology, 18*(2), 72-83. doi:DOI: 10.1016/j.tifs.2006.09.003

[6] de Noord, O. E. (1994). Multivariate calibration standardization. *Chemometrics and Intelligent Laboratory Systems, 25*(2), 85-97. doi:DOI: 10.1016/0169-7439(94)85037-2

[7] (2008). Foss NIRSystems. Retrieved July 8, 2009, from Foss NIRSystems Web site: http://www.fossnirsystems. com/index.html

[8] Lorber, Wangen and Kowalski in J. Chemometrics 1, 19-31, 1987

Table 5.1. Certificate of Analysis (CoA) concentrations of mixture components that serve as the measured concentrations for comparison against the NIR spectra predictions. These concentrations are sorted and split into training (calibration) and test (validation) sets. Samples 47-51 were split up into training and test sets as well.

Certificate of Analysis (CoA) Number	Protein %	Fat %	Moisture %	pH
1	35	3.16	3.9	6.95
2	34.62	2.96	3.9	6.91
3	34.93	2.93	3.7	6.58
4	34.81	3.21	3.9	6.94
5	35.05	2.51	3.7	6.29
6	35.06	2.85	3.8	6.95
7	35.41	2.67	3.7	6.64
8	35.54	2.79	3.9	6.88
9	34.78	2.94	3.9	6.77
10	34.24	3.03	3.8	6.46
11	34.85	2.79	3.7	6.76
12	34.65	2.96	3.8	6.86
13	35.61	3.02	3.9	6.95
14	34.34	2.85	3.8	6.8
15	34.94	3.41	4.08	6.14
16	34.11	3.58	4.18	6.57
17	34.62	3.48	4.32	6.17
18	34.66	3.11	4.08	6.26
19	35.16	3.25	3.82	6.21
20	34.88	2.78	4.09	6.31
21	34.57	3.19	3.98	6.18
22	35.37	3.27	4.36	6.28
23	34.31	2.67	4.14	6.14
24	34.27	3.32	4.16	6.16
25	34.51	3.51	4.01	6.22
26	34.19	2.99	3.9	6.77
27	35.51	2.6	3.9	6.77
28	35.59	2.82	3.8	6.91
29	35.7	3.48	3.9	6.78
30	35.84	3.36	3.7	6.77
31	34.61	2.73	3.8	6.82
32	34.85	2.6	3.8	6.59

Table 5.1. Certificate of Analysis (CoA) concentrations of mixture components that serve as the measured concentrations for comparison against the NIR spectra predictions. These concentrations are sorted and split into training (calibration) and test (validation) sets. Samples 47-51 were split up into training and test sets as well (continued).

Certificate of Analysis (CoA) Number	Protein %	Fat %	Moisture %	pH
33	35.53	2.68	3.8	6.75
34	34.94	2.53	3.8	6.79
35	35.3	2.64	3.7	6.79
36	34.77	2.85	3.8	6.84
37	34.28	2.45	3.8	6.63
38	34.33	2.69	3.9	6.78
39	35.16	2.91	3.8	6.85
40	34.15	2.8	3.9	6.8
41	34.81	2.58	3.7	6.73
42	35.75	3.06	3.8	6.87
43	34.22	2.95	3.8	6.82
44	35.45	2.75	3.9	6.96
45	35.23	2.84	3.8	6.75
46	34.36	2.64	3.8	6.9
47	80.66	5.21	5.13	6.39
48	80.66	5.21	5.13	6.39
49	48.96	4.8	5.19	6.4
50	81.62	4.89	4.17	6.46
51	82.59	4.92	4.18	6.45

Table 5.2. Numerical results of Partial Least Squares (PLS) modeling for protein% concentration. Out of the 18 factors run, it was determined that only 2 factors were needed to accurately model all of the data. Adding additional factors would do very little in improving the model; the increase in factors would risk over-fitting the PLS model to the data reducing its predictive capabilities for protein% determination of future unknown samples. The use of 2 factors yields a Root Mean Square Error of Prediction of 6.258.

	Root Mean		Training (Calibration)			Test (Validation)		
# of Factors	Square Error of Calibration (SEC)	Square Error of Prediction (SEP)	Measured Conc.	Estimated Conc.	Residuals	Measured Conc.	Estimated Conc.	Residuals
1	11.399	9.872	34.850	34.344	0.506	34.510	32.026	2.484
2	1.775	6.258	34.150	32.089	2.061	34.280	34.058	0.222
3	0.855	6.326	35.370	34.005	1.365	34.610	36.468	-1.858
4	0.738	6.275	34.940	34.146	0.795	48.960	78.023	-29.063
5	0.653	6.198	35.300	34.809	0.491	35.510	36.443	-0.933
6	0.519	6.234	35.060	37.609	-2.549	81.620	81.662	-0.042
7	0.509	6.247	34.930	36.795	-1.865	34.190	34.675	-0.485
8	0.496	6.251	34.110	31.407	2.703	34.220	33.576	0.645
9	0.396	6.083	34.850	37.921	-3.071	35.160	30.518	4.642
10	0.320	6.135	35.840	33.878	1.962	35.450	34.628	0.822
11	0.297	6.152	35.230	34.682	0.548	34.940	33.647	1.293
12	0.266	6.181	82.590	81.391	1.200	35.000	36.953	-1.953
13	0.248	6.146	35.530	33.093	2.437	34.770	34.299	0.471
14	0.223	6.118	35.410	38.566	-3.156	34.310	33.774	0.536
15	0.178	6.215	34.330	32.689	1.641	34.620	38.504	-3.884
16	0.144	6.289	35.750	34.598	1.152	34.810	38.561	-3.751
17	0.111	6.288	35.590	35.462	0.128	34.660	32.044	2.617
18	0.089	6.310	34.620	34.456	0.164	34.270	33.395	0.875
			34.810	33.746	1.064	35.160	35.962	-0.802
			80.660	80.519	0.141	35.610	36.984	-1.374
			34.340	37.427	-3.087	34.780	37.161	-2.381
			34.360	34.968	-0.608	34.880	33.363	1.517
			35.540	37.116	-1.576	34.240	36.919	-2.679
			35.050	35.964	-0.914	34.650	35.872	-1.222
			80.660	80.383	0.277			
			35.700	36.652	-0.952			
			34.570	35.428	-0.858			

Table 5.3. Numerical results of Partial Least Squares (PLS) modeling for fat% concentration. Out of the 18 factors run, it was determined that only 2 factors were needed to accurately model all of the data. Adding additional factors would do very little in improving the model; the increase in factors would risk over-fitting the PLS model to the data reducing its predictive capabilities for fat% determination of future unknown samples. The use of 2 factors yields a Root Mean Square Error of Prediction of 0.270.

	Root Mean		Training (Calibration)			Test (Validation)		
# of Factors	Square Error of Calibration (SEC)	Square Error of Prediction (SEP)	Measured Conc.	Estimated Conc.	Residuals	Measured Conc.	Estimated Conc.	Residuals
1	0.450	0.378	2.600	2.695	-0.095	3.510	3.001	0.509
2	0.244	0.270	2.800	2.707	0.093	2.450	2.587	-0.137
3	0.218	0.288	3.270	3.125	0.145	2.730	2.655	0.075
4	0.203	0.309	2.530	2.674	-0.144	4.800	4.925	-0.125
5	0.195	0.266	2.640	2.631	0.009	2.600	2.717	-0.117
6	0.188	0.268	2.850	3.046	-0.196	4.890	5.051	-0.161
7	0.186	0.277	2.930	2.853	0.077	2.990	2.368	0.622
8	0.159	0.410	3.580	3.057	0.523	2.950	2.651	0.299
9	0.152	0.410	2.790	2.977	-0.187	3.250	3.083	0.167
10	0.148	0.424	3.360	2.812	0.548	2.750	2.857	-0.107
11	0.146	0.458	2.840	2.789	0.051	3.410	3.134	0.276
12	0.139	0.464	4.920	5.017	-0.097	3.160	3.089	0.071
13	0.124	0.568	2.680	2.730	-0.050	2.850	2.690	0.160
14	0.075	0.487	2.670	2.978	-0.308	2.670	3.177	-0.507
15	0.064	0.526	2.690	2.573	0.117	2.960	3.055	-0.095
16	0.059	0.546	3.060	2.842	0.218	3.210	3.198	0.013
17	0.045	0.538	2.820	2.785	0.035	3.110	2.773	0.338
18	0.037	0.551	3.480	3.391	0.089	3.320	3.306	0.014
			2.580	2.784	-0.204	2.910	2.752	0.158
			5.210	5.103	0.107	3.020	3.090	-0.070
			2.850	2.966	-0.116	2.940	2.855	0.085
			2.640	2.574	0.067	2.780	3.391	-0.611
			2.790	3.071	-0.281	3.030	3.056	-0.026
			2.510	2.804	-0.294	2.960	2.937	0.023
			5.210	5.095	0.115			
			3.480	3.230	0.250			
			3.190	3.661	-0.471			

Table 5.4. Numerical results of Partial Least Squares (PLS) modeling for moisture% concentration. Out of the 18 factors run, it was determined that only 3 factors were needed to accurately model all of the data. Adding additional factors would do very little in improving the model; the increase in factors would risk over-fitting the PLS model to the data reducing its predictive capabilities for moisture% determination of future unknown samples. The use of 3 factors yields a Root Mean Square Error of Prediction of 0.190.

	Root Mean		Training (Calibration)			Test (Validation)		
# of Factors	Square Error of Calibration (SEC)	Square Error of Prediction (SEP)	Measured Conc.	Estimated Conc.	Residuals	Measured Conc.	Estimated Conc.	Residuals
1	0.207	0.200	3.800	3.784	0.016	4.010	3.979	0.031
2	0.210	0.195	3.900	3.865	0.035	3.800	3.713	0.087
3	0.191	0.190	4.360	3.994	0.367	3.800	3.590	0.210
4	0.185	0.210	3.800	3.801	-0.001	5.190	4.809	0.381
5	0.184	0.205	3.700	3.752	-0.052	3.900	3.698	0.202
6	0.176	0.207	3.800	3.743	0.057	4.170	4.687	-0.517
7	0.171	0.213	3.700	3.696	0.004	3.900	3.481	0.419
8	0.140	0.292	4.180	4.084	0.096	3.800	3.789	0.011
9	0.129	0.324	3.700	3.708	-0.008	3.820	4.055	-0.235
10	0.116	0.298	3.700	3.912	-0.212	3.900	3.885	0.015
11	0.108	0.294	3.800	3.807	-0.007	4.080	4.069	0.011
12	0.094	0.261	4.180	4.690	-0.510	3.900	3.842	0.058
13	0.085	0.294	3.800	3.837	-0.037	3.800	3.758	0.042
14	0.077	0.278	3.700	3.684	0.016	4.140	4.045	0.095
15	0.052	0.254	3.900	3.809	0.091	3.900	3.729	0.171
16	0.043	0.226	3.800	3.899	-0.099	3.900	3.845	0.055
17	0.033	0.245	3.800	3.732	0.069	4.080	3.895	0.185
18	0.027	0.238	4.320	4.177	0.143	4.160	4.172	-0.012
			3.700	3.951	-0.251	3.800	3.805	-0.005
			5.130	4.860	0.270	3.900	3.883	0.017
			3.800	3.719	0.081	3.900	3.740	0.160
			3.800	3.673	0.127	4.090	4.234	-0.144
			3.900	3.862	0.038	3.800	3.790	0.010
			3.700	3.784	-0.084	3.800	3.812	-0.012
			5.130	4.873	0.257			
			3.900	4.009	-0.109			
			3.980	4.278	-0.298			

Table 5.5. Numerical results of Partial Least Squares (PLS) modeling for pH concentration. Out of the 18 factors run, it was determined that only 4 factors were needed to accurately model all of the data. Adding additional factors would do very little in improving the model; the increase in factors would risk over-fitting the PLS model to the data reducing its predictive capabilities for pH determination of future unknown samples. The use of 4 factors yields a Root Mean Square Error of Prediction of 0.149.

	Root Mean		Training (Calibration)			Test (Validation)		
# of Factors	Square Error of Calibration (SEC)	Square Error of Prediction (SEP)	Measured Conc.	Estimated Conc.	Residuals	Measured Conc.	Estimated Conc.	Residuals
1	0.204	0.247	6.590	6.788	-0.198	6.220	6.218	0.002
2	0.171	0.236	6.800	6.740	0.061	6.630	6.907	-0.277
3	0.170	0.217	6.280	6.248	0.032	6.820	6.909	-0.089
4	0.147	0.149	6.790	6.772	0.018	6.400	6.436	-0.036
5	0.137	0.159	6.790	6.881	-0.091	6.770	6.885	-0.115
6	0.133	0.155	6.950	6.712	0.238	6.460	6.417	0.043
7	0.132	0.149	6.580	6.703	-0.123	6.770	6.902	-0.132
8	0.119	0.186	6.570	6.377	0.193	6.820	6.760	0.060
9	0.115	0.194	6.760	6.700	0.060	6.210	6.315	-0.105
10	0.111	0.216	6.770	6.656	0.114	6.960	6.726	0.234
11	0.107	0.217	6.750	6.709	0.041	6.140	6.444	-0.304
12	0.102	0.249	6.450	6.426	0.024	6.950	6.838	0.112
13	0.092	0.331	6.750	6.781	-0.031	6.840	6.851	-0.011
14	0.061	0.367	6.640	6.717	-0.077	6.140	6.249	-0.109
15	0.039	0.421	6.780	6.728	0.052	6.910	6.743	0.167
16	0.037	0.416	6.870	6.754	0.116	6.940	6.861	0.079
17	0.024	0.410	6.910	6.733	0.177	6.260	6.506	-0.246
18	0.023	0.422	6.170	6.333	-0.163	6.160	6.212	-0.052
			6.730	6.710	0.020	6.850	6.730	0.120
			6.390	6.391	-0.001	6.950	6.756	0.194
			6.800	6.758	0.042	6.770	6.777	-0.007
			6.900	6.912	-0.012	6.310	6.176	0.134
			6.880	6.853	0.027	6.460	6.690	-0.230
			6.290	6.726	-0.436	6.860	6.791	0.069
			6.390	6.396	-0.006			
			6.780	6.729	0.051			
			6.180	6.306	-0.126			

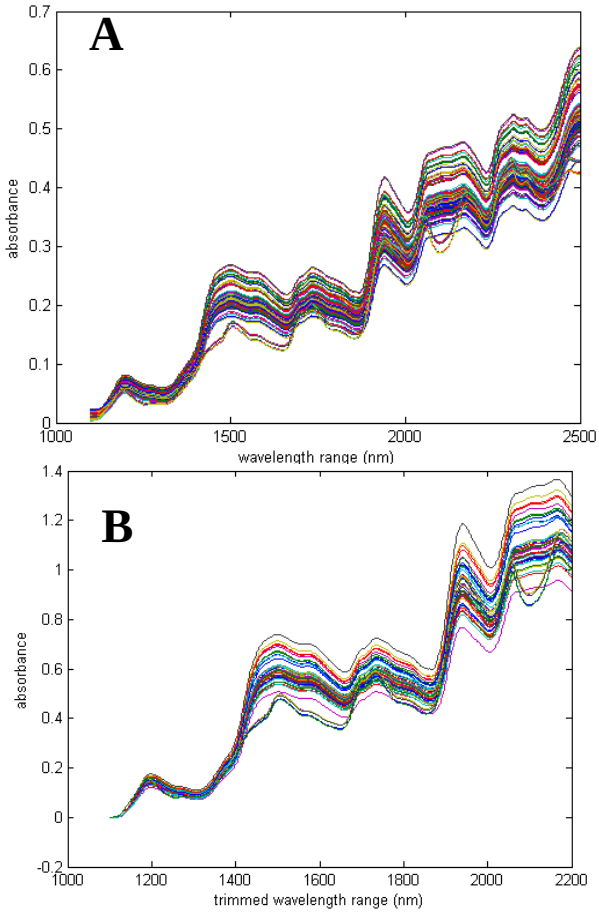

Figure 5.1. (A) NIR spectra with baseline correction, all reference and spectral data without accompanying known concentrations were deleted. (B) Spectra of figure A with triplicates averaged and wavelength trimmed to exclude upper spectral region with noise.

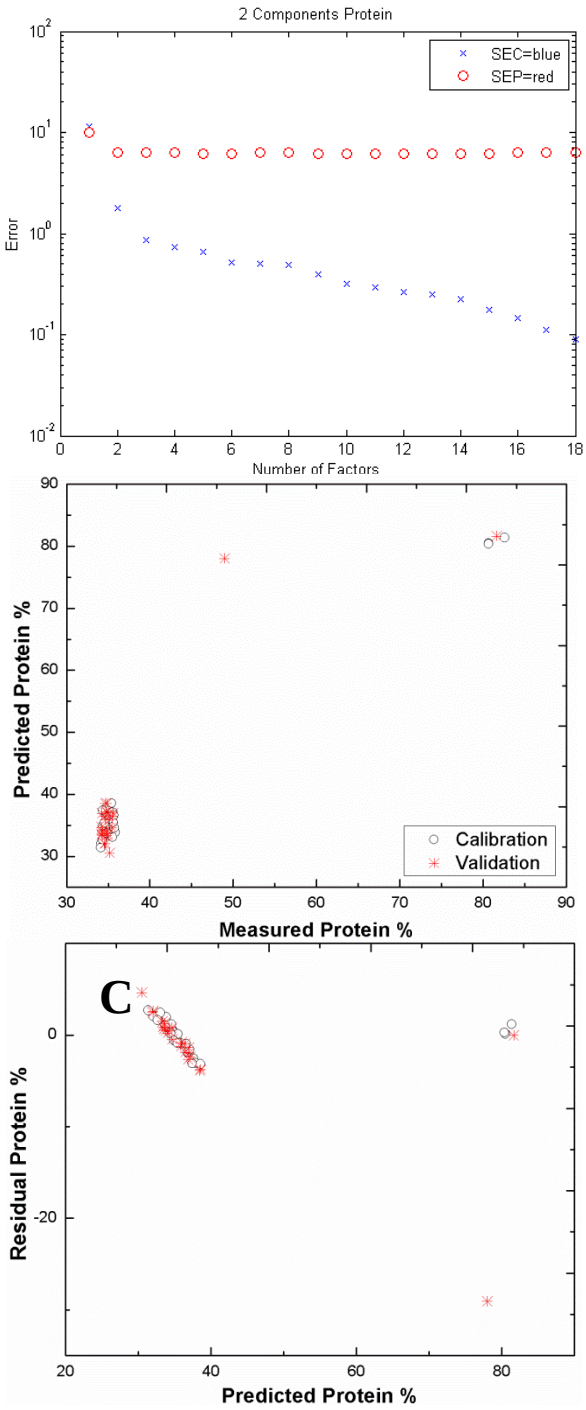

Figure 5.2. (A) factors needed to classify the protein model with a RMSEP of 6.258. (B) calibration and validation sets with measured concentrations (from CoA's) compared to predicted concentrations determined by NIR and PLS. (C) residuals from the calibration and validation models.

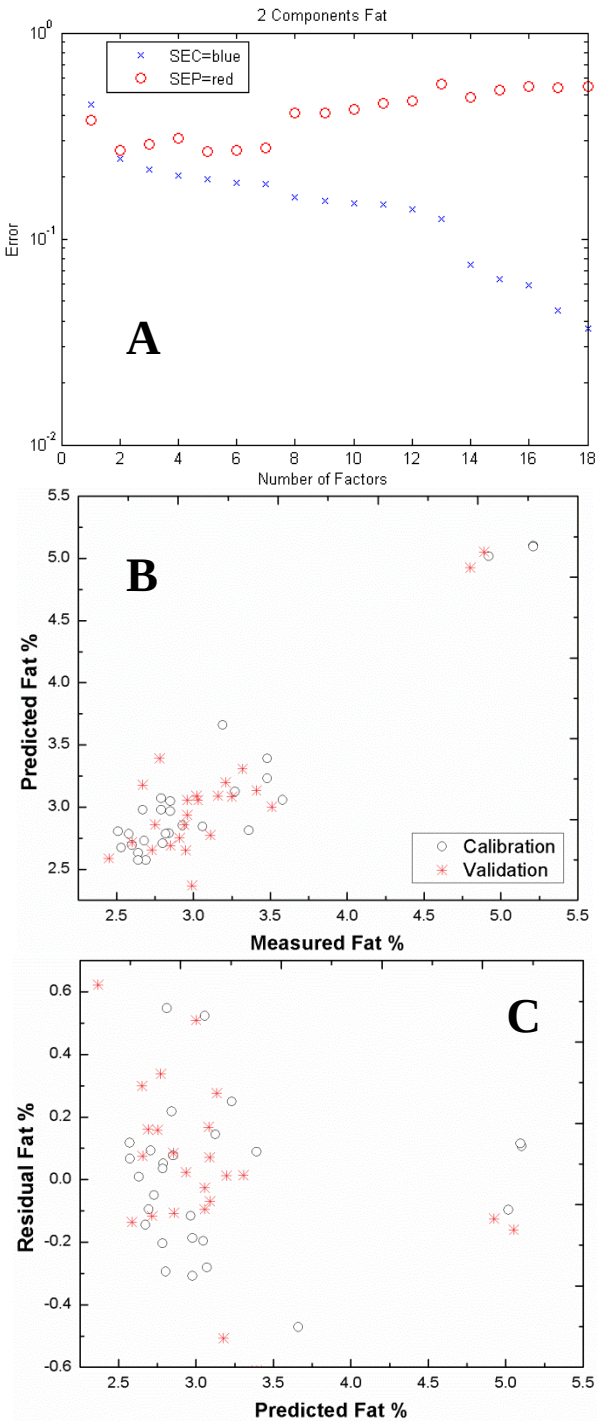

Figure 5.3. (A) factors needed to classify the fat% model with a RMSEP of 0.270. (B) calibration and validation sets with measured concentrations (from CoA's) compared to predicted concentrations determined by NIR and PLS. (C) residuals from the calibration and validation models.

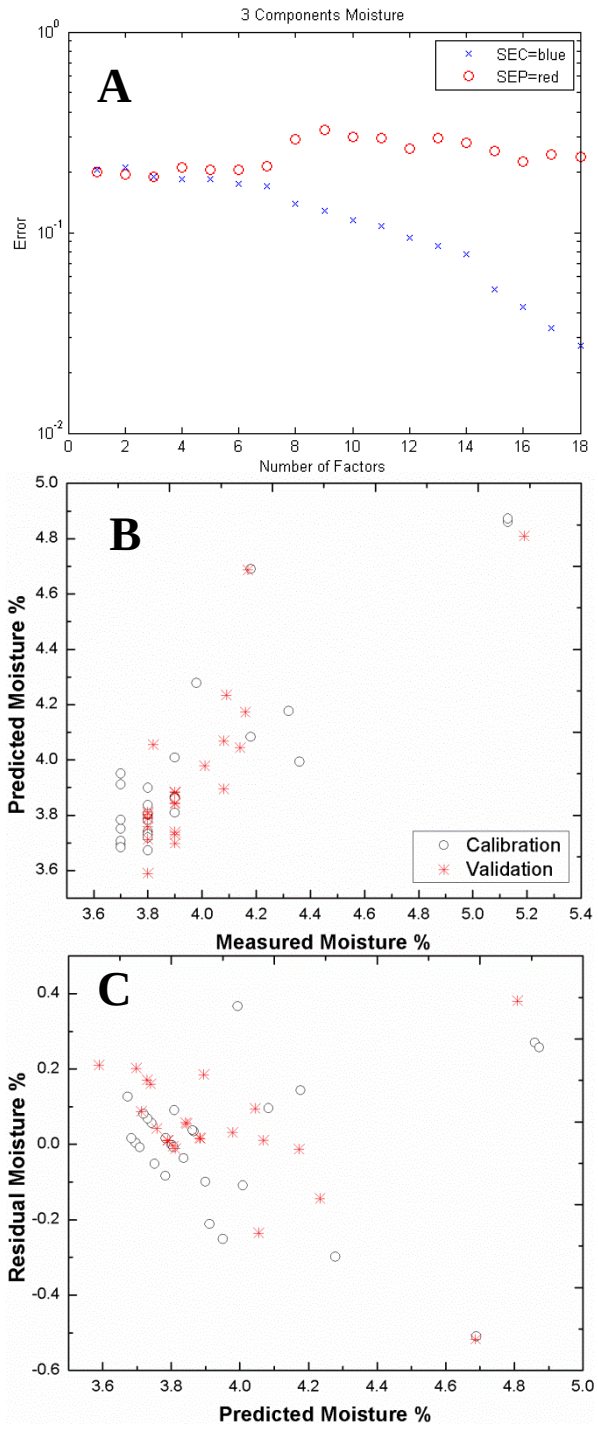

Figure 5.4. (A) factors needed to classify the moisture% model with a RMSEP of 0.190. (B) calibration and validation sets with measured concentrations (from CoA's) compared to predicted concentrations determined by NIR and PLS. (C) residuals from the calibration and validation models.

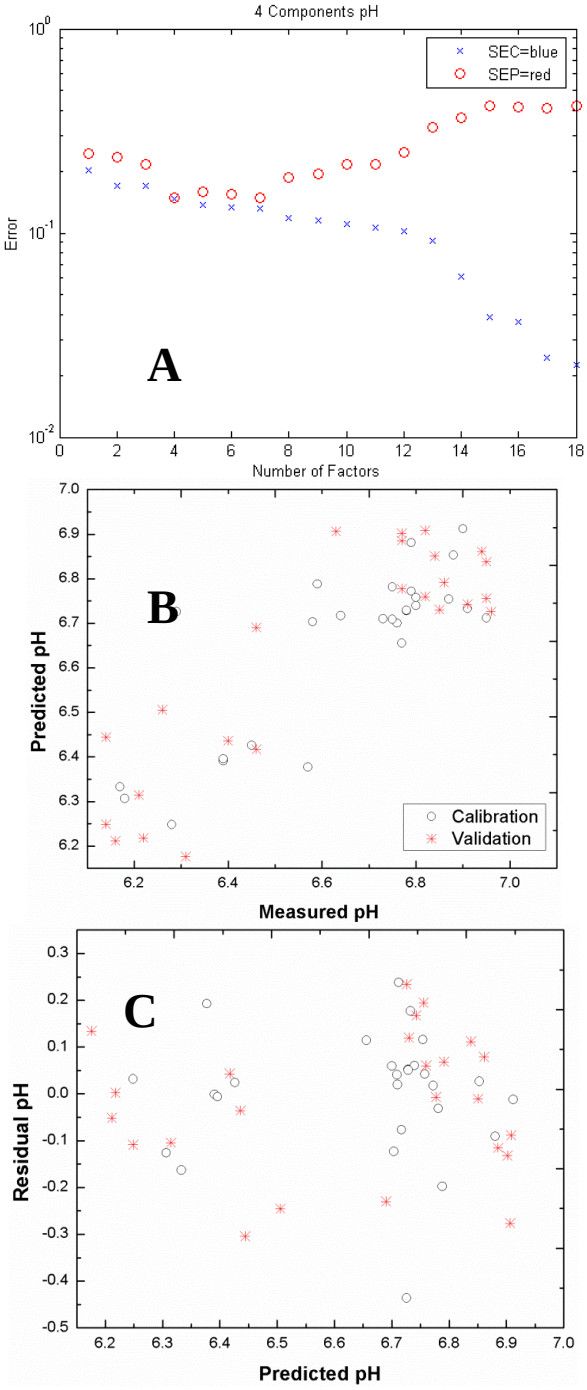

Figure 5.5. (A) factors needed to classify the pH model with a RMSEP of 0.149. (B) calibration and validation sets with measured concentrations (from CoA's) compared to predicted concentrations determined by NIR and PLS. (C) residuals from the calibration and validation models.

CHAPTER 6 Conclusions & Recommendations

Stephanie T. Sullivan

6.1 Conclusions

This investigation began when I learned about whey protein, which had been well studied at North Carolina State University (NCSU) and by the Khan Laboratory, and from searching for an additional interesting biomaterial to complex with it. I happened upon pullulan. Something produced from a fungus just did not seem that desirable at first, but it is really fascinating material. I am grateful for Hayashibara's providing this material to me when I contacted them about my research; as I am to Davisco Foods, Inc. who has been supporting NCSU for some time for supplying whey protein. I also want to thank the impetus that an anonymous donor may have had in providing funds that went towards the purchase of a rheometer at ECU. This allowed me to work closer to home while I worked at my full time position teaching there.

In the preceding chapters, we attempted to address three underlying themes:

I. Developing WP nanofibers and correlating morphology to solution properties
II. Investigating formation and microstructure of WP-pullulan gels and ways to manipulate gel properties using enzyme and salt
III. Forming and crosslinking of pullulan and pullulan blend nanofibers to render this highly water soluble material insoluble

In pursuit of these research themes, we investigated systems with electrospun nanofibers and gels. Some of the major findings are below:

6.1.1 Chapter 2 Solution Electrospinning Whey Protein

Some said it could not be done, and darn if it could not, at least with some pleasant

solvents to work with like water! However, after many efforts that resulted in interesting microstructures, we did electrospin whey protein with a spinnable polymer, poly(ethylene oxide). The most promising outcome for this chapter as well as chapter 4 was heat treating the fibers. The protein denaturing and forming bonds to render the mats insoluble in water has tremendous potential, perhaps even expanding to other proteins or protein-polymer blends.

To reiterate, in Chapter 2: We report the fabrication of a variety of whey protein (WP) nanostructures ranging from nanoparticles to nanofibers via solution electrospinning, which may be particularly well suited for flavor delivery. Aqueous whey protein solutions, both whey protein isolate (WPI) and one of its major components β–lactoglobulin (BLG), either in native or denatured form yielded interesting micro and nanostructures; while nanofiber production required blending with a spinnable polymer, poly(ethylene oxide) (PEO). WP:PEO solution composition was as high as 3:1 and average fiber diameters ranged from 312 to 690 nm depending on polymer composition and concentration. WP:PEO solutions are also successfully electrospun at acidic pH ($2 \leq pH \leq 3$), which could improve shelf life. FTIR analysis of WP:PEO fiber mat indicates some variation in WP secondary structure with varying WPI concentration (as WPI increased, % α-helix increased and β-turn decreased) and pH (as pH decreased from neutral (7.5) to acidic (2), % β-sheet decreased and α-helix increased). XPS also confirms the presence of WP on the surface of the blend fibers, augmenting the FTIR analysis. Interestingly, WP:PEO composite nanofibers maintain its fibrous morphology at temperatures as high as 100 ^{o}C, above the 60 ^{o}C PEO melting point. Further, we show that the blend mats retained a fibrous structure after the heat treatment. In

addition, the mats swell in water and retain a fibrous quality which makes them ideal for tissue scaffolding. Finally, we incorporated a small hydrophobic molecule (RhB) as a model flavenoid into WP:PEO nanofiber mats. The BLG:PEO nanofibers qualitatively exhibit improved fiber quality and RhB distribution compared to PEO nanofibers; however, no effect on the release profile was observed.

6.1.2 CHAPTER 3 Functional gels of whey protein and pullulan blends

Examining gels in situ on the rheometer has been a challenge. We started with just a cone and plate geometry, then tried a cross-hatch upper plate, and even tried sandpaper. Then we received a cross-hatched bottom plate and went to town. Although we still may have experienced some slip, which is for further study (see next section).

Of course, what is always most fascinating about working with materials is imaging them on a small scale. A picture is worth a thousand words is very true, and often necessary in science as evidence for what we are trying to explain. Gel microstructure is fascinating.

Manipulating the gels with foodsafe additives is a motivation for me. Finding STMP was thrilling and I plan to work with it and pullulan and whey protein more in the future, as the studies in this chapter were at a concentration of pullulan and/or NaOH that was not adequate to achieve gels without some presence of protein.

In summary, again: Whey protein and pullulan blend gels have been evaluated using microscopy and rheological methods. Protein gels had higher fracture stress than its blend counterparts. Also, blend gels formed at the protein isoelectric point of pH 5.2 exhibited

fracture stresses more than an order of magnitude lower than its native mix counterpart; while 100% WPI gels of different pH had fracture stresses and strains of the same order of magnitude. The presence of the pullulan in the protein aggregated solution inhibited protein heat induced crosslinking. ESEM and confocal imaging showed smooth gel microstructure at pH 6.8, but particulate gel microstructure at isoelectric point pH 5.2. Particulate blend gels contained larger voids, which indicated less crosslinking and thus may explain the lower fracture stresses. Changing the continuous network from protein to protein-pullulan blend appeared to cause an increase in water holding properties as well.

As shown by the varying gel fracture stress and strain as well as microstructure, the addition of pullulan to the whey protein gel permits new concentration controlled protein-polysaccharide blend gel design for biomedical, food and pharmaceutical application. WP:PULL blend solution and gel properties can be manipulated by heat treatment and addition of TG and STMP. Gel yield strength was increased by TG at higher WPI concentrations, while STMP reduced the magnitude of the system viscoelastic response. Depending on the pullulan/WPI blend concentration desired, TG or STMP can be used to manipulate system properties. Enzyme enhanced gel yield strain over native gels; while pullulan and STMP reduced the elasticity of the gels. ESEM revealed gels with microstructure at the protein isoelectric point, but smooth transparent gels at near neutral and pH 8. Benchtop NMR is a promising tool for evaluating species mobility in protein solutions.

6.1.3 CHAPTER 4 Pullulan Nanofiber Crosslinking by heat and chemical methods

Evaluating solutions on the rheometer and electrospinning pullulan I started as soon as I received my first shipment. It took a while at first because it required higher concentrations than the traditional PEO and PVA. And I thought heat treating the whey protein-PEO mats was cool, but pullulan whey protein is much more impressive, as it swells much more in water and retains it long after it is removed! The WP:PEO mats dry fairly quickly. Also, with this work, marrying the specific viscosity data to fiber morphology I think is a great accomplishment, thanks to Christina suggesting we get data for lower concentrations of pullulan. The three linear fit model predicts both transitions very well in accordance with other published data.

In summary for this work: we correlate PULL, PULL:WP and PULL:HPBCD fiber mat morphologies to solution dynamics. We identify three regimes in the pullulan solution specific viscosity data that indicate the pullulan critical concentration to electrospin of a minimum of 13.7 w/w%, confirmed by defect free mat produced with a 15 w/w% solution. Pullulan tends to behave as do other polymers with broad polydispersity having a high c/c* ratio to achieve fibers. All solutions evaluated had dominant Newtonian regions; and solution viscosity increased in each case with increasing pullulan concentration. Blend fibers were able to form defect free mats. The addition of WP to PULL solutions shifted the critical concentration lower, enabling defect free mats to form at lower pullulan concentrations than PULL only mats. pH also impacted the success of electrospinning PULL:WP blends, as 50:50 blends at pH 3, 5.2, 8 and 11 all achieved defect free fibers. The lowest pH of 3 enabled nearly defect free fibers of 30:70 PULL:WPI. Protein on the surface of the

PULL:WP fibers, as confirmed by XPS, enabled mats to be heat treated, presumably forming protein-protein linkages during heat treatment that rendered them insoluble in water. In fact, they formed very nice swellable, biodegradable, edible mats that would be ideal for cell seeding and tissue culture. XRD results agreed with literature data interpreted as pullulan being fully amorphous. Chemical crosslinking with EGDGE also yielded a crosslinked network. In both heat treatment of PULL:WP blends and chemical submersion of PULL or PULL:HPBCD, an insoluble gelatinous/fibrous network was formed.

6.1.4 CHAPTER 5 Near Infrared Reflectance (NIR) Spectroscopy of Commercial Whey Protein Powders

This work evaluated commercial powder whey proteins to determine if NIR would be a feasible method for quality control. Using NIR and chemometrics, models for pH, protein, fat and moisture were identified.

6.2 Recommendations

In this dissertation, we discussed the solution properties and process parameters that affected the production of aqueous biomaterial solution electrospun nanofibers. The scope of this work can be continued with many extensions of work discussed and beyond. I will briefly discuss some extensions and other research projects I have planned going forward.

6.2.1 Extensions of this work

I have many ideas for extending the works herein going forward. First, we would like to

correlate Benchtop NMR and rheology data for protein-polysaccharide complexation (collaboration with D. Cistola (MD, PhD), Associate Dean of Research, Brody Medical School and Dr. Saad Khan). Another exciting avenue is tissue scaffolding development of protein-polymer heat-treated mats (collaboration with B. Muller-Borer, Associate Professor, Brody Medical School and Dr. Saad Khan). Some factors to evaluate include:

- Investigating mat thickness vs. required heat treatment
- Cell proliferation on media swollen pullulan:WP mats
- Tensile testing of mats for cardiac cell growth potential

A third avenue is to investigate polysaccharide gelation and crosslinking (i.e. guar) by the STMP/NaOH system. Also, I have already started investigating the impact of rheometer geometry on whey protein gelation analysis and slip with traditional couette versus a vane geometery. We will also look at the smooth vs. crosshatched geometries.

6.2.2 Additional potential research

Other planned projects include the rheology of biofuels (co-PI on NSF MRI proposal for engine test laboratory). Other areas of research include bridging materials science and art together in youth education, as my father is an artist and Professor Emeritus at the Columbus College of Art & Design in Columbus, Ohio which has exposed me to art education my entire life. Also, I have a strong interest in engineering ethics, STEM (Science, Technology, Engineering and Mathematics) education and leadership as well asmilitary leadership and the support of our military veterans. If not for the sacrifice of our military men and women, I

would not have the opportunity, especially as a female, to do many of the things I have accomplished in this life. I plan to find a way to utilize my experience and expertise to help our veterans and their families.

APPENDICES

Appendix A. Excerpts from CURRICULUM VITAE (2006-2011)

Stephanie T. Sullivan extracurricular activities during time enrolled at North Carolina State University pursuing this degree:

PUBLICATIONS

Book Chapter

Sullivan, S. T., Khan, S. A., & Eissa, A. S. (2008). Whey Proteins: Functionality and Foaming under Acidic Conditions. In C. Onwulata & P. Huth (Eds.), ***Whey Processing, Functionality and Health Benefits (Institute of Food Technologists Series)*** (pp. 99-132): Wiley-Blackwell.

Refereed Journals (does not include chapters of this dissertation to be submitted)

1. Eissa, A.; Sullivan, S. T.; Khan, S. A.; Chemical and Physical Interactions in Enzymatically Modified Cold Set Acidic Whey Protein Gels. Draft Available, *Food Hydrocolloids* 2011.
2. Williams, R. R.; Klein, S.; Limberis, L.; Sullivan, S. T.; The Implementation of a Challenge-Based Curriculum into a Bioprocess Engineering Program. To be submitted, *International Journal of Engineering Education*, 2011.
3. Yao, J., Sullivan, S. T., Eckert, C., & Bartlett, E., (2009). An Orthopedic Injection Training Instrument Using Flow Impedance to Indicate Needle Tip Locations. *Journal of Clinical Monitoring and Computing* 23:347-353.
4. Hall, C., Sullivan, S. T., Kauffmann, P. J., Batts, D. & Long, J., (2009) "Are there Gender Differences in Factors Influencing Career Considerations?" *American Journal of Educational Studies* 2 (1), 23-38.
5. Kabin J.A.; Tolstedt S.L.; Sáez A.E.; Grant C.S.; Carbonell R.G. (1998). Removal of Organic Films from Rotating Disks Using Aqueous Solutions of Nonionic Surfactants: Effect of Surfactant Molecular Structure. *Journal of Colloid and Interface Science* 206 (1), 102-111.

Refereed Proceedings

1. Kauffmann, P.; Sullivan, S.; Dixon, G.; Kim, B. J. (2010) Integration of Engineering Economics, Statistics and Project Management: Reinforcing Key Concepts. *ASEE 2010 Annual Conference Proceedings.*
2. Williams, R. R.; Klein, S.; Sullivan, S.; Limberis, L.; (2009) Bioprocess Engineering Curriculum Development and Assessment. *ASEE 2009 Annual Conference Proceedings.*
3. Williams, R. R.; Sullivan, S.; Klein, S.; Limberis, L.; (2009) Design and Development of Educational Modules for Bioprocess Engineering. *2009 ASEE Annual Conference Proceedings*.
4. Sullivan, Stephanie; Hall, Cathy; Kauffmann, Paul; Batts, David; Long, Jeremy; (2008) Influences on Female Interest in Pursuit of STEM Fields in Higher Education, *2008 American Institute of Higher Education Conference Proceedings.*
5. Sullivan, Stephanie T.; Williams, Rick; Howard, William E.; Yao, Jason; Kauffmann, Paul. (2007) Identifying the content of an Engineering program using benchmarking and the Fundamentals of Engineering examination; *2007 ASEE Annual Conference Proceedings*.

Presentations

1. Sullivan, S. T.[‡]; Simmons, J.; Miller, V. L.; Khan, S. A. (2010) Poster Presentation: Solution Electrospun Nanofibers of Pullulan & Pullulan/Whey Protein Blends. *Nanofibers for the 3rd Millenium: A Summit of the World's Leaders in Nanofibers.* Raleigh, NC.

2. McLeod, S.M.ǂ; Duffrin, M.W.; Carraway-Stage, V.; Wheeler, M.; Sullivan, S.; Forsythe, W. (2010) Poster Presentation: Local Agriculture Engages Students in Classroom-Industry Partnership. *2010 Institute of Food Technologists Annual Meeting*, Chicago, IL.
3. Sullivan, S. T.ǂ; Eckert, C.; Cannon, M. & Khan, S. A., (2009) Oral Presentation and Proceedings: Functional gels of whey protein and pullulan blends. *The International Symposium on Food Rheology and Structure*, Zurich, Switzerland.
4. Sullivan, S. T.ǂ ; Talwar, S.; Khan, S.A. (2007) Oral Presentation: Solution Electrospinning Whey Protein, AIChE Annual Meeting, Salt Lake City, UT.
5. Sullivan, S. T.ǂ; Grant, C. S.; Carbonell, R. (1995) Poster Presentation: Removal of Organic Films from Rotating Disks Using Aqueous Solutions of Nonionic Surfactants: Effect of Surfactant Molecular Structure. *International Symposium on Surfactants in Solution - Micelles, Microemulsions and Monolayers: Quarter Century Progress and New Horizons* University of Florida, Gainsville, FL (300 researchers from 25 countries in attendance).

(ǂpresenter)

GRANTS AND CONTRACTS

- NSF CCLI Grant Co-PI, Award No. 0737198 ($136K over 2 years), Design and Development of Educational Modules for Bioprocess Engineering, CCLI-Phase 1. (2008-2010)
- NSF ITEST Grant ($1.3 million over 3 years); Biomechanics Curriculum Program Coordinator, 2007-2009.

EAST CAROLINA UNIVERSITY/COLLEGE/DEPARTMENT SERVICE

- College of Technology & Computer Science (CTECS) Leadership Committee, Fall 2010 – Present.
- Coordinator, CTECS Leadership Legacy Lecture Series, Spring 2010 – Present.
- Advisor (with two other faculty), ECU Engineering Honor Society, Fall 2009 – Present.
- Biomedical Engineering Concentration Curriculum Committee, Fall 2007 – Present.
- Bioprocess Engineering Concentration Curriculum Committee, Fall 2006 – Present.
- College of Technology & Computer Science Distance Education Task Force, Spring 2007.
- Engineering Management Curriculum Committee, Fall 2006 – Spring 2007.
- Engineering K-12 Outreach Committee, Fall 2006 – Spring 2010.

HONORS & AWARDS

- 2nd place, poster competition (2010) *Nanofibers for the 3rd Millennium: A Summit of the World's Leaders in Nanofibers*, Raleigh, NC.
- Identified by ECU graduate Misty Atkins as "The person at ECU who made the most significant positive contribution to her education," 2010.
- North Carolina Future Program Partner, FoodMASTER, 2008 Science Education Partnership Award, National Center for Research Resources, National Institutes of Health
- Guest Faculty, UNC Chapel Hill School of Pharmacy graduate level course PPES 180 "Pharmaceutical Research, Development & Marketing," Pharmaceutical Manufacturing, 2000 – 2004.

COURSES TAUGHT

****ENGR 3500.** Introduction to Engineering Project Management (3 hrs) *Spring 2011*

***ENGR 4501.** Special Topics: Bioprocess Validation and Quality Engineering (1 hrs) *Spring 2011*

***ITEC 4350.** Separations for Industrial Processes (3 hrs) *Spring 2011, Spring 2009*

ENGR 3901/2/3. Undergraduate Engineering Research (1-3 hrs) *ongoing since Spring 2008*

****ENGR 3300.** Introduction to Engineering Project Management (3 hrs) *Fall 2010, Spring 2010, Spring 2008, Fall 2007*

ENGR 2050. Computer Applications in Engineering (3 hrs) *Fall 2010, Spring 2010*

***ITEC 4550.** Quality for Regulatory Environments (3 hrs) *Fall 2010, Spring 2010, Spring 2008*

***ITEC 4150.** Industrial Microbiology (3 hrs) *Spring 2010, Fall 2008, Spring 2008*

***BIOE 4000.** Bioprocess Validation and Quality Engineering (4 hrs) *Fall 2009, 2008*

***ITEC 4250.** Engineering for Food Safety & Sanitation (3 hrs) *Fall 2009, Fall 2007*

COAD 1000. Student Development & Learning in Higher Education (1 hr) *Fall 2007*

ICEE 1020. Integrated Collaborative Engineering II (6 hrs) *Spring 2007 (Engineering Economics portion of course)*

****ITEC 3000.** Internet Tools Technology (3 hrs) *Spring 2007, Fall 2006*

**Developed new course*
*** Revised existing course*

Appendix B. Highlight images: 2006-2011.

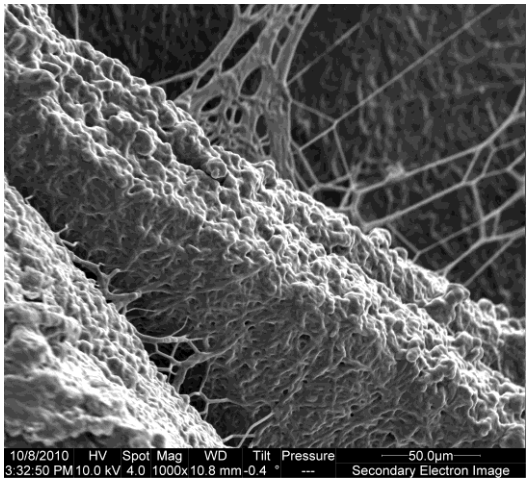

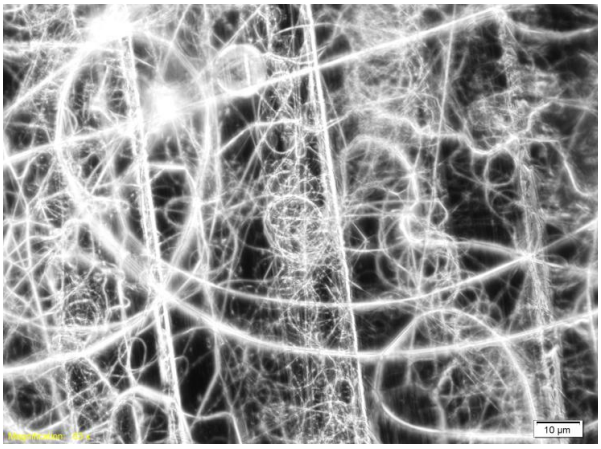

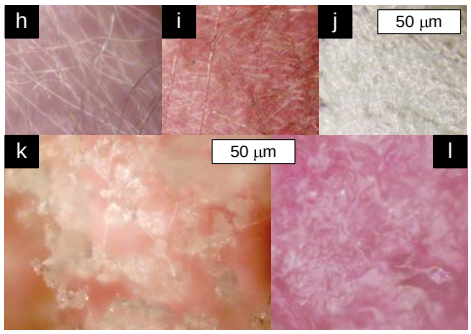

Victoria Miller on RLM

God Bless.